

Catalytic Transformations Based on Pincer and Half-Sandwich Ruthenium Complexes

By

Basujit Chatterjee
CHEM11201104001

National Institute of Science Education and Research
Bhubaneswar, Odisha – 752050

*A thesis submitted to the
Board of Studies in Chemical Sciences
In partial fulfillment of requirements
for the Degree of*

DOCTOR OF PHILOSOPHY

Of

HOMI BHABHA NATIONAL INSTITUTE

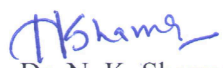


July, 2017

HomiBhabha National Institute¹

Recommendations of the Viva Voce Committee

As members of the Viva Voce Committee, we certify that we have read the dissertation prepared by Mr. Basujit Chatterjee entitled "Catalytic Transformations Based on Pincer and Half-Sandwich Ruthenium Complexes" and recommend that it may be accepted as fulfilling the thesis requirement for the award of Degree of Doctor of Philosophy.

Chairman	 Prof. A. Srinivasan	Date: 28.7.17
Guide/convenor	 Dr. C. Gunanathan	Date: 28/07/2017
External examiner	 Prof. K. P. Kaliappan	Date: 28/7/17
Member 1-	 Dr. B. L. Bhargava	Date: 28/7/17
Member 2-	 Dr. N. K. Sharma	Date: 28/07/17
Member 3-	 Dr. Debasmita P. Alone	Date: 28/07/17

Final approval and acceptance of this thesis is contingent upon the candidate's submission of the final copies of the thesis to HBNI.

I hereby certify that I have read this thesis prepared under my direction and recommend that it may be accepted as fulfilling the thesis requirement.

Date: 28/07/2017
Place: Bhubaneswar


(Dr. C. Gunanathan)
Guide

¹This page is to be included only for final submission after successful completion of viva voce.

STATEMENT BY AUTHOR

This dissertation has been submitted in partial fulfillment of requirements for an advanced degree at Homi Bhabha National Institute (HBNI) and is deposited in the Library to be made available to borrowers under rules of the HBNI.

Brief quotations from this dissertation are allowable without special permission, provided that accurate acknowledgement of source is made. Requests for permission for extended quotation from or reproduction of this manuscript in whole or in part may be granted by the Competent Authority of HBNI when in his or her judgement the proposed use of the material is in the interests of scholarship. In all other instances, however, permission must be obtained from the author.

Basujit Chatterjee
Basujit Chatterjee

DECLARATION

I, hereby declare that the investigation presented in the thesis has been carried out by me. The work is original and has not been submitted earlier as a whole or in part for a degree / diploma at this or any other Institution / University.

Basujit Chatterjee

Basujit Chatterjee

List of Publications arising from the thesis

Journal

1. *Ruthenium catalyzed selective hydrosilylation of aldehydes*, **Chatterjee, B;** Gunanathan, C. *Chem. Commun.* **2014**, 50, 888-890.
2. *Ruthenium Catalyzed Selective Hydroboration of Carbonyl Compounds*
†Kaithal, A.; †**Chatterjee, B.;** Gunanathan, C. *Org. Lett.* **2015**, 17, 4790-4793.
3. *Ruthenium Catalyzed Selective α - and α,β -Deuteration of Alcohols Using D_2O* , **Chatterjee, B.;** Gunanathan, C. *Org. Lett.* **2015**, 17, 4794-4797.
4. *The ruthenium-catalysed selective synthesis of mono-deuterated terminal alkynes*, **Chatterjee, B.;** Gunanathan, C. *Chem. Commun.* **2016**, 52, 4509-4512.
5. *Ruthenium-Catalyzed Regioselective 1,4-Hydroboration of Pyridines*,
†Kaithal, A.; †**Chatterjee, B.;** Gunanathan, C. *Org. Lett.* **2016**, 18, 3402-3405.
Highlights: *Synfacts* **2016**, 12, 0956.
6. *Selective α -Deuteration of Amines and Amino Acids Using D_2O* , †**Chatterjee, B.;** †Krishnakumar, V.; Gunanathan, C. *Org. Lett.* **2016**, 18, 5892-5895.
7. *Ruthenium-catalysed multicomponent synthesis of borasiloxanes*, **Chatterjee, B.;** Gunanathan, C. **2017**, 53, 2515-2518.
8. *Ruthenium-Catalyzed Urea Synthesis by N-H Activation of Amines*,
†Krishnakumar, V.; †**Chatterjee, B.;** Gunanathan, C. *Inorg. Chem.* **2017**, 56, 7278-7284.
(†Equal contribution).

Publication not included in thesis

9. *Ruthenium-Catalyzed Selective Hydroboration of Nitriles and Imines*, †Kaithal, A.; †Chatterjee, B.; Gunanathan, C. *J. Org. Chem.*, **2016**, *81*, 11153-11161. Highlights: *Synfacts* **2017**, *13*, 0078.

(†Equal contribution).

Conferences

1. **11th J-NOST Conference for Research Scholars (J-NOST 2015)**. School of Chemical Sciences, NISER, Bhubaneswar, December 14-17, 2015, *Ruthenium Catalyzed Selective α - and α,β -Deuteration of Alcohols Using D_2O* . Chatterjee, B.; Gunanathan, C. Duration: 25 minutes (**Oral Presentation**).
2. **11th J-NOST Conference for Research Scholars (J-NOST 2015)**, School of Chemical Sciences, NISER, Bhubaneswar, December 14-17, 2015. *Ruthenium Catalyzed Selective Hydroboration of Carbonyl Compounds*, †Kaithal, A.; †Chatterjee, B.; Gunanathan, C. (†Equal contribution) (**Poster Presentation**).
3. Attended **Indo-French Symposium on Functional Metal Organics: Applications in Materials and Catalysis**. School of Chemical Sciences, NISER, Bhubaneswar, February 24-26, 2014.
4. Attended **Indo-European Symposium on Frontiers of Chemistry**, School of Chemical Sciences, NISER, Bhubaneswar, November 10 - 12, 2011.



Basujit Chatterjee

To my parents

ACKNOWLEDGEMENTS

First and above all, I praise God, the almighty for providing me this opportunity and granting me the capability to proceed successfully. This thesis appears in its current form due to the assistance and guidance of several people. I would therefore like to offer my sincere thanks to all of them. First of all, I would like to thank my supervisor Dr. C. Gunanathan for providing me the opportunity to work on this exciting and inventive project. Also, I would like to express my gratitude to him for his guidance, patience, knowledge, sincere advices and support during this long-standing learning period of my life. I appreciate all his contributions of valuable time, stimulating ideas, and funding to make my project experience interesting and productive. My sincere gratitude goes to Prof. Sudhakar Panda, Director (NISER), Prof. T. K. Chandrashekar, founder-Director (NISER) and Prof. V. Chandrashekhar, former-Director (NISER). I would like to thank my doctoral committee members, Prof. A. Srinivasan, Dr. B. L. Bhargava, Dr. N. K. Sharma and Dr. Debasmita P. Alone for their support and suggestions. I would also like to thank Dr. Arindam Ghosh for his kind help in NMR studies and Dr. C. S. Purohit for his valuable suggestion and help in X-ray analysis. I also would like to recognize Mr. Sanjaya Mishra for his kind help in recording NMR data, Mr. Deepak Kumar Behera for his kind help in X-ray analysis and Mr. Amit sankar sahu and Mr. Rajkumar Lakra for their kind help in ESI-MS analysis.

This would not have been possible without the continuous, unconditional help from my labmates Dr. V. Krishnakumar, Dr. Arun Kumar Shil, Akash, Suhash, Thiagarajan, Suresh, Biplab, Prakash, Sesha, Kishore, Apurba, Preet and Steffi. I would also like to thank my friends and well-wishers for their kind suggestion and help. Financial assistance (fellowship) by University Grants Commission (UGC), Govt. of India is gratefully acknowledged. I would also like to acknowledge DST-SERB, New Delhi, Govt. of India for research funding.

Finally, I would like to thank my parents, and family who were a witness to every step of the way and provided me support and confidence whenever I needed it the most. Thank you all so much for your unconditional love and untiring support.

...Basujit Chatterjee

SYNOPSIS

1. Name of the Student:	Basujit Chatterjee
2. Name of the Constituent Institution :	National Institute of Science Education and Research (NISER)
3. Enrolment No:	CHEM11201104001
4. Title of the Thesis:	Catalytic Transformations Based on Pincer and Half-Sandwich Ruthenium Complexes
5. Board of Studies:	Chemical Science

Introduction:

Isolation and characterization of intermediates in catalytic processes are uncommon and challenging owing to their inevitable low stability. However, overcoming this barrier and succeeding in isolating and characterizing the intermediates involved in the catalytic transformations can be highly beneficial in further fine tuning and optimization of catalysts, and for the fundamental understanding of reaction mechanisms. By employing pincer and half-sandwich ruthenium complexes, simple, atom-economical and important catalytic transformations were developed in which interesting and hitherto unknown intermediates were identified and uncovered. Identified catalytic intermediates were independently synthesized and further successfully used as efficient catalysts.

Selective deuteration of alcohols, terminal alkynes and synthesis of urea derivatives using DMF as a CO surrogate were developed by employing ruthenium pincer complexes that operate via amine-amide metal-ligand cooperation and elaborated in **Part A**. While **Part B**, demonstrates chemistry using half-sandwich ruthenium complexes as catalysts. Efficient chemoselective hydroelementation reactions (hydroboration and hydrosilylation), and atom-economical synthesis of borasiloxanes

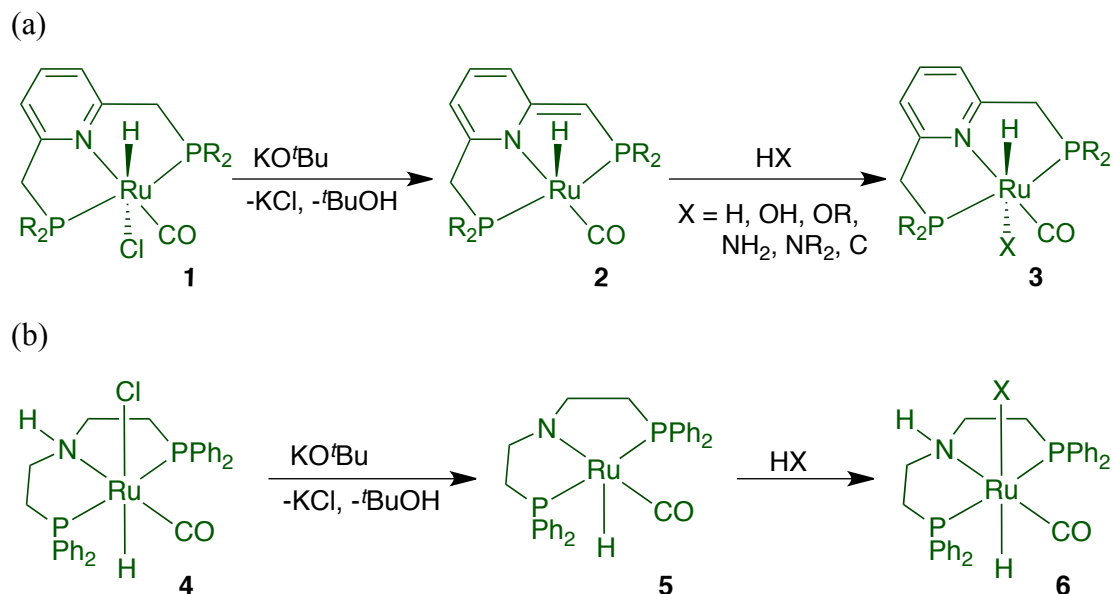
were devised. The unexpected intermediate involved in the hydroelementation reactions turned out to be an efficient catalyst for the challenging selective deuteration of amines and amino acids. Notably, direct deuteration of organic compounds using heavy water (D₂O) as a source of deuterium was established in four different catalytic processes

Part A: Catalysis Based on Ruthenium Pincer Complexes

CHAPTER 1: Ruthenium Pincer Complexes and Their Reactivity

Activation of unreactive chemical bonds by transition metal complexes is an area of utmost significance. Efficient bond activation by catalysts is highly demanding and can provide greener approach towards benign organic transformations. Pincer complexes are composed of tridentate pincer ligands, which enforces meridional geometry at the metal center upon complexation with metals. Embedded with bulky donor substituents and planar framework these complexes are highly stable and capable of exhibiting versatile reactivity. Although the first pincer complex was discovered in late 1980's their unusual reactivity came to limelight by the discovery of Metal-Ligand Cooperation (MLC) by Milstein and coworkers in 2005.¹ MLC can be operative in different pathways, two representative pathways are demonstrated (Scheme 1), where a pincer complex upon facile deprotonation of the acidic α -CH₂ protons can generate a reactive and unsaturated complex **2** where the pyridine core of the ligand is dearomatized. The complex **2** can activate several unreactive bonds of small molecules (H₂, H₂O, ROH, NH₃, H-NR₂, C-H, etc) and can generate a saturated complex **3** (Scheme 1a). Similarly, bond activation is also conceivable by amine-amide MLC, where in a similar fashion deprotonation of coordinated amine functionality can provide a reactive and unsaturated complex **5**, which also capable of activating unreactive bonds to generate a saturated complex **6** (Scheme 1b). The area

of amine-amide MLC is not fully explored and needs further attention. Thus in **part A** efforts were made to explore different catalytic protocols involving amine-amide Metal-Ligand Cooperation.



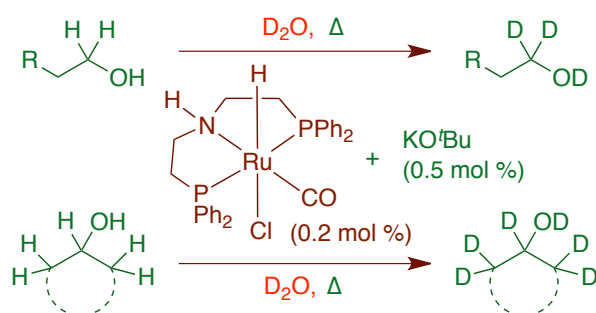
Scheme 1. (a) Metal-Ligand Cooperation via dearomatization-aromatization pathway.

(b) Metal-Ligand Cooperation via amine-amide pathway.

CHAPTER 2: Ruthenium Catalyzed Selective α - and α,β -Deuteration of Alcohols Using D_2O

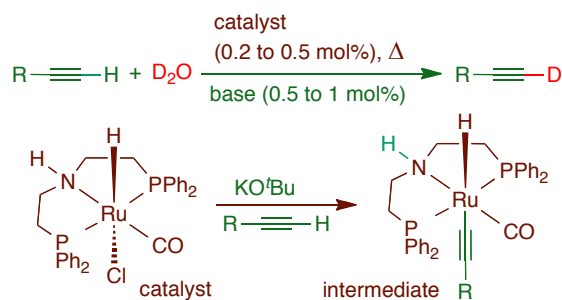
Synthesis of deuterium labeled alcohols with high percentage of deuteration and selectivity is an important transformation in organic synthesis as deuterated pharmaceuticals and bio-active organic molecules play a vital role in the metabolism of alcohols and enzymes, in addition to the regular use as NMR solvents and also as reliable chemical probes.² Ru on carbon support is reported to catalyze selective deuteration of the protons at the α -position of alcohols with the catalyst loading of 20% of Ru (relative to the substrate) and under the atmosphere of hydrogen.³ Exclusive deuteration at the β -positions also occurred with 3 mol % of aminoalcohol ligated in situ-generated ruthenium catalyst.⁴ We have developed highly selective ruthenium-catalyzed α -deuteration of primary alcohols and α,β -deuteration of

secondary alcohols using deuterium oxide (D_2O) as a source of deuterium and reaction solvent. Minimal load of catalyst (Ru-macho), base (KO^tBu) and low temperature heating provided efficient selective deuteration of alcohols making the process practically attractive and environmentally benign. Mechanistic studies indicate the D–O(D/R) bond activations by metal-ligand cooperation and intermediacy of carbonyl compounds resulting from dehydrogenation of alcohols.⁵



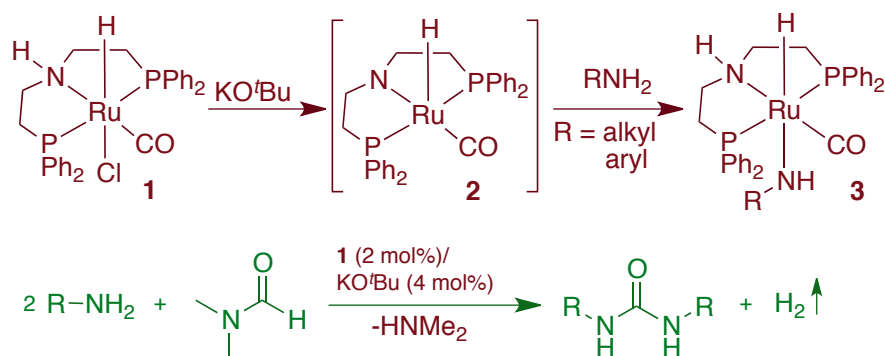
CHAPTER 3: The Ruthenium-Catalyzed Selective Synthesis of *mono*-Deuterated Terminal Alkynes

Terminal alkyne motifs are found in numerous natural products, pharmaceuticals and they have widespread applications in chemical synthesis,⁶ pharmaceuticals, live cell imaging of biomolecules and material science. Deuterated terminal alkynes are currently obtained using conventional organic synthesis. Reaction of alkynes with n -BuLi and 9-D-9-phenylfluorene, a pre-synthesized deuterium label derived from multi-step synthesis,⁷ Grignard reagents with large excess of deuterium oxide at sub-ambient temperatures are used.⁸ The chapter 3 describes an efficient catalytic method for the synthesis of *mono*-deuterated terminal alkynes directly from deuterium oxide, catalyzed by a Ru(II) pincer complex in which the reaction proceeds via Ru-acetylide intermediates and amine-amide metal-ligand cooperation.⁹



CHAPTER 4. Ruthenium-Catalyzed Urea Synthesis by N–H Activation of Amines

N,N'-disubstituted urea derivatives are an important class of organic compounds. In particular *N,N'*-dialkyl urea derivatives have potential applications as efficient organocatalyst,¹¹ green solvent,¹² promising materials for nonlinear optical properties, and also possess high viscoelastic properties. Urea embedded biologically active molecules find widespread applications in pharmacological and physiological activities.¹³ Despite the notable advances, the urea derivatives are in general obtained using phosgene and isocyanates.¹⁴ Urea derivatives are also synthesized by various transition metal-catalyzed reactions¹⁵ using excessive additives, high pressure carbon monoxide, which also generates large amount of waste. Chapter 5 describes a Ru(II)-catalyzed urea synthesis from amines using DMF as a carbon monoxide source (C1 feedstock) in which the carbonylation of amines occurs with liberation of dihydrogen. The developed protocol is applicable for a wide range of simple and functionalized amines, devoid of any stoichiometric activating reagents and avoids direct use of fatal carbon monoxide. At low temperature, a formamide was isolated. The reactions are proposed to proceed via formyl C–H activation of DMF by a ruthenium pincer complex operating via “amine-amide” metal-ligand cooperation.



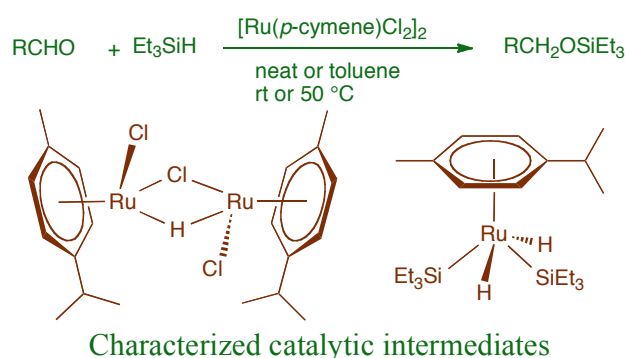
Part B: Catalysis Based on Ruthenium Half-Sandwich Complexes

CHAPTER 5. Half-Sandwich Ruthenium Complexes and Their Reactivity

In 1952 the discovery of ferrocene and its hapticity bonding pattern by Woodward and Wilkinson was a breakthrough in organometallic chemistry. Afterwards several metallocenes were synthesized using various transition metals. When sandwich type complexes possess a single cyclic polyhapto ligand along with other monodentate ligands they generate half-sandwich complexes. The half-sandwich complexes of ruthenium exhibit versatile reactivity, serve as excellent precursors for various inorganic synthetic protocols, and also find potential applications in many organic transformations as effective catalysts.¹⁶ The unique properties such as, milder synthetic procedure, high yields, and wide range of stability expanded the scope and usage of these half-sandwich arene ruthenium complexes. Some of these complexes are also stable in aqueous medium at high temperature, thus providing further opportunity to understand the reaction mechanism in aqueous medium.¹⁷ **Part B** demonstrates different catalytic protocols for hydroelementation reactions, an atom-economic protocol for synthesizing borasiloxanes from boranes, silanes and water and an effective deuteration strategy to provide α -deuterated primary, secondary amines and amino acids using a highly reactive catalyst which was isolated as an intermediate during our hydroelementation studies.

CHAPTER 6. Ruthenium-Catalyzed Selective Hydrosilylation of Aldehydes

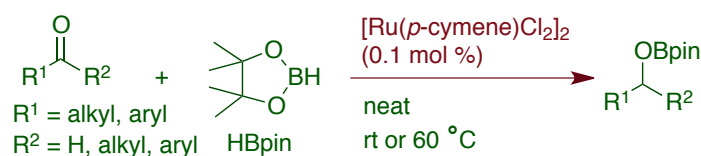
Hydrosilylation of carbonyl compounds is a valuable transformation in chemical synthesis as a single step operation that serves on both reduction of carbonyl motifs and protection of resulting alcohols featuring high atom-economy. Catalytic hydrosilylation, which can be carried out under mild experimental conditions is often used as a convenient alternative to hydrogenation reaction and advantageous over the traditional and harsh reducing agents.¹⁸ Alkoxysilanes function as useful synthetic intermediates, used for the synthesis of silicon-containing polymers, ceramic materials and thus produced in both small as well as large-scales.¹⁹ The chapter 7 describes a chemoselective hydrosilylation method for aldehydes using a ruthenium catalyst $[(\text{Ru}(p\text{-cymene})\text{Cl}_2)_2]$ and triethylsilane; a mono hydride bridged dinuclear complex $[\{(\eta^6\text{-}p\text{-cymene})\text{RuCl}\}_2(\mu\text{-H}-\mu\text{-Cl})]$ and a Ru(IV) mononuclear dihydride complex $[(\eta^6\text{-}p\text{-cymene})\text{Ru}(\text{H})_2(\text{SiEt}_3)_2]$ are identified as potential intermediates in the reaction and the proposed catalytic cycle involves a 1,3-hydride migration.²⁰



CHAPTER 7. Ruthenium-Catalyzed Selective Hydroboration of Carbonyl Compounds

Boronate esters are excellent synthetic surrogates in organic synthesis and an assortment of chemical transformation is developed to incorporate them into organic

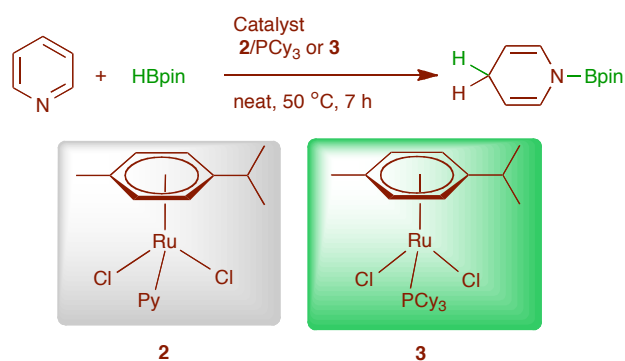
substrates.²¹ The organoboronates are stable, non-toxic compounds and thus preferred over the other organometallic compounds. Thus, a number of catalytic methods are employed for the synthesis of alkyl and vinyl boronates.²² However, chemoselective hydroboration of aldehydes over ketones is a synthetically valuable and unknown transformation. Using $[\text{Ru}(p\text{-cymene})\text{Cl}_2]_2$ (**1**) complex, catalytic hydroboration of aldehydes and ketones with pinacolborane under neat and mild conditions is described in this chapter. At room temperature, chemoselective hydroboration of aldehydes over the ketones is also attained. Mechanistic studies confirmed the immediate formation of mono hydride bridged dinuclear complex $[\{(\eta^6\text{-}p\text{-cymene})\text{RuCl}\}_2(\mu\text{-H}-\mu\text{-Cl})]$ (**1b**) from the reaction of **1** with pinacolborane, which catalyzed the highly efficient hydroboration reactions. The catalytic cycle containing mononuclear Ru–H species and intramolecular 1,3-hydride transfer is postulated.²³



CHAPTER 8. Ruthenium-Catalyzed Regioselective 1,4-Hydroboration of Pyridines

1,4-Dihydropyridines are prevalently present in nature and also commercially available as they possess pharmacological applications.²⁴ NAD^+/NADH redox couple undergoes dearomatization/aromatization of pyridine motifs, plays important role in biological systems²⁵ and 1,4-dihydropyridines are also widely used as reducing agents in organocatalysis.²⁶ Selective synthesis of dihydropyridines from pyridine is a fundamental and challenging transformation, which conventionally performed using

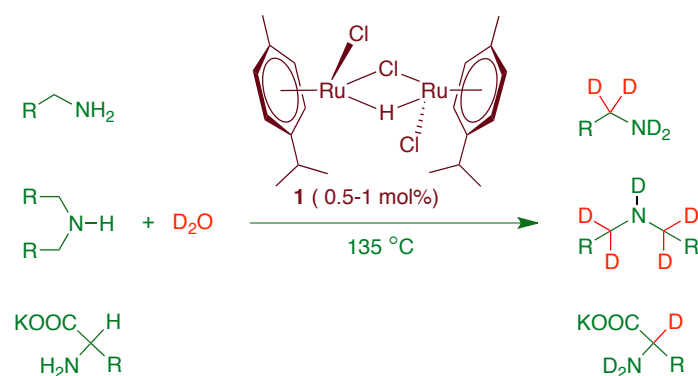
excessive amount of alkali metals or metal-hydrides leading to a mixture of 1,2 and 1,4-dihydropyridines. Strategies towards selective synthesis of dihydropyridines from pyridines are more limited. While the direct catalytic hydrogenation resulted in over reduction of pyridines to piperidines,²⁷ hydrosilylation, silaboration, phosphinoboration and hydroboration allow the selective synthesis. The groups of Suginome²⁸ and Marks²⁹ developed Rh(I) and La(III) catalyzed elegant hydroboration of pyridine in which insertion of pyridine C=N bond into the M–H bond provided selective 1,2-hydroboration. Recently, Wang et al. discovered that a bulky organoborane forms a FLP with pyridine and provides selective 1,4-hydroboration of pyridines.³⁰ The chapter 9 describes simple Ru-catalyzed regioselective 1,4-hydroboration of pyridines using pinacolborane in which four catalytic intermediates, [Ru(*p*-cymene)Cl₂Py] **2**, [Ru(*p*-cymene)Cl₂(P(Cy)₃)] **3**, [Ru(*p*-cymene)Cl₂(Py)(P(Cy)₃)] **4** and [Ru(*p*-cymene)(H)Cl(Py)(P(Cy)₃)] **5** are identified and an intramolecular selective 1,5-hydride transfer in **5** leading to the selective 1,4-hydroboration of pyridines is suggested as possible mechanism.³¹



CHAPTER 9. Ruthenium-Catalyzed Selective Synthesis of Borasiloxane

Borasiloxanes have found numerous applications in functional inorganic material synthesis for their inherent molecular properties such as high stability providing resistance to heat and chemical reactions.³² The conventional synthetic methods comprise the reaction of hydroxyborane with silane derivatives or the reaction of

Selective deuteration of organic compounds is one of the important transformations in chemical synthesis as deuterated organic compounds find widespread applications as NMR solvents, mechanistic probe in chemical and biological processes, biologically active compounds and pharmaceuticals.³⁷ When metabolism of drugs involve cleavage of C–H bonds, deuteration of those covalently bound hydrogen atoms can provide improved metabolomics profile and prevent formation of toxic metabolites.³⁸ Thus, direct catalytic deuteration of these target molecules by C–H activation³⁹ is a highly desired protocol. Very recently, the groups of Rousseau and Chaudret developed polymer supported ruthenium nanoparticle catalyzed α -deuteration of amines.⁴⁰ Nevertheless, this method suffers from the requirement of expensive deuterium gas (1-2 bar D₂) as a deuterium source and only 40% deuteration occurred on primary amines. Moreover, α -selective deuteration of amino acids remains a challenge for which there exist no effective catalytic methods.⁴¹ The chapter 11 describes mono hydrido bridged ruthenium complex $[\{(\eta^6\text{-}p\text{-cymene})\text{RuCl}\}_2(\mu\text{-H-}\mu\text{-Cl})]$ **1** as an effective catalyst for α -selective deuteration of primary amines, secondary amines, amino acids and biologically active molecules. Mechanistic investigations revealed involvement of unprecedented N–H activation of benzylamine. 1,3-Deuteride transfers to imine ligand (formed in situ from β -hydride elimination) on a ruthenium center leading to the selective deuteration at α -CH₂ protons of amine functionality is proposed as possible reaction mechanism.



References:

- (1) (a) Gunanathan, C.; Milstein, D. *Chem. Rev.* **2014**, *114*, 12024-12087. (b) Gunanathan, C.; Milstein, D. *Acc. Chem. Res.* **2011**, *44*, 588-602. (c) Gunanathan, C.; Milstein, D. *Top. Organomet. Chem.* **2011**, *37*, 55-84.
- (2) *Synthesis and Application of Isotopically Labeled Compounds* Pleiss, U.; Voges, R. (Eds) Vol. 7 Wiley: New York, 2001.
- (3) Maegawa, T.; Fujiwara, Y.; Inagaki, Y.; Monguchi, Y.; Sajiki, H. *Adv. Synth. Catal.* **2008**, *350*, 2215-2218.
- (4) Tse, S. K. S.; Xue, P.; Lau, C. W. S.; Sung, H. H. Y.; Williams, I. D.; Jia, G. *Chem. Eur. J.* **2011**, *17*, 13918-13925.
- (5) Chatterjee, B.; Gunanathan, C. *Org. Lett.* **2015**, *17*, 4794-4797.
- (6) Thirumurugan, P.; Matosiuk, D.; Jozwiak, K. *Chem. Rev.* **2013**, *113*, 4905-4979.
- (7) Cintrat, J. C.; Pillion, F.; Rousseau, B. *Tetrahedron Lett.* **2001**, *42*, 5001-5003.
- (8) Hashmi, A. S. K.; Rudolph, M.; Siehl, H. -U.; Tanaka, M.; Bats, J. W.; Frey, W. *Chem. Eur. J.* **2008**, *14*, 3703-3708.
- (9) Chatterjee, B.; Gunanathan, C. *Chem. Commun.* **2016**, *52*, 4509-4512.
- (10) (a) Smart, K. A.; Mothes-Martin, E.; Annaka, T.; Grellier, M.; Sabo-Etienne, S. *Adv. Synth. Catal.* **2014**, *356*, 759-764. (b) Campos, J.; Esqueda, A. C.; Lo'pez-Serrano, J.; Sa'nchez, L.; Cossio, F. P.; Cozar, A. D.; A'lvarez, E.; Maya, C.; Carmona, E. *J. Am. Chem. Soc.* **2010**, *132*, 16765-16767.

- (11) Gore, S.; Baskaran, S.; Konig, B. *Org. Lett.* **2012**, 4568-4571.
- (12) Imperato, G.; Eibler, E.; Niedermeier, J.; Konig, B. *Chem. Commun.* **2005**, 1170-1172.
- (13) Guan, A.; Liu, C.; Yang, X.; Dekeyser, M. *Chem. Rev.* **2014**, *114*, 7079-7107.
- (14) Le, H. V.; Ganem, B. *Org. Lett.* **2011**, *13*, 2584-2585.
- (15) Díaz, D. J.; Darko, A. K.; McElwee-White, L. *Eur. J. Org. Chem.* **2007**, 4453-4465.
- (16) Flegeau, E. F.; Bruneau, C.; Dixneuf, P. H. Jutand, A. *J. Am. Chem. Soc.* **2011**, *133*, 10161-10170. (b) Mirtschin, S.; Slabon-Turski, A.; Scopelliti, R.; Velders, A. H.; Severin, K. *J. Am. Chem. Soc.* **2010**, *132*, 14004-14005. (c) Smith, G. S.; Therrien, B.; *Dalton Trans.* **2011**, *40*, 10793-10800. (d) Farrer, N. J.; Sadler, P. J. in *Bioinorganic Medicinal Chemistry*, ed. Alessio, E. Wiley-VCH, 2011, vol. 1, pp. 1-47.
- (17) Arockiam, P. B.; Bruneau, C.; Dixneuf, P. H. *Chem. Rev.* **2012**, *112*, 5879-5918.
- (18) *Hydrosilylation: A Comprehensive Review on Recent Advances*, (Ed.: B. Marciniak), Springer, Heidelberg, 2009.
- (19) *The Chemistry of Organic Silicon Compounds, Vol. 3* (Eds.: Z. Rappoport, Y. Apeloig) Wiley, New York, 2001.
- (20) Chatterjee, B.; Gunanathan, C. *Chem. Commun.* **2014**, *50*, 888-890.
- (21) *Boronic Acids. Preparation and Applications in Organic Synthesis and Medicine*; Hall, D. G., Ed.; 2nd ed.; Wiley-VCH: Weinheim, 2011.
- (22) Lennox, A. J.; Lloyd-Jones, G. C. *Chem. Soc. Rev.* **2014**, *43*, 412-443.
- (23) Kaithal, A.; Chatterjee, B.; Gunanathan, C. *Org. Lett.* **2015**, *17*, 4790-4793.
- (24) Kumar, P. P.; Stotz, S. C.; Paramashivappa, R.; Beedle, A. M.; Zamponi, G. W.; Rao, A. S. *Mol. Pharm.* **2002**, *3*, 649-658.

- (25) Pollak, N.; Dölle, C.; Ziegler, M. *Biochem. J.* **2007**, *402*, 205-218.
- (25) Ouellet, S. G.; Walji, A. M.; Macmillan, D. W. C. *Acc. Chem. Res.* **2007**, *40*, 1327-1339.
- (26) F. Glorius, *Org. Biomol. Chem.*, 2005, *3*, 4171-4175.
- (27) Oshima, K.; Ohmura, T.; Suginome, M. *J. Am. Chem. Soc.* **2012**, *134*, 3699-3702.
- (28) Dudnik, A. S.; Weidner, V. L.; Motta, A.; Delferro, M.; Marks, T. J. *Nat. Chem.* **2014**, *6*, 1100-1107.
- (29) Fan, X.; Zheng, J.; Li, Z. H.; Wang, H. *J. Am. Chem. Soc.* **2015**, *137*, 4916-4919.
- (30) Kaithal, A.; Chatterjee, B.; Gunanathan, C. *Org. Lett.* **2016**, **2016**, *18*, 3402-3405.
- (31) Rees, W. S.; *CVD of Nonmetals*, VCH, New York, 1996.
- (32) Pascu, M.; Ruggi, A.; Scopelliti, R.; Severin, K. *Chem. Commun.* **2013**, *49*, 45-47.
- (33) Masaoka, S.; Banno, T.; Ishikawa, M. *J. Organomet. Chem.* **2006**, *691*, 174-181.
- (34) Marciniak, B.; Walkowiak, J. *Chem. Commun.* **2008**, 2695-2697.
- (35) Ito, M.; Itazaki, M.; Nakazawa, H. *J. Am. Chem. Soc.* **2014**, *136*, 6183-6186.
- (36) *Synthesis and Application of Isotopically Labeled Compounds*; Pleiss, U., Voges, R., Eds.; Wiley: New York, 2001; Vol. 7.
- (37) Meanwell, N. A. *J. Med. Chem.* **2011**, *54*, 2529-2591.
- (38) Choi, J.; MacArthur, A. H. R.; Brookhart, M.; Goldman, A. S. *Chem. Rev.* **2011**, *111*, 1761-1779.
- (39) Pieters, G.; Taglang, C.; Bonnefille, E.; Gutmann, T.; Puente, C.; Berthet, J. -C.; Dugave, C.; Chaudret, B.; Rousseau, B. *Angew. Chem., Int. Ed.* **2014**, *53*, 230-234.

(40) Azrodt, J.; Derdau, V.; Fey, T.; Zimmermann, J. *Angew. Chem., Int. Ed.* **2007**, *46*, 7744-7765.

	List of Schemes	Page No
1	Scheme 1.1 Different Modes of MLC	35
2	Scheme 1.2 Hydrogenolysis of Esters Catalyzed by Ru-macho	36
3	Scheme 1.3 Hydrogenation of Fluorinated Esters Catalyzed by 4	37
4	Scheme 1.4 Schematic pathway for Methanol Reforming	38
5	Scheme 2.1 Selective α -Deuteration of Aryl Methanols Catalyzed by Ru-macho	43
6	Scheme 2.2 Synthesis and Reactivities of Intermediates	48
7	Scheme 2.3 Dehydrogenation of 2-Norbornanemethanol by 1	49
8	Scheme 2.4 Proposed Catalytic Cycle	50
9	Scheme 3.1 Scope of the Ru-Catalyzed Deuteration of Aryl Terminal Alkynes Using D ₂ O	69
10	Scheme 3.2 Scope of the Ruthenium-Catalyzed Synthesis of <i>mono</i> -Deuterated Terminal Aliphatic Alkynes Using D ₂ O	71
11	Scheme 3.3 Selective Catalytic Synthesis of Eudatin-d1	74
12	Scheme 3.4 Reactions of Terminal Alkynes with Ru-Complex 1	76
13	Scheme 3.5 Proposed Mechanism for the Synthesis of <i>mono</i> -Deuterated Terminal Alkynes	78
14	Scheme 4.1 N-H activation by "Amine-Amide" MLC	102
15	Scheme 4.2 Synthesis of Arylmethyl and Arylalkyl Urea Derivatives	104
16	Scheme 4.3 Synthesis of <i>N,N'</i> -Dialkyl Urea Derivatives	105
17	Scheme 4.4 Catalytic Synthesis of <i>N</i> -Benzylformamide	106

18	Scheme 4.5 Synthesis of Unsymmetrical Urea Derivatives	106
19	Scheme 4.6 Proposed Mechanism	108
20	Scheme 5.1 Half-Sandwich Complexes of Ruthenium	132
21	Scheme 5.2 Preparation of the Ruthenium Allenylidene Complexes	134
22	Scheme 5.3 RCM Using Ru-Allenylidene Catalysts	134
23	Scheme 5.4 Hydrosilylation of Alkenes by a Ruthenium Silylene Complex	135
24	Scheme 6.1 Chemoselective Hydrosilylation of Aldehydes Catalyzed by $[\text{Ru}(p\text{-cymene})\text{Cl}_2]_2$	144
25	Scheme 6.2 Synthesis and X-ray Structure of 3	147
26	Scheme 6.3 Synthesis of Complex $[(\eta^6\text{-}p\text{-cymene})\text{Ru}(\text{H})_2$ $(\text{SiEt}_3)_2](\mathbf{3})$ from 1 or 2	147
27	Scheme 6.4 Proposed Mechanism for Hydrosilylation	149
28	Scheme 7.1 Hydroboration of Aldehydes Catalyzed by 1	178
29	Scheme 7.2 Hydroboration of Ketones Catalyzed by 1	179
30	Scheme 7.3 Chemoselective Hydroboration of Aldehydes Catalyzed by $[\text{Ru}(p\text{-cymene})\text{Cl}_2]_2$	180
31	Scheme 7.4 Reaction of $[\text{Ru}(p\text{-cymene})\text{Cl}_2]_2$ 1 with Pinacolborane: Preparation of Intermediate 1b	182
32	Scheme 7.5 Catalytic Hydroboration by an Isolated Intermediate 1b $[\{(\eta^6\text{-}p\text{-cymene})\text{RuCl}\}_2(\mu\text{-H}-\mu\text{-Cl})]$	183
33	Scheme 7.6 Plausible Mechanism for the Hydroboration of Carbonyl Compounds	184
34	Scheme 8.1 1,4-Dihydropyridines: Applications, Role in Nature and Recent Advances in Synthesis	199

35	Scheme 8.2 Preparation of Intermediates	202
36	Scheme 8.3 Ruthenium Catalyzed Regioselective 1,4-Hydroboration of Pyridines	204
37	Scheme 8.4 Stoichiometric Experiments, <i>in situ</i> Observation of Intermediates and Reaction Progress	205
38	Scheme 8.5 Proposed Reaction Mechanism for the Regioselective 1,4-Hydroboration of Pyridines	208
39	Scheme 9.1 Recent Advances in the Synthesis of Borasiloxanes	232
40	Scheme 9.2 Synthesis of Borasiloxanes	235
41	Scheme 9.3 Ru-Catalyzed Synthesis of (Diboryl)siloxanes and (Disilyl)boroxanes	236
42	Scheme 9.4 Synthesis of Borasiloxanes Using Boric Acid	237
43	Scheme 9.5 Mechanistic Studies	240
44	Scheme 9.5 Proposed Mechanism for the Formation of Borasiloxanes	241
45	Scheme 10.1 Catalytic Deuteration of Pharmaceuticals	270
46	Scheme 10.2 Proposed Mechanism for α -Selective Deuteration of Amines and Amino Acids	272

List of Figures

Page No

1	Figure 2.1 ^1H NMR Monitoring of % D Incorporation	45
2	Figure 2.2 Selective α -Deuteration of Diols	46
3	Figure 2.3-2.17 NMR Spectra of Deuterated Alcohols	58
4	Figure 3.1 Representative Natural Products, Drugs and Bioactive Molecules Containing Terminal Alkyne Functionality	74
5	Figure 3.2 Stacked ^{31}P NMR Spectrum of Reaction Mixture	77
6	Figure 3.3-3.11 NMR Spectra of Deuterated Terminal Alkynes	94

7	Figure 4.1 Biologically Active Urea Derivatives	101
8	Figure 4.2 Single Crystal X-ray Structure of 3b	102
9	Figure 4.3-4.8 NMR Spectra of Urea Derivatives	128
10	Figure 6.1 NMR Monitoring of the Reaction Progress	145
11	Figure 6.2 NMR Study of the Reaction Progress Shows Formation of Hydride Peaks at Different Time (min) Interval	146
12	Figure 6.3 X-ray Structure of 3	148
13	Figure 6.4-6.17 NMR Spectra of Silyl Ethers and Complexes	169
14	Figure 7.1 ORTEP Diagram of 2-(2,2-diphenylethyl)-4,4,5,5- tetramethyl-1,3,2- dioxaborolane	179
15	Figure 7.2 ¹ H NMR Monitoring of Reaction Progress	181
16	Figure 7.3-7.9 NMR Spectra of Products and Reaction Mixture	193
17	Figure 8.1 NMR Monitoring of the Reaction Progress	207
18	Figure 8.2 Determination of the Rate Equation	223
19	Figure 8.3-8.8 NMR Spectra of the Isolated Compounds	228
20	Figure 9.1 ¹ H NMR Spectrum of Labeling Experiment with D ₂ O	253
21	Figure 9.2-9.3 Mass Spectrum of Intermediates	256
22	Figure 9.4-9.9 NMR Spectra of Borasiloxanes	260
23	Figure 10.1 X-ray Structure of [$\{\eta^6\text{-}p\text{-cymene}\}\text{RuHCl}\}\{\text{NHCH}_2\text{Ph}\}$ (NH ₂ CH ₂ Ph)]Cl	271
24	Figure 10.2 ORTEP Structure of Complex 2 in Unit Cell	283
25	Figure 10.3-10.9 NMR Spectra of Deuterated Amines	289

List of Tables

Page No

1	Table 2.1 Selective α -Deuteration of Linear Alcohols	44
2	Table 2.2 Selective α,β -Deuteration of Secondary Alcohols	46

3	Table 3.1 Optimization of Aryl Terminal Alkyne Deuteration	68
4	Table 3.2 Optimization of Aliphatic Terminal Alkyne Deuteration	70
5	Table 3.3 Substrate Scope for Chemoselective Deuteration	72
6	Table 4.1 Optimization of Reaction Conditions	103
7	Table 6.1 Screening of Ruthenium Catalysts	140
8	Table 6.2 Optimization of Reaction Conditions with 1	141
9	Table 6.3 Optimization of Silanes	141
10	Table 6.4 Hydrosilylation of Aldehydes by 1	142
11	Table 8.1 Optimization of Reaction Condition Using [Ru(<i>p</i> -cymene)Cl] ₂ Cl ₂ as a Catalyst	200
12	Table 8.2 Optimization of Experimental Conditions for 1,4- Hydroboration of Pyridine	201
13	Table 9.1 Screening of Catalysts and Reaction Conditions for the Selective Synthesis of Borasiloxanes	234
14	Table 10.1 Selective α -Deuteration of Primary Amines	266
15	Table 10.2 Selective α -Deuteration of Secondary Amines	267
16	Table 10.3 Selective α -Deuteration of Amino Acids	269

List of Abbreviations Used

Å	Angstrom
Anal.	Analytically
Anhyd	Anhydrous
aq	Aqueous
bp	Boiling Point
br	Broad
°C	Degree Celcius
Calcd	Calculated
cm	Centimeter
Conc	Concentrated
conv	Conversion
d	Doublet, Days
DCM	Dichloromethane
dd	Doublet of a Doublet
DMF	<i>N,N</i> -Dimethyl Formamide
eq	Equation
equiv	Equivalent
Et	Ethyl
g	Grams
h	Hours
HRMS	High-resolution Mass Spectrometry
IR	Infrared
K	Kelvin
kcal	Kilo calories
lit	Liter
m	Multiplet
M	Molar
MeCN	Acetonitrile
mp	Melting point
Me	Methyl
MHz	Mega Hertz
Min	Minutes

mL	Milliliter
mM	Millimolar
mmol	Millimole
mol	Mole
MS	Mass Spectra
N	Normal
NMR	Nuclear Magnetic Resonance
ppm	Parts per Million
rt	Room Temperature
s	Singlet, Seconds
TLC	Thin Layer Chromatography
TOF	Turn Over Frequency
TON	Turn Over Number
XRD	X-Ray Diffraction
NaOMe	Sodium methoxide
RCM	Ring Closing Metathesis

Table of Contents

Synopsis	Catalytic Transformations Based on Pincer and Half-Sandwich Ruthenium Complexes	iX
List of Schemes		XXiii
List of Figures		XXV
List of Tables		XXVi
Chapter 1	Ruthenium Pincer Complexes and their Reactivity	33
Chapter 2	Ruthenium-Catalyzed Selective α- and α,β-Deuteration of Alcohols Using D₂O	40
	2.1 Abstract	40
	2.2 Introduction	40
	2.3 Results and Discussions	42
	2.4 Conclusions	51
	2.5 Experimental Section	51

2.6 Notes and References	55
¹ H and ¹³ C NMR spectra	58
Chapter 3 The Ruthenium-Catalyzed Selective Synthesis of <i>mono-</i>	
Deuterated Terminal Alkynes	66
3.1 Abstract	66
3.2 Introduction	66
3.3 Results and Discussions	67
3.4 Conclusions	78
3.5 Experimental Section	79
3.6 Notes and References	91
¹ H and ¹³ C NMR spectra	94
Chapter 4 Ruthenium-Catalyzed Urea Synthesis by N–H Activation	
of Amines	99
4.1 Abstract	99
4.2 Introduction	99
4.3 Results and Discussions	101
4.4 Conclusions	108
4.5 Experimental Section	109
4.6 Notes and References	123
¹ H and ¹³ C NMR spectra	128
Chapter 5 Half-Sandwich Ruthenium Complexes and their Reactivity	131
Chapter 6 Ruthenium-Catalyzed Selective Hydrosilylation of Aldehydes	138
6.1 Abstract	138
6.2 Introduction	138
6.3 Results and Discussions	139

6.4	Conclusions	149
6.5	Experimental Section	150
6.6	Notes and References	163
	¹ H and ¹³ C NMR spectra	169
Chapter 7 Ruthenium-Catalyzed Selective Hydroboration of Carbonyl		
	Compounds	176
7.1	Abstract	176
7.2	Introduction	176
7.3	Results and Discussions	177
7.4	Conclusions	184
7.5	Experimental Section	185
7.6	Notes and References	188
	¹ H and ¹³ C NMR spectra	193
Chapter 8 Ruthenium-Catalyzed Regioselective 1,4-Hydroboration		
	of Pyridines	197
8.1	Abstract	197
8.2	Introduction	197
8.3	Results and Discussions	199
8.4	Conclusions	208
8.5	Experimental Section	209
8.6	Notes and References	224
	¹ H and ¹³ C NMR spectra	228
Chapter 9 Ruthenium-Catalyzed Selective Synthesis of Borasiloxanes		
9.1	Abstract	231
9.2	Introduction	231

9.3 Results and Discussions	233
9.4 Conclusions	241
9.5 Experimental Section	242
9.6 Notes and References	257
¹ H and ¹³ C NMR spectra	260
Chapter 10 Ruthenium-Catalyzed Selective α-Deuteration of Amines and	
 Amino Acids Using Deuterium Oxide	263
10.1 Abstract	263
10.2 Introduction	263
10.3 Results and Discussions	265
10.4 Conclusions	272
10.5 Experimental Section	273
10.6 Notes and References	283
¹ H and ¹³ C NMR spectra	289
Summary	292

Part A

Catalysis Based on Ruthenium Pincer Complexes

CHAPTER 1

Ruthenium Pincer Complexes and their Reactivity

Activation of small molecules is of utmost importance, as it leads to the successful design of a catalytic cycle and can provide greener approach to the synthetic processes. Usually ligands are employed to stabilize transition metals via coordination, thus enhancing their ability to sustain in solution also at elevated temperature. In recent years ligands are designed to participate actively in the catalytic cycle by stabilizing the metal center and their unusual oxidation states, referred as non-innocent ligands. “Pincer complexes” are the coordination complexes of tridentate “pincer ligands” that enforces meridional geometry at the metal center upon complexation.¹ Pincer ligands coordinated to the transition metals are able to show diverse reactivity by metal-ligand cooperation, particularly in activation of unreactive bonds and small molecules, hence unraveling a wide scope of new catalytic processes and their successful utilization towards synthetic chemistry. The planar framework along with the bulky substituents covers much of the coordination sphere around the metal center, thus offers control over other coordination sites and enhances stability of the resulting complexes. The rational design of ligands with fine modification of stereo-electronic properties of the anchoring sites can generate an excellent catalyst. In the mid 1970s the pioneering reports by Bernerd Shaw disclosed the chemistry of pincer complexes.² The exciting development of these complexes as highly efficient

catalysts has occurred in the last two decades, particularly in activation of unreactive bonds and small molecules.^{1,3}

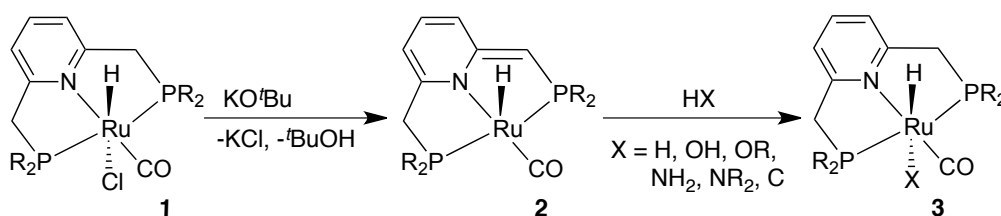
The unusual catalytic efficiency showed by pincer complexes are mainly emanated from the metal-ligand cooperation (MLC).¹ Hydrogenase, a metalloenzyme, can exhibit chemical transformations based on MLC, is also attributable as bifunctional catalysis.⁴ Similarly, hemoglobin (Hb) also capable of exhibiting a different mode of metal-ligand cooperation, which stimulate in change of spin state for the coordinated iron center and enhances the affinity of Hb towards oxygen.⁵ In recent years, the active participation of a ligand in a catalytic cycle by helping metal to change the coordination mode without changing the formal oxidation state, generated superior mode of catalysis and uncovered interesting chemical transformations.¹ The metal-ligand cooperation based on aromatization and dearomatization is described in Scheme 1.1a. Typically, a pyridine based pincer complexes of type **1** undergo deprotonation at the pyridinyl-methylene carbon to result in dearomatization of the pyridine ring. The dearomatized five-coordinated pincer complexes of type **2** then react stoichiometrically with various small molecules and unreactive bonds (H-X; X = H, C, OH, OR, NH₂, NR₂) and heterolytically cleave them, in which the proton is accepted by the basic “methine carbon” and the X-fragments (X-type ligands) occupy the vacant coordination site on the ruthenium center and generates rearomatized, coordinatively saturated pincer complexes of type **3** (Scheme 1.1a).

MLC can also be operative in the metal complexes embedded with tridentate aliphatic backbone, containing coordinated amine moiety. In presence of base the complexes of type **4** undergo deprotonation and generate unsaturated and reactive intermediates of type **5**. Like the unsaturated complexes of type **2** (Scheme 1.1a) the deprotonated five

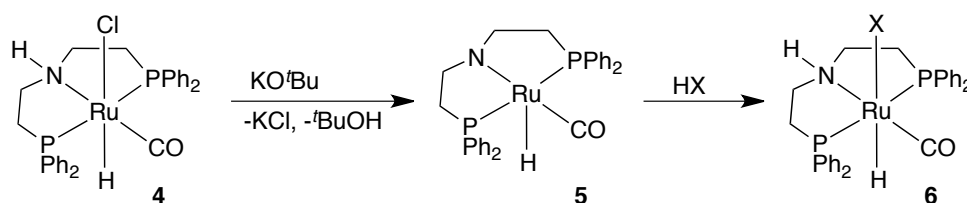
coordinated complexes of type **5** can react with various small molecules and unreactive bonds (H–X) to cleave them heterolytically in which the proton is accepted by the basic nitrogen (amide type) atom of the ligand backbone and the X-fragments (X-type ligands) occupy the vacant coordination site on the ruthenium center and generate protonated, coordinatively saturated pincer complexes of type **6** (Scheme 1.1b).¹

Scheme 1.1 Different Modes of MLC (a) MLC Based on Aromatization-De aromatization (b) MLC Based on Amine-Amide

a)



b)

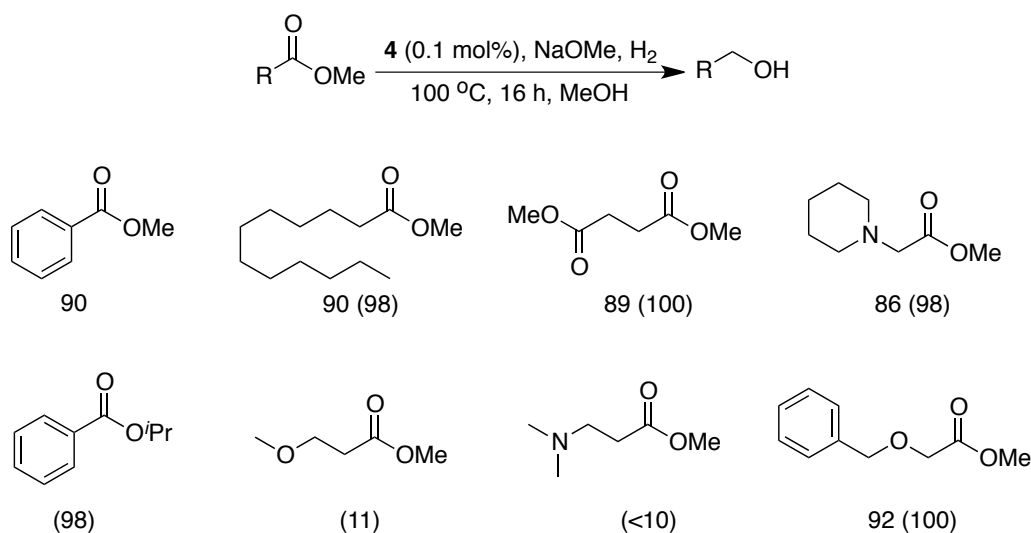


The MLC operative by “amine-amide” pathway is comparatively less explored and ample scope exists to develop this chemistry. Thus our present studies described in **PART A** will explore this topic.

Recently, Saito and coworkers disclosed the hydrogenation of esters to alcohols catalyzed by complex **4**. The reactions were performed using methanol as solvent under pressurized H_2 (50 bar) atmosphere.⁶ An assortment of esters were reduced with good conversion and selectivity in the presence of NaOMe . Aromatic and alkanolic acid methyl esters were effectively reduced. The reduction of diesters was also performed to obtain the diols in good yields. Oxygen and nitrogen embedded functional groups at the α -position of ester groups did not impact the activity of the

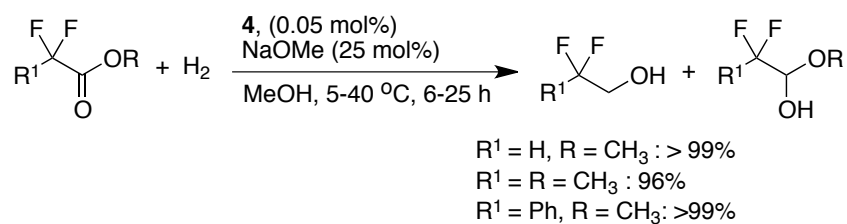
catalyst. However, substrates containing heteroatom at β -position gave low yield with decomposition of substrates. *iso*-Propyl and *tert*-butyl phenyl esters also gave the corresponding alcohols in good yields (Scheme 1.2).

Scheme 1.2: Hydrogenolysis of Esters Catalyzed by Ru-macho (**4**)



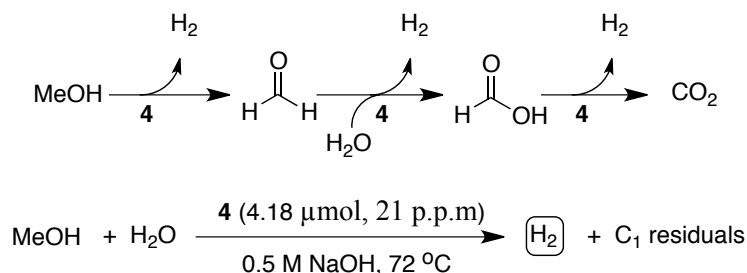
Later, Ikariya and coworkers revealed practical and selective hydrogenation of α -fluorinated esters catalyzed by pincer complex, $\text{RuHCl}(\text{CO})(\text{dpa})$ **4** (dpa = bis-(2-diphenylphosphinoethyl)amine) under mild conditions.⁷ The method is highly beneficial for its application to synthesize fluorinated alcohols and fluoral hemiacetal intermediates from fluorinated esters. This report disclosed efficient hydrogenation of several α -fluorinated esters to the corresponding fluorinated alcohol by employing complex **4** as catalyst. Aliphatic and aromatic difluoro esters were hydrogenated with excellent conversion and selectivity (Scheme 1.3).

Scheme 1.3: Hydrogenation of Fluorinated Esters Catalyzed by Complex **4**



Production of hydrogen from renewable resources is possible source of energy. The implementation of “Hydrogen economy” is important as it leads to the greener approach to the existing energy problem. Unfortunately, handling and storage of hydrogen is troublesome. However, this difficulty can be resolved by using methanol as a hydrogen storage material, provided efficient catalytic protocol available to reform methanol. Recently, Beller and workers disclosed an interesting example of an efficient low temperature aqueous-phase methanol dehydrogenation process⁸ (methanol reforming) catalyzed by complex **4**. The first dehydrogenation step of methanol results in formaldehyde. The subsequent conversion to formate and hydrogen occurs rapidly under alkaline aqueous conditions. Further dehydrogenation of formate leads to the generation of one molecule of hydrogen and carbon dioxide. Compared to previously known heterogeneous systems, this method liberates less amounts of contaminant gases CO and CH₄ (10 ppm). The well-defined complex **4** displayed very high activities up to 4,700 h⁻¹ (TOF) and catalyst productivities of >350,000 (TON) in methanol reforming reaction to provide overall three molecule of H₂ and one molecule of CO₂ from one MeOH molecule, base and water (Scheme 1.4).

Scheme 1.4: Schematic Pathway for a Homogeneously Catalyzed Methanol Reforming



NOTES AND REFERENCES

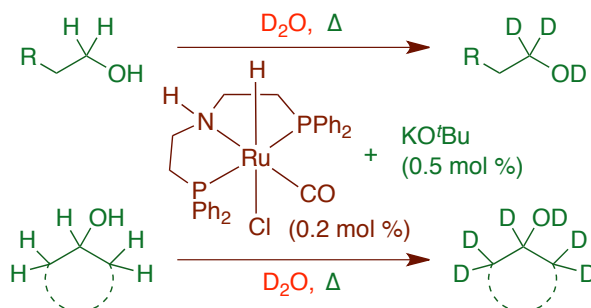
- (1) (a) Gunanathan, C.; Milstein, D. *Acc. Chem. Res.* **2011**, *44*, 588-602. (b) Gunanathan, C.; Milstein, D. *Top. Organomet. Chem.* **2011**, *37*, 55-84. (c) Gunanathan, C.; Milstein, D. *Chem. Rev.* **2014**, *114*, 12024-12087.
- (2) (a) Moulton, C. J.; Shaw, B. L. *J. Chem. Soc., Dalton Trans.* **1976**, 1020-1024. (b) Empsall, H. D.; Hyde, E. M.; Markham, R.; McDonald, W. S.; Norton, M. C.; Shaw, B. L.; Weeks, B. *J. Chem. Soc., Chem. Commun.* **1977**, 589-590. (c) Crocker, C.; Errington, R. J.; Markham, R.; Moulton, C. J.; Odell, K. J.; Shaw, B. L. *J. Am. Chem. Soc.* **1980**, *102*, 4373-4379. (d) Crocker, C.; Errington, R. J.; Markham, R.; Moulton, C. J.; Shaw, B. L. *J. Chem. Soc., Dalton Trans.* **1982**, 387-395. (e) Crocker, C.; Empsall, H. D.; Errington, R. J.; Hyde, E. M.; McDonald, W. S.; Markham, R.; Norton, M. C.; Shaw, B. L.; Weeks, B. *J. Chem. Soc., Dalton Trans.* **1982**, 1217-1224. (f) Briggs, J. R.; Constable, A. G.; McDonald, W. S.; Shaw, B. L. *J. Chem. Soc., Dalton Trans.* **1982**, 1225-1230. (g) Errington, R. J.; McDonald, W. S.; Shaw, B. L. *J. Chem. Soc., Dalton Trans.* **1982**, 1829-1835.
- (3) (a) Albrecht, M.; van Koten, G. *Angew. Chem., Int. Ed.* **2001**, *40*, 3750-3781. (b) Vigalock, A.; Milstein, D. *Acc. Chem. Res.* **2001**, *34*, 798-807. (c) van der Boom, M. E.; Milstein, D. *Chem. Rev.* **2003**, *103*, 1759-1792.

- (4) (a) Evans, D. J.; Pickett, C. J. *Chem. Soc. Rev.* **2003**, *32*, 268-275. (b) Whittaker, J. W. *Arch. Biochem. Biophys.* **2005**, *433*, 227-239. (c) Peters, J. W.; Lanzilotta, W. N.; Lemon, B. J.; Seefeldt, L. C. *Science* **1998**, *282*, 1853-1858. (d) Bifunctional Molecular Catalysis; Ikariya, T., Shibasaki, M., Eds.; Springer-Verlag: Heidelberg, 2011.
- (5) Chou, K.C. *trends Biochem. Sci.* **1989**, *14*, 212-213.
- (6) (a) Kuriyama, W.; Matsumoto, T.; Ogata, O.; Ino, Y.; Aoki, K.; Tanaka, S.; Ishida, K.; Kobayashi, T.; Sayo, N.; Saito, T. *Org. Process Res. Dev.* **2012**, *16*, 166-171. (b) Kuriyama, W.; Matsumoto, T.; Ino, Y.; Ogata, O. Patent WO2011048727A1, Takasago International Corp., Japan, 2011.
- (7) Otsuka, T.; Ishii, A.; Dub, P. A.; Ikariya, T. *J. Am. Chem. Soc.* **2013**, *135*, 9600-9603.
- (8) Nielsen, M.; Alberico, E.; Baumann, W.; Drexler, H, J.; Junge, H.; Gladiali, S.; Beller, M. *Nature* **2013**, *495*, 85-90.

CHAPTER 2

Ruthenium Catalyzed Selective α - and α,β -Deuteration of Alcohols Using D_2O

2.1 ABSTRACT



Highly selective ruthenium catalyzed α -deuteration of primary alcohols and α,β -deuteration of secondary alcohols are achieved using deuterium oxide (D_2O) as a source of deuterium and reaction solvent. Minimal loading of catalyst (*Ru-macho*), base (*KO^tBu*), and low temperature heating provided efficient selective deuteration of alcohols making the process practically attractive and environmentally benign. Mechanistic studies indicate the $D-O(D/R)$ bond activations by metal–ligand cooperation and intermediacy of carbonyl compounds resulting from dehydrogenation of alcohols.

2.2 INTRODUCTION

Synthesis of deuterium labeled alcohols with high percentage of deuteration and selectivity is an important transformation in organic synthesis as deuterated pharmaceuticals and bioactive organic molecules play a vital role in the metabolism of alcohols and enzymes, in addition to the regular use as NMR solvents and also as reliable chemical probes.¹ All the deuterium atoms present in the commercially available or synthesized chemicals are either directly or indirectly derived from

deuterium oxide. Selectively deuterated alcohols are currently synthesized from elongated multistep procedures using reductive reagents such as NaBD₄, LiAlD₄ and SiDMe₂Ph/F⁻ from aldehyde or carbonyl derivatives of alcohols, which result in enormous hazardous waste and the cost of the deuterated alcohols becomes prohibitively high.² Thus, direct synthesis of selectively deuterated alcohols from H/D exchange reactions with cheap deuterium oxide is highly attractive. Selective efficient deuteration and activation of CH bonds under mild reaction conditions is a tantalizing task.³⁻⁵ Iridium,³ and molybdenum⁴ based catalytic systems were reported and they required higher loading of catalyst (5 mol %). While iridium catalyzed deuteration of alcohols required expensive benzene-d₆ as a deuterium source (reaction solvent), molybdenum based catalyst is effective for only benzylic protons of alcohols.⁴ Both homogeneous and heterogeneous ruthenium catalysts received great attention for the H/D exchange reaction of alcohols.⁵ Ru on carbon support is reported to catalyze selective deuteration of the protons at the α -position of alcohols with the catalyst loading of 20% of Ru (relative to the substrate) and under the atmosphere of hydrogen.^{5d} Ruthenium and osmium pincer complexes catalyzed the selective deuteration of alcohols using 2-propanol-d₈ as the deuterium source.^{5b} Under the microwave irradiation a ruthenium based soluble catalyst provided selective deuteration of alcohols with 5% catalyst load.^{5e} Exclusive deuteration at the β -positions also occurred with 3 mol % of aminoalcohol ligated *in situ*-generated ruthenium catalyst.^{5f}

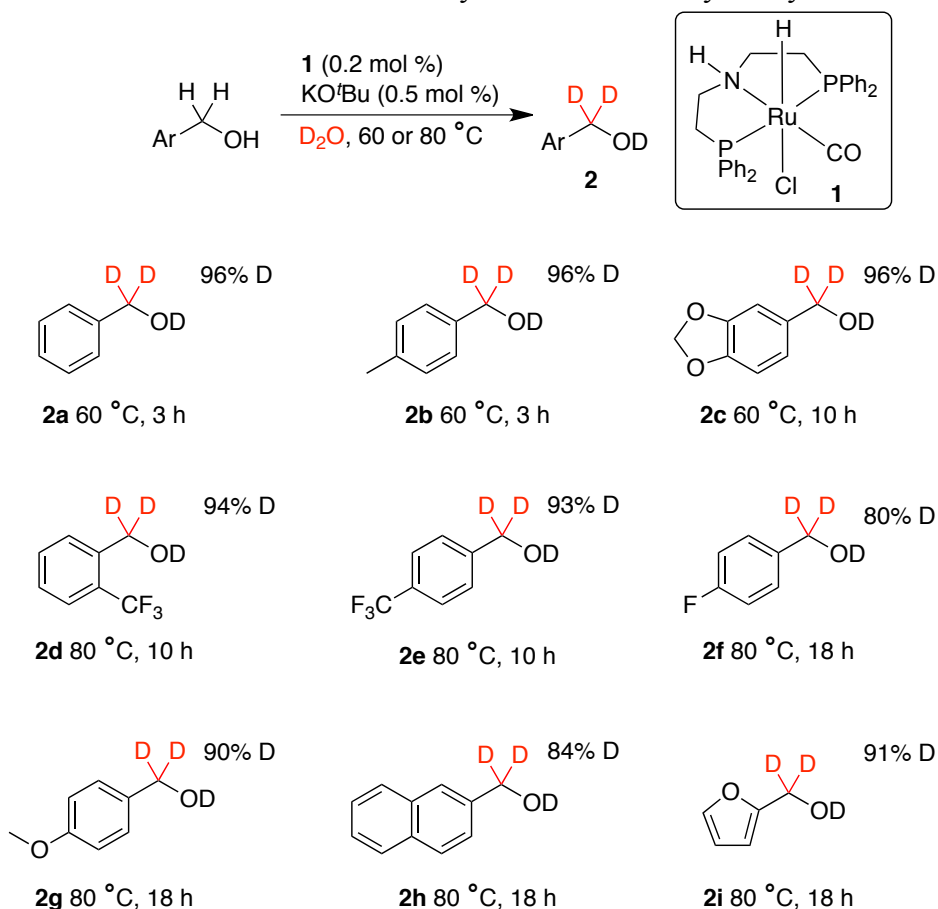
Very recently, Milstein reported an interesting selective deuteration of alcohols catalyzed by bipyridine derived PNN (6-di-*tert*-butylphosphinomethyl-2,2'-bipyridine) ruthenium pincer complex,^{3a} which exhibited remarkable reactivity as a result of metal-ligand cooperation.⁶ However, in general ruthenium catalyzed

deuteration of alcohols required high temperature-refluxing deuterium oxide conditions (120-150 °C), and higher loading of base (15 to 20 mol % relative to substrate). Except Milstein system all other ruthenium catalyzed H/D exchange reaction also require higher loading of catalyst (1-20 mol %).⁵ Ru-macho catalyst, which exhibits amine-amide metal-ligand cooperation, is reported to catalyze a wide range of organic transformations including dehydrogenation of methanol under aqueous basic conditions.⁷ Inspired by these reports, we set to explore the H/D exchange of alcohols using Ru-macho catalyst. Thus, in this chapter we demonstrate the facile and highly efficient selective α -deuteration of primary alcohols, and selective α,β -deuteration of secondary alcohols catalyzed by Ru-macho using deuterium oxide.

2.3 RESULTS AND DISCUSSIONS

At the outset deuteration of aryl methyl alcohols (**2a-2i**) was tested (Scheme 2.1). When benzyl alcohol (0.5 mmol) was reacted with Ru-macho catalyst (0.2 mol %) with KO^tBu (0.5 mol %) in deuterium oxide, a facile and highly selective α -deuteration is observed at 60 °C. While 96% deuteration occurred at the α -position to provide benzyl alcohol-d₃ in only 3 h, no detectable H/D exchange is observed with aryl protons.⁸ Under similar experimental conditions catalyst **1** selectively deuterated the α -CH₂ protons of other benzyl alcohols such as 4-methylbenzyl alcohol and piperonyl alcohol (Scheme 2.1). Other aryl methanols and heteroaryl methanols required heating the reaction mixture at 80 °C for a prolonged period. Percentage of deuterium also largely depends on the substrate; the reaction conditions may be further optimized for the individual alcohols to obtain higher deuteration. Upon completion of the reaction, the α -deuterated alcohols were easily separated from the reaction mixture by extraction with dichloromethane.

Scheme 2.1 Selective α -Deuteration of Aryl Methanols Catalyzed by Ru-macho **1**^a

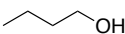
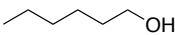
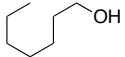
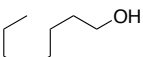
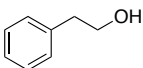
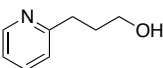
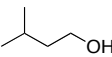
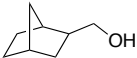


^aConditions: Alcohol (0.5 mmol), catalyst **1** (0.001 mmol), KO^tBu (0.0025 mmol) and D₂O (0.4 mL, 20 mmol) were charged in a screw cap NMR tube under nitrogen atmosphere and the reaction mixture heated at the indicated temperature. The Percentage of deuterium incorporation was monitored by integration of residual signals of ¹H NMR spectroscopy. Maximum possible % deuteration for these aryl methanols is 96.4%.

Deuteration of linear aliphatic alcohols catalyzed by **1** is investigated and the results are summarized in Table 2.1. In general, aliphatic alcohols, Ru-macho **1** (0.2 mol %) and KO^tBu (0.5 mol %) in deuterium oxide are heated at 80 °C over the period indicated. Linear alcohols such as 1-butanol, 1-hexanol, 1-heptanol and 1-octanol underwent facile deuteration predominantly at the α -position (92 to 94%); however, among these alcohols deuteration at the β -position of alcohols is also observed in the range of 9-12% (Table 2.1, entries 2-5). Progress of the α -deuteration of 1-butanol catalyzed by **1** in D₂O is monitored using ¹H NMR spectroscopy (Figure 2.1a).

However, when ethanol was subjected to the reaction, deuteration occurred non-selectively; 87% and 86% deuteration observed at α and β -positions of ethanol, respectively (Table 2.1, entry 1). Linear alcohols appended with aryl and heteroaryl ring systems provided selectivity for α -deuteration in the range of 90-95% (Table 2.1, entries 6-7), while 10-20% β -deuteration occurred as observed similarly in other linear alcohols. Selective α -deuteration alone also observed for functionalized and sterically hindered alcohols (Table 2.1, entries 8-10).

Table 2.1 Selective α -Deuteration of Linear Alcohols^a

entry	alcohol	time (h)	temp (°C)	α , β (%) deuteration
1 ^b		24	100	87; 86
2		18	80	94; 9
3		12	80	94; 12
4		16	80	92; 12
5		16	80	92.5; 10
6		5	80	90; 10
7		18	80	95; 20
8		20	80	66
9		12	80	95.5; --
10		10	80	95; --

^aConditions: as indicated in the footnote of Scheme 2.1. ^b1,4-dioxane (0.05 mmol) is used as an internal standard

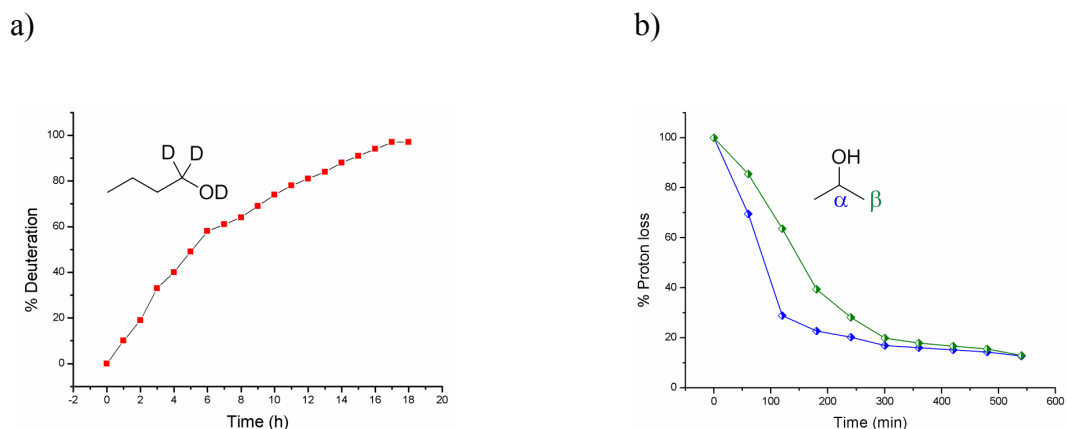


Figure 2.1 ^1H NMR monitoring of % D incorporation: (a) α -position of 1-butanol (0.5 mmol) in D_2O (0.4 mL). Integration of α -position is done taking integration of δ - CH_3 -protons of 1-butanol as a standard. (b) ^1H NMR monitoring of rate of proton loss of 2-propanol at 80°C .

Further to expand the substrate scope, diols (**3a-3d**) were tested in the selective deuteration reaction catalyzed by Ru-macho catalyst **1**. Benzene-1,4-dimethanol and pyridine-2,6-dimethanol were reacted with **1** (0.2 mol %) and KO^tBu (0.5 mol %) and D_2O , which delivered the corresponding (both α -positions) deuterated diols. No detectable deuterium incorporation among aryl proton was observed (Figure 2.2). Surprisingly, when acyclic diols such as 1,4-butanediol, and 1,6-hexanediol were subjected to deuteration under standard conditions, deuteration occurred selectively only at both α -positions to hydroxyl functionality (81%). No deuteration was observed at the β -positions of these substrates (Figure 2.2).

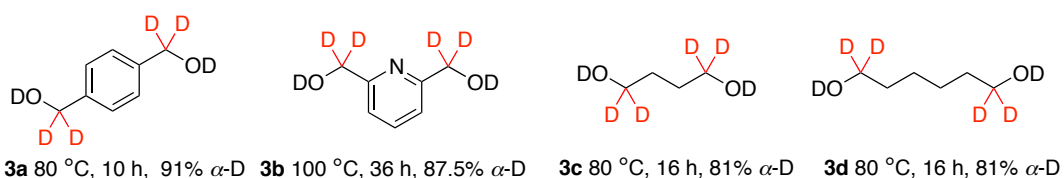
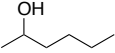
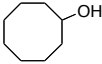
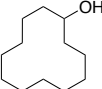


Figure 2.2 Selective α -Deuteration of Diols

Upon reaction with Ru-macho **1** under standard reaction conditions, secondary alcohols underwent efficient deuteration at both α - and β -positions, contrary to the α -selective deuteration observed in primary alcohols. Perhaps the intermediate ketones were more long lived than aldehydes, resulting in the effective β -deuteration by H/D exchange via keto-enol tautomerism and the subsequent hydrogenation providing α,β -deuterated secondary alcohols. 2-Propanol underwent 88% and 87% α,β -deuteration, respectively (maximum possible deuteration is 90.9%, Table 2.2, entry 1). The incorporation of deuterium in the α,β -positions of 2-propanol was unambiguously demonstrated by monitoring the progress of the H/D-exchange reaction (Figure 2.1b). 1-Phenylethanol exhibited both α,β -deuteration in 94% (entry 2). While 2-hexanol showed predominantly selective α -deuteration like linear alcohols, diphenylmethanol provided 97% α -deuteration. Under the standard experimental conditions, cyclic secondary alcohols also afforded the effective α,β -deuteration with excellent selectivity and efficiency (Table 2.2, entries 5-7).

Table 2.2 Selective α,β -Deuteration of Secondary Alcohols^a

entry	diol	time (h)	temp (°C)	α ; β (%) deuteration
1 ^b		9	80	88; 87 (90.9)
2		12	80	94; 94 (94)
3		10	80	80; 10 (92)
4		12	80	97 (97.6)
5		10	80	90; 89 (93)

6		12	80	90; 89 (93)
7		16	80	86; 85 (93)

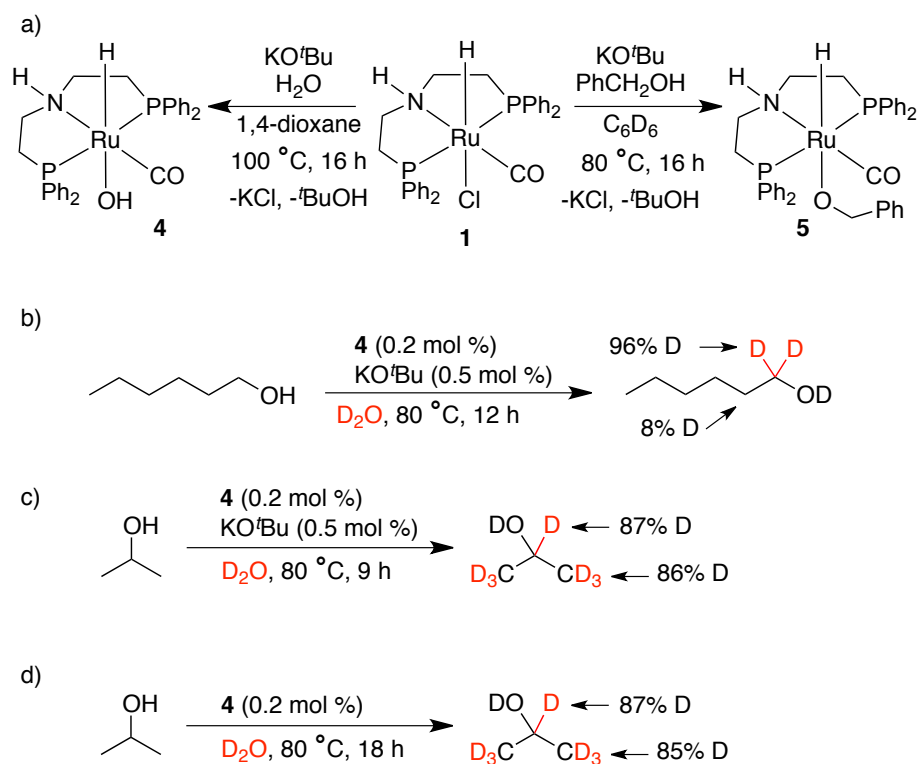
^aAs indicated in the footnote of Scheme 2.1. ^b1,4-dioxane (0.5 mmol) is used as an internal standard. Maximum possible % deuteration of substrates is given in the parenthesis.

Stoichiometric reactions were performed to obtain mechanistic insight. Upon reaction of complex **1** with water and base, a Ru(II) complex **4** (³¹P NMR δ = 57.3 ppm) with hydroxyl-ligand is obtained (Scheme 2.2a).⁹ A similar reaction of **1** with benzyl alcohol provided benzyloxy-ligated complex **5**; interestingly, presence of benzaldehyde coordinated ruthenium complex (9%) is also found in the reaction mixture.¹⁰ These reactions involve a base promoted, in situ formed unobserved amide-ligated unsaturated intermediate (**6**, Scheme 2.4), which reacted with H₂O and BnOH to provide **4** and **5**, respectively as a result of O–H activation by metal-ligand cooperation.^{6,11}

When isolated complex **4** (0.2 mol %) is used as a catalyst in the presence of base using D₂O, selective 96% α -deuteration of 1-hexanol (Scheme 2.2b, along with 8% D at the β -position; see Table 2.1, entry 3) and 87% and 86% α,β -deuteration of 2-propanol occurred in 12 h and 9 h, respectively (Scheme 2.2c and see Table 2.2, entry 1). These observations indicate the comparable reactivity of Ru–OH complex **4** compared to that of Ru-macho catalyst **1** and its potential involvement in the reaction. In principle, complex **4** does not require base to catalyze the H/D exchange reaction between alcohols and D₂O. Thus, deuteration of 2-propanol was carried out using **4** under neutral conditions. As anticipated, reaction proceeded in the absence of base; however only after 18 h similar % deuteration as that of basic conditions was obtained

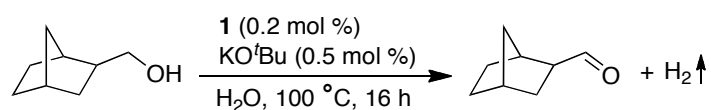
(Scheme 2.2d). This observation indicates that base may promote the H/D exchange reactions with solvent and catalytic system in one or more steps.

Scheme 2.2 Synthesis and Reactivities of Intermediates



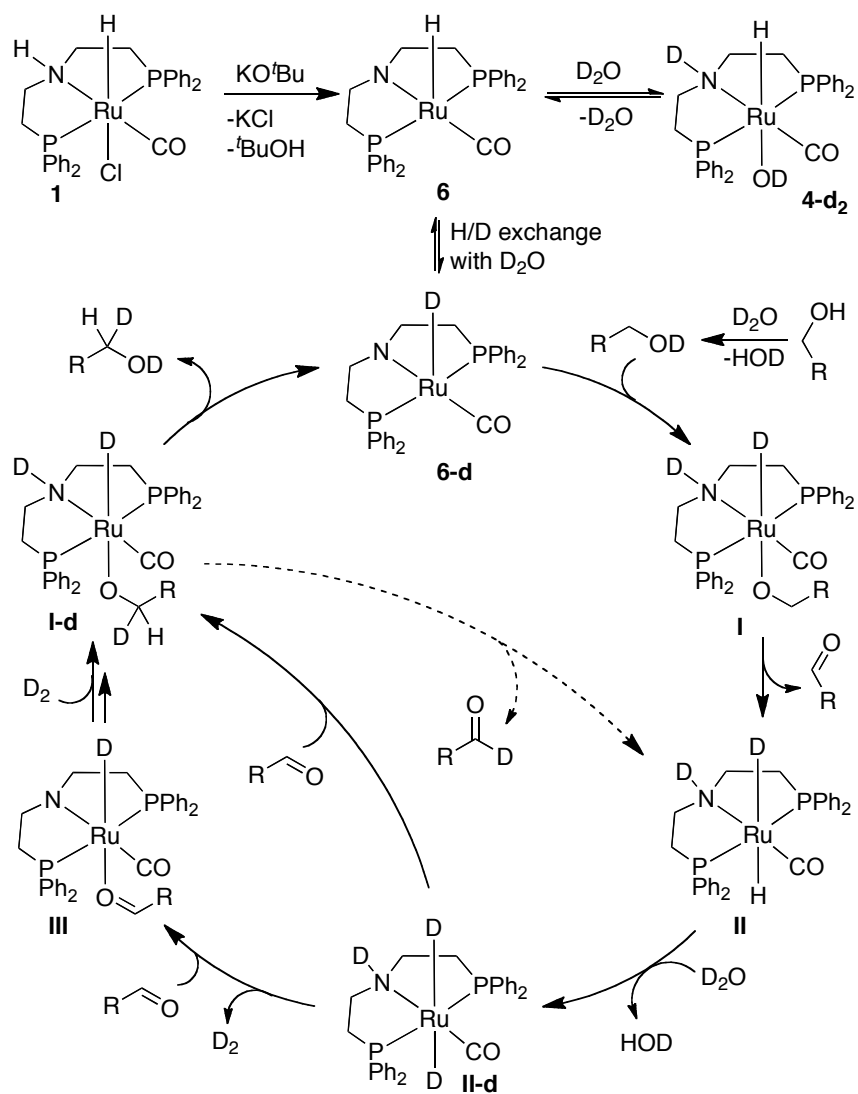
Attempts were made to observe the intermediates, if any from alcohol dehydrogenation during the catalysis.¹² When 2-norbornanemethanol was reacted with H₂O using catalyst **1** (0.2 mol %) and base (0.5 mol %) under open conditions, formation of the corresponding aldehyde was observed in the reaction mixture (Scheme 2.3).¹³ Since the reaction is performed with minimal amount of base using water as a solvent, potential competing pathways such as subsequent dehydrogenation of aldehyde to carboxylic acid¹⁴ or coupling with alcohol to provide the corresponding self-coupled esters^{7d} are minimized and the formation of intermediate aldehyde in the reaction mixture was observed (Scheme 2.3).

Scheme 2.3 Dehydrogenation of 2-Norbornanemethanol by **1**



Although more evidence is required based on the above observations, a possible catalytic cycle for the selective deuteration of alcohols is postulated in Scheme 2.4. Reaction of complex **1** with a base provided the unsaturated Ru(II) intermediate **6**, which reacts with D₂O by “amine-amide” metal-ligand cooperation^{6,10} and result in complex **4-d₂** as observed in reaction of complex **1** with H₂O (Scheme 2.2a). Under experimental conditions, **6** is in equilibrium with **4-d₂** and **6-d** by O–D activation or Ru–H/D exchange with D₂O, respectively. Perhaps, base assisted H/D exchange or involvement of Ru(0) intermediate cannot be ruled out, which may also play a crucial role in the deuterium scrambling. Complex **6-d** further reacts with alcohols (RCH₂OD) to provide saturated intermediate **I** (as observed in stoichiometric reaction, Scheme 2.2a). Further, β -hydride elimination of alkoxide ligand can result in Ru-dihydride **II**. Base assisted Ru–H/D exchange of **II** with solvent (D₂O) provides **II-d**. Either by direct aldehyde insertion into Ru–D bond of **II-d** or by D₂ liberation followed by aldehyde coordination (**III**)/decoordination pathways mono-deuterated alkoxy-ligated intermediate **I-d** was generated. Reductive elimination of alcohols from intermediate **I-d** can provide alcohols with mono-deuteration at the α -position, regenerating **6-d** to complete one cycle. Alternatively, **I-d** may also undergo β -hydride elimination to result in **II** and the subsequent transformations would result in **I-d₂** that can reductively eliminate alcohols with complete deuteration at the α -position of alcohols (RCD₂OD).

Scheme 2.4 Proposed Catalytic Cycle



2.4 CONCLUSIONS

In conclusion, Ru-macho catalyzed highly efficient selective deuteration of assorted primary and secondary alcohols are developed using deuterium oxide, the cheapest source of deuterium. While primary alcohols underwent deuteration predominantly at the α -position, the secondary alcohols were deuterated at both α - and β -positions. The reaction proceeded by O–D activation of deuterium oxide and alcohols by the Ru-macho catalyst, and subsequently the alkoxide ligands were dehydrogenated to the carbonyl compounds via amine-amide metal-ligand cooperation. While the catalytic hydrogenation of carbonyl motif resulted in α -deuteration, β -deuteration perhaps occurred via keto-enol tautomerization, which was varied based on substrate and steric hindrance. High percentage selective deuteration, mild experimental conditions and low loading and commercial availability of the catalyst make the process highly attractive for both laboratory as well as large-scale preparation of useful deuterated alcohols.

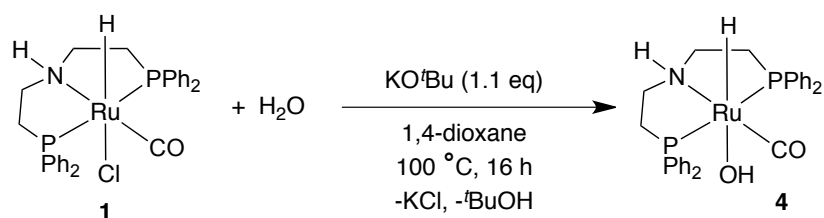
2.5 EXPERIMENTAL SECTION

General Experimental: All catalytic reactions were performed under nitrogen atmosphere. All stoichiometric reactions were performed in nitrogen atmosphere MBraun glove box. Chemicals were purchased from Acros, Sigma-Aldrich, Alfa-aesar, Himedia Chemicals and used without further purification. ^1H , ^{13}C , ^2H spectra were recorded at Bruker AV-400 (^1H : 400 MHz, ^{13}C : 100.6 MHz, ^2H : 61.42 MHz). ^1H and $^{13}\text{C}\{^1\text{H}\}$ NMR chemical shifts were reported in ppm downfield from tetramethyl silane. Assignment of spectra was done based on one dimensional (dept-135) NMR techniques.

General Procedure for Catalytic H/D Exchange Reaction: Alcohol (0.5 mmol), catalyst (0.001 mmol), KO^tBu (0.0025 mmol) were charged in a screw cap NMR tube

inside the nitrogen atmosphere glove-box. The NMR tube was brought out and degassed D₂O (0.4 mL) was added under N₂ atmosphere and then immersed in a pre-heated oil bath. The progress of the reaction was monitored by ¹H NMR spectroscopy. The decrease of signals intensity of α - and β -CH₂ protons is clearly observed in the ¹H NMR. The reactions were stopped at the saturation point of percentage deuterium incorporation. The reaction mixture is extracted with dichloromethane and the combined organic layer is washed with brine solution. The removal of solvent under reduced pressure provided pure products for further analysis.

Synthesis of Ru–OH Complex (4):

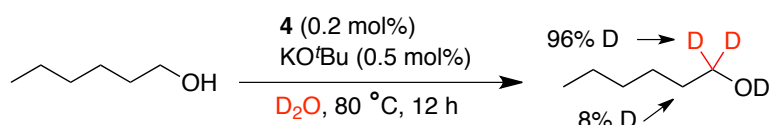


To a screw cap NMR tube, Ru-macho **1** (0.05 mmol, 30 mg), KO^tBu (0.055 mmol, 6 mg), degassed H₂O (0.25 mmol, 4.5 μ l) and 0.3 mL 1,4-dioxane was added inside a nitrogen atmosphere glove-box. The NMR tube was then brought out and heated to 100 °C on a preheated oil bath for 16 h. The ³¹P NMR monitoring of the reaction mixture indicates the formation of a new peak at 57.29 ppm along with the disappearance of the signal at 52.4 ppm corresponds to complex **1**. Attempts made to isolate the complex **4** from solution remain unsuccessful as it leads to the partial decomposition along with the reformation of the parent complex **1**. Thus, 1,4-dioxane solution of complex **4** in benzene-d₆ is used for spectral analyses. ¹H NMR (C₆D₆): δ 7.93 (d, J = 8 Hz, 4H, ArCH), 7.77 (d, J = 8 Hz, 4H, ArCH), 7.36-7.21 (m, 12H, ArCH), 3.71 (t, 4H, J = 6 Hz, CH₂), 3.55 (t, 4H, J = 4 Hz, CH₂), -17.2 (t, J = 20 Hz, 1H, Ru–H). ¹³C{¹H} NMR (C₆D₆): 31.37 (vt, J = 36 Hz, CH₂ (PPh₂)), 48.24 (s,

CH₂NH), 128.19 (ArCH), 129.30 (quat-C), 132.01 (ArCH), 133.46 (ArCH), 202.58 (Ru–CO). ³¹P {¹H} NMR: 57.29 ppm.

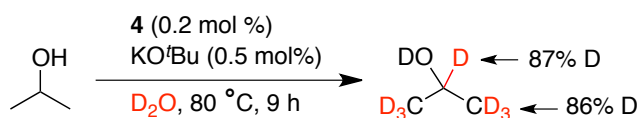
Procedures for the Reactivity Experiments of Ru–OH Complex 4:

Deuteration of 1-Hexanol with 4 as Catalyst:



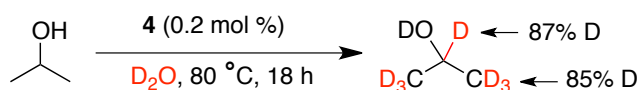
To a screw cap NMR tube, 1-hexanol (0.5 mmol, 62 μ l), complex 4 (0.001 mmol, 0.6 mg), KO^tBu (0.0025 mmol, 0.28 mg) and degassed D₂O (0.4 mL, 20 mmol) were charged under nitrogen atmosphere glove box. The NMR tube was brought out and the reaction mixture was heated to 80 °C on a preheated oil-bath. The H/D exchange phenomenon was monitored by ¹H NMR.

Deuteration of Isopropanol with Complex 4:



To a screw cap NMR tube, isopropanol (0.5 mmol, 38 μ l), complex 4 (0.001 mmol, 0.6 mg), KO^tBu (0.0025 mmol, 0.28 mg) and degassed D₂O (0.4 mL, 20 mmol) were charged under nitrogen atmosphere glove-box. The tube was brought out and the reaction mixture was heated to 80 °C on a preheated oil-bath. The H/D exchange phenomenon was monitored by ¹H NMR.

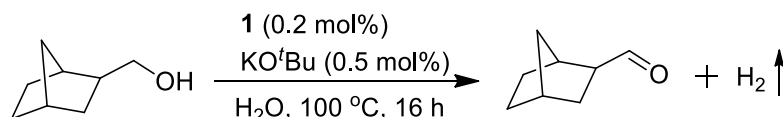
Deuteration of 2-Propanol Catalyzed by Complex 4 in the Absence of Base:



To a screw cap NMR tube, 2-propanol (0.5 mmol, 38 μ l), complex 4 (0.001 mmol, 0.6 mg) and degassed D₂O (0.4 mL, 20 mmol) were charged under nitrogen

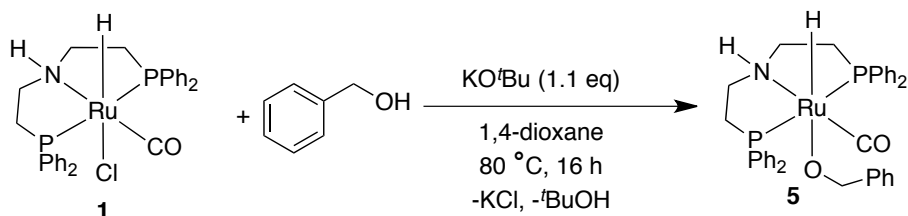
atmosphere glove box. The NMR tube was brought out and the reaction mixture was heated to 80 °C on a preheated oil-bath. The percentage deuterium incorporation was monitored by ¹H NMR.

Dehydrogenation of 2-Norbornanemethanol by Complex 1:



2-Norbornanemethanol (1 mmol, 134 μl), complex **1** (0.002 mmol, 1.2 mg), KO^tBu (0.005 mmol, 0.6 mg) and H₂O (1 mL) were added to a Schlenk tube. The reaction mixture was heated to 100 °C for 16 h under the nitrogen flow. After cooling, the reaction mixture was extracted with dichloromethane. The combined organic layers were washed with brine and the solvents were removed under the reduced pressure. The reaction mixture was analyzed by ¹H NMR spectroscopy.

In-Situ Observation of Ru-OR (5a) Complex:



To a screw cap NMR tube, Ru-macho **1** (0.0025 mmol, 15 mg), KO^tBu (0.0275 mmol, 3 mg), benzyl alcohol (0.0031 mmol, 3.2 μl) and 0.3 mL C₆D₆ were charged inside a nitrogen atmosphere glove box. The NMR tube was then brought out and heated to 80 °C on a preheated oil bath for 16 h. The ³¹P NMR monitoring of the reaction mixture indicates the formation of a new doublet at 56.69 ppm.

2.6 NOTES AND REFERENCES

(1) (a) Atzrodt, J.; Derdau, V.; Fey, T.; Zimmerman, J. *Angew. Chem. Int. Ed.* **2007**, *46*, 7744-7765. (b) *Synthesis and Application of Isotopically Labeled Compounds*

Pleiss, U.; Voges, R. (Eds) Vol. 7 Wiley: New York, 2001. (c) Junk, T.; Catallo, W. J. *Chem. Soc. Rev.* **1997**, *26*, 401-406.

(2) (a) Wang, Q.; Sheng, X.; Horner, J. H.; Newcomb, M. *J. Am. Chem. Soc.* **2009**, *131*, 10629-10636. (b) Klomp, D.; Maschmeyer, T.; Hanefeld, U.; Peters, J. A. *Chem. Eur. J.* **2004**, *10*, 2088-2093. (c) Xu, L.; Price, N. P. *J. Carbohydr. Res.* **2004**, *339*, 1173-1178. (d) Miyazaki, D.; Nomura, K.; Ichihara, H.; Ohtsuka, Y.; Ikeno, T.; Yamada, T. *New J. Chem.* **2003**, *27*, 1164-1166. (e) Jensen, D. R.; Schultz, M. J.; Mueller, J. A.; Sigman, M. S. *Angew. Chem. Int. Ed.* **2003**, *42*, 3810-3813. (f) Rasmussen, T.; Jensen, J. F.; Østergaard, N.; Tanner, D.; Ziegler, T.; Norrby, P. *Chem. Eur. J.* **2002**, *8*, 177-184. (g) Andersson, P. G. *J. Org. Chem.* **1996**, *61*, 4154-4156. (h) Liguori, A.; Mascaro, P.; Sindona, G.; Uccella, N. *J. Labelled Compd. Radiopharm.* **1990**, *28*, 1277-1283. (i) Polavarapu, P. L.; Fontana, L. P.; Smith, H. E. *J. Am. Chem. Soc.* **1986**, *108*, 94-99.

(3) (a) Yung, C. M.; Skaddan, M. B.; Bergman, R. G. *J. Am. Chem. Soc.* **2004**, *126*, 13033-13043. (b) Nishioka, T.; Shibata, T.; Kinoshita, I. *Organometallics* **2007**, *26*, 1126-1128. (c) Klei, S. R.; Golden, J. T.; Tilley, T. D.; Bergman, R. G. *J. Am. Chem. Soc.* **2002**, *124*, 2092-2093.

(4) (a) Balzarek, C.; Weakley, T. J. R.; Tyler, D. R. *J. Am. Chem. Soc.* **2000**, *122*, 9527-9534. (b) Breno, K. L.; Tyler, D. R. *Organometallics* **2001**, *20*, 3864-3868.

(5) For Ru catalyzed reactions: (a) Khaskin, E.; Milstein, D. *ACS Catal.* **2013**, *3*, 448-452. (b) Bossi, G.; Putignano, E.; Rigo, P.; Baratta, W. *Dalton Trans.* **2011**, *40*, 8986-8995 (D₂O used as a deuterium source in one entry). (c) Fujiwara, Y.; Iwata, H.; Sawama, Y.; Monguchi, Y.; Sajiki, H. *Chem. Commun.*, **2010**, *46*, 4977-4979. (d) Maegawa, T.; Fujiwara, Y.; Inagaki, Y.; Monguchi, Y.; Sajiki, H. *Adv. Synth. Catal.* **2008**, *350*, 2215-2218. (e) Takahashi, M.; Oshima, K.; Matsubara, S. *Chem. Lett.*

2005, *34*, 192-193. (f) Tse, S. K. S.; Xue, P.; Lau, C. W. S.; Sung, H. H. Y.; Williams, I. D.; Jia, G. *Chem. Eur. J.* **2011**, *17*, 13918–13925.

(6) For reviews, see: (a) Gunanathan, C.; Milstein, D. *Acc. Chem. Res.* **2011**, *44*, 588-602. (b) Gunanathan, C.; Milstein, D. *Top. Organomet. Chem.* **2011**, *37*, 55-84. (c) Gunanathan, C.; Milstein, D. *Chem. Rev.* **2014**, *114*, 12024-12087.

(7) (a) Kuriyama, W.; Matsumoto, T.; Ogata, O.; Ino, Y.; Aoki, K.; Tanaka, S.; Ishida, K.; Kobayashi, T.; Sayo, N.; Saito, T. *Org. Process Res. Dev.* **2012**, *16*, 166-171. (b) Nielsen, M.; Alberico, E.; Baumann, W.; Drexler, H. -J.; Junge, H.; Gladiali, S.; Beller, M. *Nature* **2013**, *495*, 85-89. (c) Otsuka, T.; Ishii, A.; Dub, P. A.; Ikariya, T. *J. Am. Chem. Soc.* **2013**, *135*, 9600-9603. (d) Oldenhuis, N. J.; Dong, V. M.; Guan, Z. *Tetrahedron* **2014**, *70*, 4213-4218. (e) Oldenhuis, N. J.; Dong, V. M.; Guan, Z. *J. Am. Chem. Soc.* **2014**, *136*, 12548-12551. (f) Monney, A.; Barsch, E.; Sponholz, P.; Junge, H.; Ludwig, R.; Beller, M. *Chem. Commun.*, **2014**, *50*, 707-709.

(8) For ruthenium catalyzed H/D exchange with aromatic hydrocarbons, see (a) Prechtel, M. H. G.; Hoelscher, M.; Ben-David, Y.; Theyssen, N.; Milstein, D.; Leitner, W. *Eur. J. Inorg. Chem.* **2008**, *22*, 3493-3500. (b) Prechtel, M. H. G.; Hoelscher, M.; Ben-David, Y.; Theyssen, N.; Loschen, R.; Milstein, D.; Leitner, W. *Angew. Chem. Int. Ed.* **2007**, *46*, 2269-2272.

(9) For other Ru(II) hydroxyl-ligated complexes, see (a) Reference 5a; (b) Kohl, S. W.; Weiner, L.; Schwartsburd, L.; Konstantinovski, L.; Shimon, L. J. W.; Ben-David, Y.; Iron, M. A.; Milstein, D. *Science* **2009**, *324*, 74-77.

(10) See Figure 2.16.

(11) Schneider, S.; Meiners, J.; Askevold, B. *Eur. J. Inorg. Chem.* **2012**, 412-429.

(12) In situ monitoring of benzyl alcohol and 2-propanol deuteration reactions catalyzed by complex **1** failed to predict involvement of any carbonyl compounds.

(13) ^1H and ^{13}C NMR analyses of the reaction mixture indicated the presence of unreacted 2-norbornanemethanol and the corresponding ester in addition to the aldehyde.

(14) Balaraman, E.; Khaskin, E.; Leitus, G.; Milstein, D. *Nat. Chem.* **2013**, *5*, 122-125.

^1H and ^{13}C NMR Spectra of Deuterated Alcohols:

Figure 2.3 ^1H NMR spectrum of benzo[d][1,3]dioxol-5-ylmethanol-d₃ (**2c**): NMR Solvent: CDCl_3 (^1H : 400 MHz)

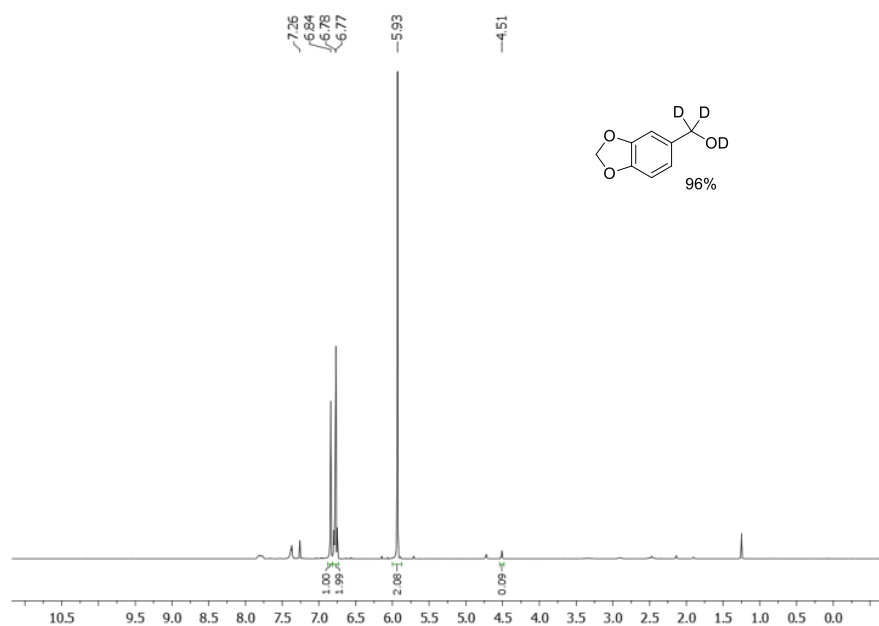


Figure 2.4 ^{13}C NMR spectrum of benzo[d][1,3]dioxol-5-ylmethanol-d₃ (**2c**): NMR Solvent: CDCl_3 (^{13}C : 100.6 MHz)

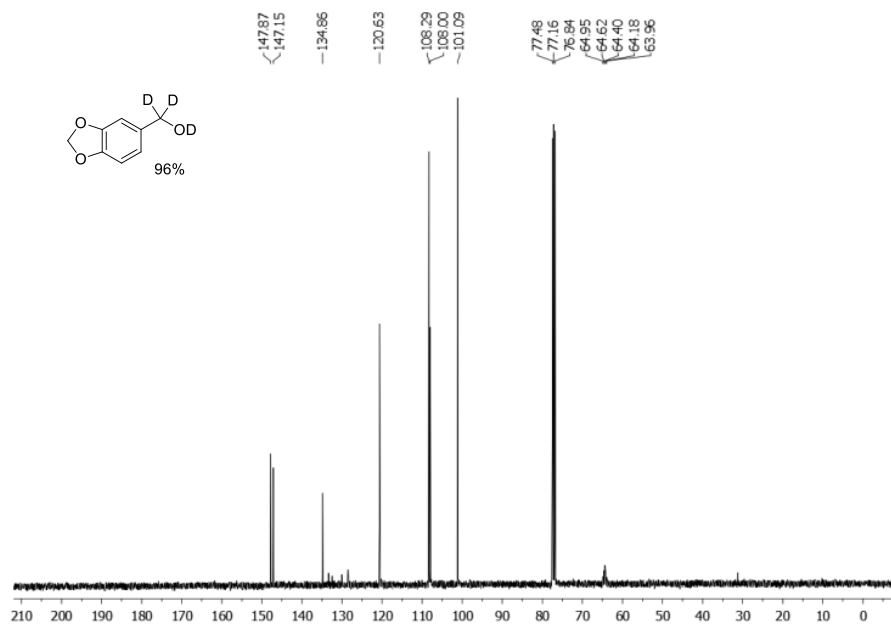


Figure 2.5 ^2H NMR spectrum of benzo[d][1,3]dioxol-5-ylmethanol- d_3 (**2c**): NMR Solvent: CDCl_3 (^2H : 61.42 MHz)

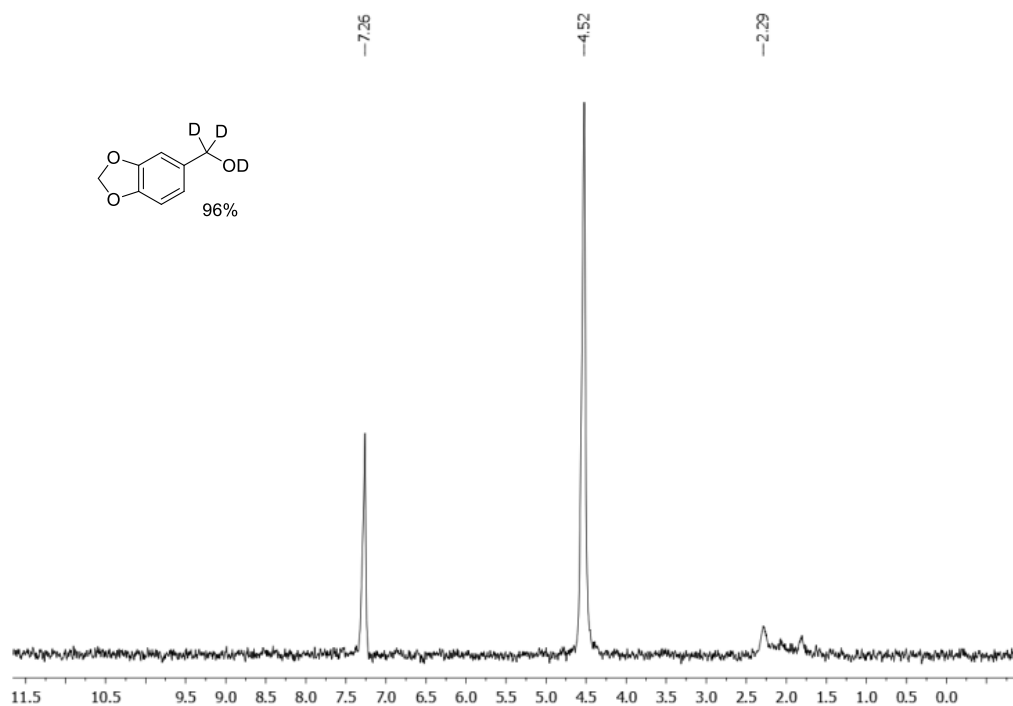


Figure 2.6 Stacked ^1H NMR spectra of furfuryl alcohol and furfuryl alcohol- d_3 (**2i**): NMR Solvent: D_2O (^1H : 400 MHz)

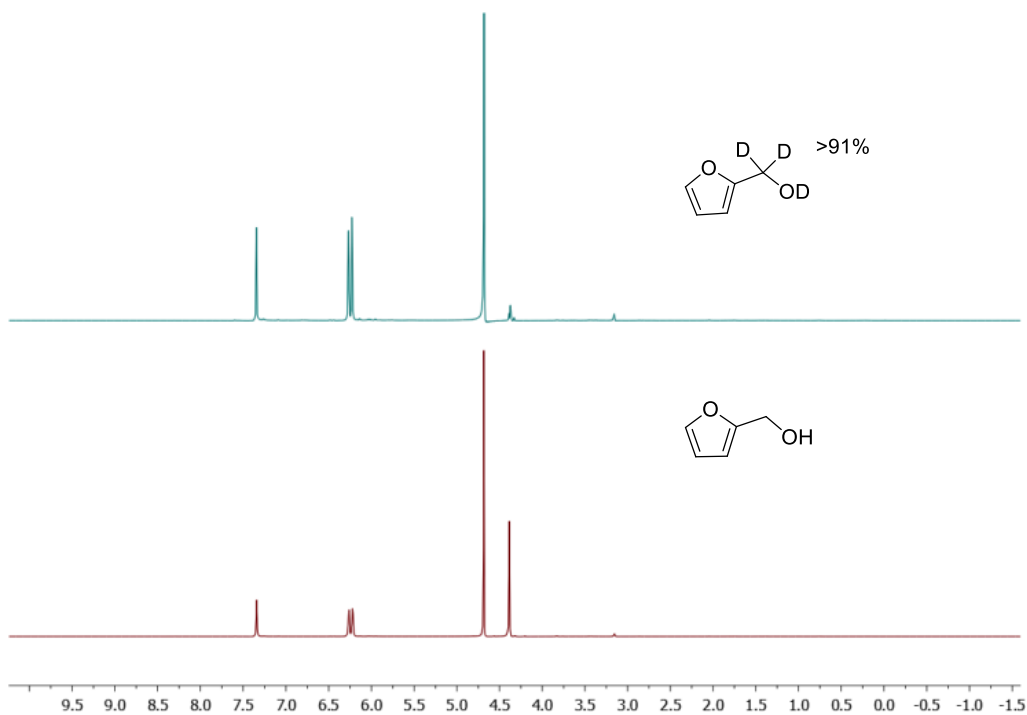


Figure 2.7 Stacked ^1H NMR spectra of ethanol and ethanol-d3 (Table 2.1: Entry 1): NMR Solvent: D_2O (^1H : 400 MHz)

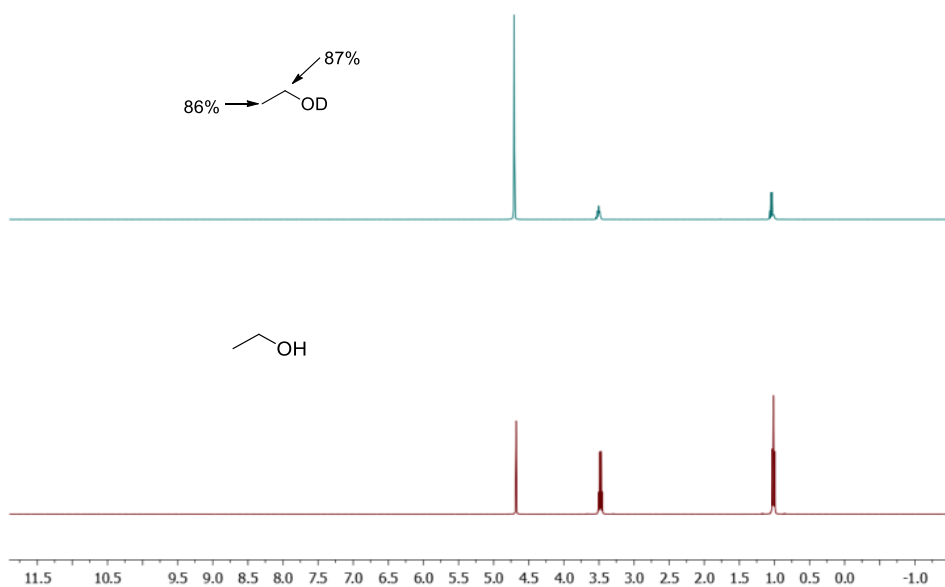


Figure 2.8 ^1H NMR spectrum of ethanol-d3 (Table 2.1: Entry 1): NMR Solvent: D_2O (^1H : 400 MHz)

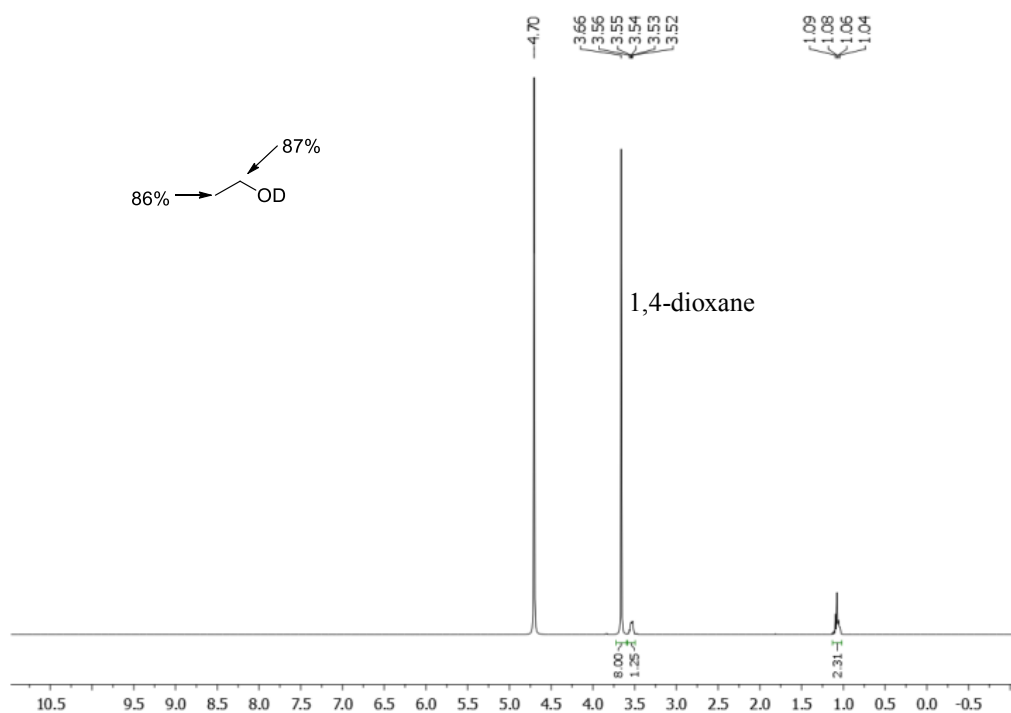


Figure 2.9 ^{13}C NMR spectra of ethanol-d3 (Table 2.1: Entry 1): NMR Solvent: D_2O (^{13}C : 100.6 MHz)

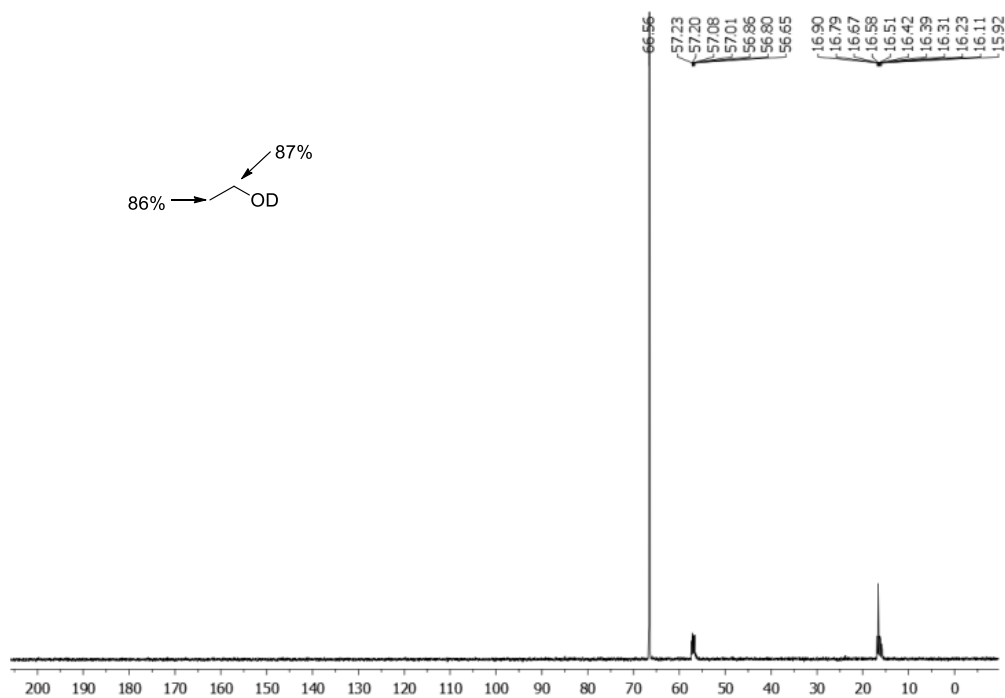


Figure 2.10 Stacked ^1H NMR spectra of 1,4-butane diol and 1,4-butane diol-d6 (Figure 2.2: **3c**): NMR Solvent: D_2O (^1H : 400 MHz)

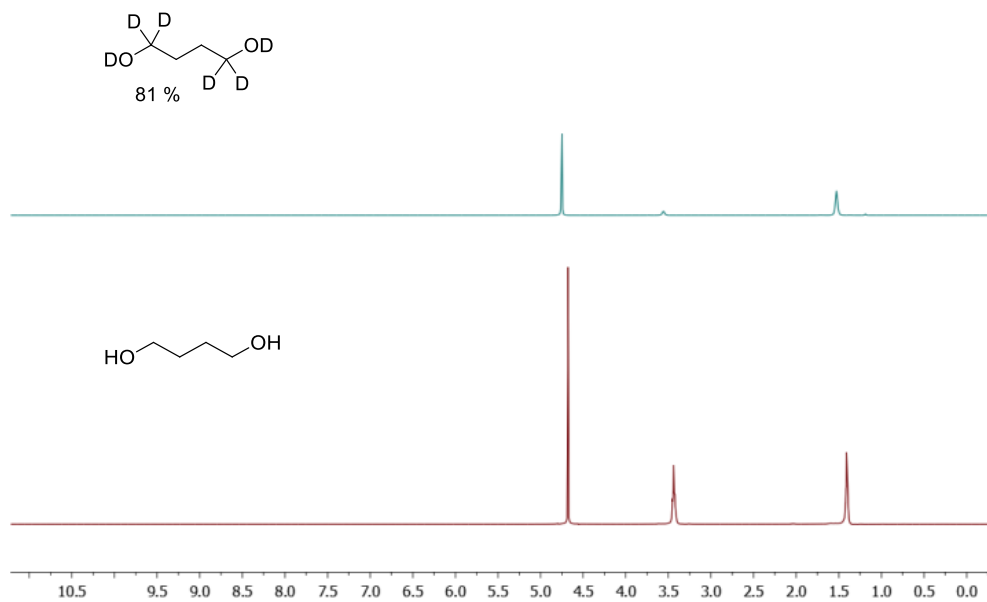


Figure 2.11 ^1H NMR spectrum of 1,6-hexane diol- d_6 (Figure 2.2: **3d**): NMR Solvent: D_2O (^1H : 400 MHz)

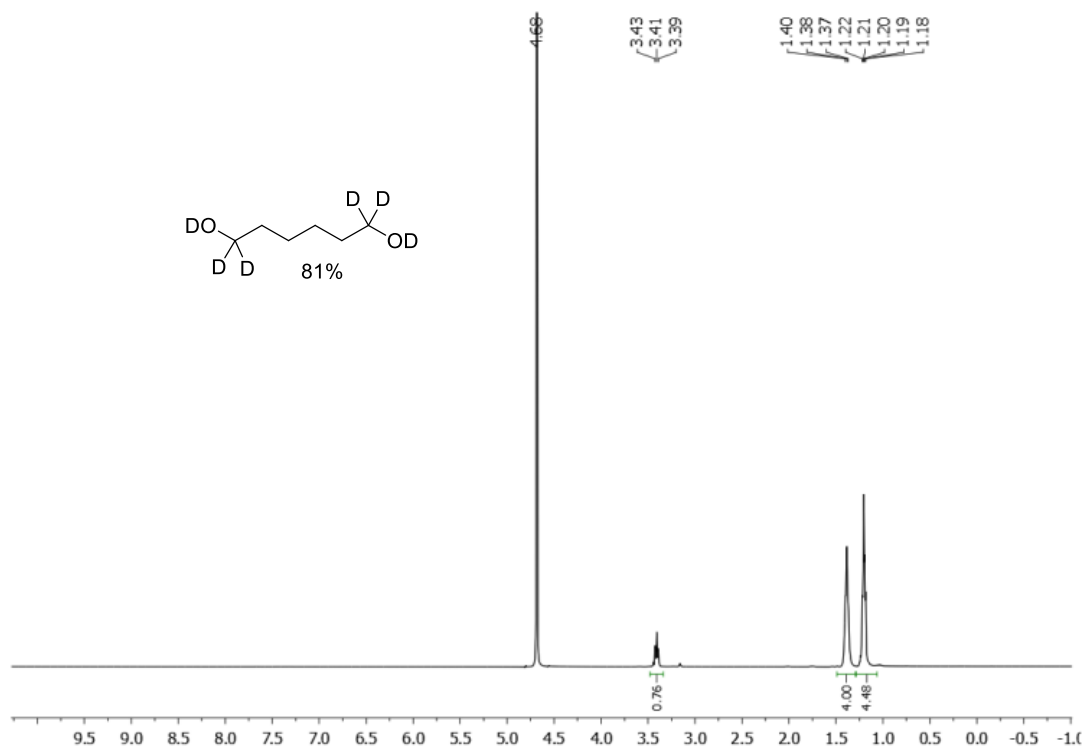


Fig 2.12 Deuteration of 2-propanol in D_2O . 1,4-dioxane (0.5 mmol) is used as internal standard.

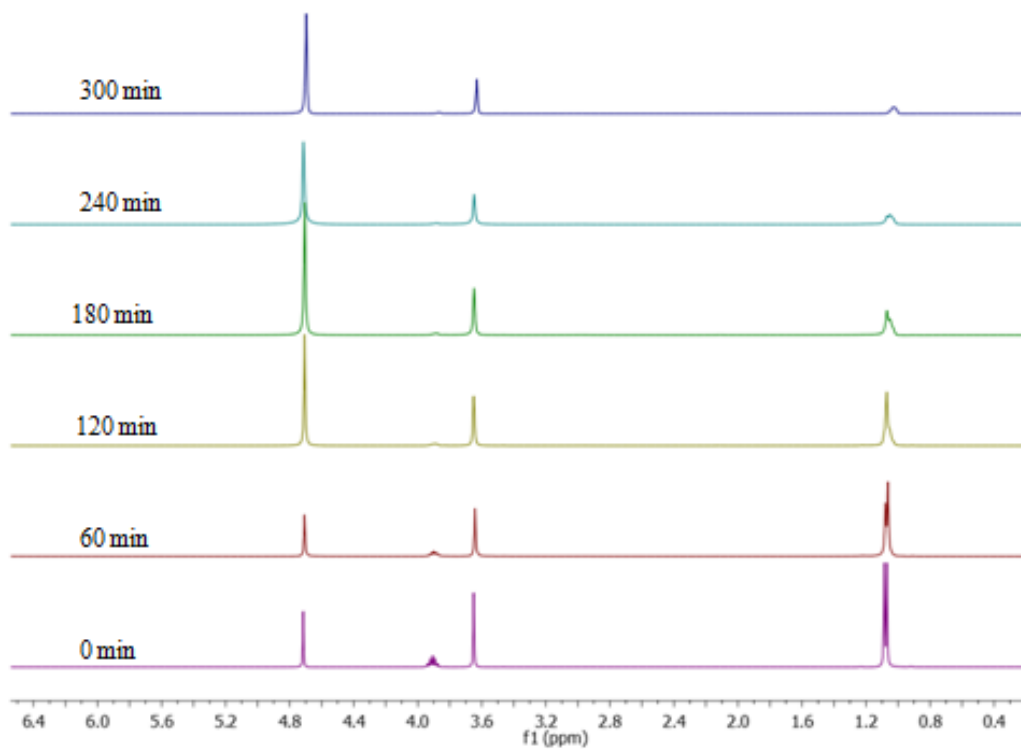


Figure 2.13 ^1H NMR spectrum of cyclododecanol-d6 (Table 2.2: Entry 7): NMR Solvent: CDCl_3 (^1H : 400 MHz)

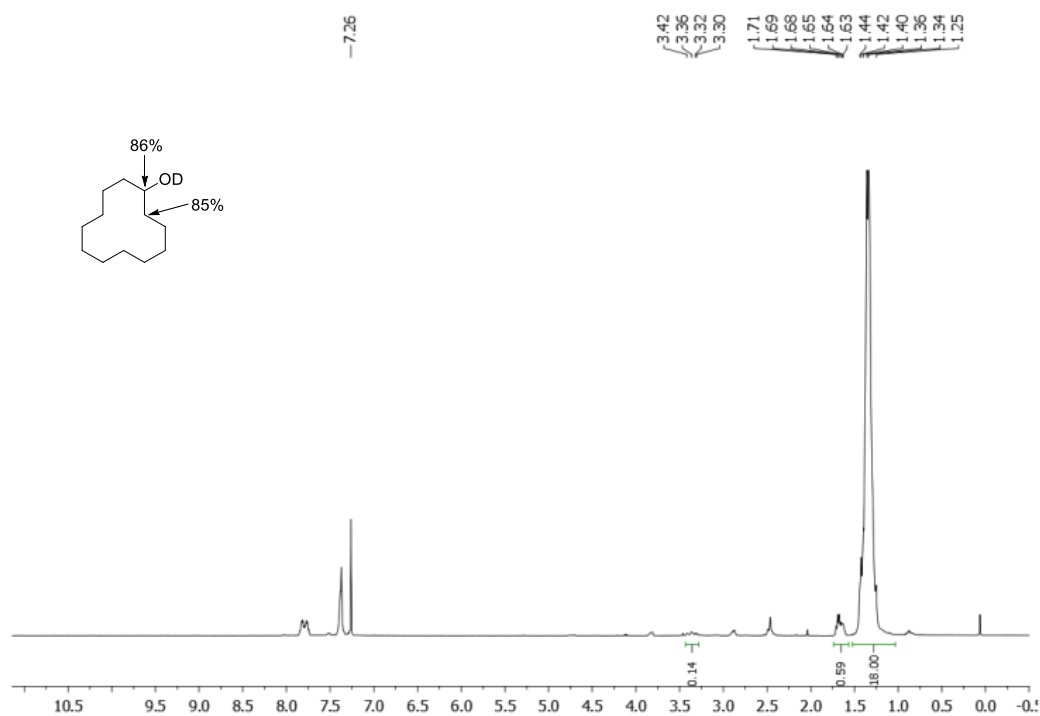


Figure 2.14 ^{13}C NMR spectrum of cyclododecanol-d6 (Table 2.2: Entry 7): NMR Solvent: CDCl_3 (^{13}C : 100.6 MHz)

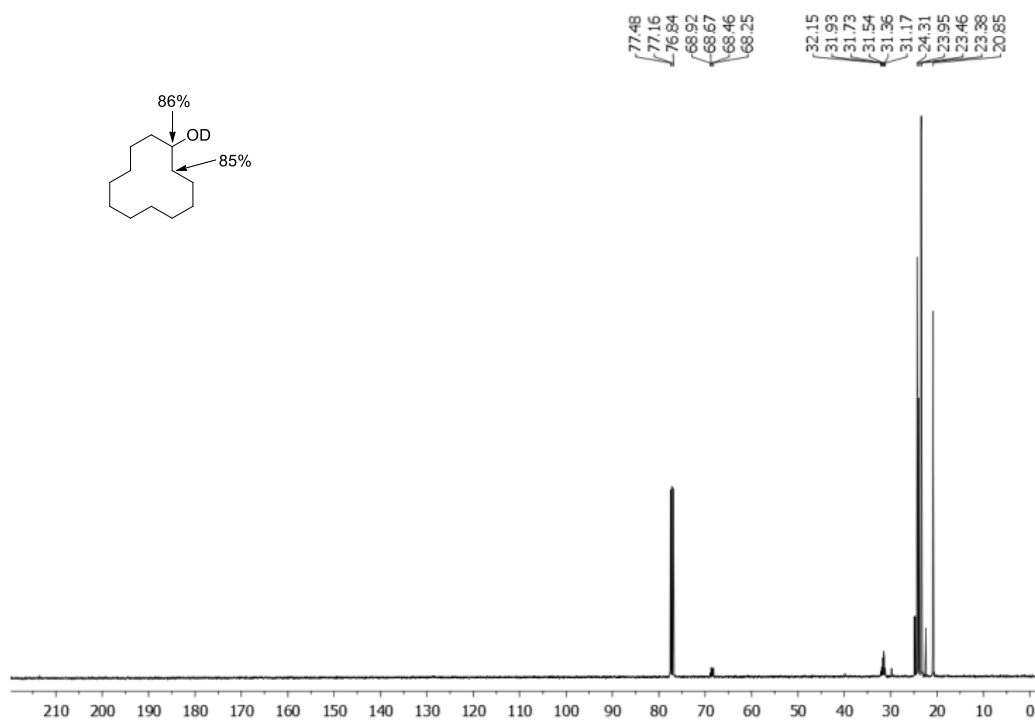


Fig 2.15 Stacked spectra from ^1H NMR monitoring for the deuteration of pyridine-2-propanol (0.5 mmol) in D_2O . Integration of α , β , γ position is measured with respect to the residual integration of aromatic (ArCH) protons.

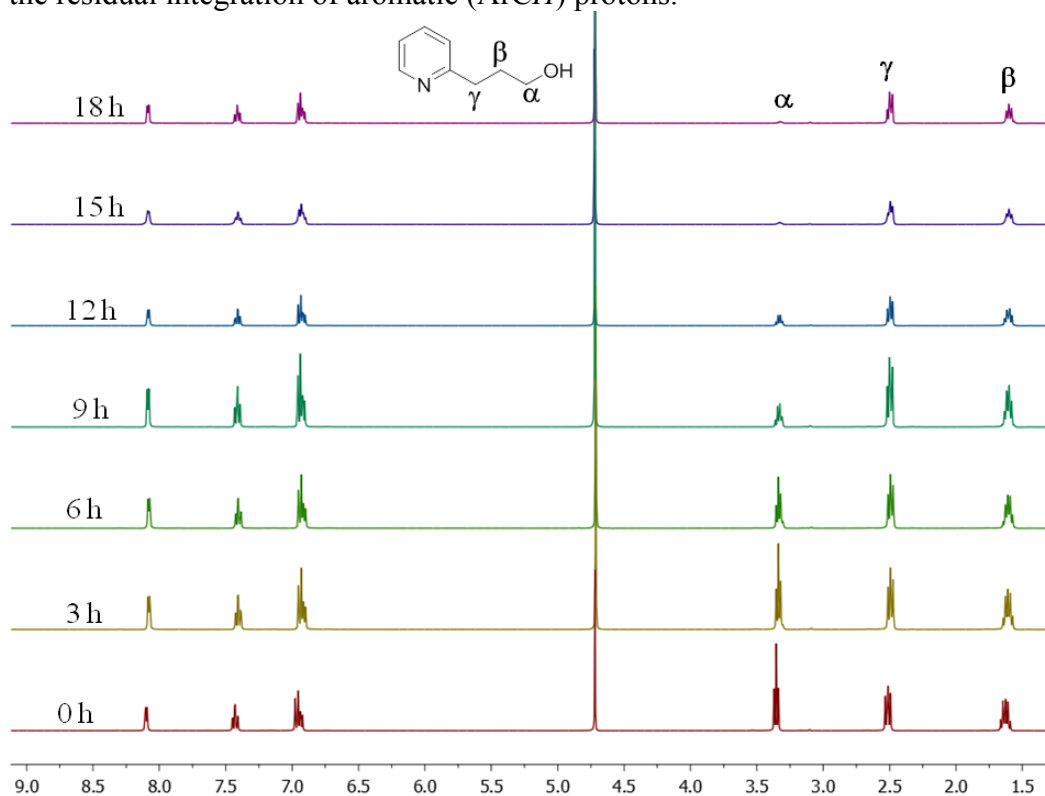


Figure 2.16 ^1H NMR of the reaction mixture of In-situ monitoring of Ru-OR (R= Ph, **5a**) complex:

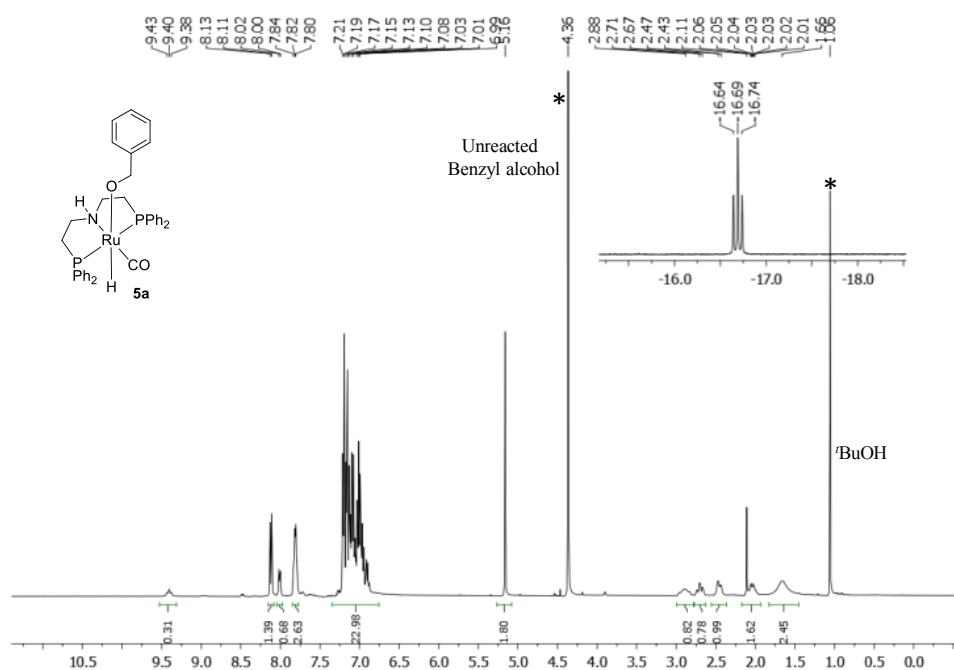
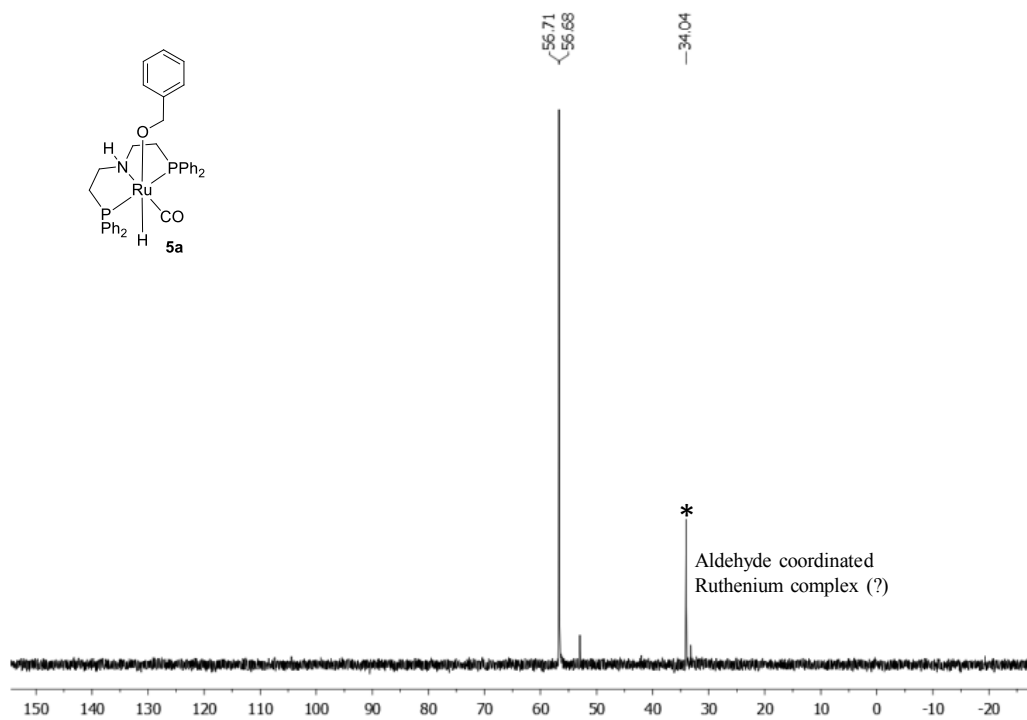


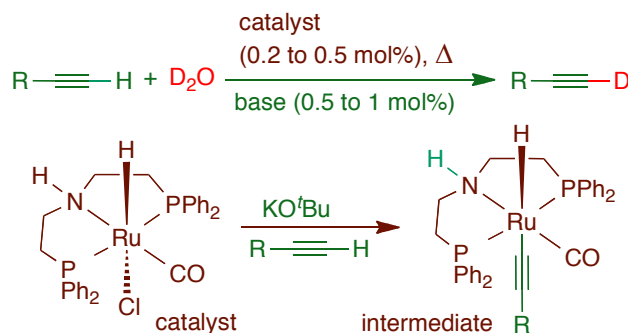
Figure 2.17 ^{31}P NMR of the reaction mixture of In-situ monitoring of Ru-OR (R= Ph, **5a**) complex:



CHAPTER 3

The Ruthenium-Catalyzed Selective Synthesis of *mono*-Deuterated Terminal Alkynes

3.1 ABSTRACT



We describe an efficient catalytic method for the synthesis of mono-deuterated terminal alkynes directly from deuterium oxide, catalyzed by a Ru(II) pincer complex in which the reaction proceeds via Ru-acetylide intermediates and amine-amide metal-ligand cooperation.

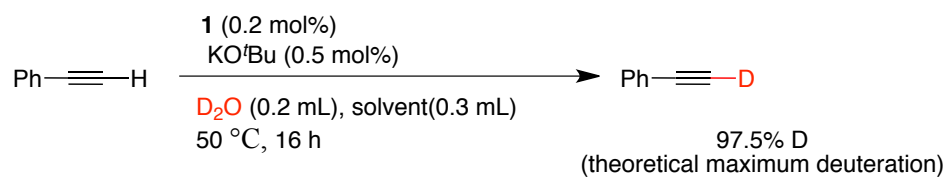
3.2 INTRODUCTION

Selective synthesis of deuterated organic compounds is a fundamental and challenging transformation.¹ Terminal alkyne motifs are found in numerous natural products,² and pharmaceuticals and they have widespread applications in chemical synthesis,³ pharmaceuticals, live cell imaging of biomolecules⁴ and material science.⁵ Deuterated terminal alkynes are also often used as highly reliable probe in mechanistic investigation of chemical transformations.⁶ Deuterated terminal alkynes are currently obtained using conventional organic synthesis. Reaction of alkynes with *n*-BuLi and 9-D-9-phenylfluorene, a pre-synthesized deuterium label derived from multi-step synthesis,⁷ Grignard reagents with large excess of deuterium oxide at sub-ambient temperatures are used.⁸ In the reactions involving stoichiometric amounts of toxic reagents,

different bases, alkali metals and basic resin with exceedingly large amount of deuterium oxide (> 50 equivalents) and deuterium chloride (DCl),⁹ often together with expensive co-solvents such as CD₃OD, and CD₃CN are employed.¹⁰ Discreet reactions involving H/D exchange of terminal alkyne with various expensive deuterated compounds such as CD₃COOD, and 2-propanol-d₈ are known.¹¹ An efficient catalytic method for the selective synthesis of terminal alkynes using deuterium oxide is highly desirable. As a part of our ongoing development of green catalytic synthesis of deuterated organic compounds using deuterium oxide, we have reported the selective α - and α, β -deuteration of alcohols catalyzed by a ruthenium pincer complex [(PNP^{Ph})RuHCl(CO)] **1** (PNP = **bis(2-(diphenylphosphino)ethyl)amine**).¹² In the current chapter we describe complex **1** catalyzed highly efficient, selective and direct synthesis of *mono*-deuterated terminal alkynes using deuterium oxide.

3.3 RESULTS AND DISCUSSIONS

As the aqueous solution of alkyne reaction mixture did not attain homogeneity, at the outset, deuteration of phenylacetylene using deuterium oxide catalyzed by complex **1** (0.2 mol%) and base (KO^tBu, 0.5 mol%) was performed in different polar organic solvents such as acetone, THF, 1,4-dioxane and DME (1,2-dimethoxyethane, see Table 3.1). Although the ether solvents are compatible, DME is the most suitable solvent in which 97% deuteration occurred on phenylacetylene terminal CH proton in 16 h at 50 °C against the theoretical maximum possible deuteration of 97.5% (Scheme 3.1). Control experiments under optimized conditions with and without base resulted in 10% and 7% deuteration of phenylacetylene, respectively, perhaps due to the weak acidity of terminal alkynes (see Table 3.1).

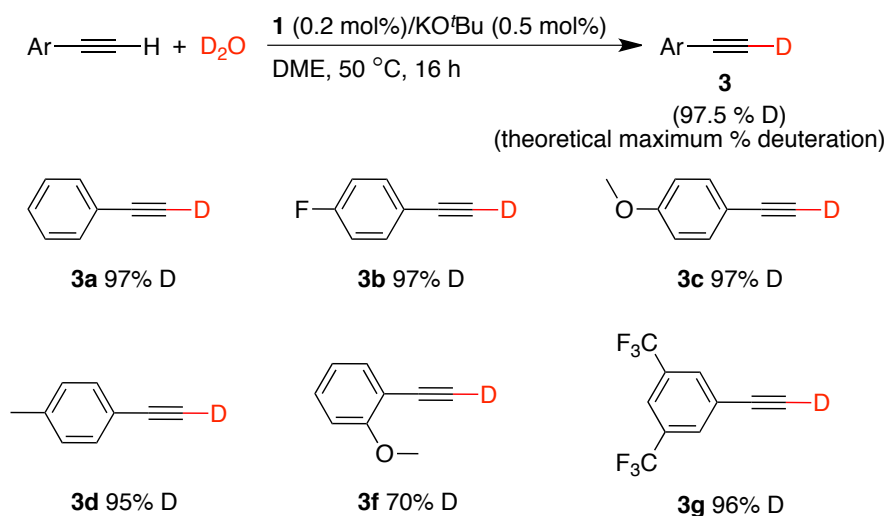
Table 3.1 Optimization of Aryl Terminal Alkyne Deuteration

Entry	Solvent	% Deuteration
1	Acetone	43
2	THF	95
3	1,4-Dioxane	92
4	DME	97
5 ^{a,b,d}	DME	10
6 ^{c,d}	DME	7

^a Reaction performed without using catalyst under otherwise similar conditions. ^b Reaction carried out in absence of catalyst. ^c Reaction carried out in the absence of both catalyst and base. ^d Data verified from two independent experiments.

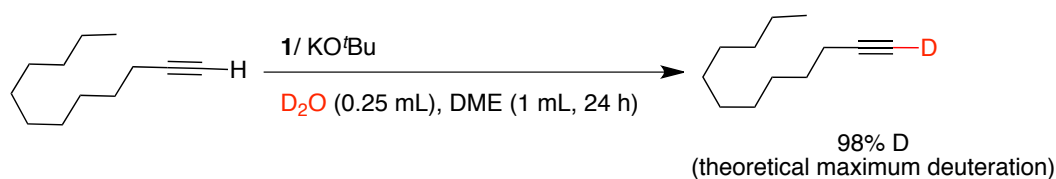
Under the optimized experimental conditions other aryl alkynes were subjected to the direct *mono*-deuteration with deuterium oxide (**3a-3g**, Scheme 3.1). Both electron donating and withdrawing groups were well tolerated on the *meta*- and *para*-positions of aryl alkynes. However, 2-methoxy phenylacetylene provided 70% mono-deuteration indicating that these reactions are sensitive to the steric hindrance. Notably, arene-CH bonds were not deuterated.¹⁴

Scheme 3.1 Scope of the Ru-Catalyzed Deuteration of Aryl Terminal Alkynes Using D₂O^a



^aValues reported are % deuteration determined by means of ¹H NMR. Standard conditions were as follows: catalyst **1** (0.2 mol%), KO^tBu (0.5 mol%), alkyne (0.5 mmol), D₂O (0.2 mL), DME (0.3 mL) were stirred in a closed vial at 50 °C for 16 h.

Aliphatic terminal alkynes with long chains required more organic solvent to attain homogeneity and hence the reactions were performed using 1 mL of DME (Table 3.2). When dodec-1-yne was subjected to the deuteration under the experimental conditions optimized for aryl alkyne, only 27% deuterium incorporation occurred after 24 h. Further optimization with slight increased loadings of catalyst (0.5 mol%), base (1 mol%) and temperature (90 °C) provided near maximum deuteration (96%) (Table 3.2). Control experiments under these conditions with and without base led to 19% and 15% deuteration of dodec-1-yne, respectively indicating influence of alkyne acidity and temperature (Table 3.2).

Table 3.2 Optimization of Aliphatic Terminal Alkyne Deuteration

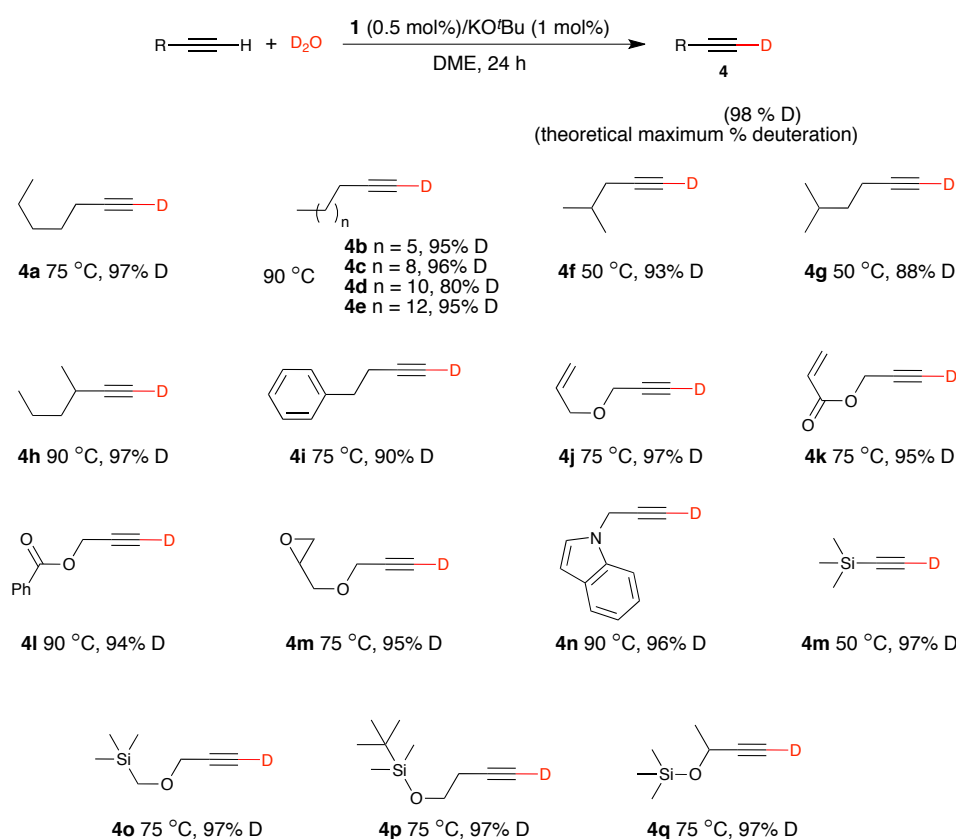
Entry	Catalyst 1 (mol%)	KO ^t Bu (mol%)	Temp (°C)	% Deuteration
1	0.2	0.5	50	27
2	0.2	1	50	30
3	0.2	1	75	84
4	0.5	1	90	96
5 ^{a,b,d}	-	1	90	19
6 ^{c,d}	-	-	90	15

^aReaction performed without using catalyst under otherwise similar conditions. ^bReaction carried out in the absence catalyst. ^cReaction carried out in the absence of both catalyst and base. ^dData verified from two independent experiments.

Structural variations in the aliphatic terminal alkynes were well tolerated, and simple and functionalized substrates were effectively deuterated (**4a-4q**, Scheme 3.2). While terminal alkynes embedded with linear hydrocarbons showed excellent deuteration, branched hydrocarbon substrates resulted in marginally decreased % of deuteration due to the increase of steric encumbrance. Gratifyingly, this method is chemoselective to the alkyne *sp*-C-H; alkene *sp*²-C-H bonds remained unaffected. Allyl ether, vinyl ester,

benzoate, epoxide, indole, silyl, silylmethyl ether and silyl ether containing terminal alkynes exhibited percentage deuteration almost close to the theoretical maximum (98%, Scheme 3.2) and provided the corresponding *mono*-deuterated terminal alkyne products.

Scheme 3.2 Scope of the Ruthenium-Catalyzed Synthesis of *mono*-Deuterated Terminal Aliphatic Alkynes Using D₂O^a



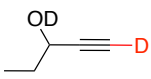
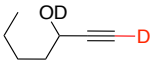
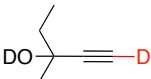
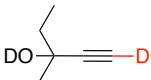
^aValues reported are % deuteration determined by means of ¹H NMR. Standard conditions were as follows: catalyst **1** (0.5 mol%), KO^tBu (1 mol%), alkyne (0.5 mmol), D₂O (0.25 mL), DME (1 mL) were stirred for 24 h at the indicated temperature.

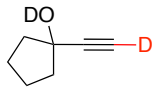
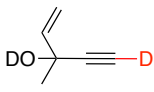
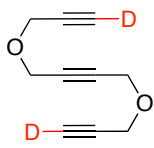
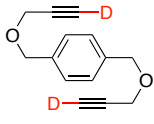
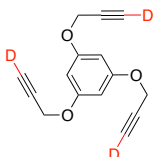
We have also planned competitive and selective *mono*-deuteration of terminal alkynes over the α,β -deuteration of alcohols.¹² Reaction of pent-1-yn-3-ol and hept-1-yn-3-ol provided 80% and 95% of the respective *mono*-deuterated terminal alkynes, while only insignificant deuteration occurred on α,β -positions

of alcohol functionality (Table 3.3, entries 1,2), confirming that the *sp*-CH activation and deuteration processes prevail over the other competing pathways. Moreover, presence of hydroxyl and amine functionalities on alkynes was beneficial as they enhance the substrate solubility in D₂O, and hence the experiments can be performed without use of solvent (DME) at 60 °C (Table 3.3, entries 1-7); under this mild conditions excellent % of deuteration was observed on terminal alkyne *sp*-C–H only in 7 h.

Further, deuteration of terminal alkynes was also demonstrated on substrates containing multiple terminal alkyne units (Table 3.3, entries 8-10). Di-terminal alkynes (0.25 mol% of **1**/alkyne) and tri-terminal alkynes (0.17 mol% of **1**/alkyne) displayed efficient deuteration even though the catalyst loading of **1** per alkyne unit on these reactions were very minimal.

Table 3.3 Substrate Scope of Chemoselective Deuteration of Highly Functionalized Terminal Alkynes Using D₂O^a

Entry	Product	Temp (°C)	Theoretical % deuteration	Observed % deuteration
1		60	90.9	80 (α: 10; β: 1)
2		60	90.9	95 (α: 5; β: 1)
3		60	96	89
4		60	96	92

5		60	96	89
6		60	96	87
7		75	89	87
8 ^{†,§}		90	98	97
9 ^{†,§}		75	98	80
10 ^{‡,§}		90	98	77

^aValues reported are % deuteration determined by means of ¹H NMR. Standard conditions were as follows: catalyst **1** (0.5 mol%), KO^tBu (1 mol%), alkyne (0.5 mmol) and D₂O (0.25 mL) were stirred at the indicated temperature for 7 h. [†]0.5 mL D₂O, 2 mL DME used. [‡] 0.75 mL D₂O, 3 mL DME used. [§]Reaction performed for 24 h.

Deuterium incorporation is found to enhance the overall therapeutic and metabolic profile of a drug.¹⁵ Interestingly, the pharmaceuticals such as Eudatin[®], Ovastol[®] and Parsal[®] and other bioactive molecules¹⁶ are embedded with terminal alkyne units (Figure 3.1) and provide the potential opportunity to derive their deuterated analogues, which could enable the direct tracing of these molecules in the body and enhance their therapeutic abilities.¹⁷

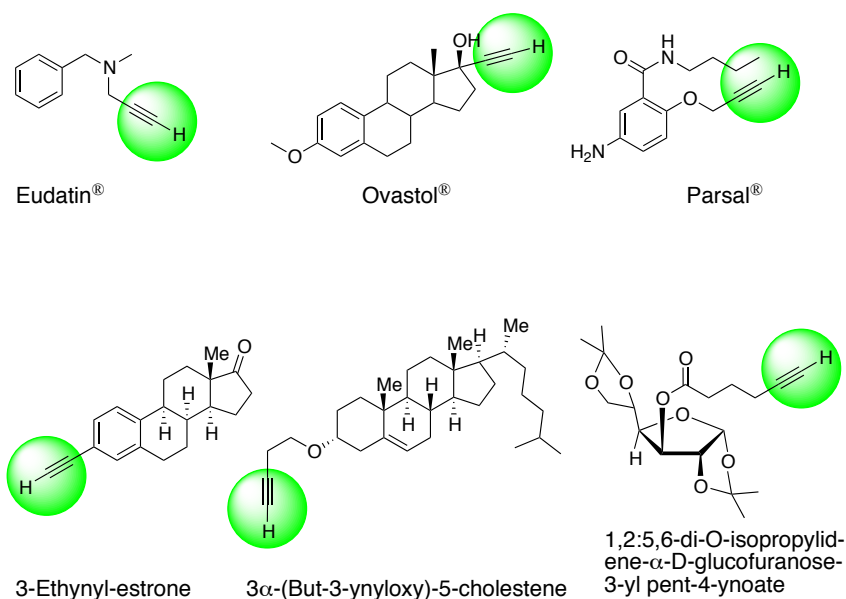
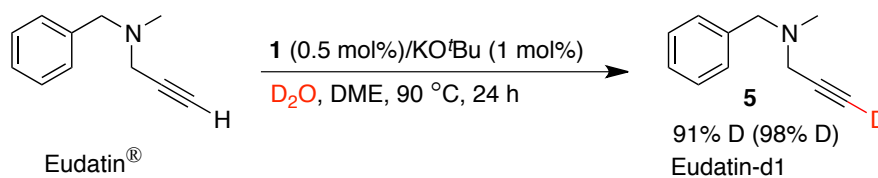


Figure 3.1 Representative natural products, drugs and bioactive molecules containing terminal alkyne functionality.¹⁸

Eudatin[®] is a monoamine oxidase inhibitor used for the treatment of hypertension, when it was subjected to the reaction, 91% *mono*-deuterated Eudatin-d1 **5** was obtained, demonstrating potential utility of this method for selective deuteration of terminal alkynes (Scheme 3.3) present in drugs and bioactive molecules.

Scheme 3.3 Selective Catalytic Synthesis of Eudatin-d1

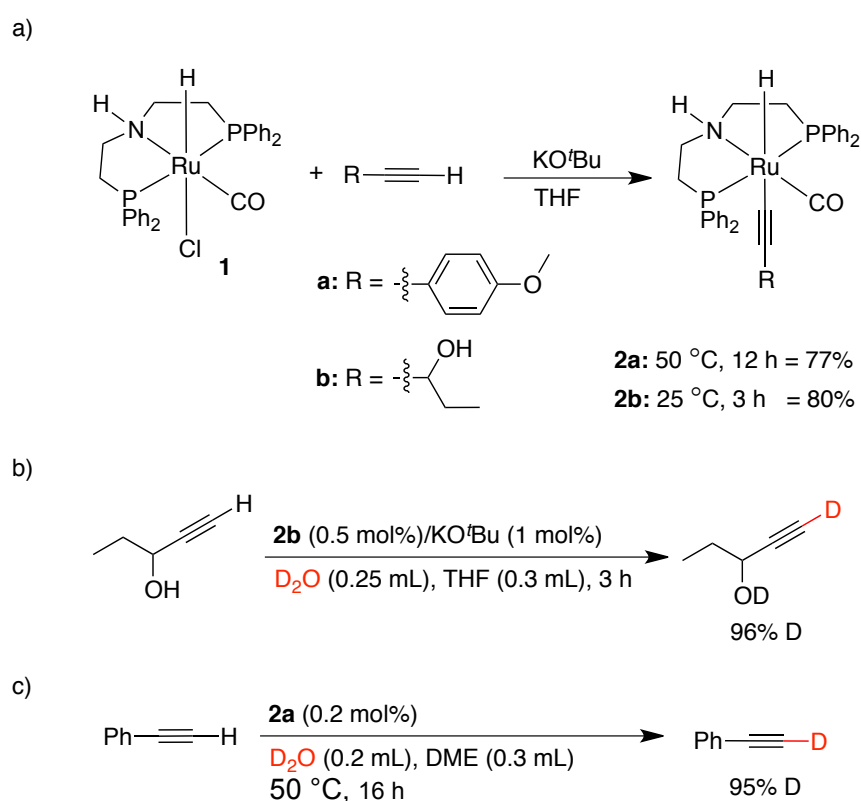


Stoichiometric experiments were performed to understand the reaction mechanism of this interesting catalytic process. Upon reaction of **1** with 4-methoxy phenylacetylene and base the corresponding Ru-acetylide complex **2a** was obtained, which exhibited characteristic ¹H (t, -7.68 ppm, *J*_{P-H} = 20 Hz)

and $^{31}\text{P}\{^1\text{H}\}$ (s, 58.61 ppm) NMR signals. Similar reaction of **1** with 1-pentyne-3-ol occurred rapidly at room temperature and resulted in Ru-acetylide **2b**, which displayed ^1H (t, -7.76 ppm, $J_{\text{P-H}} = 20$ Hz) and $^{31}\text{P}\{^1\text{H}\}$ (s, 58.21 ppm) NMR signals (Scheme 3.4a) confirming the *sp*-CH activation in both reactions. Further, structure of complex **2b** was unequivocally corroborated using single crystal X-ray analysis (Figure 3.2), which indicates the distorted octahedral geometry around ruthenium center and the formation of Ru-acetylide rather than Ru-vinylidene. Remarkably, under the experimental conditions *sp*-C-H activation of terminal alkynes by ruthenium pincer complex **1** prevails over the O-H activation of alcohols.¹⁹ The reaction of terminal alkyne with ruthenium is well known to provide Ru-vinylidene complexes with hydride migration to the internal carbon of alkynes.^{6a,20} Furthermore, Ru-vinylidene complexes are known to react with water to provide the Ru-hydroxycarbene complexes.²¹ Notably, such side reactions were not observed with complex **1** despite the presence of a metal-hydride. When the deuteration of 4-methoxy phenylacetylene and 1-pentyne-3-ol catalyzed by **1** were monitored in situ using ^{31}P and ^1H NMR, intermediate signals corresponding to the complexes **2a** and **2b**, respectively were exclusively observed, indicating their intermediacy in the catalysis (see Figure 3.3 and 3.4). Moreover, under these experimental conditions the previously observed corresponding Ru-OH complex that can be formed *via* reaction of complex **1** with base and water is also not observed,¹² demonstrating the facile and predominant activation of *sp*-C-H bond. Further, 1-pentyne-3-ol was subjected to selective deuteration using the isolated intermediate **2b** (0.5 mol%) as a catalyst (Scheme 3.4b); 1-pentyne-3-ol-d₂ was obtained in which terminal alkyne-CH was 96%

deuterated in only 3 h. In principle, Ru-acetylide complexes can catalyze the deuteration under neutral conditions. Thus, upon use of intermediate **2a** as the catalyst (0.2 mol%), phenylacetylene-d1 with 95% deuterium was obtained (without using base, Scheme 3.4c) in 16 h confirming the potential intermediacy of Ru-acetylide in the catalytic deuteration reaction.

Scheme 3.4: Mechanistic Studies



(a) Reactions of Terminal Alkynes with Ru-Complex **1**. (b) Catalysis Using Isolated Intermediate **2b**. (c) Catalysis Using Isolated Intermediate **2a**.

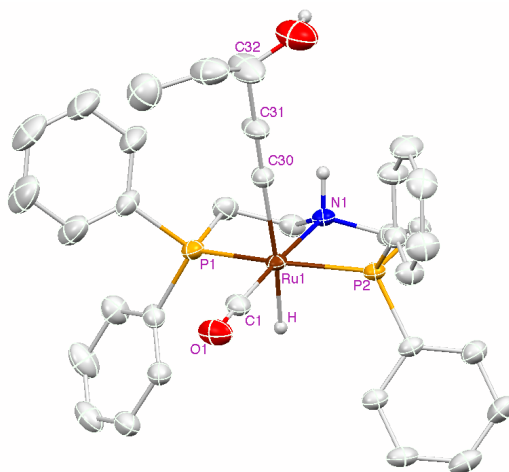
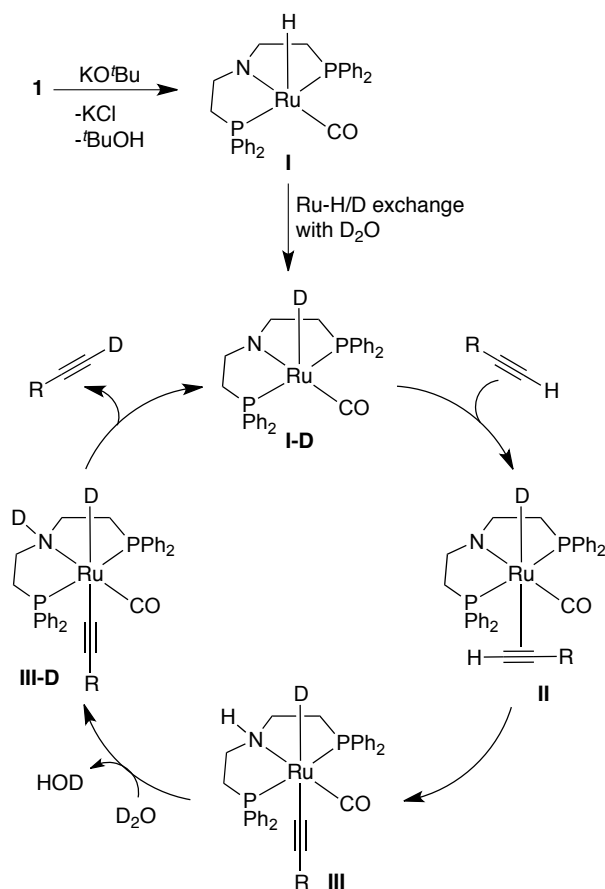


Figure 3.2: Single Crystal X-ray Structure of **2b**. Ellipsoids are drawn with 50% probability. Selected bond lengths (Å) and angles (deg) of **2b**: Ru1–H: 1.65, Ru1–C30: 2.10, C30–C31: 1.20, C31–C32: 1.48, P2–Ru1–P1: 164.01, P2–Ru1–H: 93(3), C1–Ru1–H: 87(3), C1–Ru1–N1: 176.03, C1–Ru1–C30: 93.27.

On the basis of the above experimental observations, a catalytic cycle for the chemoselective deuteration of terminal alkynes by complex **1** is proposed (Scheme 3.5). The reaction of complex **1** with base generates the amide-ligated unobserved unsaturated intermediate **I**, which undergoes Ru–H/D exchange with deuterium oxide to generate **I-D**. The reaction of intermediate **I-D** with terminal alkyne leads to the formation of alkyne coordinated initial intermediate **II** in which the terminal alkyne undergoes selective oxidative addition of *sp*-C–H bond at the ruthenium center to provide the amine-ligated saturated intermediate **III** (notably, oxidation state of ruthenium remains +2 as amide became amine in **III**; verified by the preparation and observation of complexes **2a** and **2b** in catalysis).^{13,22} H/D exchange reaction of **III** with deuterium oxide, perhaps also base assisted¹² provides **III-D**, which upon reductive elimination provides the deuterated terminal alkynes and regenerates the catalytically active intermediate **I-D** closing a catalytic cycle.

Scheme 3.5 Proposed Mechanism for the Synthesis of *mono*-Deuterated Terminal Alkynes



3.4 CONCLUSIONS

In summary, an efficient catalytic method for the synthesis of *mono*-deuterated terminal alkynes was developed using a ruthenium pincer complex **1** and deuterium oxide, a cheapest source of deuterium. Reactions proceed via the formation of Ru-acetylide intermediates and H/D exchange with deuterium oxide via amine-amide metal-ligand cooperation. Remarkably, this catalytic process is chemoselective and is devoid of any deleterious side reactions. As this transformation uses low loading of a commercially available ruthenium-catalyst, is practically simple and environmental friendly, it will have a major

impact on the way *mono*-deuterated terminal alkynes, pharmaceuticals and materials are synthesized.

3.5 EXPERIMENTAL SECTION

General Experimental: All catalytic reactions were performed under nitrogen atmosphere. All stoichiometric reactions were performed in nitrogen atmosphere MBraun glove box. Chemicals were purchased from Acros, Sigma-Aldrich, Alfa-aesar, Spectrochem and used without further purification. ^1H , ^{13}C , and ^{31}P NMR spectra were recorded at Bruker AV-400 (^1H : 400 MHz, ^{13}C : 100.6 MHz, ^{31}P : 162 MHz). ^1H and $^{13}\text{C}\{^1\text{H}\}$ NMR chemical shifts were reported in ppm downfield from tetramethyl silane. Multiplicity is abbreviated as: s, Singlet; d, doublet; t, triplet; q, quartet; sept, septet; m, multiplate. Assignment of spectra was done based on one dimensional (dept-135) NMR technique. IR Spectra were recorded in Perkin-Elmer FT-IR Spectrometer.

General Procedure for the Deuteration of Terminal Aromatic Alkynes: To a screw cap scintillation vial terminal aromatic alkyne (0.5 mmol), catalyst (0.001 mmol), KO^tBu (0.0025 mmol), 1,2-dimethoxyethane (0.5 mL) and degassed D₂O (0.2 mL) were added under nitrogen atmosphere. The reaction vial was wrapped with aluminium foil and immersed into a pre-heated oil bath. The reactions were stopped at the optimized time of deuterium incorporation and solvent was evaporated under reduced pressure. The resulted residue was extracted with dichloromethane and the combined organic phase is dried over sodium sulfate. Removal of solvent under reduced pressure provided pure products for further analysis.

General Procedure for the Deuteration of Terminal Aliphatic Alkynes: To a screw cap scintillation vial terminal aliphatic alkyne (0.5 mmol), catalyst (0.0025 mmol), KO^tBu (0.005 mmol), 1,2-dimethoxyethane (1 mL) and degassed D₂O (0.25

mL) were added under nitrogen atmosphere. Vial was covered with aluminium foil and immersed into a pre-heated oil bath. The reactions were stopped after 24 h and the solvent was evaporated under reduced pressure. The resulted residue was extracted with dichloromethane and combined organic phase is dried over sodium sulfate. Removal of solvent under reduced pressure provided pure products for further analysis.

Spectral Data of Deuterated Terminal Alkynes:

Ethynylbenzene-d1 (3a): ^1H NMR (CDCl_3 , 400 MHz) δ 7.24-7.21 (m, 2H, ArCH), 7.08-7.03 (m, 3H, ArCH). $^{13}\text{C}\{^1\text{H}\}$ NMR (101 MHz, CDCl_3) δ 131.29 (ArCH), 127.96 (ArCH), 127.58 (ArCH), 121.63 (quat-C), 82.47-82.32 (t, quat-C), 76.97-76.20 (t).

1-Ethynyl-4-fluorobenzene-d1 (3b): ^1H NMR (CDCl_3 , 400 MHz) δ 7.50-7.45 (m, 2H, ArCH), 7.04-6.99 (m, 2H, ArCH). $^{13}\text{C}\{^1\text{H}\}$ NMR (101 MHz, CDCl_3) δ 158.69 (quat-C), 133.72 (ArCH), 118.23 (quat-C), 115.10 (ArCH), 83.24-83.05 (t, quat-C), 76.78-75.97 (t).

1-Ethynyl-4-methoxybenzene-d1 (3c): ^1H NMR (CDCl_3 , 400 MHz) δ 7.44 (d, $J = 8$ Hz, 2H, ArCH), 6.84 (d, $J = 8$ Hz, 2H, ArCH). $^{13}\text{C}\{^1\text{H}\}$ NMR (101 MHz, CDCl_3) δ 160.02 (quat-C), 133.67 (ArCH), 114.25 (quat-C), 114.03 (ArCH), 83.39-83.24 (t, quat-C), 76.05-75.29 (t), 55.33 (OCH_3).

1-Ethynyl-4-methylbenzene-d1 (3d): ^1H NMR (CDCl_3 , 400 MHz) δ 7.43 (d, $J = 8$ Hz, 2H, ArCH), 7.15 (d, $J = 8$ Hz, 2H, ArCH), 2.38 (s, 3H, CH_3). $^{13}\text{C}\{^1\text{H}\}$ NMR (101 MHz, CDCl_3) δ 139.01 (quat-C), 132.11 (ArCH), 129.16 (ArCH), 119.15 (quat-C), 83.58-83.42 (t, quat-C), 76.74-76.97 (t), 21.55 (CH_3).

1-Ethynyl-2-methoxybenzene-d1 (3f): ^1H NMR (CDCl_3 , 400 MHz) δ 7.48-7.45 (m, 1H, ArCH), 7.34-7.30 (m, 1H, ArCH), 6.93-6.88 (m, 2H, ArCH), 3.90 (s, 3H, OCH_3).

$^{13}\text{C}\{^1\text{H}\}$ NMR (101 MHz, CDCl_3) δ 160.09 (quat-C), 134.35 (ArCH), 129.43 (ArCH), 124.10 (ArCH), 111.90 (quat-C), 111.12 (ArCH), 83.32-83.19 (t, quat-C), 76.15-75.36 (t), 55.20 (OCH_3).

1-Ethynyl-3,5-bis(trifluoromethyl)benzene-d1 (3g): ^1H NMR (CDCl_3 , 400 MHz) δ 7.91 (s, 2H, ArCH), 7.84 (s, 1H, ArCH). $^{13}\text{C}\{^1\text{H}\}$ NMR (101 MHz, CDCl_3) δ 132.22 (ArCH), 132.18 (quat-C, $J = 33.03$ Hz), 124.62 (ArCH), 122.95 (CF_3 , $J = 273.71$ Hz), 122.45 (quat-C), 81.05-80.25 (t, quat-C), 78.11-77.36 (t).

Hept-1-yne-d1 (4a): ^1H NMR (CDCl_3 , 400 MHz) δ 2.18 (t, $J = 8$ Hz, 2H, CH_2), 1.55-1.40 (m, 2H, CH_2), 1.39-1.27 (m, 4H, CH_2), 0.90 (t, $J = 8$ Hz, 3H, CH_3). $^{13}\text{C}\{^1\text{H}\}$ NMR (101 MHz, CDCl_3) δ 84.58-84.43 (t, quat-C), 68.29-67.54 (t), 31.08 (CH_2), 28.34 (CH_2), 22.31 (CH_2), 18.48 (CH_2), 14.08 (CH_3).

Non-1-yne-d1 (4b): ^1H NMR (CDCl_3 , 400 MHz) δ 2.17 (t, $J = 8$ Hz, 2H, CH_2), 1.52 (m, 2H, CH_2), 1.29-1.27 (m, 8H, CH_2), 0.88 (t, $J = 8$ Hz, 3H, CH_3). $^{13}\text{C}\{^1\text{H}\}$ NMR (101 MHz, CDCl_3) δ 84.50-84.35 (t, quat-C), 68.29-67.53 (t), 31.86 (CH_2), 28.92 (CH_2), 28.86 (CH_2), 28.65 (CH_2), 27.75 (CH_2), 18.50 (CH_2), 14.19 (CH_3).

Dodec-1-yne-d1 (4c): ^1H NMR (CDCl_3 , 400 MHz) δ 2.17 (t, $J = 8$ Hz, 2H, CH_2), 1.58-1.50 (m, 2H, CH_2), 1.48-1.26 (m, 14H, CH_2), 0.88 (t, $J = 8$ Hz, 3H, CH_3). $^{13}\text{C}\{^1\text{H}\}$ NMR (101 MHz, CDCl_3) δ 84.46-84.31 (t, quat-C), 68.27-67.54 (t), 32.04 (CH_2), 29.78 (CH_2), 29.66 (CH_2), 29.46 (CH_2), 29.26 (CH_2), 28.91 (CH_2), 28.65 (CH_2), 22.82 (CH_2), 18.50 (CH_2), 14.22 (CH_3).

Tetradec-1-yne-d1 (4d): ^1H NMR (CDCl_3 , 400 MHz) δ 2.17 (t, $J = 8$ Hz, 2H, CH_2), 1.54-1.50 (m, 2H, CH_2), 1.48-1.26 (m, 18H, CH_2), 0.88 (t, $J = 8$ Hz, 3H, CH_3). $^{13}\text{C}\{^1\text{H}\}$ NMR (101 MHz, CDCl_3) δ 84.42-84.27 (t, quat-C), 68.28-67.53 (t), 32.09 (CH_2), 29.83 (CH_2), 29.81 (CH_2), 29.79 (CH_2), 29.69 (CH_2), 29.52 (CH_2), 29.29 (CH_2), 28.93 (CH_2), 28.68 (CH_2), 22.85 (CH_2), 18.51 (CH_2), 14.23 (CH_3).

Hexadec-1-yne-d1 (4e): ^1H NMR (CDCl_3 , 400 MHz) δ 2.17 (t, $J = 8$ Hz, 2H, CH_2), 1.56-1.50 (m, 2H, CH_2), 1.48-1.26 (m, 22H, CH_2), 0.88 (t, $J = 8$ Hz, 3H, CH_3). $^{13}\text{C}\{^1\text{H}\}$ NMR (101 MHz, CDCl_3) δ 84.51-84.37 (t, quat-C), 68.29-67.54 (t), 32.09 (CH_2), 29.85 (CH_2), 29.84 (CH_2), 29.82 (CH_2), 29.78 (CH_2), 29.67 (CH_2), 29.52 (CH_2), 29.28 (CH_2), 28.93 (CH_2), 28.67 (CH_2), 22.85 (CH_2), 18.52 (CH_2), 14.26 (CH_3).

4-Methylpent-1-yne-d1 (4f): ^1H NMR (CDCl_3 , 400 MHz) δ 2.08 (d, $J = 8$ Hz, 2H, CH_2), 1.82 (Sept, $J = 6$ Hz, 1H, $^i\text{PrCH}$), 0.99 ((d, $J = 4$ Hz, 6H, $^i\text{PrCH}_3$). $^{13}\text{C}\{^1\text{H}\}$ NMR (101 MHz, CDCl_3) δ 83.91-83.17 (t, quat-C), 67.93-67.15 (t), 33.88 (CH_2), 28.17 (CH), 21.97 (CH_3).

5-Methylhex-1-yne-d1 (4g): ^1H NMR (CDCl_3 , 400 MHz) δ 2.18 (t, $J = 8$ Hz, 2H, CH_2), 1.73-1.66 (m, 1H, $^i\text{PrCH}$), 1.46-1.39 (m, 2H, CH_2), 0.89 (d, $J = 4$ Hz, 6H, $^i\text{PrCH}_3$). $^{13}\text{C}\{^1\text{H}\}$ NMR (101 MHz, CDCl_3) δ 83.97-83.27 (t, quat-C), 67.23-66.55 (t), 42.77 (CH_2), 26.78 (CH), 22.33 (CH_3), 18.51(CH_3).

3-Methylhex-1-yne-d1 (4h): ^1H NMR (CDCl_3 , 400 MHz) δ 2.43 (m, 1H, CH), 1.49-1.39 (m, 4H, CH_2), 1.17 (d, $J = 8$ Hz, 3H, CH_3), 0.91 (t, $J = 6$ Hz, 3H, CH_3). $^{13}\text{C}\{^1\text{H}\}$ NMR (101 MHz, CDCl_3) δ 84.15-83.57 (t, quat-C), 67.33-66.85 (t), 38.12 (CH_2), 33.90 (CH), 20.54 (CH_3), 19.11 (CH_2), 13.45 (CH_3).

But-3-yn-1-ylbenzene-d1 (4i): ^1H NMR (CDCl_3 , 400 MHz) δ 7.30 (m, 2H, ArCH), 7.23 (m, 3H, ArCH), 2.86 (t, $J = 8\text{Hz}$, 2H, CH_2), 2.49 (t, $J = 8\text{Hz}$, 2H, CH_2). $^{13}\text{C}\{^1\text{H}\}$ NMR (101 MHz, CDCl_3) δ 140.57 (quat-C), 128.55 (ArCH), 128.54 (ArCH), 126.50 (ArCH), 83.55-83.40 (t, quat-C), 69.18-68.78 (t), 34.99 (CH_2), 20.67 (CH_2).

3-(Prop-2-yn-1-yloxy)prop-1-ene-d1 (4j): ^1H NMR (CDCl_3 , 400 MHz) δ 5.94-5.84(m, 1H, Olefinic-CH), 5.32-5.22 (m, 2H, Olefinic- CH_2), 4.14 (s, 2H, CH_2), 4.06 (d, $J = 8$ Hz, 2H, CH_2). $^{13}\text{C}\{^1\text{H}\}$ NMR (101 MHz, CDCl_3) δ 133.95 (Olefinic-CH),

118.06 (Olefinic-CH₂), 79.37-79.22 (t, quat-C), 74.64-73.88 (t), 70.67 (CH₂), 57.14 (CH₂).

Prop-2-yn-1-yl acrylate-d1 (4k): ¹H NMR (CDCl₃, 400 MHz) δ 6.43 (d, *J* = 20 Hz, 1H, Olefinic-CH), 6.12 (m, 1H, Olefinic-CH₂), 5.86 (d, *J* = 12 Hz, 1H, Olefinic-CH), 4.73 (s, 2H, OCH₂). ¹³C{¹H} NMR (101 MHz, CDCl₃) δ 165.33 (Carbonyl-C), 131.97 (Olefinic-CH), 127.64 (Olefinic-CH₂), 77.61-77.08 (t, quat-C), 75.21-74.44 (t), 52.09 (CH₂).

Prop-2-yn-1-yl benzoate-d1 (4l): ¹H NMR (CDCl₃, 400 MHz) δ 8.06 (d, *J* = 8 Hz, 2H, ArCH), 7.56 (t, *J* = 6 Hz, 1H, ArCH), 7.43 (t, *J* = 8 Hz, 2H, ArCH), 4.91 (s, 2H, OCH₂). ¹³C{¹H} NMR (101 MHz, CDCl₃) δ 165.80 (Carbonyl-C), 133.37 (ArCH), 129.84 (ArCH), 129.45 (quat-C), 128.48 (ArCH), 77.43-77.28 (t, quat-C), 75.26-74.49 (t), 52.47 (CH₂).

2-((Prop-2-yn-1-yloxy)methyl)oxirane-d1 (4m): ¹H NMR (CDCl₃, 400 MHz) δ 4.20 (d, *J* = 4 Hz, 2H, CH₂), 3.80 (t, *J* = 8 Hz, 1H, CH), 3.47 (t, *J* = 8 Hz, 1H, CH), 3.15 (m, 1H, CH), 2.78 (t, *J* = 4 Hz, 1H, OCH₂), 2.61 (m, 1H, OCH₂). ¹³C{¹H} NMR (101 MHz, CDCl₃) δ 79.06-78.91 (t, quat-C), 75.19-74.43 (t), 70.49 (OCH₂), 58.60 (OCH₂), 50.67 (CH), 44.45 (CH₂).

1-(Prop-2-yn-1-yl)-1H-indole-d1 (4n): ¹H NMR (CDCl₃, 400 MHz) δ 7.74 (d, *J* = 8 Hz, 1H, ArCH), 7.47 (d, *J* = 8 Hz, 1H, ArCH), 7.34 (t, *J* = 8 Hz, 1H, ArCH), 7.27-7.22 (m, 2H, ArCH), 6.63 (d, *J* = 4 Hz, 1H, ArCH), 4.89 (s, 2H, CH₂). ¹³C{¹H} NMR (101 MHz, CDCl₃) δ 135.86 (quat-C), 128.97 (quat-C), 127.33 (ArCH), 121.97 (ArCH), 121.21 (ArCH), 119.97 (ArCH), 109.42 (ArCH), 102.16 (ArCH), 77.33-76.84 (t, quat-C), 73.74-72.97 (t), 35.79 (CH₂).

Ethynyltrimethylsilane-d1 (4o): ^1H NMR (CDCl_3 , 400 MHz) δ 0.06 (s, 9H, CH_3). $^{13}\text{C}\{^1\text{H}\}$ NMR (101 MHz, CDCl_3) δ 89.11-88.67(t, quat-C), 73.55-76.94 (t), 3.09 (CH_3).

(But-3-yn-1-yloxy)(tert-butyl)dimethylsilane-d1 (4p): ^1H NMR (CDCl_3 , 400 MHz) δ 3.72 (t, $J = 8$ Hz, 2H, OCH_2), 1.94 (t, $J = 6$ Hz, 2H, CH_2), 0.88 (s, 9H, CH_3), 0.06 (s, 6H, CH_3). $^{13}\text{C}\{^1\text{H}\}$ NMR (101 MHz, CDCl_3) δ 81.21-81.06 (t, quat-C), 69.57-68.82 (t), 61.88 (OCH_2), 26.00 (CH_3), 22.94 (CH_2), 18.45 (quat-C), 5.18 (CH_3).

Trimethyl((prop-2-yn-1-yloxy)methyl)silane-d1 (4q): ^1H NMR (CDCl_3 , 400 MHz) δ 4.26 (s, 2H, OCH_2), 0.15 (s, 9H, CH_3), 0.06 (s, 2H, TMS- CH_2). $^{13}\text{C}\{^1\text{H}\}$ NMR (101 MHz, CDCl_3) δ 81.75-81.60 (t, quat-C), 74.10-73.34 (t), 50.86 (OCH_2), 2.07(CH_3), 1.42 (TMS- CH_2).

(But-3-yn-2-yloxy)trimethylsilane-d1: ^1H NMR (CDCl_3 , 400 MHz) δ 4.51 (q, $J = 6$ Hz, 1H, CH), 1.46 (d, $J = 8$ Hz, 3H, CH_3), 0.15 (s, 9H, CH_3). $^{13}\text{C}\{^1\text{H}\}$ NMR (101 MHz, CDCl_3) δ 85.57-85.42 (t, quat-C), 72.31-71.93 (t), 58.12 (OCH), 24.26 (CH_3), 2.06 (CH_3).

Pent-1-yn-3-ol-d2: ^1H NMR (CDCl_3 , 400 MHz) δ 4.29 (t, $J = 8$ Hz, 1H, OCH), 1.76-1.68 (m, 2H, CH_2), 1.00 (t, $J = 8$ Hz, 3H, CH_3). $^{13}\text{C}\{^1\text{H}\}$ NMR (101 MHz, CDCl_3) δ 84.52-84.37 (t, quat-C), 73.09-72.33 (t), 63.43 (OCH), 30.73 (CH_2), 9.38 (CH_3).

Hept-1-yn-3-ol-d2: ^1H NMR (CDCl_3 , 400 MHz) δ 4.33 (t, $J = 8$ Hz, 1H, OCH), 1.74-1.67 (m, 2H, CH_2), 1.47-1.30 (m, 4H, CH_2), 0.91 (t, $J = 8$ Hz, 3H, CH_3). $^{13}\text{C}\{^1\text{H}\}$ NMR (101 MHz, CDCl_3) δ 84.83-84.68 (t, quat-C), 72.82-72.58 (t), 62.12 (OCH), 37.33 (CH_2), 27.25 (CH_2), 22.40 (CH_2), 14.03 (CH_3).

3-Methylpent-1-yn-3-ol-d2: ^1H NMR (CDCl_3 , 400 MHz) δ 1.70-1.62 (m, 2H, CH_2), 1.44 (s, 3H, CH_3), 1.01 (t, $J = 8$ Hz, 3H, CH_3). $^{13}\text{C}\{^1\text{H}\}$ NMR (101 MHz, CDCl_3) δ

87.67-87.15 (t, quat-C), 71.50-70.74 (t), 68.49 (quat-C), 36.36 (CH₃), 29.15 (CH₂), 8.91 (CH₃).

3-Ethylpent-1-yn-3-ol-d2: ¹H NMR (CDCl₃, 400 MHz) δ 1.68-1.61 (m, 4H, CH₂), 1.03-0.98 (m, 6H, CH₃). ¹³C{¹H} NMR (101 MHz, CDCl₃) δ. 86.19-86.05 (t, quat-C), 72.51-71.05 (t), 71.94 (quat-C), 34.22 (CH₂), 8.48 (CH₃).

1-Ethynylcyclopentanol-d2: ¹H NMR (CDCl₃, 400 MHz) δ 1.94-1.91 (m, 4H, CH₂), 1.80-1.70 (m, 4H, CH₂). ¹³C{¹H} NMR (101 MHz, CDCl₃) δ 87.59-87.44 (t, quat-C), 74.15 (quat-C), 71.31-70.55 (t), 42.30 (CH₂), 23.44 (CH₂).

3-Methylpent-1-en-4-yn-3-ol-d2: ¹H NMR (CDCl₃, 400 MHz) δ 5.94 (m, 1H, Olefinic-CH), 5.51 (d, *J* = 16 Hz, 1H, Olefinic-CH₂), 5.12 (d, *J* = 12 Hz, 1H, Olefinic-CH), 1.54 (s, 3H, CH₃). ¹³C{¹H} NMR (101 MHz, CDCl₃) δ 141.62 (Olefinic-CH), 114.08 (Olefinic-CH₂), 85.90-85.38 (t, quat-C), 73.11-72.35, (t), 68.09 (quat-C), 29.96 (CH₃).

Prop-2-yn-1-amine-d3: ¹H NMR (CDCl₃, 400 MHz) δ 3.39 (s, 2H, CH₂). ¹³C{¹H} NMR (101 MHz, CDCl₃) δ 85.56-85.05 (t, quat-C), 71.58-70.63 (t), 31.18 (CH₂).

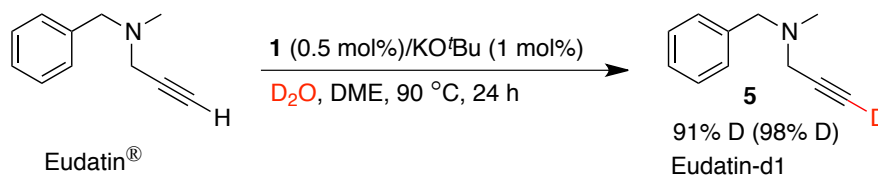
1,4-Bis(prop-2-yn-1-yloxy)but-2-yne-d2: ¹H NMR (CDCl₃, 400 MHz) δ 4.26 (s, 4H, OCH₂), 4.20 (s, 4H, OCH₂). ¹³C{¹H} NMR (101 MHz, CDCl₃) δ 82.09 (quat-C), 78.44-78.29 (t, quat-C), 75.29-74.52 (t), 56.65 (OCH₂), 56.45 (OCH₂).

1,4-Bis((prop-2-yn-1-yloxy)methyl)benzene-d2: ¹H NMR (CDCl₃, 400 MHz) δ 7.35 (s, 4H, ArCH), 4.60 (s, 4H, OCH₂), 4.16 (s, 4H, OCH₂). ¹³C{¹H} NMR (101 MHz, CDCl₃) δ 137.06 (quat-C), 128.28 (ArCH), 79.31-79.16 (t, quat-C), 74.92-74.15 (t), 71.27 (OCH₂), 57.09 (OCH₂).

1,3,5-Tris(prop-2-yn-1-yloxy)benzene-d3: ¹H NMR (CDCl₃, 400 MHz) δ 6.26 (s, 3H, ArCH), 4.63 (s, 6H, OCH₂). ¹³C{¹H} NMR (101 MHz, CDCl₃) δ

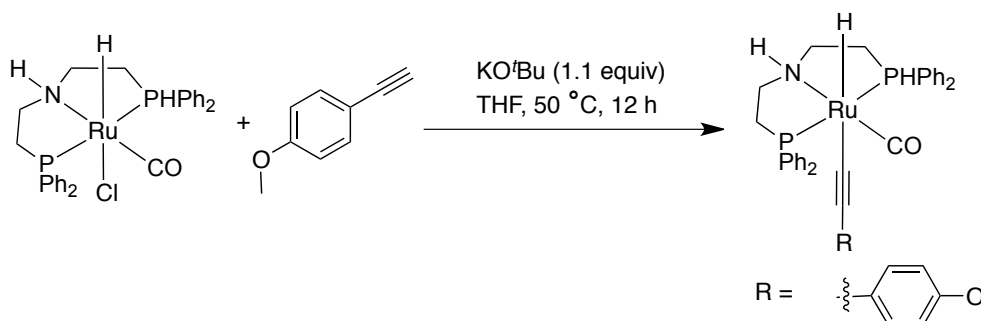
162.19 (quat-C), 92.77 (ArCH), 84.27-83.15 (t, quat-C), 77.58-76.10 (t), 56.89 (OCH₂).

Synthesis of Eudatin-d1 (5):



In a screw-cap scintillation vial *N*-benzyl-*N*-methylprop-2-yn-1-amine (0.5 mmol, 80 mg), **1** (0.0025 mmol, 1.5 mg), KO^tBu (0.005 mmol, 0.6 mg) and 1,2-dimethoxyethane (1 mL) were added under nitrogen atmosphere. Degassed D₂O (0.25 mL, 12.5 mmol) was added under nitrogen atmosphere and the reaction vial immersed into a preheated oil bath of 90 °C. After 24 h the solvent is evaporated and the product is extracted with dichloromethane. The combined organic layers then dried over sodium sulfate and after removal of solvent under vacuum provided 91% deuterium incorporated Eudatin-d1. ¹H NMR (CDCl₃, 400 MHz) δ 7.41-7.29 (m, 5H, ArCH), 3.63 (CH₂), 3.36 (CH₂), 2.40 (CH₃). ¹³C{¹H} NMR (101 MHz, CDCl₃) δ 138.38 (quat-C), 129.23 (ArCH), 128.37 (ArCH), 127.28 (ArCH), 78.20-78.06 (t, quat-C), 73.60-72.85 (t), 59.99 (CH₂), 44.85 (CH₂), 41.78 (CH₃).

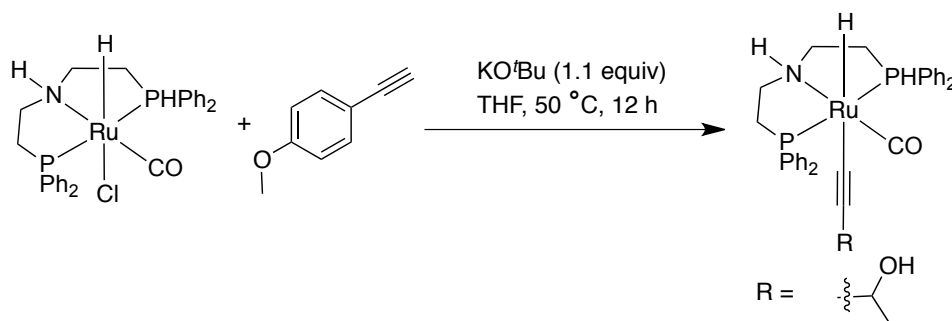
Synthesis and Characterization of Ru-Acetylide Complex 2a:



In a screw cap scintillation vial Ru-macho **1** (0.032 mmol, 20 mg), KO^tBu (1.1 equiv, 0.035 mmol, 4 mg) and THF (1 mL) were added and the resulting mixture was

allowed to stir at room temperature for 30 min. To the reddish-brown solution 4-ethynyl-anisole (1.1 equiv. 0.035 mmol, 4 μ l) was added dropwise. The resulting solution then stirred for another 12 h at 50 °C. The volume of light yellow solution was reduced under vacuum and slow addition of cold hexane (2 mL) provided light yellow precipitate. The solution was decanted and the precipitate was washed with hexane (1 mL) three times. The precipitate was dried under vacuum for overnight to afford **2a** as light yellow solid in 77% yield (17.30 mg). IR (C₆H₆): 3428, 2092 (Ru-H), 1915, 1610, 1384, 1266, 1176, 1100, 962, 896, 741 cm⁻¹. ¹H NMR (CDCl₃): δ 8.21 (m, 4H, ArCH), 7.98 (m, 4H, ArCH), 7.09 (m, 16H, ArCH), 3.28 (s, 3H, OCH₃), 3.13 (br s, 1H, NH), 2.42 (br, 2H, CH₂), 2.25 (br, 2H, CH₂), 2.09 (t, *J* = 16 Hz, 2H, CH₂), 1.92 (t, *J* = 12 Hz, 2H, CH₂), -7.68 (t, *J* = 20 Hz, 1H, Ru-H). ³¹P{¹H} NMR (CDCl₃): δ 58.21 (s).

Synthesis and Characterization of Ru-Acetylide Complex **2b**:



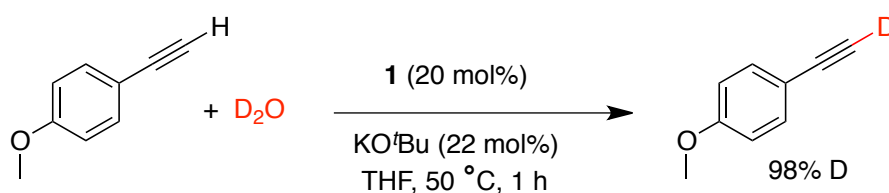
In a screw cap scintillation vial Ru-macho **1** (0.032 mmol, 20 mg), KO^tBu (1.1 equiv, 0.035 mmol, 4 mg) and THF (1 mL) were added and the resulting mixture was allowed to stir at room temperature for 30 min. To the light yellow solution pent-1-yn-3-ol (1.1 equiv. 0.035 mmol, 3 μ l) was added dropwise. The resulting solution then stirred for another 3 h. The volume of light yellow solution was then reduced under vacuum and slow addition of cold hexane (2 mL) provided light yellow precipitate. The solution was decanted and the precipitate was washed with hexane (1

mL) three times. The resulted yellow complex was dried under vacuum for overnight (17 mg, 80%). IR (C₆H₆): 3431, 2923, 2038 (Ru–H), 1924, 1734, 1603, 1495, 1177, 1100, 835, 729 cm⁻¹. ¹H NMR (CDCl₃): δ 8.05 (m, 4H, ArCH), 7.99 (m, 4H, ArCH), 7.00 (m, 12H, ArCH), 4.30 (t, *J* = 8 Hz, 1H, OCH), 3.38 (br s, 1H, NH), 2.37 (br, 4H, CH₂), 2.14 (br, 2H, CH₂), 1.91 (br, 2H, CH₂), 1.64 (m, 2H, CH₂), 0.91 (t, *J* = 8 Hz, 3H, CH₃), -7.76 (t, *J* = 20 Hz, 1H, Ru–H). ³¹P{¹H} NMR (CDCl₃): δ 58.61 (s).

Determination of the Molecular Structure of 2b in the Solid State by X-ray Single Crystal Diffraction: Single crystals of complex **2b** suitable for X-ray analysis were obtained from a solution of benzene and hexane. A crystal suited for single crystal x-ray diffraction measurements was mounted on a glass fibre. Geometry and intensity data were collected with a Bruker SMART D8 goniometer equipped with an APEX CCD detector and with an Incoatec microsource (Mo-K α radiation, λ = 0.71073 Å, multilayer optics). Temperature was controlled using an Oxford Cryostream 700 instrument. Intensities were integrated with SAINT⁺²³ and corrected for absorption with SADABS.²⁴ The structure was solved by direct methods and refined on *F*² with SHELXL-97.^{25,26}

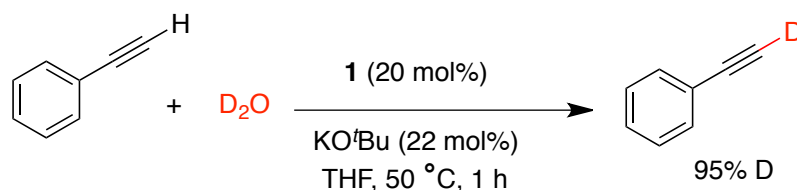
Crystal Data of Ru-Acetylide Complex 2b: C₄₀H₄₃NO₂P₂Ru, crystal dimensions: 0.1 × 0.1 × 0.09, monoclinic with space group P121/c, *a* = 13.3813 (7)Å, *b* = 13.5583 (7) Å, *c* = 20.6709 (11) Å, α = 90°, β = 104.397 (3)°, γ = 90°, *V* = 3632.5 (3)Å³, *Z* = 4, *T* = 100 K, $2\theta_{\max}$ = 29.587, ρ_{calcd} = 1.340 g/cm³, μ (MoK α) = 0.554 mm⁻¹. min/max transmission factors = 0.6087/0.7459, 10155 Reflections collected, 8833 unique (*R*1 = 0.0574), *WR*2 = 0.1611 (all data). The structure has been deposited at the CCDC data center and can be retrieved by using the number CCDC **1445337**.

Catalytic Experiment to Observe the Intermediacy of 2a:



In a screw cap NMR tube Ru-macho **1** (0.024 mmol, 15 mg), KO^tBu (0.026 mmol, 3 mg) and THF (0.4 mL) were added under nitrogen atmosphere and the resulting reaction mixture shaken for 10 minutes. 4-Ethynyl anisole (0.12 mmol, 16 μ l) was added slowly and then deuterium oxide (0.1 mL) was added under nitrogen atmosphere. The NMR tube then heated to 50 °C and monitored by 1H and ^{31}P NMR spectroscopy.

Catalytic Experiment in Absence of Base Using 2a as Catalyst:



In a screw cap scintillation vial phenylacetylene (0.5 mmol, 55 μ l), **2a** (0.00099 mmol, 0.7 mg), DME (0.3 mL) and D_2O (0.2 mL) were added under nitrogen atmosphere. The reaction vial then heated to 50 °C. After 16 h the resulted residue was extracted with dichloromethane and the combined organic phase is dried over sodium sulfate. Solvent was removed under reduced pressure and the product was analysed by 1H and ^{13}C NMR spectroscopy.

3.6 NOTES AND REFERENCES

- (1) (a) Junk, T.; Catallo, W. J. *Chem. Soc. Rev.* **1997**, *26*, 401-406. (b) Derdau, J. V.; Fey, T.; Zimmermann, J. *Angew. Chem. Int. Ed.* **2007**, *46*, 7744-7765.
- (2) Zhu, X.; Liu, J.; Zhang, W. *Nat. Chem. Biol.* **2015**, *11*, 115-120.
- (3) Thirumurugan, P.; Matosiuk, D.; Jozwiak, K. *Chem. Rev.* **2013**, *113*, 4905-4979.
- (4) Wei, L.; Hu, F.; Shen, Y.; Chen, Z.; Yu, Y.; Lin, C.; Wang, M. C.; Min, W. *Nature Methods* **2014**, *11*, 410-412.
- (5) (a) Minto, R. E.; Blacklock, B. J. *Prog. Lipid Res.* **2008**, *47*, 233-306. (b) Sin, N.; Meng, L.; Auth, H.; Crews, C. M. *Bioorg. Med. Chem.* **1998**, *6*, 1209-1217.
- (6) For selected examples, see (a) Gunanathan, C.; Hölscher, M.; Pan, F.; Leitner, W. *J. Am. Chem. Soc.* **2012**, *134*, 14349-14352. (b) Oh, C. H.; Jung, H. H.; Kim, K. S.; Kim, N. *Angew. Chem., Int. Ed.*, **2003**, *42*, 805-808. (c) Chou, M.; Mandal, A. B.; Leung, M. *J. Org. Chem.* **2002**, *67*, 1501-1505.
- (7) Cintrat, J. C.; Pillion, F.; Rousseau, B. *Tetrahedron Lett.* **2001**, *42*, 5001-5003.
- (8) Hashmi, A. S. K.; Rudolph, M.; Siehl, H. -U.; Tanaka, M.; Bats, J. W.; Frey, W. *Chem. Eur. J.* **2008**, *14*, 3703-3708.
- (9) (a) Sirokán, G.; Molnar, á.; Bartók, M. *J. Labelled Compds. Radiopharm.* **1989**, *27*, 439-448. (b) Zhang, G.; Cui, L.; Wang, Y.; Zhang, L. *J. Am. Chem. Soc.* **2010**, *132*, 1474-1475 (c) Yabe, Y.; Sawama, Y.; Monguchi, Y.; Sajiki, H. *Chem. Eur. J.* **2013**, *19*, 484-488. (d) Yamada, T.; Park, K.; Monguchi, Y.; Sawama, Y.; Sajiki, H. *RSC Adv.*, **2015**, *5*, 92954-92957.
- (10) (a) Tsuchimoto, T.; Matsubayashi, H.; Kaneko, M.; Nagase, Y.; Miyamura, T.; Shirakawa, E. *J. Am. Chem. Soc.* **2008**, *130*, 15823-15835. (b) Bew, S. P.; Hiatt-Gipson, G. D.; Lovell, J. A.; Poullain, C. *Org. Lett.* **2012**, *14*, 456-459. (c)

Perez, F.; Ren, Y.; Boddaert, T.; Rodriguez, J.; Coquerel, Y. *J. Org. Chem.*, **2015**, *80*, 1092-1097.

(11) (a) Lewandos, G. S.; Maki, J. W.; Ginnebaug, J. P. *Organometallics* **1982**, *1*, 1700-1705. (b) Sabot, C.; Kumar, K. A.; Antheaume, C.; Mioskowski, C. *J. Org. Chem.* **2007**, *72*, 5001-5004. (c) Ito, J.; Asai, R.; Nishiyama, H. *Org. Lett.* **2010**, *12*, 3860-3862.

(12) Chatterjee, B.; Gunanathan, C. *Org. Lett.* **2015**, *17*, 4794-4797.

(13) See Figures 3.2 and 3.3.

(14) For ruthenium catalyzed arene C-H deuteration using deuterium oxide, see (a) Prechtel, M. H. G.; Hoelscher, M.; Ben-David, Y.; Theyssen, N.; Loschen, R.; Milstein, D.; Leitner, W. *Angew. Chem. Int. Ed.* **2007**, *46*, 2269-2272. (b) Prechtel, M. H. G.; Hoelscher, M.; Ben-David, Y.; Theyssen, N.; Milstein, D.; Leitner, W. *Eur. J. Inorg. Chem.* **2008**, 3493-3500.

(15) Sanderson, K. *Nature* **2009**, *458*, 269.

(16) Zhang, Z.; Jiang, X. *Org. Lett.* **2014**, *16*, 4400-4403.

(17) Yu, R. P.; Hesk, D.; Rivera, N.; Pelczer, I.; Chirik, P. J. *Nature* **2016**, *529*, 195-199.

(18) Zhang, Z.; Jiang, X. *Org. Lett.* **2014**, *16*, 4400-4403.

(19) For reviews on O-H activation by ruthenium pincer complexes, see: (a) Gunanathan, C.; Milstein, D. *Acc. Chem. Res.* **2011**, *44*, 588-602. (b) Gunanathan, C.; Milstein, D. *Chem. Rev.* **2014**, *114*, 12024-12087.

(20) Bruneau, C.; Dixneuf, P. H. *Angew. Chem. Int. Ed.* **2006**, *45*, 2176-2203.

(21) (a) Yang, H.; Chung, C.; Lin, Y.; Liu, Y. *Dalton Trans.* **2011**, *40*, 3703-3710.

- (22) Khusnutdinova, J. R.; Milstein, D. *Angew. Chem. Int. Ed.* **2015**, *54*, 12236-12273.
- (23) Bruker AXS, SAINT+, Program for Reduction of Data collected on Bruker CCD Area Detector Diffractometer V. 6.02. Bruker AXS Inc., Madison, Wisconsin, USA, 1999.
- (24) Bruker AXS, SADABS, Program for Empirical Absorption Correction of Area Detector Data V 2004/1, Bruker AXS Inc., Madison, Wisconsin, USA, 2004.
- (25) Sheldrick, G. M. *Acta Crystallogr.* **2008**, *A64*, 112-122.
- (26) Dolomanov, O. V.; Bourhis, L. J.; Gildea, R. J.; Howard, J. A. K.; Puschmann, H. J. *Appl. Crystallogr.* **2009**, *42*, 339-341.

NMR Spectra of Deuterated Terminal Alkynes:

Figure 3.3 Stacked ^{31}P NMR spectra of the catalytic reaction for the deuteration of 4-ethynyl anisole catalyzed by **2a**

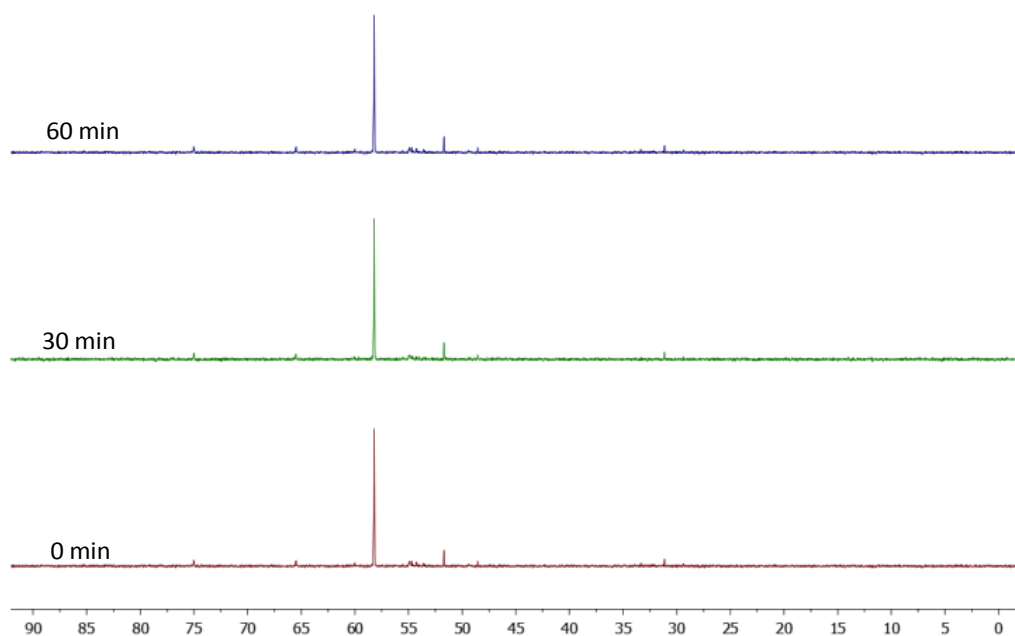


Figure 3.4 Stacked ^1H NMR spectra (- ppm) of the catalytic reaction for the deuteration of 4-ethynyl anisole catalyzed by **2a**

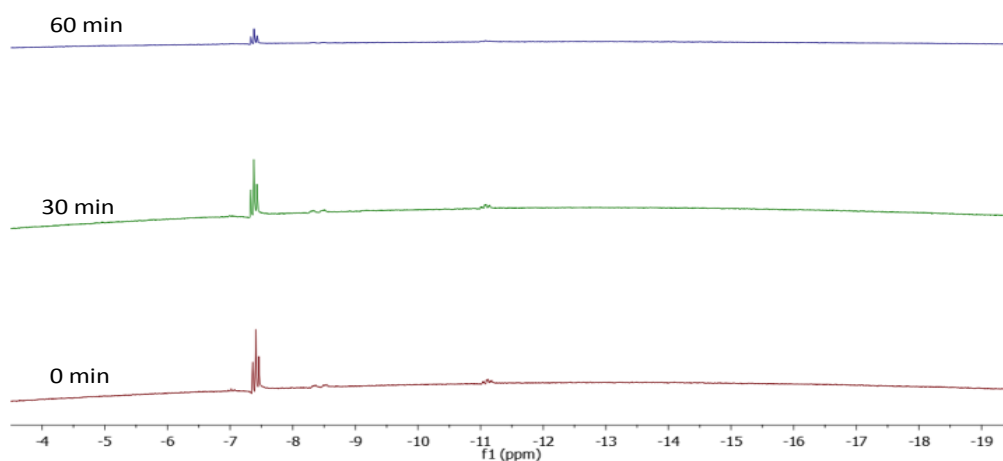


Figure 3.5 ^1H NMR spectrum of 1-ethynyl-4-methoxybenzene-d1 (400 MHz, CDCl_3):

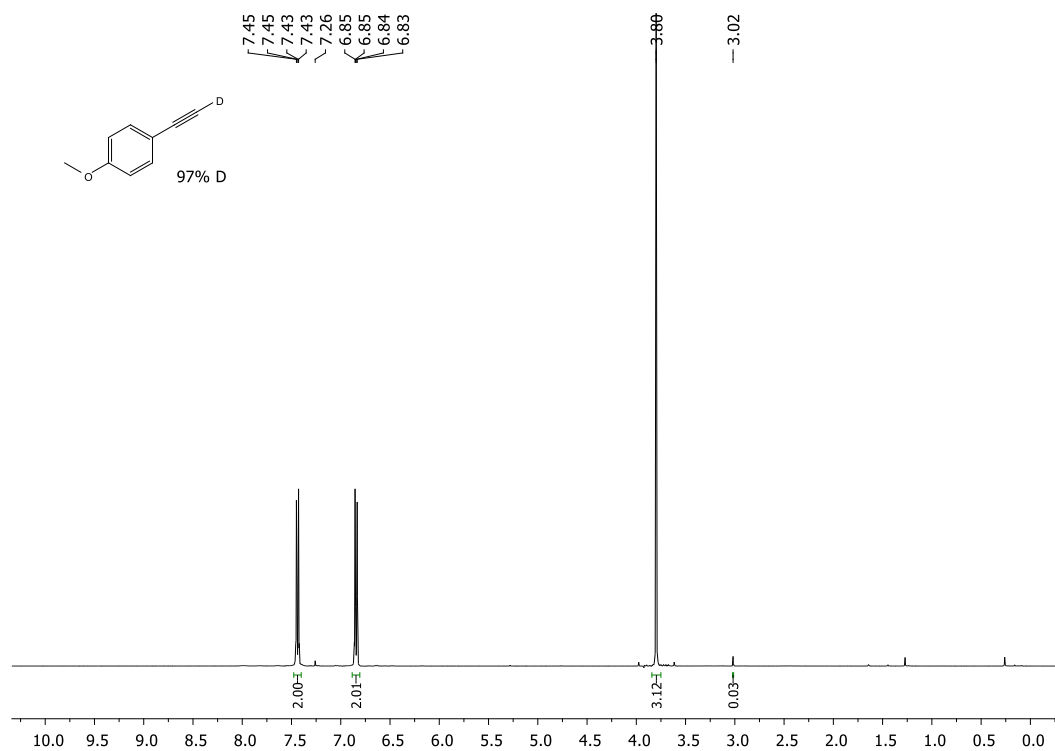


Figure 3.6 ^{13}C NMR spectrum of 1-ethynyl-4-methoxybenzene-d1 (100.6 MHz, CDCl_3):

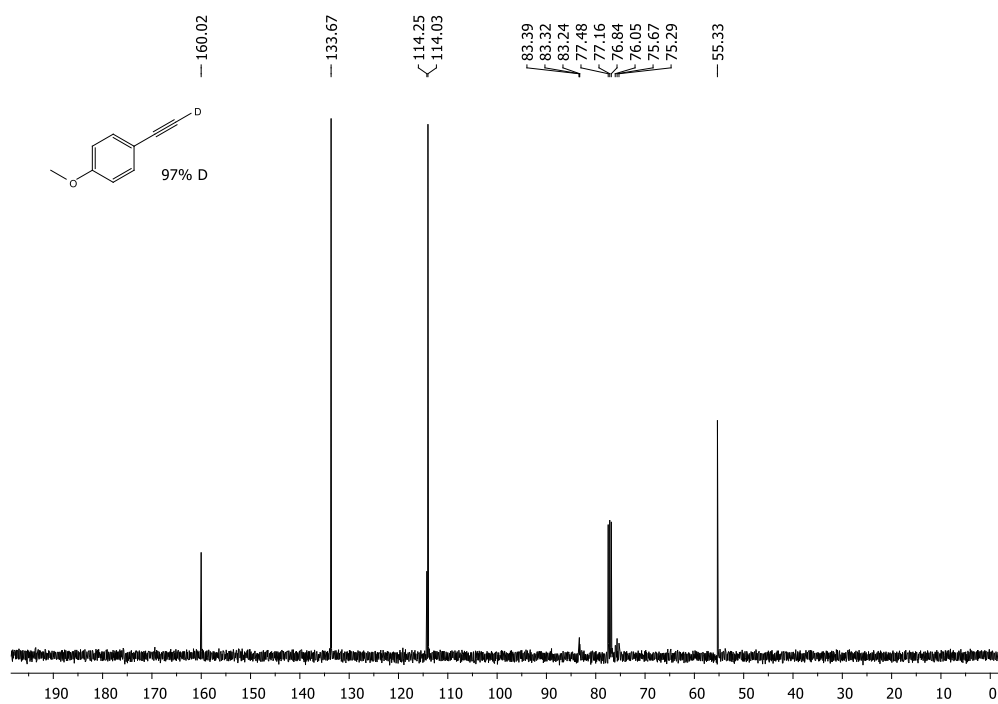


Figure 3.7 ^1H NMR spectrum of 1,4-bis(prop-2-yn-1-yloxy)but-2-yne-d₂ (400 MHz, CDCl_3):

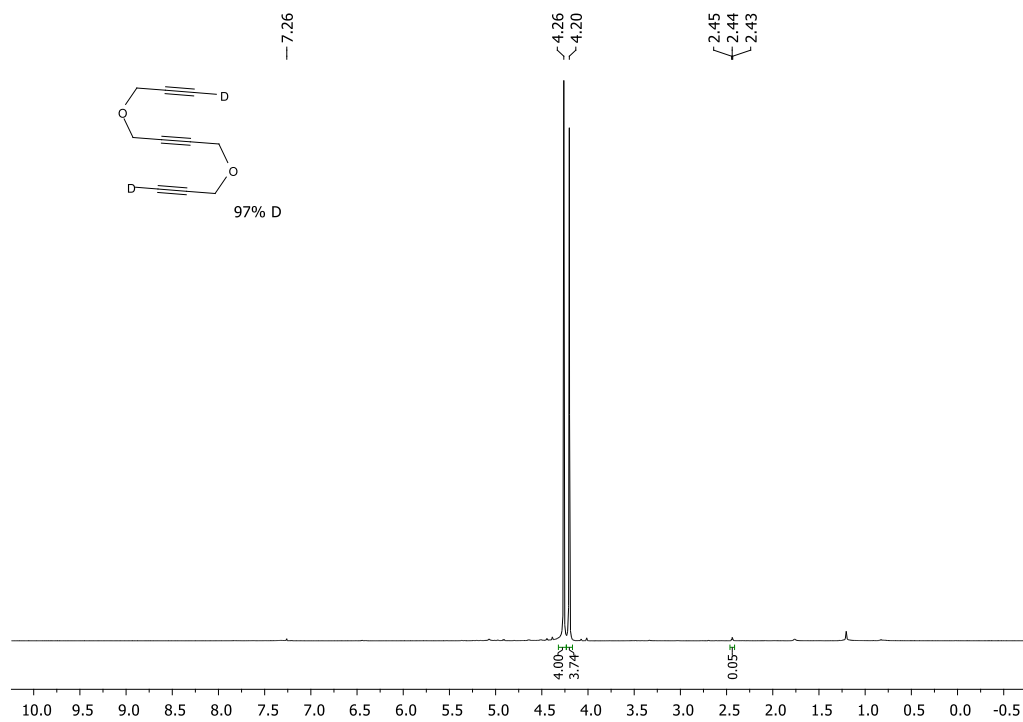


Figure 3.8 ^{13}C NMR spectrum of 1,4-bis(prop-2-yn-1-yloxy)but-2-yne-d₂ (100.6 MHz, CDCl_3):

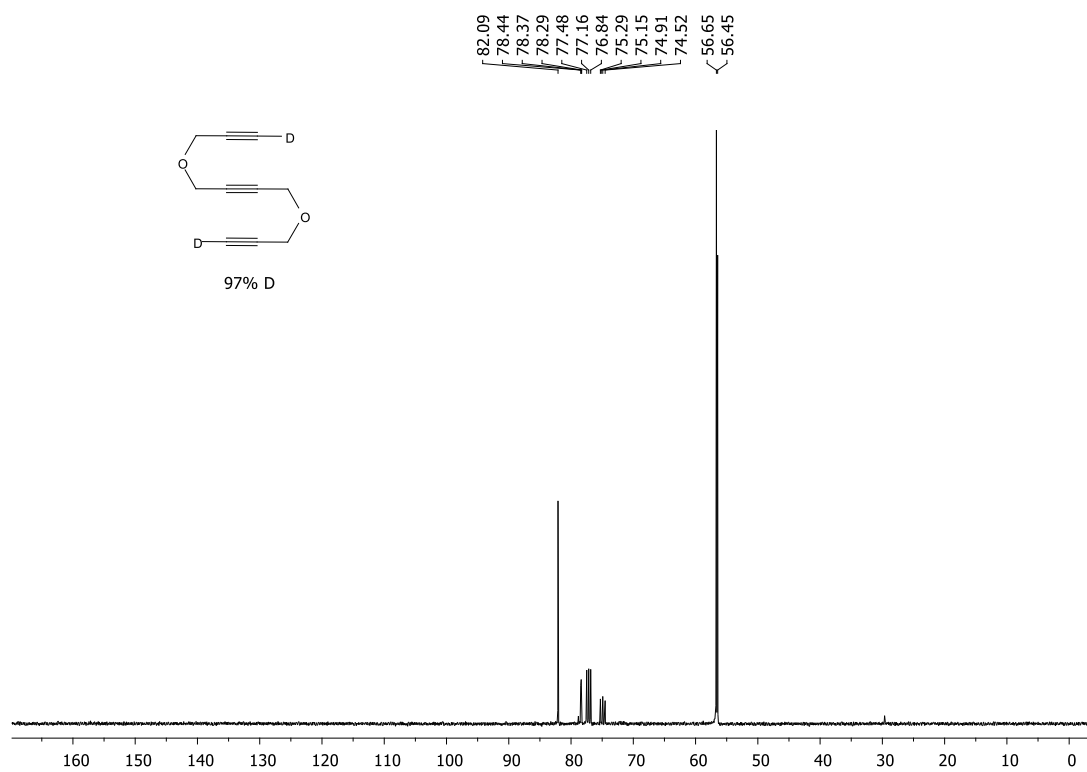


Figure 3.9 ^1H NMR spectrum of 1,4-bis((prop-2-yn-1-yloxy)methyl)benzene-d₂ (400 MHz, CDCl_3):

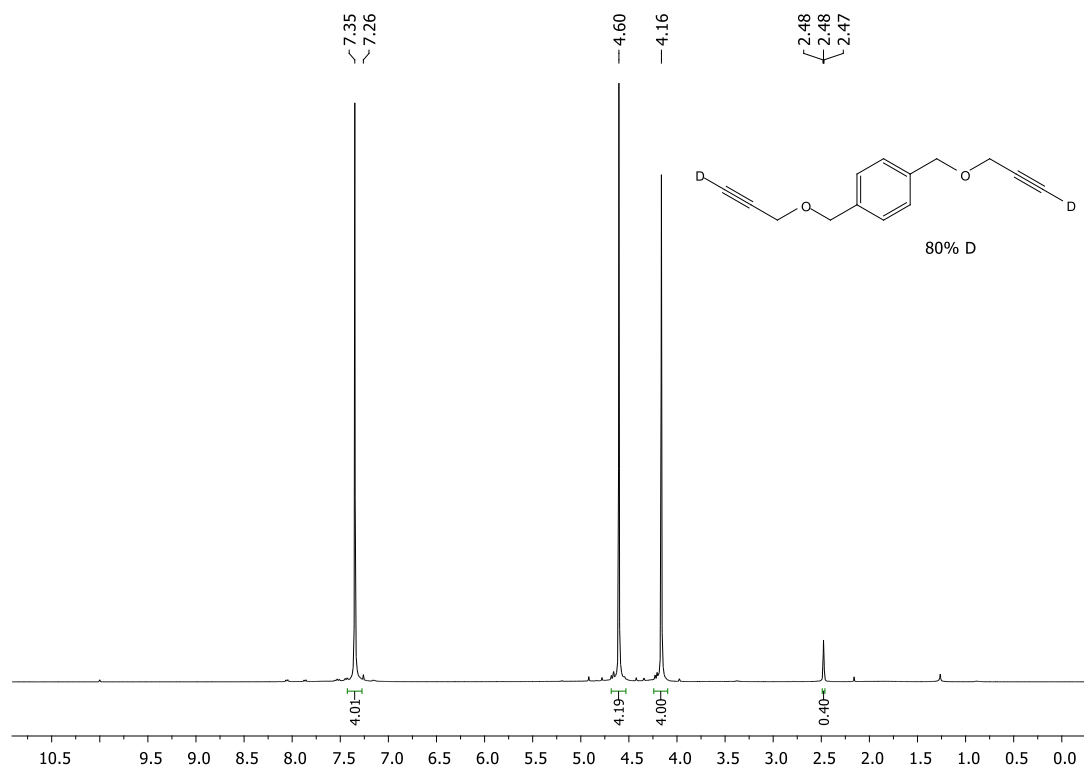


Figure 3.10 ^{13}C NMR spectrum of 1,4-bis((prop-2-yn-1-yloxy)methyl)benzene-d₂ (100.6 MHz, CDCl_3):

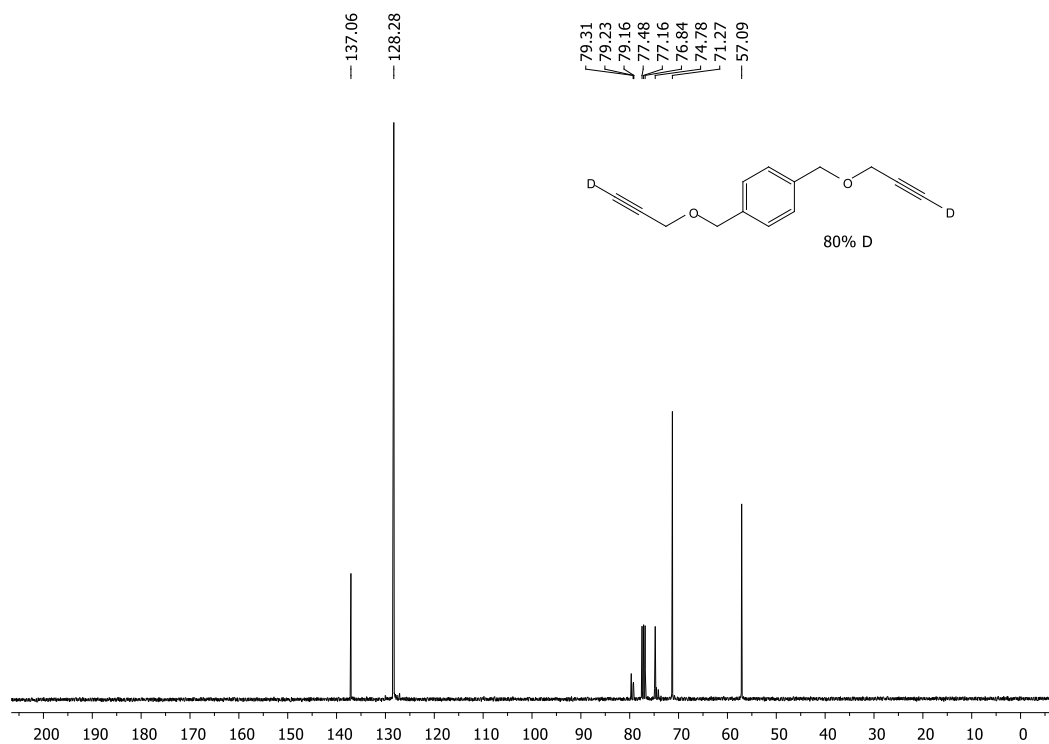


Figure 3.11 ^1H NMR spectrum of N-benzyl-N-methylprop-2-yn-1-amine-d1 (400 MHz, CDCl_3):

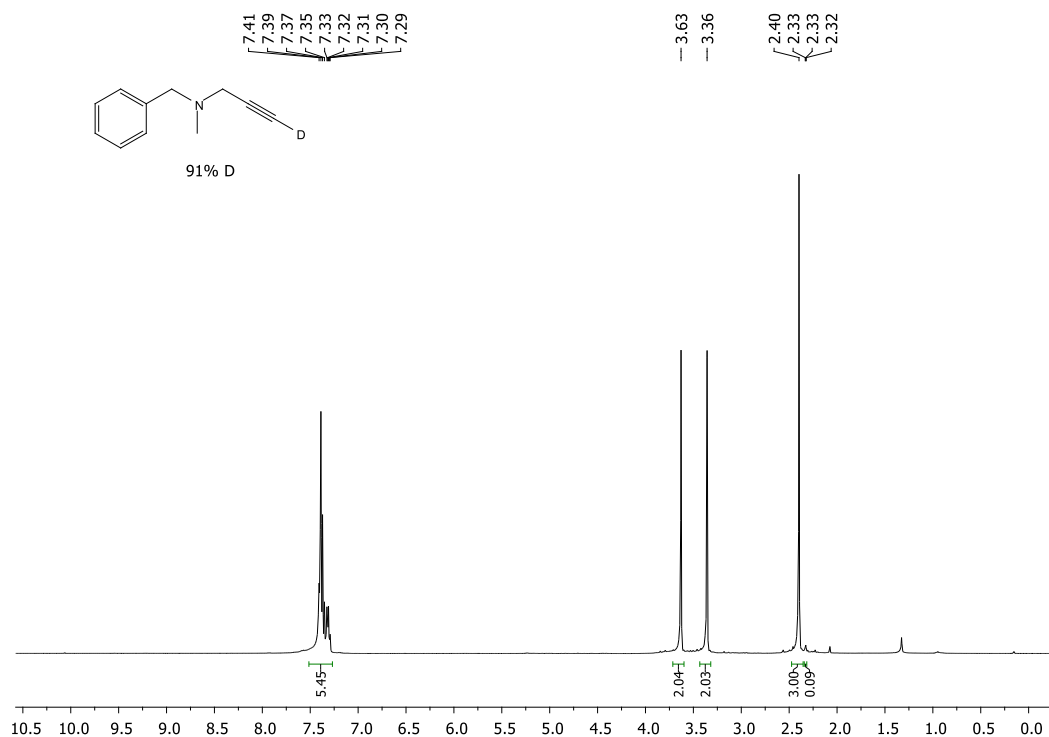
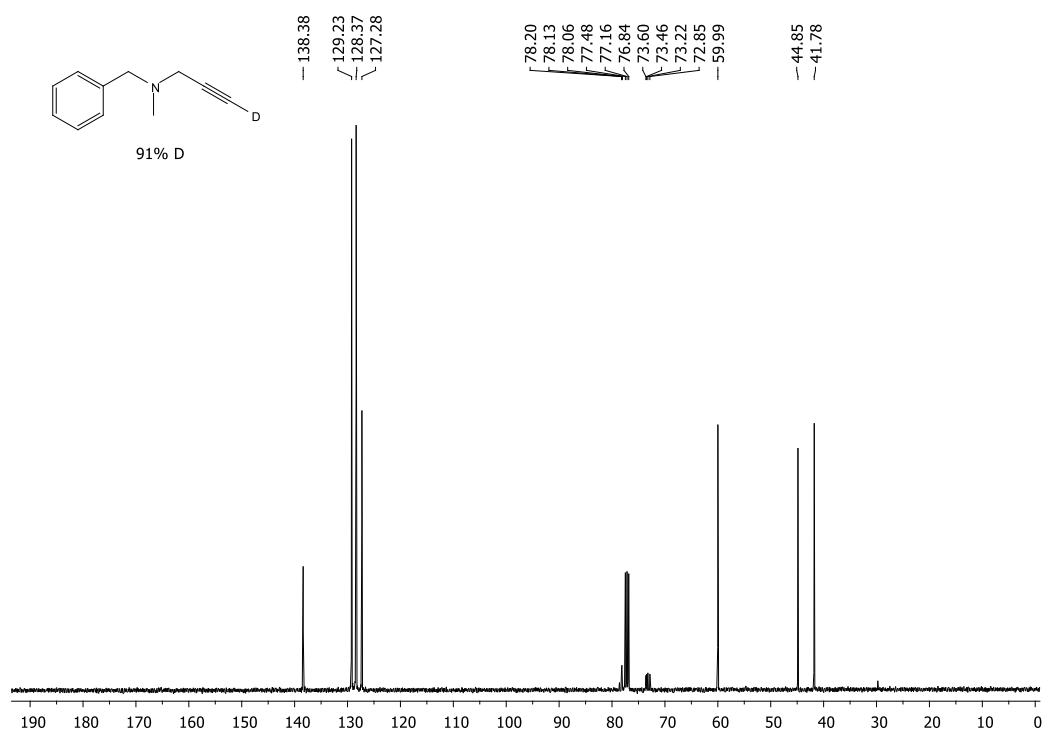


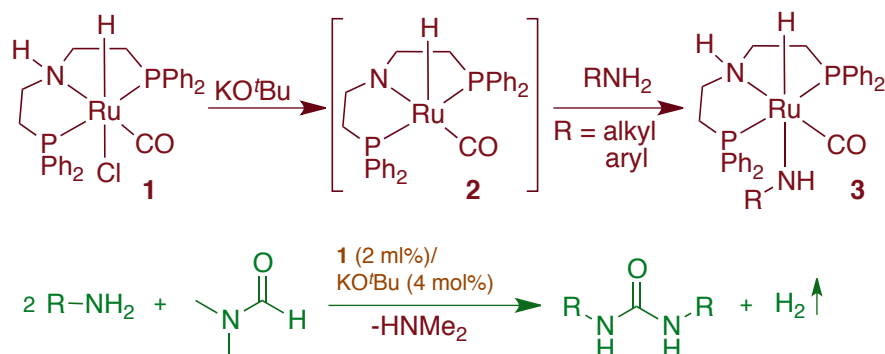
Figure 3.12 ^{13}C NMR spectrum of N-benzyl-N-methylprop-2-yn-1-amine-d1 (100.6 MHz, CDCl_3):



CHAPTER 4

Ruthenium-Catalyzed Urea Synthesis by N–H Activation of Amines

4.1 ABSTRACT



Activation of N–H bond of amines by a ruthenium pincer complex operating via “amine-amide” metal-ligand cooperation (MLC) is demonstrated. The scope of this new mode of bond activation is extended to the synthesis of urea derivatives from amines using DMF as a carbon monoxide surrogate. This catalytic protocol allows the synthesis of simple and functionalized urea derivatives, devoid of any stoichiometric activating reagents and avoids direct use of fatal CO. Consecutive addition of different amines provided unsymmetrical urea compounds. At low temperature, a formamide intermediate was isolated. The reactions are proposed to proceed via N–H activation of amines followed by CO insertion from DMF and with liberation of dihydrogen.

4.2 INTRODUCTION

The reactivity of the lone pair of electrons available on the nitrogen atom dominates the chemistry of amines, resulting in Lewis acid-base interaction and thus generally leads to the formation of Werner type of complexes when treated with transition metals.¹ As a result, the activation of N–H bond, which has enormous potential in

catalytic transformation remains scarce.² In contrast, the suitable ligand design resulted in activation of N–H bond of amines on the metal center to provide the ‘amide’ type ligand. Milstein and coworkers introduced non-innocent ligand mediated N–H activation of amines in which the metal oxidation state remains same due to MLC.^{3,4} Despite that tremendous strides have been made in various bond activation and catalytic applications thereof, the chemistry of N–H activation remain limited to stoichiometric reactions.⁵ Recently, we demonstrated facile N–H activation of amine functionality by a monohydrido-bridged dinuclear ruthenium complex, which resulted in selective α -deuteration of amines and amino acids with excellent catalytic efficiency.⁶

N,N'-disubstituted urea derivatives have potential applications as efficient organocatalyst,⁷ green solvent,⁸ promising NLO materials,⁹ and pharmacological compounds (Figure 4.1).¹⁰⁻¹²

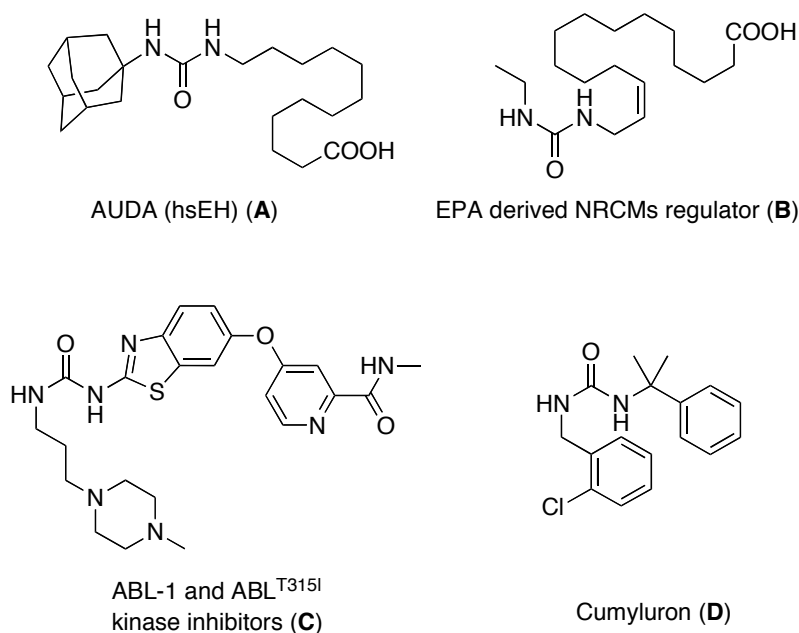


Figure 4.1 Biologically Active Urea Derivatives. **(A)** soluble epoxide hydrolase inhibitors. **(B)** regulator of cardiomyocyte contraction **(C)** ABL-1 and ABL^{T315I} kinase inhibitors **(D)** pesticides such as cumyluron.

Despite the notable synthetic advances, the urea derivatives are in general obtained using phosgene and isocyanates,¹³ which generates toxic by-products. Synthesis of urea compounds using phosgene alternates requires multi-step synthesis.¹⁴ Catalytic carbonylation reactions have profound influence in chemical synthesis and are known to employ different compounds as carbon monoxide surrogate.¹⁵ Although direct carbonylation of amines to urea offers attractive alternative protocol¹⁶⁻¹⁸ they often suffer from low yield,¹⁶ requirement of additional and stoichiometric amount of oxidant,¹⁷ use of toxic pressurized carbon monoxide gas¹⁸ and chromatographic purifications. Thus, environmentally benign and mild reaction condition for urea synthesis still remains a challenge. In continuation of our studies on N–H⁶, O–D and C_{sp}–H bond activation reactions, which resulted in highly selective deuteration of amines, amino acids, alcohols and terminal alkynes using D₂O,¹⁹ we report herein the facile N–H bond activation by a ruthenium pincer complex [(PNP^{Ph})RuHCl(CO)] **1** (PNP = bis(2-(diphenylphosphino)ethyl)amine), and its direct catalytic application to the synthesis of valuable urea derivatives using DMF as a CO alternative.

4.3 RESULTS AND DISCUSSIONS

Upon deprotonation of the ruthenium pincer complex **1** with a base (KO^tBu) in presence of benzylamine generated the complex **3a** at room temperature. When 4-fluorobenzylamine and 4-nitroaniline were subjected to the reaction under similar condition, complexes **3b** and **3c** were obtained, respectively as a result of facile N–H activations of alkyl and arylamines. Complexes **3a-c** exhibited the characteristic ¹H, ¹³C and ³¹P NMR signals (Scheme 4.1). Further, the structure of complex **3b** was unequivocally corroborated using single crystal X-ray analysis (Figure 4.2).²⁰

Scheme 4.1 N–H activation by “Amine-Amide” MLC Operative in Complex **1**

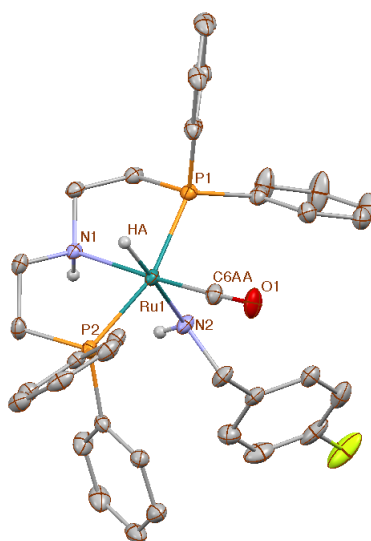
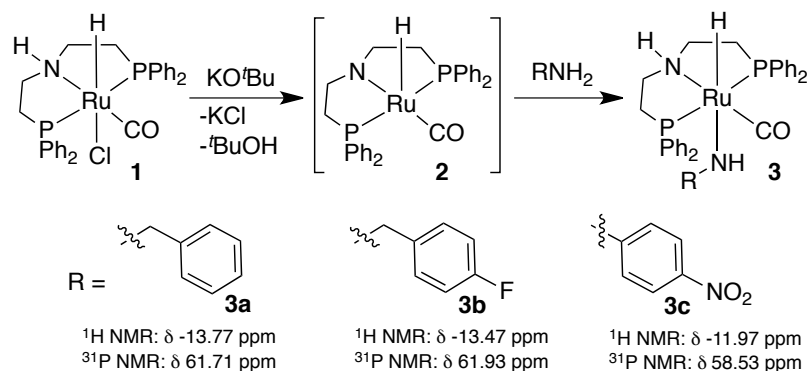
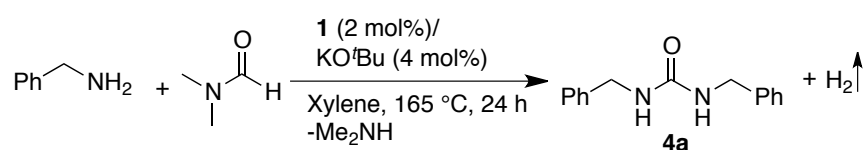


Figure 4.2: Single Crystal X-ray Structure of **3b** (ellipsoids are drawn with 50% probability)

To explore the catalytic application of N–H activation reactions, direct carbonylation of amines using DMF was planned. DMF is established as a safe alternative to the toxic carbon monoxide.²¹ At the outset, optimization studies were performed for carbonylation of benzylamine to urea using DMF as a carbon monoxide surrogate catalyzed by ruthenium pincer complex **1** and the results are summarized in Table 1. Experiments with 0.5 mol% and 1 mol% of Ru-catalyst **1** and benzylamine (1 mmol) and 3-5 mmol of DMF resulted in poor yields (12-29%) of *N,N'*-dibenzyl urea (Table 1, entries 1-3). Upon use of 2 mol% of catalyst **1** with excess amount of DMF (3-7

equiv.) under open condition provided enhanced product formation (Table 1, entries 4-6). When 2 mol% of catalyst **1** and 10 equivalent of DMF were reacted with benzylamine, *N,N'*-dibenzylurea was isolated in 91% yield (Table 1, entry 7). Control experiment in absence of catalyst confirmed that the catalyst is essential for this transformation (Table 1, entry 8).

Table 4.1 Optimization of Reaction Conditions^a



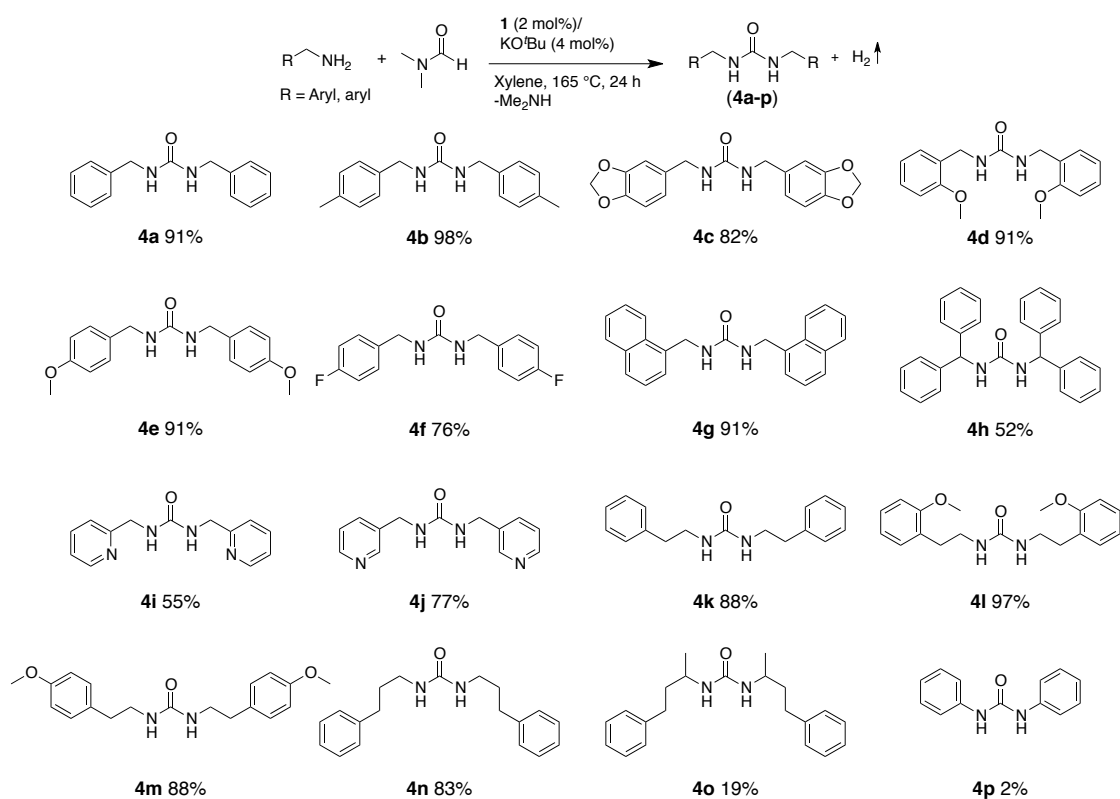
Entry	Catalyst load (mol%)	DMF (equiv.)	Yield (%) ^b
1	0.5	3	12
2	0.5	5	22
3	1.0	3	29
4	2.0	3	46
5	2.0	5	67
6	2.0	7	74
7	2.0	10	91
8 ^c	-	10	-

^aAmine (1 mmol), xylene (1.5 mL) and catalyst **1** were heated at 165 °C for 24 h in an open condition under argon atmosphere. ^bIsolated yields. ^cControl experiment in the absence of catalyst.

Under the optimized condition an assortment of aryl methylamines was tested for the urea synthesis using catalyst **1** and DMF (Scheme 4.2). Benzylamine with electron donating groups provided dialkyl urea products in very good yields (Scheme 4.2, **4b-4e**), while 4-fluoro benzylamine provided the corresponding urea in diminished yield (**4f**, 76%). Use of 1-naphthylmethylamine resulted in 91% dinaphthylmethyl urea (Scheme 4.2, **4g**). Furthermore, reactions of phenethylamine and its derivatives displayed good reactivity (Scheme 4.2, **4k-4n**). In general, benzylamines and alkylamines provided the urea products in good yields. While substitution at ortho-

position of benzylamine was tolerated, substitution at α -amine functionality (**4h**, **4o**) and heteroaryl methylamine (2- and 3-picolylamines) delivered the urea products in moderate yields (**4i**, **4j**). However, when aniline was subjected to this catalytic transformation, *N,N'*-diphenyl urea was obtained only in 2% yield, implying that nucleophilicity of amines is an essential requirement for efficient formation of urea.

Scheme 4.2 Synthesis of Arylmethyl and Arylalkyl Urea Derivatives^a

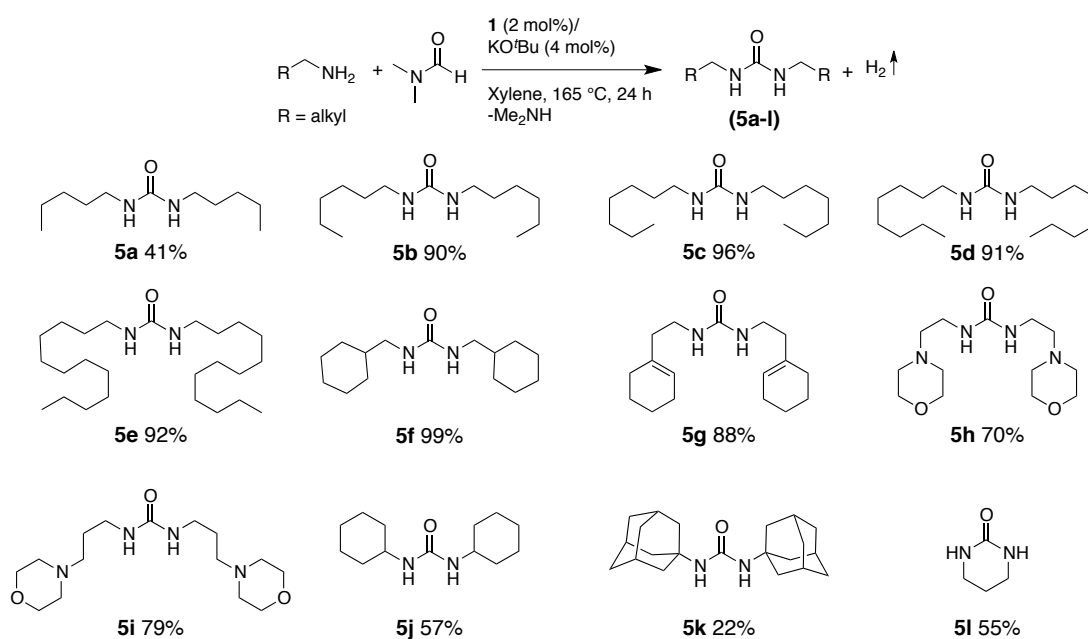


^aAmine (1 mmol), catalyst **1** (2 mol %), KO^tBu (4 mol%), DMF (10 mmol) and xylene (1.5 mL) were heated at 165 °C for 24 h in an open condition under argon atmosphere. Yields correspond to isolated products.

Further linear *n*-alkyl and cycloalkyl amines were utilized in the synthesis of *N,N'*-dialkyl urea derivatives. When *n*-pentylamine was reacted with DMF under the optimized condition dipentyl urea was obtained in 41% yield, perhaps due to the lower bp (104 °C) of amines. However, when long chain amines were reacted, the corresponding urea derivatives were isolated in excellent yields. Likewise,

cyclohexylmethylamine, morpholine and cyclohexenyl incorporated amines were subjected in the reaction, which furnished the corresponding dialkyl urea products in good yields (Scheme 4.3, **5f-5i**). The cyclohexylamine displayed moderate yield (Scheme 4.3, **5j**) and in case of bulkier adamantyl amine the reaction was sluggish and provided poor yield (Scheme 4.3, **5k**) due to steric hindrance. Interestingly, use of 1,3-diaminopropane under the optimized condition provided a cyclic urea (**5l**).

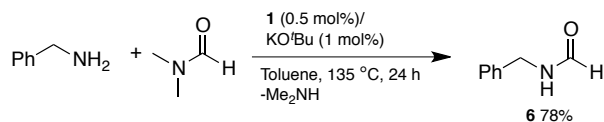
Scheme 4.3 Synthesis of *N,N'*-Dialkyl Urea Derivatives^a



^aAmine (1 mmol), catalyst **1** (2 mol %), KO^tBu (4 mol%), DMF (10 mmol) and xylene (1.5 mL) were heated at 165 °C for 24 h in an open condition under argon atmosphere. Yields correspond to isolated products.

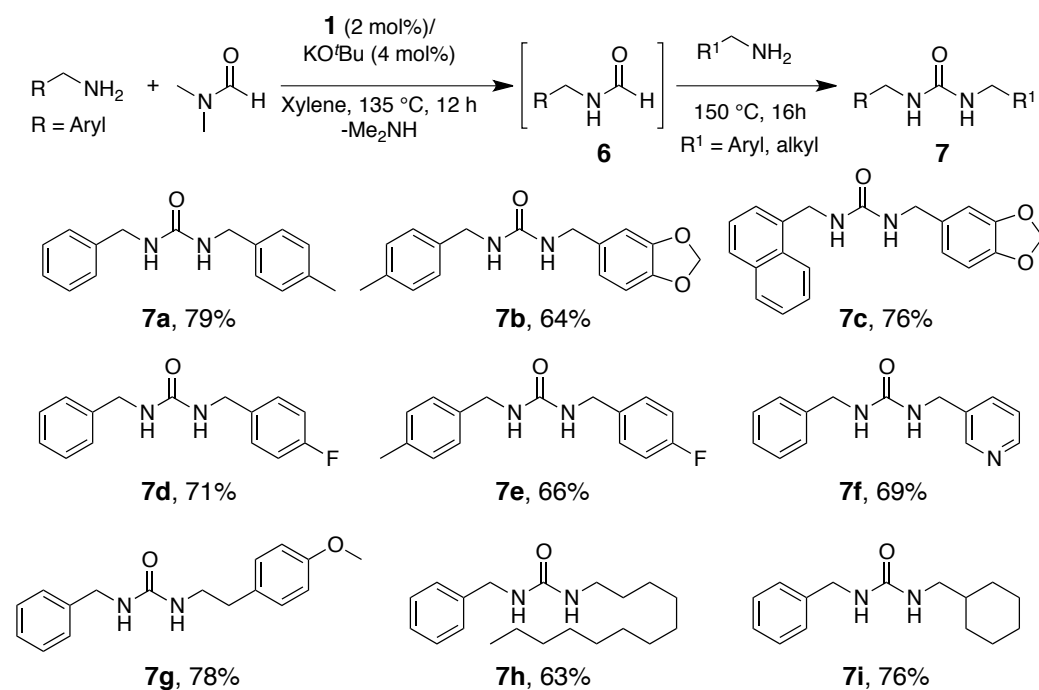
To understand further mechanistic insight of this useful process, reaction of benzylamine with DMF (4 equiv.) catalyzed by **1** (0.5 mol%) was carried out at low temperature (135 °C), which provided *N*-benzylformamide in 78% yield, indicating the involvement of formamide as potential intermediate in synthesis of urea derivatives (Scheme 4.4).

Scheme 4.4 Catalytic Synthesis of *N*-Benzylformamide



As formamides can be further used as a reagent for urea synthesis, this observation revealed the possibility for the synthesis of unsymmetrical urea derivatives. Thus, upon catalytic formation of formamides, different amines was added to the same reaction mixture and heated at elevated temperature, which provided the unsymmetrical urea derivatives in good to excellent yield (Scheme 4.5, **7a-7i**).

Scheme 4.5 Synthesis of Unsymmetrical Urea Derivatives^a



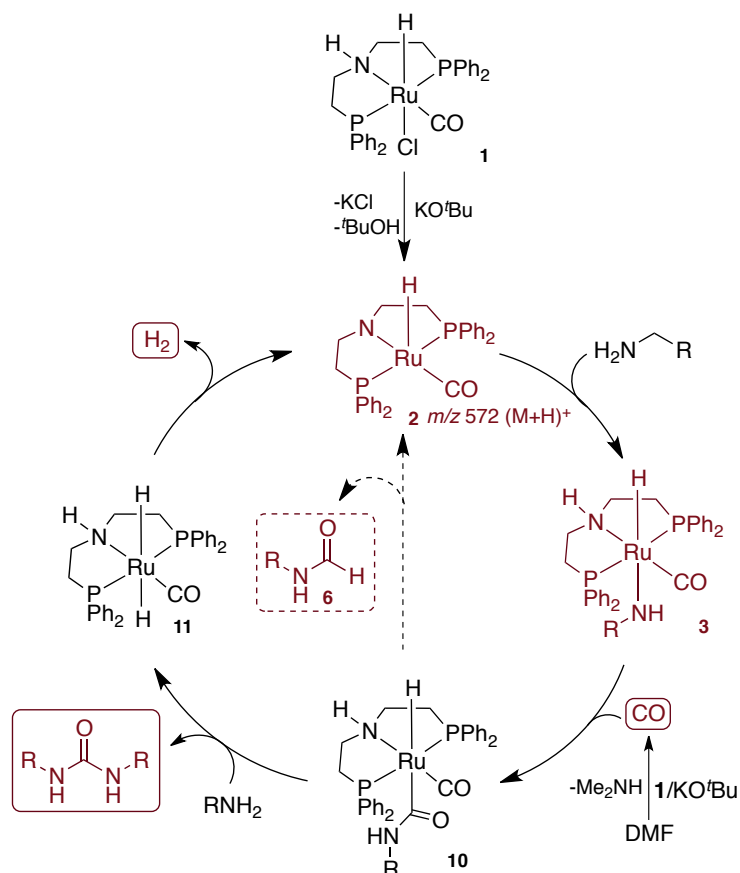
^aAmine (1 mmol), **1** (2 mol %), KO^tBu (4 mol%), DMF (10 mmol) and xylene (1.5 mL) were heated at 135 °C for 12 h in an open condition under argon atmosphere. Subsequently, different amine (1 mmol) was added and the reaction mixture was heated at 150 °C for 16 h. Yields correspond to isolated products.

The catalytic synthesis of N,N'-dibenzylurea was performed in closed conditions, and after 1 h, the gas phase of the reaction mixture was subjected to gas chromatography (GC) analysis, which allowed us to detect the in situ formed CO and dihydrogen.

Further, upon reaction of the ruthenium pincer complex **1** with a base in DMF, we observed the C–H activation of the formyl functionality of DMF by the in situ formed unsaturated complex **2** at room temperature. However, the generated complex (^{31}P , 64.28 ppm; IR, 1876 cm^{-1}) remains elusive to complete characterization, as repeated attempts for its isolation failed.

Further, on the basis of stoichiometric reaction of complex **1** with different amines and base (Scheme 4.1), other experimental observations, a mechanism for catalytic carbonylation of amines to urea derivatives is proposed in Scheme 4.6. The reaction of complex **1** with base, KO^tBu generates unsaturated Ru(II) intermediate **2**. The formation of transient intermediate **2** is observed in situ using ^1H ($\delta_{\text{Ru-H}}-5.85\text{ ppm}$), ^{31}P NMR (δ 48.45 ppm) and ESI-MS analyses (m/z 572(M^+)). The N–H bond activation of amine functionality by complex **2** occurs via “amine–amide” MLC^{4,19} to generate intermediate **3** (Scheme 4.1). An intermolecular nucleophilic reaction between coordinated amide ligand and a DMF molecule with concomitant liberation of Me_2NH , perhaps occurs via coordination/decordination pathway leading to the formation of intermediate **8**. The amide ligated saturated complex **8** reductively eliminates formamide **6** at low temperature ($135\text{ }^\circ\text{C}$) and can regenerate complex **2** (Scheme 2). At higher temperature ($>150\text{ }^\circ\text{C}$), a second intermolecular nucleophilic attack by amine on metal coordinated amide motif occurs leading to the formation of urea and a saturated Ru-dihydride complex **9**,²² which upon liberation of a dihydrogen regenerates **2** for further catalysis. The liberated CO and H_2 gas were detected further by GC analysis. Overall, the catalytic carbonylation of amines to urea derivatives proceeds with liberation of molecular hydrogen.

Scheme 4.6 Proposed Mechanism for the N–H Activation and Catalytic Carbonylation of Amines to Urea Using DMF as a CO Surrogate



4.4 CONCLUSIONS

In conclusion, A facile N–H activation of amines is demonstrated. This bond activation is further applied for developing an efficient protocol for the synthesis of urea derivatives catalyzed by a ruthenium catalyst **1**. A clean synthetic method using DMF as an effective surrogate for the CO is attained and an assortment of urea derivatives were synthesized by carbonylation of primary amines. Operating at open condition and devoid of any deleterious side products make this method highly attractive and advantageous over the related reported procedures for the synthesis of urea derivatives. As these reactions progress under mild condition without the requirement of any pressure set-up, the potential applications of this protocol in other organic transformations are currently being explored.

4.5 EXPERIMENTAL SECTION

General experimental procedure: All catalytic reactions were performed using standard Schlenk line technique under argon atmosphere. All stoichiometric reactions were performed under nitrogen atmosphere in MBraun glove box. Chemicals were purchased from Acros, Alfa-aesar, Sigma-Aldrich, Spectrochem and used without further purification. Dry solvents were prepared according to the standard procedure. ^1H , ^{13}C , and ^{31}P NMR spectra were recorded at Bruker AV-400 (^1H : 400 MHz, ^{13}C : 100.6 MHz, ^{31}P : 162 MHz). ^1H and $^{13}\text{C}\{^1\text{H}\}$ NMR chemical shifts were reported in ppm downfield from tetramethyl silane. Multiplicity is abbreviated as: s, singlet; d, doublet; t, triplet; q, quartet; m, multiplet. Assignment of spectra was done based on one-dimensional (dept-135) NMR technique. IR Spectra were recorded through Perkin-Elmer FT-IR Spectrometer. Mass spectra were recorded on Bruker micrOTOF-Q II Spectrometer.

Synthesis of Ru-amide complexes:

In a screw cap scintillation vial Ru-macho **1** (0.032 mmol, 20 mg), KO^tBu (1.1 equiv, 0.035 mmol, 4 mg) and THF (1 mL) were added and the resulting mixture was allowed to stir at room temperature for 30 min. To the reddish-brown solution amines (2.2 equiv) was added dropwise. The resulting solution then stirred for 5 minutes at room temperature. The brownish yellow solution immediately turns to red color. The resulting solution was reduced under vacuum and slow addition of cold hexane (2 mL) provided yellow precipitate. The solution was decanted and the precipitate was washed with hexane (1 mL) three times. The precipitate was dried under vacuum for 4 hours to afford the product as yellow solids.

Ru-amide complex (3a): Yellow solid, Yield – 18.9 mg (87%), IR (C_6H_6): 3026, 2279 (Ru–H), 1918, 1603, 1495, 1459, 1221, 1081, 1029, 895, 812, 726, 793 cm^{-1} . ^1H

NMR (C₆D₆): δ 7.66 (m, 4H, ArCH), 7.36 (m, 4H, ArCH), 6.57 (m, 17H, ArCH), 3.35 (br, 1H, NH), 3.17 (m, 5H, CH₂), 2.79 (br, 2H, CH₂), 2.49 (t, $J = 8$ Hz, 1H, NH), 1.95 (br, 2H, CH₂), 1.46 (bs, 2H, CH₂), -13.77 (t, $J = 16$ Hz, 1H, Ru-H). ³¹P{¹H} NMR (C₆D₆): δ 61.71 (s).

Ru-amide complex (3b): Yellow solid, Yield – 18.2 mg (75%), IR (C₆H₆): 3228, 2192 (Ru-H), 1915, 1610, 1483, 1216, 1176, 1100, 911, 896, 745 cm⁻¹. ¹H NMR (C₆D₆): δ 6.73 (m, 4H, ArCH), 6.30 (m, 4H, ArCH), 5.72 (m, 16H, ArCH), 2.25 (br, 1H NH), 1.53 (br, 1H, NH), 0.98 (br, 1H, CH₂), 0.93 (bs, 2H, CH₂), 0.88 (bs, 2H, CH₂), -13.47 (t, $J = 20$ Hz, 1H, Ru-H). ¹³C NMR: δ 162.42 (quat-C), 159.99 (quat-C), 138.54 (C=O), 133.89 (quat-C), 133.81, 133.75, 130.83, 130.78, 130.72, 129.82, 128.82, 128.33, 128.01, 114.30 (CH₂), 66.82 (CH₂), 24.82 (CH₂). ³¹P{¹H} NMR (C₆D₆): δ 61.93 (s).

Ru-amide complex (3c): Light yellow solid, Yield – 13.6 mg (60%), IR (C₆H₆): 3197, 2194 (Ru-H), 1893, 1623, 1478, 1216, 1173, 1156, 941, 887, 746 cm⁻¹. ¹H NMR (C₆D₆): δ 8.12 (m, 4H, ArCH), 8.01 (m, 4H, ArCH), 7.77 (m, 4H, ArCH), 7.48 (m, 4H, ArCH), 6.99 (m, 8H, ArCH), 3.59 (m, 3H, CH₂ and NH), 3.36 (s, 1H, NH), 3.28 (br, 2H, CH₂), 2.36 (br, 2H, CH₂), 2.21 (br, 2H, CH₂), -11.97 (t, $J = 16$ Hz, 1H, Ru-H). ¹³C NMR: δ 147.11 (quat-C), 133.88 (quat-C), 133.81 (C=O), 130.72, 129.92, 128.87, 128.32, 127.82, 126.82, 124.42, 124.35, 66.82 (CH₂), 24.82 (CH₂). ³¹P{¹H} NMR (C₆D₆): δ 58.53 (s).

Determination of the Molecular Structure of 3b in the Solid State by X-ray

Single Crystal Diffraction: Single crystals of complex **3b** suitable for X-ray analysis were obtained from a solution of benzene and hexane. A crystal suited for single crystal x-ray diffraction measurements was mounted on a glass fiber. Geometry and intensity data were collected with a Bruker SMART D8 goniometer equipped with an

APEX CCD detector and with an Incoatec microsource (Mo-K α radiation, $\lambda = 0.71073$ Å, multilayer optics). Temperature was controlled using an Oxford Cryostream 700 instrument. Intensities were integrated with SAINT²³ and corrected for absorption with SADABS.²⁴ The structure was solved by direct methods and refined on F^2 with SHELXL-97.^{25,26}

Crystal Data of Ru-amide Complex 3b: C₇₉H₈₀Cl₂F₂N₄O₂P₄Ru₂, crystal dimensions: 0.3 × 0.15 × 0.12, triclinic with space group P₋₁, $a = 13.1153$ (5) Å, $b = 14.6254$ (5) Å, $c = 21.0142$ (7) Å, $\alpha = 83.896$ (2)°, $\beta = 76.029$ (2)°, $\gamma = 67.637$ (2)°, $V = 3617.0$ (2) Å³, $Z = 2$, $T = 100$ K, $2\theta_{\max} = 30.21$, $\rho_{\text{calcd}} = 1.425$ g/cm³, μ (MoK α) = 0.635 mm⁻¹. min/max transmission factors = 0.6892/0.7460, 21358 Reflections collected, 18086 unique ($R1 = 0.0427$), $WR2 = 0.0531$ (all data). The structure has been deposited at the CCDC data center and can be retrieved by using the number CCDC 1526189.

General procedure for the synthesis of urea derivatives: To an oven dried Schlenk tube, catalyst **1** (2 mol%, 0.019 mmol, 12 mg), KO^tBu (4 mol%, 0.039 mmol, 4.4 mg) and xylene (1.5 mL) were added and the reaction mixture was stirred for 10 minutes at room temperature. After that to the above reaction mixture, amine (1 mmol) and DMF (10 mmol) were added and the Schlenk tube was fitted with a condenser. Schlenk tube was immediately immersed into a preheated oil bath at 165 °C and heated for 24 h with stirring. Upon completion, the reaction mixture was allowed to cool at room temperature. Hexane (5 mL) was added to the reaction mixture and the precipitated urea derivative was further washed with hexane (3 mL). The solid was dried under vacuum.

Spectral data of urea derivatives:

1,3-dibenzylurea (4a): Pale yellow solid, Yield: 123 mg (91%), IR (DCM) 3667, 3093, 2061, 1594, 1241, 751 cm^{-1} . ^1H NMR (400 MHz, CDCl_3) δ 7.27-7.31 (m, 4H, ArCH), 7.22-7.25 (m, 6H, ArCH), 5.09 (s, 2H, NH), 4.29-4.31 (d, $J = 8$ Hz, 2H, NH). ^{13}C NMR (101 MHz, CDCl_3) δ 158.38 (C=O), 139.34 (quat-C), 128.72 (ArCH), 127.52 (ArCH), 127.37 (ArCH), 44.60 (CH_2). HRMS (EI) calcd for $\text{C}_{15}\text{H}_{16}\text{N}_2\text{O}$: m/z 241.1335 ($\text{M}+\text{H}^+$), found 241.1252.

1,3-Bis(4-methylbenzyl)urea²⁷ (4b): White solid. Yield: 146 mg (98%). IR (DCM) 3641, 2922, 1613, 1573, 1241, 774 cm^{-1} . ^1H NMR (CDCl_3): δ 7.11-7.17 (m, 8H, ArCH), 4.52 (s, 2H, NH), 4.33-4.34 (d, $J = 4$ Hz, 4H, CH_2), 2.33 (s, 6H, CH_3). $^{13}\text{C}\{^1\text{H}\}$ NMR (DMSO-d_6): δ 162.88 (C=O), 143.04 (quat-C), 140.75 (quat-C), 133.95 (ArCH), 132.20 (ArCH), 47.92 (CH_2), 25.86 (CH_3). HRMS (EI) calcd for $\text{C}_{17}\text{H}_{20}\text{N}_2\text{O}$: m/z 269.1609 ($\text{M}+\text{H}^+$), found 269.1642.

1,3-Bis(benzo[*d*][1,3]dioxol-5-ylmethyl)urea²⁸ (4c): White solid. Yield: 136 mg (76%). IR (DCM) 3668, 2874, 1681, 1585, 1245, 808 cm^{-1} . ^1H NMR (DMSO-d_6): δ 6.78-6.83 (t, $J = 8$ Hz, 4H, ArCH), 6.69-6.71 (d, $J = 8$ Hz, 2H, ArCH), 6.37 (s, 2H, NH), 5.95 (s, 4H, OCH_2O), 4.11 (s, 4H, NCH_2). $^{13}\text{C}\{^1\text{H}\}$ NMR (DMSO-d_6): δ 158.22 (C=O), 147.32 (quat-C), 146.00 (quat-C), 134.96 (quat-C), 120.25 (ArCH), 108.09 (ArCH), 107.83 (ArCH), 100.87 (OCH_2O), 42.88 (NCH_2). HRMS (EI) calcd for $\text{C}_{17}\text{H}_{16}\text{N}_2\text{O}_5$: m/z 329.1093 ($\text{M}+\text{H}^+$), found 329.1105.

1,3-Bis(2-methoxybenzyl)urea (5d): Pale yellow solid. Yield: 150 mg (91%). IR (DCM) 3877, 2066, 1685, 1578, 1239, 749 cm^{-1} . ^1H NMR (DMSO-d_6): δ 7.16-7.24 (m, 4H, ArCH), 6.87-6.96 (m, 4H, ArCH), 6.29-6.32 (t, $J = 4$ Hz, 2H, NH), 4.16-4.18 (d, $J = 4$ Hz, 2H, NH), 3.79 (s, 6H, CH_3). $^{13}\text{C}\{^1\text{H}\}$ NMR (DMSO-d_6): δ 158.56 (C=O), 157.14 (quat-C), 128.65 (quat-C), 128.35 (ArCH), 128.24 (ArCH), 120.54

(ArCH), 110.83 (ArCH), 55.71 (OCH₂), 38.68 (NCH₂). HRMS (EI) calcd for C₁₇H₂₀N₂O: m/z 301.1547 (M+H⁺), found 301.1562.

1,3-Bis(4-methoxybenzyl)urea²⁷ (4e): Pale yellow solid. Yield: 110 mg (81%). IR (DCM) 3668, 3078, 1694, 1583, 1252, 806 cm⁻¹. ¹H NMR (DMSO-d₆): δ 7.15-7.20 (m, 4H, ArCH), 6.43-6.90 (m, 4H, ArCH), 4.16 (s, 2H, NH), 3.74 (s, 4H, CH₂), 2.50 (s, 6H, CH₃). ¹³C {¹H} NMR (DMSO-d₆): δ 158.11 (C=O), 158.09 (quat-C), 132.88 (quat-C), 128.38 (ArCH), 113.67 (ArCH), 55.09 (OCH₂), 42.45 (NCH₂). HRMS (EI) calcd for C₁₇H₂₀N₂O: m/z 301.1547 (M+H⁺), found 301.1559.

1,3-Bis(4-fluorobenzyl)urea²⁹ (4f): Pale yellow solid. Yield: 125 mg (82%). IR (DCM) 3656, 3132, 1608, 1508, 1221, 831cm⁻¹. ¹H NMR (CDCl₃): δ 7.23-7.25 (m, 4H, ArCH), 6.98-7.02 (t, *J* = 8 Hz, 4H, ArCH), 4.60 (s, 2H, NH), 4.35-4.36 (d, *J* = 4 Hz, 4H, CH₂). ¹³C {¹H} NMR (DMSO-d₆): δ 155.08 (C=O), 152.67 (quat-C, Ar-CF), 151.42 (quat-C, Ar-CF), 127.91 (quat-C), 127.88 (quat-C), 120.61 (ArCH), 120.53 (ArCH), 106.65 (ArCH), 106.44 (ArCH), 34.57 (CH₂). HRMS (EI) calcd for C₁₅H₁₄N₂O: m/z 299.0966 (M+H⁺), found 2299.0960.

1,3-Bis(naphthalen-1-ylmethyl)urea³⁰ (4g): Pale yellow solid. Yield: 168 mg (91%). IR (DCM) 3692, 2920, 1694, 1572, 1248, 772 cm⁻¹. ¹H NMR (DMSO-d₆): δ 8.18-8.21 (d, *J* = 12 Hz, 2H, ArCH), 8.00-8.03 (m, 2H, ArCH), 7.90-8.00 (t, *J* = 4 Hz, 2H, ArCH), 7.59-7.65 (m, 4H, ArCH), 7.52-7.55 (m, 4H, ArCH), 6.58.6.61 (t, *J* = 4 Hz, 2H, NH), 4.80-4.81 (d, *J* = 4 Hz, 4H, CH₂). ¹³C {¹H} NMR (DMSO-d₆): δ 157.86 (C=O), 136.07 (quat-C), 133.39 (quat-C), 130.96 (quat-C), 128.56 (ArCH), 127.46 (ArCH), 126.23 (ArCH), 125.84 (ArCH), 125.50 (ArCH), 125.15 (ArCH), 123.64 (ArCH), 41.11 (CH₂). HRMS (EI) calcd for C₂₃H₂₀N₂O: m/z 363.1468 (M+H⁺), found 363.1464.

1,3-Dibenzhydrylurea (4h): Pale yellow solid. Yield: 110 mg (52%), IR (DCM) 3709, 2973, 1646, 1551, 1271, 740 cm^{-1} . ^1H NMR (CDCl_3): δ 7.27-7.33 (m, 12H, ArCH), 7.18-7.20 (m, 8H, ArCH), 5.94-5.96 (d, $J = 8$ Hz, 2H, CH_2), 5.05-5.07 (d, $J = 8$ Hz, 2H, NH). $^{13}\text{C}\{^1\text{H}\}$ NMR (CDCl_3): δ 158.35 (C=O), 139.33 (quat-C), 128.73 (ArCH), 127.53 (ArCH), 127.38 (ArCH), 44.61 (CH_2). HRMS (EI) calcd for $\text{C}_{27}\text{H}_{24}\text{N}_2\text{O}$: m/z 393.1922 ($\text{M}+\text{H}^+$), found 393.1903.

1,3-Bis(pyridin-2-ylmethyl)urea²⁷ (4i): Brown solid. Yield: 75 mg (55%). IR (DCM) 3639, 2138, 1635, 1472, 776 cm^{-1} . ^1H NMR (CDCl_3): δ 8.54-8.55 (d, $J = 4$ Hz, 2H, ArCH), 7.66-7.69 (m, 2H, ArCH), 7.29-7.33 (t, $J = 8$ Hz, 2H, ArCH), 7.19-7.22 (t, $J = 8$ Hz, 2H, ArCH), 5.82 (s, 2H, NH), 4.56-4.57 (d, $J = 4$ Hz, 2H, CH_2). $^{13}\text{C}\{^1\text{H}\}$ NMR (CDCl_3): δ 158.56 (C=O), 158.16 (quat-C), 136.88 (ArCH), 122.29 (ArCH), 122.06 (ArCH), 45.82 (CH_2). HRMS (EI) calcd for $\text{C}_{13}\text{H}_{14}\text{N}_4\text{O}$: m/z 243.1240 ($\text{M}+\text{H}^+$), found 243.1226.

1,3-Bis(pyridin-3-ylmethyl)urea²⁷ (4j): Brown solid. Yield: 105 mg (77%). IR (DCM) 3671, 2132, 1676, 1565, 1243, 749 cm^{-1} . ^1H NMR (CDCl_3): δ 8.47 (s, 4H, ArCH), 7.61-7.63 (d, $J = 8$ Hz, 2H, ArCH), 7.21-7.24 (m, 2H, ArCH), 5.33 (s, 2H, NH), 4.37-4.38 (d, $J = 4$ Hz, 4H, CH_2). $^{13}\text{C}\{^1\text{H}\}$ NMR (CDCl_3): δ 158.70 (C=O), 148.59 (ArCH), 148.40 (ArCH), 135.48 (ArCH), 135.45 (quat-C), 123.67 (ArCH), 41.70 (CH_2). HRMS (EI) calcd for $\text{C}_{13}\text{H}_{14}\text{N}_4\text{O}$: m/z 243.1240 ($\text{M}+\text{H}^+$), found 243.1232.

1,3-Diphenethylurea²⁷ (4k): Pale yellow solid. Yield: 131 mg (88%). IR (DCM) 3651, 3136, 2063, 1609, 1514, 1239, 746 cm^{-1} . ^1H NMR (CDCl_3): δ 7.28-7.32 (t, $J = 8$ Hz, 4H, ArCH), 7.16-7.24 (m, 6H, ArCH), 4.73 (s, 2H, NH), 3.35-3.40 (m, 2H, CH_2), 2.75-2.79 (t, $J = 8$ Hz, 4H, NCH_2). $^{13}\text{C}\{^1\text{H}\}$ NMR (CDCl_3): δ 158.33 (C=O), 139.33

(quat-C), 128.91 (ArCH), 128.65 (ArCH), 126.46 (ArCH), 41.70 (CH₂), 36.57 (NCH₂). HRMS (EI) calcd for C₁₇H₂₀N₂O: m/z 269.1648 (M+H⁺), found 269.1658.

1,3-Bis(2-methoxyphenethyl)urea (4l): Pale yellow solid. Yield: 173 mg (97%). IR (DCM) 3607, 3023, 2950, 1615, 1581, 1240, 745 cm⁻¹. ¹H NMR (CDCl₃): δ 7.18-7.23 (m, 2H, ArCH), 7.10-7.13 (m, 2H, ArCH), 6.84-6.90 (m, 4H, ArCH), 4.44 (s, 2H, NH), 3.79 (s, 6H, OCH₃), 3.33-3.38 (q, *J* = 8 Hz, *J* = 4 Hz, 4H, NCH₂), 2.79-2.83 (t, *J* = 8 Hz, 4H, CH₂). ¹³C{¹H} NMR (CDCl₃): δ 158.39 (C=O), 157.63 (quat-C), 130.78 (ArCH), 127.88 (ArCH), 127.63 (quat-C), 120.76 (ArCH), 110.48 (ArCH), 55.36 (OCH₃), 40.83 (NCH₂), 31.18 (CH₂). HRMS (EI) calcd for C₁₉H₂₄N₂O₃: m/z 329.1860 (M+H⁺), found 329.2016.

1,3-Bis(4-methoxyphenethyl)urea (4m): White solid. Yield: 157 mg (88%). IR (DCM) 3626, 2839, 1621, 1515, 1246, 813 cm⁻¹. ¹H NMR (CDCl₃): δ 7.08-7.10 (d, *J* = 8 Hz, 4H, ArCH), 6.83-6.85 (d, *J* = 8 Hz, 4H, ArCH), 4.15 (s, 2H, NH), 3.79 (s, 6H, OCH₃), 3.34-3.39 (q, *J* = 8 Hz, *J* = 4 Hz, 4H, NCH₂), 2.70-2.74 (t, *J* = 8 Hz, 4H, CH₂). ¹³C{¹H} NMR (CDCl₃): δ 158.30 (C=O), 158.21 (quat-C), 131.27 (quat-C), 129.84 (ArCH), 114.10 (ArCH), 55.36 (OCH₃), 41.92 (NCH₂), 35.59 (CH₂). HRMS (EI) calcd for C₁₉H₂₄N₂O₃: m/z 329.1860 (M+H⁺), found 329.1864.

1,3-Bis(3-phenylpropyl)urea²⁷ (4n): Pale yellow solid. Yield: 135 mg (83%). IR (DCM) 3709, 3347, 2940, 1656, 1557, 1274, 748 cm⁻¹. ¹H NMR (CDCl₃): δ 7.22-7.24 (m, 4H, ArCH), 7.13-7.17 (m, 4H, ArCH), 3.11-3.16 (q, *J* = 8 Hz, *J* = 4 Hz, 4H, NCH₂), 2.59-2.63 (t, *J* = 8 Hz, 4H, CH₂), 1.74-1.81 (m, 4H, CH₂). ¹³C{¹H} NMR (CDCl₃): δ 158.44 (C=O), 147.74 (quat-C), 128.56 (ArCH), 128.50 (ArCH), 126.06 (ArCH), 40.24 (NCH₂), 33.34 (CH₂), 31.96 (CH₂). HRMS (EI) calcd for C₁₉H₂₄N₂O: m/z 297.1961 (M+H⁺), found 297.2103.

1,3-Bis(4-phenylbutan-2-yl)urea (4o): Pale yellow solid. Yield: 34 mg (19%). IR (DCM) 3634, 3099, 1628, 1548, 1288, 779 cm^{-1} . ^1H NMR (CDCl_3): δ 7.27-7.30 (m, 4H, ArCH), 7.18-7.20 (m, 6H, ArCH), 4.10-4.12 (d, $J = 8$ Hz, 2H, NH), 3.73-3.80 (m, 2H, CH), 2.65-2.69 (m, 4H, CH_2), 1.72-1.75 (m, 4H, CH_2), 1.15-1.17 (d, $J = 8$ Hz, 6H, CH_3). $^{13}\text{C}\{^1\text{H}\}$ NMR (CDCl_3): δ 158.44 (C=O), 141.74 (quat-C), 128.56 (ArCH), 128.50 (ArCH), 126.06 (ArCH), 40.24 (CH_3), 40.12 (CH), 33.34 (CH_2), 31.96 (CH_3). HRMS (EI) calcd for $\text{C}_{27}\text{H}_{24}\text{N}_2\text{O}$: m/z 393.1961 ($\text{M}+\text{H}^+$), found 393.1928.

1,3-Diphenylurea³¹ (4p): White solid. Yield: 2 mg (2%). ^1H NMR (DMSO-d_6): δ 8.65 (s, 2H, NH), 7.42-7.44 (d, $J = 8$ Hz, 4H, ArCH), 7.25-7.29 (t, $J = 8$ Hz, 4H, ArCH), 6.94-6.98 (t, $J = 8$ Hz, 2H, ArCH).

1,3-Dipentylurea (5a): Pale yellow solid. Yield: 47 mg (41%). IR (DCM) 3685, 2954, 1667, 1574, 1263, 694 cm^{-1} . ^1H NMR (CDCl_3): δ 4.37 (s, 2H, NH), 3.12-3.17 (q, $J = 8$ Hz, $J = 4$ Hz, 4H, NCH_2), 1.35-1.52 (m, 4H, CH_2), 1.28-1.31 (m, 8H, CH_2), 0.87-0.91 (t, $J = 8$ Hz, 6H, CH_3). $^{13}\text{C}\{^1\text{H}\}$ NMR (CDCl_3): δ 158.92 (C=O), 40.58 (NCH_2), 30.13 (CH_2), 29.21 (CH_2), 22.54 (CH_2), 14.11 (CH_3). HRMS (EI) calcd for $\text{C}_{11}\text{H}_{24}\text{N}_2\text{O}$: m/z 201.1961 ($\text{M}+\text{H}^+$), found 201.1970.

1,3-Dihexylurea³² (5b): Pale yellow solid. Yield: 116 mg (90%). IR (DCM) 3651, 2930, 1609, 1250, 728 cm^{-1} . ^1H NMR (CDCl_3): δ 4.27 (s, 2H, NH), 3.13-3.16 (q, $J = 8$ Hz, $J = 4$ Hz, 4H, NCH_2), 1.47-1.50 (m, 4H, CH_2), 1.29-1.31 (m, 12H, CH_2), 0.86-0.90 (t, $J = 8$ Hz, 6H, CH_3). $^{13}\text{C}\{^1\text{H}\}$ NMR (CDCl_3): δ 158.40 (C=O), 40.87 (NCH_2), 31.67 (CH_2), 30.32 (CH_2), 26.71 (CH_2), 22.72 (CH_2), 14.16 (CH_3). HRMS (EI) calcd for $\text{C}_{13}\text{H}_{28}\text{N}_2\text{O}$: m/z 229.2274 ($\text{M}+\text{H}^+$), found 229.2370.

1,3-Diheptylurea¹ (5c): Pale yellow solid. Yield: 137 mg (96%). IR (DCM) 3704, 2927, 1631, 1577, 1246, 698 cm^{-1} . ^1H NMR (CDCl_3): δ 4.20 (s, 2H, NH), 3.13-3.16 (t, $J = 4$ Hz, 4H, NCH_2), 1.47-1.49 (m, 4H, CH_2), 1.29-1.30 (m, 16H, CH_2), 0.86-0.89

(t, $J = 4$ Hz, 6H, CH_3). $^{13}C\{^1H\}$ NMR ($CDCl_3$): δ 158.57 ($C=O$), 40.78 (NCH_2), 31.91 (CH_2), 30.40 (CH_2), 29.17 (CH_2), 27.02 (CH_2), 22.73 (CH_2), 14.20 (CH_3). HRMS (EI) calcd for $C_{19}H_{24}N_2O_3$ m/z 329.1860 ($M+H^+$), found 329.1864.

1,3-Dioctylurea³³ (5d): Pale yellow solid. Yield: 143 mg (91%). IR (DCM) 3450, 2850, 1650, 1248, 772 cm^{-1} . 1H NMR ($CDCl_3$): δ 4.38 (s, 2H, NH), 3.11-3.16 (q, $J = 8$ Hz, $J = 4$ Hz, 4H, NCH_2), 1.46-1.49 (m, 4H, CH_2), 1.26-1.29 (m, 20H, CH_2), 0.85-0.89 (t, $J = 8$ Hz, 6H, CH_3). $^{13}C\{^1H\}$ NMR ($CDCl_3$): δ 158.50 ($C=O$), 40.81 (NCH_2), 31.95 (CH_2), 30.41 (CH_2), 29.47 (CH_2), 29.38 (CH_2), 27.07 (CH_2), 27.78 (CH_2), 14.22 (CH_3). HRMS (EI) calcd for $C_{17}H_{36}N_2O$: m/z 285.29 ($M+H^+$), found 285.28.

1,3-Didodecylurea (5e): Pale yellow solid. Yield: 196 mg (92%). IR (DCM) 3651, 3154, 29555, 2076, 1610, 1577, 1466, 1240, 617 cm^{-1} . 1H NMR ($CDCl_3$): δ 4.17 (s, 2H, NH), 3.12-3.17 (t, $J = 8$ Hz, 4H, $N-CH_2$), 1.47-1.49 (m, 4H, CH_2), 1.25 (s, 36H, CH_2), 0.86-0.90 (t, $J = 8$ Hz, 6H, CH_3). $^{13}C\{^1H\}$ NMR ($CDCl_3$): δ 157.93 ($C=O$), 40.89 (NCH_2), 32.07 (CH_2), 30.36 (CH_2), 29.80 (CH_2), 29.78 (CH_2), 29.75 (CH_2), 29.72 (CH_2), 29.50 (CH_2), 27.05 (CH_2), 22.84 (CH_2), 14.22 (CH_3). HRMS (EI) calcd for $C_{25}H_{52}N_2O$: m/z 397.4152 ($M+H^+$), found 397.4189.

1,3-Bis(cyclohexylmethyl)urea³⁴ (5f): Pale yellow solid. Yield: 139 mg (99%). IR (DCM) 3672, 3068, 2917, 2850, 1688, 1575, 1249, 834 cm^{-1} . 1H NMR ($CDCl_3$): δ 4.37 (s, 2H, NH), 2.98-3.01 (t, $J = 8$ Hz, 4H, NCH_2), 1.64-1.73 (m, 10H, CH_2), 1.40-1.44 (m, 2H, CH), 1.09-1.27 (m, 6H, CH_2), 0.87-0.95 (m, 4H, CH_2). $^{13}C\{^1H\}$ NMR ($CDCl_3$): δ 158.78 ($C=O$), 47.07 (NCH_2), 38.62 (CH_2), 32.03 (CH_2), 26.62 (CH), 26.02 (CH_2). HRMS (EI) calcd for $C_{15}H_{28}N_2O$: m/z 253.2274 ($M+H^+$), found 253.2396.

1,3-Bis(2-(cyclohex-1-en-1-yl)ethyl)urea (5g): Pale yellow solid. Yield: 134 mg (88%). IR (DCM) 3666, 3142, 1631, 1554, 1291, 755 cm^{-1} , 1H NMR ($CDCl_3$): δ 5.46

(s, 2H, olefin CH), 4.31 (s, 2H, NH), 3.19-3.23 (q, $J = 8$ Hz, $J = 4$ Hz, 4H, NCH₂), 1.98-2.14 (m, 4H, CH₂), 1.76-1.91 (m, 8H, CH₂), 1.51-1.64 (m, 8H, CH₂). ¹³C{¹H} NMR (CDCl₃): δ 158.51 (C=O), 134.94 (olefin C), 123.36 (quat-C), 38.43 (NCH₂), 38.37 (CH₂), 28.05 (CH₂), 25.32 (CH₂), 22.93 (CH₂), 22.45 (CH₂). HRMS (EI) calcd for C₁₇H₂₈N₂O: m/z 277.2235 (M+H⁺), found 277.2246.

1,3-bis(2-morpholinoethyl)urea (5h): Pale yellow solid Yield: 103 mg (70%). IR (DCM) 3634, 3166, 1646, 1550, 1248, 773 cm⁻¹. ¹H NMR (CDCl₃): δ 4.98 (s, 2H, NH), 3.69-3.71 (m, 8H, CH₂), 3.26-3.30 (m, 4H, CH₂), 2.44-2.50 (m, 12H, CH₂). ¹³C{¹H} NMR (CDCl₃): δ 158.50 (C=O), 67.06 (OCH₂), 58.07 (CH₂), 53.56 (CH₂), 36.92 (NCH₂). HRMS (EI) calcd for C₁₃H₂₆N₄O₃ m/z 287.2078 (M+H⁺), found 287.2073.

1,3-Bis(3-morpholinopropyl)urea (5i): Pale yellow solid. Yield: 130 mg (79%). IR (DCM) 3619, 3147, 1640, 1531, 1274, 722 cm⁻¹. ¹H NMR (CDCl₃): δ 5.26 (s, 2H, NH), 3.69-3.72 (m, 8H, CH₂), 3.21-3.25 (m, 4H, CH₂), 2.40-2.44 (m, 12H, CH₂), 1.64-1.71 (m, 4H). ¹³C{¹H} NMR (CDCl₃): δ 159.11 (C=O), 66.76 (OCH₂), 56.46 (CH₂), 53.56 (CH₂), 38.79 (NCH₂), 26.70 (CH₂). HRMS (EI) calcd for C₁₅H₃₀N₄O₃: m/z 315.2351 (M+H⁺), found 315.2388.

1,3-Dicyclohexylurea²⁷ (5j): Pale yellow solid. Yield: 72 mg (82%). IR (DCM) 3703, 2927, 1646, 1541, 1242, 750 cm⁻¹. ¹H NMR (CDCl₃): δ 4.02-4.04 (d, $J = 8$ Hz, 2H, NH), 3.47-3.49 (t, $J = 4$ Hz, 2H, CH), 1.91-1.95 (m, 4H, CH₂), 1.57-1.71 (m, 6H, CH₂), 1.25-1.40 (m, 4H, CH₂), 1.05-1.19 (m, 6H, CH₂). ¹³C{¹H} NMR (CDCl₃): δ 156.89 (C=O), 49.30 (CH₂), 34.11 (CH₂), 25.77 (CH₂), 25.09 (CH). HRMS (EI) calcd for C₁₃H₂₄N₂O: m/z 247.1781 (M+H⁺), found 247.1792.

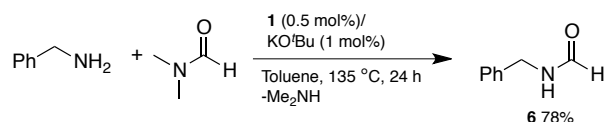
1,3-Di((3S,5S,7S)-adamantan-1-yl)urea²⁷ (5k): Pale yellow solid. Yield: 39 mg (22%). IR (DCM) 3659, 3118, 2905, 2846, 1609, 1294, 749 cm⁻¹. ¹H NMR (DMSO-

d₆): δ 3.88 (s, 2H, NH), 2.04 (s, 6H, CH), 1.94 (s, 10H, CH₂), 1.65 (s, 14H, CH₂).

HRMS (EI) calcd for C₂₁H₃₂N₂O: m/z 329.2548 (M+H⁺), found 329.2528.

Tetrahydropyrimidin-2(1H)-one²⁷ (5I): Pale yellow solid. Yield: 55 mg (55%). IR (DCM) 3657, 3030, 1683, 1557, 1318, 812 cm⁻¹. ¹H NMR (DMSO-d₆): δ 6.00 (s, 2H, NH), 3.07-3.08 (d, *J* = 4 Hz, 4H, NCH₂), 1.66-1.69 (m, 2H, CH₂). ¹³C{¹H} NMR (DMSO-d₆): δ 156.00 (C=O), 39.48 (NCH₂), 21.46 (CH₂). HRMS (EI) calcd for C₄H₈N₂O: m/z 101.0709 (M+H⁺), found 101.0705.

Synthesis of *N*-benzylformamide (6) at lower temperature:



To an oven dried Schlenk tube, catalyst **1** (0.5 mol%, 0.0049 mmol, 3 mg), KO^tBu (1 mol%, 0.0098 mmol, 1.1 mg) and toluene (1.5 mL) were added. The reaction mixture was stirred for 10 minutes. Then benzylamine (0.5 mmol, 54 μ l) and DMF (2 mmol, 154 μ l) were added to the above reaction mixture. The Schlenk tube was fitted with a condenser and immediately immersed into a preheated oil bath at 135 °C and heated for 24 h with stirring. Upon completion, the reaction mixture was allowed to cool to room temperature. Hexane (5 mL) was added to the reaction mixture and kept in freezer (-20 °C), for 12 h. The precipitated formamide was further washed with hexane (3 mL) and the obtained solid was dried under vacuum.

***N*-Benzylformamide (6):** White solid. Yield: 86 mg (78%). ¹H NMR (CDCl₃): δ 8.22 (s, 1H, N-CHO), 7.32-7.39 (m, 3H, ArCH), 7.27-7.30 (m, 2H, ArCH), 6.23 (s, 1H, NH), 4.45-4.47 (d, *J* = 8 Hz, 2H, CH₂). ¹³C{¹H} NMR (CDCl₃): δ 161.22 (C=O), 137.70 (quat-C), 128.85 (ArCH), 127.85 (ArCH), 127.74 (ArCH), 42.22 (CH₂).

General procedure for the synthesis of unsymmetrical urea derivatives: To an oven dried Schlenk tube, catalyst **1** (2 mol%, 0.019 mmol, 12 mg), KO^tBu (4 mol%,

0.039 mmol, 4.4 mg) and xylene (1.5 mL) were added and the reaction mixture was stirred for 10 minutes at room temperature. After that to the above reaction mixture, amine (1 mmol) and DMF (10 mmol) were added and the Schlenk tube was fitted with a condenser. Schlenk tube was immediately immersed into a preheated oil bath at 135 °C and heated for 12 h with stirring. Further different amine (1 mmol) was added to the reaction mixture and heated to 150 °C and heated for 16 h. Upon completion, the reaction mixture was allowed to cool at room temperature. Hexane (5 mL) was added to the reaction mixture and the precipitated urea derivative was further washed with hexane (3 mL). The solid was dried under vacuum.

1-Benzyl-3-(4-methylbenzyl)urea (7a): White solid, Yield – 180 mg (79%), mp 176–178 °C, IR (DCM) 3317, 2919, 2360, 1615, 1564, 1236, 749, 694 cm^{-1} , ^1H NMR (400 MHz, CDCl_3) δ 7.27-7.34 (m, 6H, ArCH), 7.11-7.17 (m, 3H, ArCH), 4.74 (s, 2H, NH), 4.30-4.37(m, 4H, CH_2), 2.33 (s, 3H, CH_3). ^{13}C NMR (101 MHz, CDCl_3) δ 158.11 (C=O), 139.23 (quat-C), 137.18 (quat-C), 136.09 (quat-C), 129.47, 128.79, 127.60, 127.49, 127.47, 44.77 (CH_2), 44.58 (CH_2), 21.21 (CH_3). HRMS [ESI] calcd for $\text{C}_{16}\text{H}_{18}\text{N}_2\text{O}$ m/z 255.1492 [M+H], found 255.1519 [M+H].

1-(Benzo[d][1,3]dioxol-5-ylmethyl)-3-(4-methylbenzyl)urea (7b): White solid, Yield – 218 mg (73%), mp 190–192 °C, IR (DCM) 3316, 2917, 2853, 1931, 1613, 1562, 1491, 1243, 1035, 927, 807 cm^{-1} , ^1H NMR (400 MHz, CDCl_3) δ 7.25-7.28 (t, J = 8 Hz, 1H, ArCH), 7.13-7.14 (m, 4H, ArCH), 6.72-6.76 (m 2H, ArCH), 5.96 (s, 2H, CH_2), 4.65 (s, 2H, NH), 4.25-4.32 (m, 4H, CH_2), 2.32 (s, CH_3). ^{13}C NMR (101 MHz, CDCl_3) δ 158.02 (C=O), 146.92 (quat-C), 137.17 (quat-C), 136.09 (quat-C), 133.20 (quat-C), 130.62 (quat-C), 129.46, 127.61, 120.78, 108.37, 108.26, 101.15, 44.58 (CH_2), 31.07 (CH_2), 21.21 (CH_3). HRMS [ESI] calcd for $\text{C}_{17}\text{H}_{18}\text{N}_2\text{O}_3$ m/z 299.1390 [M+H], found 299.1402 [M+H].

1-(Benzo[d][1,3]dioxol-5-ylmethyl)-3-(naphthalen-1-ylmethyl)urea (7c): White solid, Yield – 254 mg (76%), mp 193–195 °C, IR (DCM) 3316, 2829, 1611, 1566, 1496, 1440, 1247, 1037, 929, 775 cm^{-1} , ^1H NMR (400 MHz, CDCl_3) δ 7.99-8.04 (t, $J = 8$ Hz, 1H, ArCH), 7.74-7.78 (m, 1H, ArCH), 7.47-4.52 (m, 2H, ArCH), 7.35-7.39 (m, 2H, ArCH), 6.68-6.75 (m, 3H, ArCH), 5.90 (s, 2H, CH_2), 4.77-4.81 (m, 2H, CH_2), 4.69 (s, 2H, NH), 4.20-4.23 (m, 2H, CH_2). ^{13}C NMR (101 MHz, CDCl_3) δ 157.84 (C=O), 148.97 (quat-C), 146.97 (quat-C), 133.98 (quat-C), 131.48, 128.99 (quat-C), 128.49 (quat-C), 126.61, 126.27, 126.02 (quat-C), 125.53, 123.68, 123.31, 120.75, 108.34, 108.23, 101.13, 44.58 (CH_2), 42.86. (CH_2). HRMS [ESI] calcd for $\text{C}_{20}\text{H}_{18}\text{N}_2\text{O}_3$ m/z 335.1390 [M+H], found 335.1392 [M+H].

1-Benzyl-3-(4-fluorobenzyl)urea (7d): White solid, Yield – 165 mg (71%), mp 180–182 °C, IR (DCM) 3316, 2946, 2858, 1633, 1562, 1265, 1165, 731, 697 cm^{-1} , ^1H NMR (400 MHz, CDCl_3) δ 7.29-7.31 (m, 2H, ArCH), 7.19-7.23 (m, 6H, ArCH), 6.96-7.00 (t, $J = 8$ Hz, 2H, ArCH), 4.37 (s, 2H, NH), 4.31-4.37 (dd, $J = 8$ Hz, $J = 4$ Hz, 4H, CH_2). ^{13}C NMR (101 MHz, CDCl_3) δ 158.20 (C=O), 139.25 (quat-C), 139.23 (quat-C), 129.22, 129.14, 128.78, 127.55, 127.47, 115.51 (d, $J = 84$ Hz, C-F), 44.71 (CH_2), 43.90 (CH_2). HRMS [ESI] calcd for $\text{C}_{16}\text{H}_{18}\text{N}_2\text{O}$ m/z 259.1241 [M+H], found 259.1282 [M+H].

1-(4-Fluorobenzyl)-3-(4-methylbenzyl)urea (7e): White solid, Yield – 182 mg (66%), mp 203–205 °C, IR (DCM) 3320, 2878, 1937, 1611, 1567, 1507, 1221, 754 cm^{-1} , ^1H NMR (400 MHz, CDCl_3) δ 7.20-7.25 (m, 2H, ArCH), 7.11-7.15 (m, 4H, ArCH), 6.96-7.01 (m, 2H, ArCH), 4.60 (s, 2H, NH), 4.32-4.34 (m, 4H, CH_2), 2.32 (s, 3H, CH_3). HRMS [ESI] calcd for $\text{C}_{16}\text{H}_{17}\text{FN}_2\text{O}$ m/z 273.1398 [M+H], found 273.1406 [M+H].

1-Benzyl-3-(pyridin-3-ylmethyl)urea (7f): Pale yellow solid, Yield – 150 mg (69%), mp 157–159 °C, IR (DCM) 3314, 2921, 2872, 1613, 1562, 1238, 735, 695 cm^{-1} , ^1H NMR (400 MHz, CDCl_3) δ 7.23-7.31 (m, 9H, ArCH), 4.84 (s, 2H, NH), 4.32-4.34 (d, $J = 8$ Hz, 4H, CH_2). ^{13}C NMR (101 MHz, CDCl_3) δ 158.80 (C=O), 148.61, 148.31, 139.23 (quat-C), 135.15 (quat-C), 128.63, 128.55, 127.24, 127.17, 123.49, 44.17 (CH_2), 41.51 (CH_2). HRMS [ESI] calcd for $\text{C}_{14}\text{H}_{15}\text{N}_3\text{O}$ m/z 242.1288 [M+H], found 242.1350 [M+H].

1-Benzyl-3-(4-methoxyphenethyl)urea (7g): White solid, Yield – 199 mg (78%), mp 118–120 °C, IR (DCM) 3315, 2930, 1630, 1565, 1509, 1241, 1177, 1032, 819, 731, 696 cm^{-1} , ^1H NMR (400 MHz, CDCl_3) δ 7.27-7.33 (m, 5H, ArCH), 7.06-7.09 (m, 2H, ArCH), 6.81-6.85 (m, 2H, ArCH), 4.84 (s, 2H, NH), 4.30-4.37 (dd, $J = 8$ Hz, $J = 4$ Hz, 2H, CH_2), 3.79 (s, 3H, OCH_3), 3.33-3.39 (m, 2H, CH_2), 2.68-2.73 (m, 2H, CH_2). ^{13}C NMR (101 MHz, CDCl_3) δ 158.33 (C=O), 139.36 (quat-C), 131.23 (quat-C), 129.87, 128.73, 127.55, 127.40, 127.37 (quat-C), 114.13, 55.39 (OCH_3), 44.63 (CH_2), 41.92 (CH_2), 35.55 (CH_2). HRMS [ESI] calcd for $\text{C}_{17}\text{H}_{20}\text{N}_2\text{O}_2$ m/z 285.1598 [M+H], found 285.1586 [M+H].

1-Benzyl-3-dodecylurea (7h): White solid, Yield – 180 mg (63%), mp 127–129 °C, IR (DCM) 3322, 2920, 2850, 1619, 1572, 1259, 733, 698 cm^{-1} , ^1H NMR (400 MHz, CDCl_3) δ 7.26-7.31 (m, 5H, ArCH), 4.86 (s, 2H, NH), 4.33-4.36 (m, 2H, CH_2), 3.08-3.13 (m, 2H, CH_2), 1.25-1.45 (m, 20H, CH_2), 0.86-0.89 (t, $J = 8$ Hz, 3H, CH_3). ^{13}C NMR (101 MHz, CDCl_3) δ 158.40 (C=O), 139.45 (quat-C), 128.75 (ArCH), 127.58 (ArCH), 127.41 (ArCH), 44.68 (CH_2), 40.79 (CH_2), 32.06 (CH_2), 30.33 (CH_2), 29.80 (CH_2), 29.75 (CH_2), 29.49 (CH_2), 27.05 (CH_2), 22.83 (CH_2), 14.25 (CH_3). HRMS [ESI] calcd for $\text{C}_{14}\text{H}_{22}\text{N}_2\text{O}_2$ m/z 341.2563 [M+ Na], found 341.2558 [M+Na].

1-Benzyl-3-(cyclohexylmethyl)urea (7i): White solid, Yield – 168 mg (76%), mp >300 °C, IR (DCM) 3325, 2925, 2858, 1623, 1568, 1251, 730, 691 cm⁻¹, ¹H NMR (400 MHz, CDCl₃) δ 7.29-7.33 (m, 5H, ArCH), 4.77 (s, 2H, NH), 4.37 (s, 2H, CH₂), 3.12-3.15 (t, *J* = 4 Hz, 2H, CH₂), 1.59 (s, 3H, CH₂), 1.46 (s, 1H, CH), 1.27 (s, 5H, CH₂) 0.86-0.89 (m, 2H, CH₂). ¹³C NMR (101 MHz, CDCl₃) δ 158.38 (C=O), 139.36 (quat-C), 128.56, 127.38, 127.18, 44.42 (CH₂), 40.60 (CH₂), 31.52 (CH), 30.14 (CH₂), 26.53 (CH₂), 22.57 (CH₂), 14.03 (CH₂). HRMS [ESI] calcd for C₁₅H₂₂N₂O *m/z* 246.1732 [M+H], found 246.1726 [M+H].

4.6 NOTES AND REFERENCES

- (1) (a) Jackson, W. G.; McKeon, J. A.; Cortez, S. *Inorg. Chem.* **2004**, *43*, 6249-6254.
(b) James, K. B. *Acc. Chem. Res.* **2005**, *38*, 671-678.
- (2) (a) Casalnuovo, A. L.; Calabrese, J. C.; Milstein, D. *J. Am. Chem. Soc.* **1988**, *110*, 6738-6744. (b) Dorta, R.; Egli, P.; Zucher, F.; Togni, A. *J. Am. Chem. Soc.* **1997**, *119*, 10857-10858. (c) Muniz, K.; Lishchynskiy, A.; Streuff, J.; Nieger, M.; Escudero-Adana, E. C.; Belmontea, M. M. *Chem. Commun.*, **2011**, *47*, 4911-4913. (d) Teltewskoi, M.; Kallane, S. I.; Braun, T.; Herrmann, R. *Eur. J. Inorg. Chem.* **2013**, 5762-5768.
- (3) (a) Khaskin, E.; Iron, M. A.; Shimon, L. J. W.; Zhang, J.; Milstein, D. *J. Am. Chem. Soc.* **2010**, *132*, 8542-8543. (b) Feller, M.; Diskin-Posner, Y.; Shimon, L. J. W.; Ben-Ari, E.; Milstein, D. *Organometallics* **2012**, *31*, 4083-4101.
- (4) For reviews on MLC, see: (a) Gunanathan, C.; Milstein, D. *Acc. Chem. Res.* **2011**, *44*, 588-602. (b) Gunanathan, C.; Milstein, D. *Top. Organomet. Chem.* **2011**, *37*, 55-84. (c) Gunanathan, C.; Milstein, D. *Chem. Rev.* **2014**, *114*, 12024-12087. (d) Khusnutdinova, J. R.; Milstein, D. *Angew. Chem., Int. Ed.*, **2015**, *54*, 12236–12273.

- (5) (a) Casalnuovo, A. L.; Calabrese, J. C.; Milstein, D. *Inorg. Chem.* **1987**, *26*, 971-973. (b) Schaad, D. R.; Landis, C. R. *J. Am. Chem. Soc.* **1990**, *112*, 1628-1629. (c) Kanzelberger, M.; Zhang, X.; Emge, T. J.; Goldman, A. S.; Zhao, J.; Incarvito, C.; Hartwig, J. F. *J. Am. Chem. Soc.* **2003**, *125*, 13644-13645. (d) Zhao, J.; Goldman, A. S.; Hartwig, J. F. *Science* **2005**, *307*, 1080-1082. (e) Sykes, A. C.; White, P.; Brookhart, M. *Organometallics* **2006**, *25*, 1664-1675. (f) Morgan, E.; MacLean, D. F.; McDonald, R.; Turculet, L. *J. Am. Chem. Soc.* **2009**, *131*, 14234-14236. (g) Huang, Z.; Zhou, J. S.; Hartwig, J. F. *J. Am. Chem. Soc.* **2010**, *132*, 11458-11460.
- (6) Chatterjee, B.; Krishnakumar, V.; Gunanathan, C. *Org. Lett.* **2016**, *18*, 5892-5895.
- (7) Gore, S.; Baskaran, S.; Konig, B. *Org. Lett.* **2012**, 4568-4571.
- (8) Imperato, G.; Eibler, E.; Niedermeier, J.; Konig, B. *Chem. Commun.* **2005**, 1170-1172.
- (9) Dragovich, P. S. *et al. J. Med. Chem.* **1996**, *39*, 1872-1884.
- (10) Semple, G.; Ryder, H.; Rooker, D. P.; Batt, A. R.; Kendrick, D. A.; Szelke, M.; Ohta, M.; Satoh, M.; Nishida, A.; Akuzawa, S.; Miyata, K. *J. Med. Chem.* **1997**, *40*, 331-341.
- (11) (a) Kim, I.; Tsai, H.; Nishi, K.; Kasagami, T.; Morisseau, C.; Hammock, B. D. *J. Med. Chem.* **2007**, *50*, 5217-5226. (b) Shen, H. C.; Hammock, B. D. *J. Med. Chem.* **2012**, *55*, 1789-1808. (c) Falck, J. R.; Wallukat, G.; Puli, N.; Goli, M.; Arnold, C.; Konkel, A.; Rothe, M.; Fischer, R.; Müller, D. N.; Schunck, W. H. *J. Med. Chem.* **2011**, *54*, 4109-4118. (d) El-Damasy, A. K.; Lee, J. H.; Seo, S. H.; Cho, N. C.; Pae, A. N.; Keum, G. *Eur. J. Med. Chem.* **2016**, *115*, 201-216. (e) Guan, A.; Liu, C.; Yang, X.; Dekeyser, M. *Chem. Rev.* **2014**, *114*, 7079-7107.

- (12) Getman, D. P.; DeCrescenzo, J. G. A.; Heintz, R. M.; Reed, K. L.; Talley, J. J.; Bryant, M. L.; Clare, M.; Houseman, K. A.; Marr, J. J.; Mueller, R. A.; Vazquez, M. L.; Shieh, H. S.; Stallings, W. C.; Stegemanl, R. A.; *J. Med. Chem.* **1993**, *36*, 288-291.
- (13) Le, H. V.; Ganem, B. *Org. Lett.* **2011**, *13*, 2584-2585.
- (14) Bigi, F.; Maggi, R.; Sartori, G. *Green Chem.* **2000**, *2*, 140-148.
- (15) (a) Cheng, W. H. *Acc. Chem. Res.* **1999**, *32*, 685-691. (b) Díaz, D. J.; Darko, A. K.; McElwee-White, L. *Eur. J. Org. Chem.* **2007**, 4453-4465. (c) Ueda, T.; Konishi, H.; Manabe, K. *Angew. Chem. Int. Ed.* **2013**, *52*, 8611-8615. (d) Kim, S. H.; Hong, S. H. *Org. Lett.* **2016**, *18*, 212-215. (e) Zhang, Y.; Chen, J. L.; Chen, Z. B.; Zhu, Y. M.; Ji, S. J. *J. Org. Chem.* **2015**, *80*, 10643-10650.
- (16) Giannoccaro, P.; Nobile, C. F.; Mastroilli, P.; Ravasio, N. *J. Organomet. Chem.* **1991**, *419*, 251-258.
- (17) Guan, Z. H.; Lei, H.; Chen, M.; Ren, Z. H.; Bai, Y.; Wanga, Y.Y. *Adv. Synth. Catal.* **2012**, *354*, 489-496.
- (18) (a) Zhao, J.; Li, Z.; Yan, S.; Xu, S.; Wang, M. A.; Fu, B.; Zhang, Z. *Org. Lett.* **2016**, *18*, 1736-1739. (b) Gabriele, B.; Salerno, G.; Mancuso, R.; Costa, M. *J. Org. Chem.* **2004**, *69*, 4741-4750. (c) Park, J. H.; Yoon, J. C.; Chunga, Y. K. *Adv. Synth. Catal.* **2009**, *351*, 1233-1237.
- (19) (a) Chatterjee, B.; Gunanathan, C. *Org. Lett.* **2015**, *17*, 4794-4797. (b) Chatterjee, B.; Gunanathan, *Chem. Commun.* **2016**, *52*, 4509-4512.
- (20) Thermal ellipsoids are drawn at 50% probability. Two molecules were present in unit cell. A chloride counter ion bound to the N1H proton (ligand backbone amine) is removed for the clarity.
- (21) Ding, S.; Jiao, N. *Angew. Chem. Int. Ed.* **2012**, *51*, 9226-9237.

- (22) Kothandaraman, J.; Czaun, M.; Goepfert, A.; Haiges, R.; Jones, J.P.; May, R. B.; Surya Prakash, G. K.; Olah, G. A. *ChemSusChem* **2015**, *8*, 1442- 1451.
- (23) Bruker AXS, SAINT+, Program for Reduction of Data collected on Bruker CCD Area Detector Diffractometer V. 6.02. Bruker AXS Inc., Madison, Wisconsin, USA, 1999.
- (24) Bruker AXS, SADABS, Program for Empirical Absorption Correction of Area Detector Data V 2004/1, Bruker AXS Inc., Madison, Wisconsin, USA, 2004.
- (25) Sheldrick, G. M. *Acta Crystallogr.* **2008**, *A64*, 112-122.
- (26) Dolomanov, O. V.; Bourhis, L. J.; Gildea, R. J.; Howard, J. A. K.; Puschmann, H. J. *Appl. Crystallogr.* **2009**, *42*, 339-341.
- (27) Kim, S. H.; Hong, S. H. *Org. Lett.*, **2016**, *18*, 212-215.
- (28) Orito, K.; Miyazawa, M.; Nakamura, T.; Horibata, A. ; Ushito, H.; Nagasaki, H.; Yuguchi, M.; Yamashita, S. ; Yamazaki, T.; Tokuda, M. *J. Org. Chem.*, **2006**, *71*, 5951-5958.
- (29) Shelton, P. A.; Zhang, Y.; Nguyen, T. H. H.; White, L. M. *Chem. Commun.*, **2009**, 947-949.
- (30) Atanasova, I.; Petrov, I.; Mollov, N. *Synth. Commun.*, **1989**, *19*, 147-153.
- (31) Busschaert, N.; Kirby, I. L.; Young, S.; Coles, S. J.; Horton, P. N.; Light, M. E.; Gale, P. A. *Angew. Chem. Int. Ed.*, **2012**, *51*, 4426-4430.
- (32) Mizuno, T.; Nakai, T.; Mihara, M. *Synthesis*, **2010**, *24*, 4251-4255.
- (33) Mizuno, T.; Mihara, M.; Iwai, T.; Ito, T.; Ishino, Y. *Synthesis*, **2006**, *17*, 2825-2830.
- (34) Mueller, K.; Koc, F.; Ricken, S.; Eilbracht, P. *Org. Biomol. Chem.*, **2006**, *4*, 826-835.

^1H and ^{13}C NMR spectra of urea derivatives:

Figure 4.3 ^1H NMR spectrum of 1-Benzyl-3-(4-methylbenzyl)urea (**7a**):

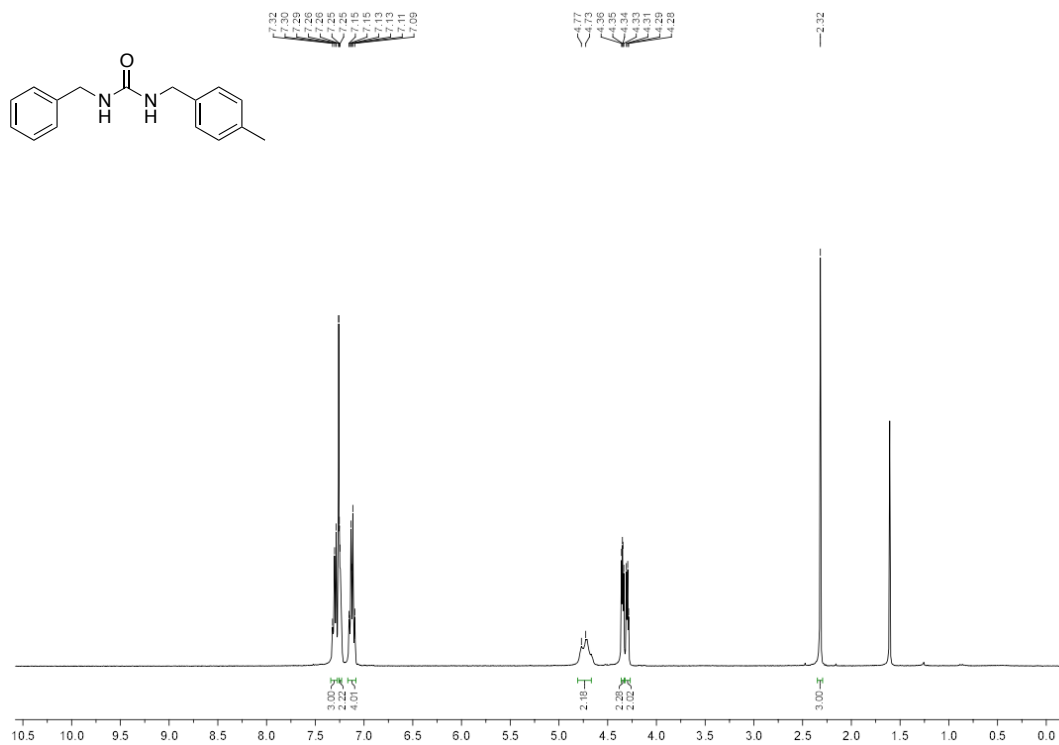


Figure 4.4 ^{13}C NMR spectrum of 1-Benzyl-3-(4-methylbenzyl)urea (**7a**):

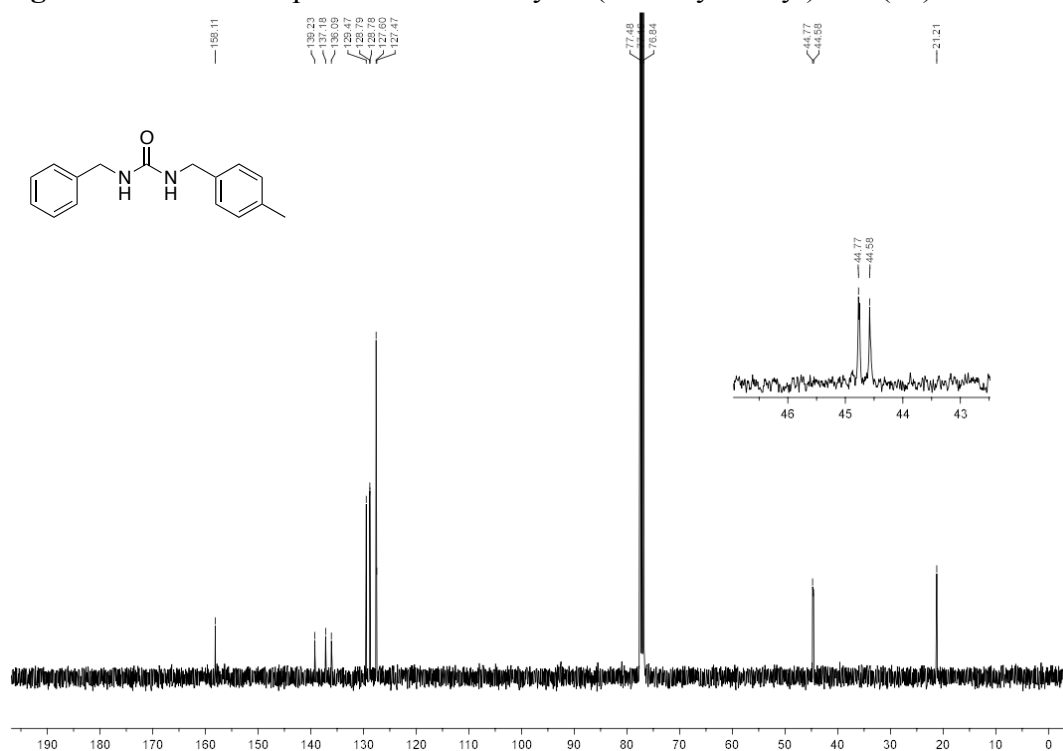


Figure 4.5 ^1H NMR spectrum of 1-Benzyl-3-(cyclohexylmethyl)urea (**7i**):

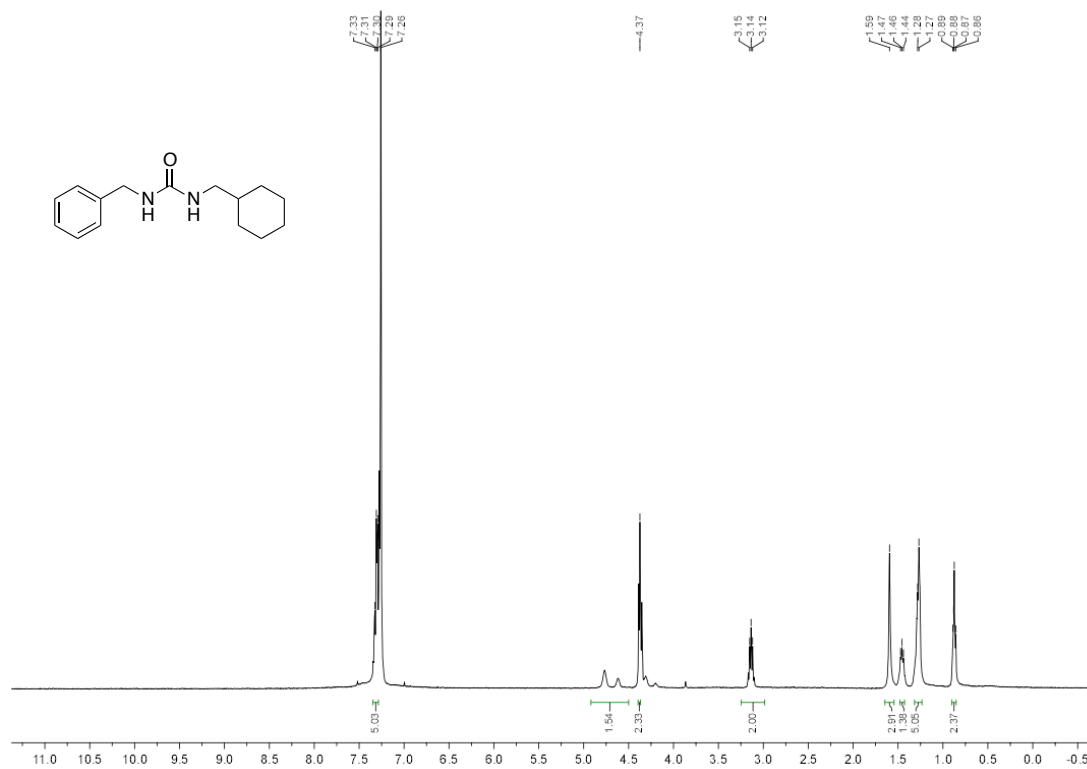


Figure 4.6 ^{13}C NMR spectrum of 1-Benzyl-3-(cyclohexylmethyl)urea (**7i**):

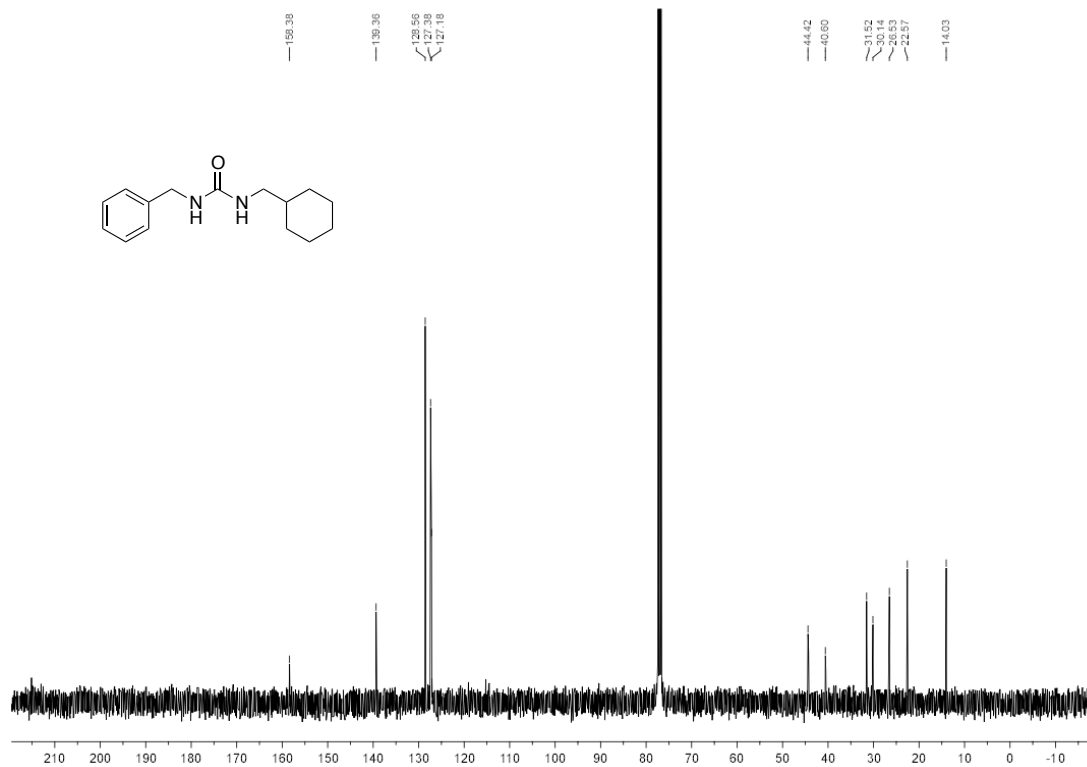


Figure 4.7 ^1H NMR Spectrum of 1,3-Dihexylurea (**5b**):

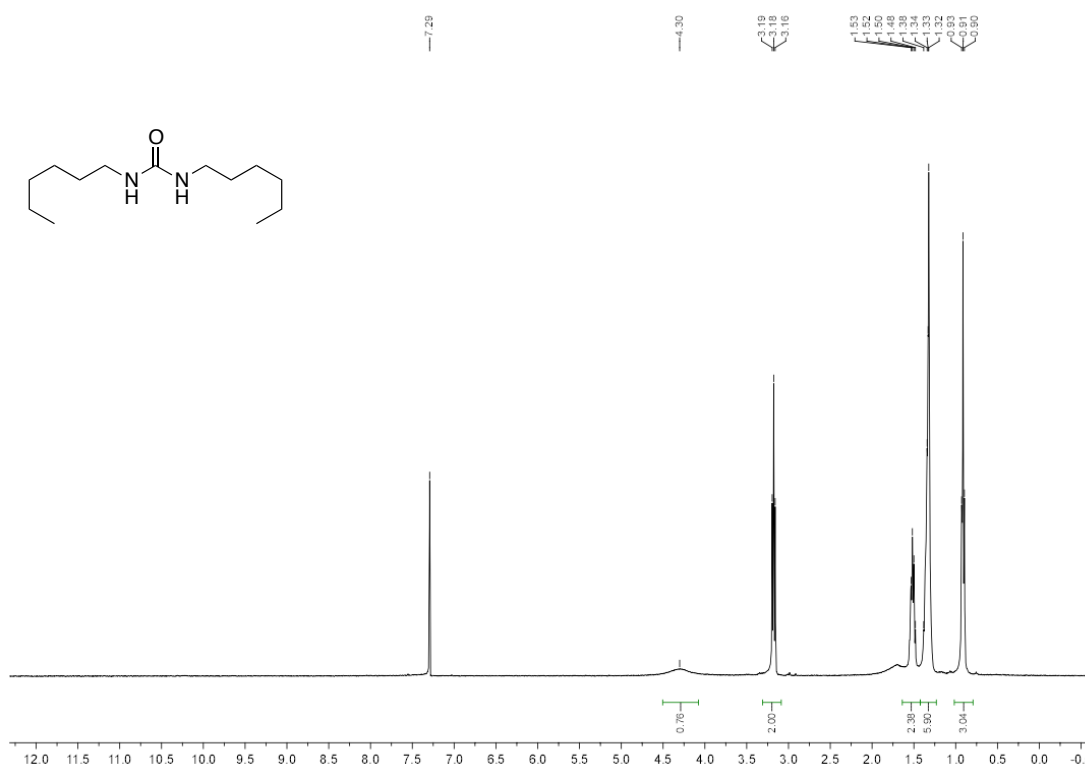
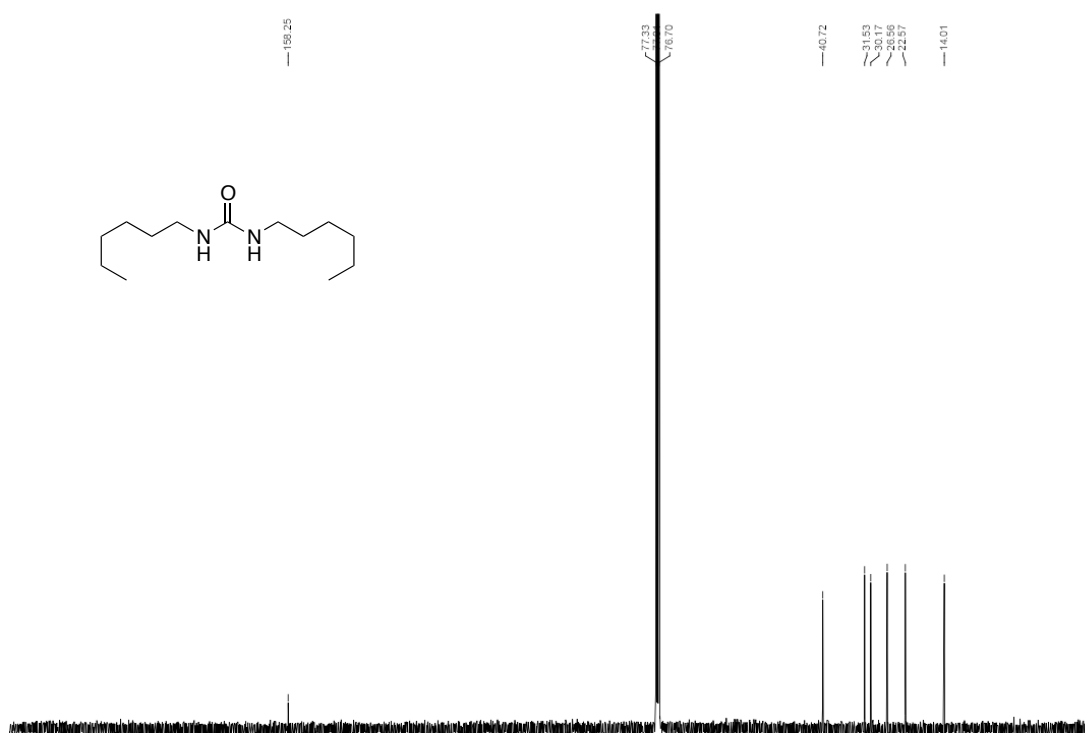


Figure 4.8 ^{13}C NMR Spectrum of 1,3-Dihexylurea (**5b**):



Part B

Catalysis Based on Ruthenium Half-Sandwich Complexes

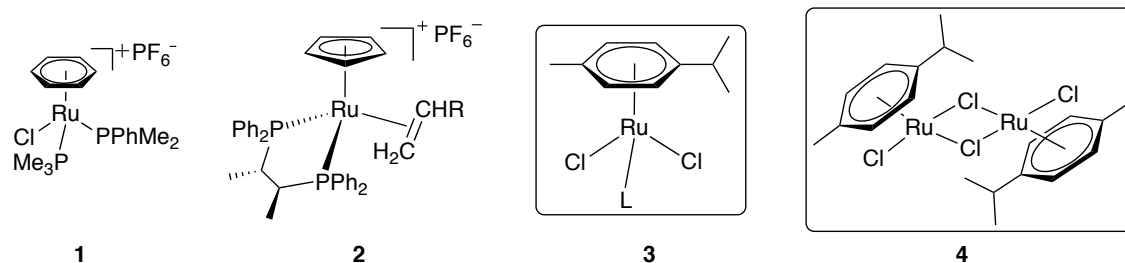
CHAPTER 5

Half-sandwich Ruthenium Complexes and their Reactivity

Half sandwich compounds are a class of organometallic complexes. When transition metals possess single cyclic polyhaptic ligands along with other ligands they are called half-sandwich complexes. The discovery of η -type bonding fashion in ferrocene molecule by Woodward and Wilkinson in 1952 was landmark in organometallic chemistry.¹ Afterwards several sandwich and half sandwich type of complexes possessing various transition metals are isolated and characterized. Ruthenium also exhibits several half-sandwich type complexes such as cationic complex of type **1** and **2** where benzene and cyclopentadiene (Cp) ligands are coordinated in η^6 and η^5 fashion respectively (Scheme 5.1). Complex **1** and **2** are known to possess diverse catalytic activity.² The neutral half sandwich of type **3** and **4** are also important class of ruthenium complexes as they exhibit versatile reactivity in different catalytic processes like hydrogenation, transfer hydrogenation, C–H activation, hydroelementation, cycloaddition, esterification and olefin-metathesis reactions.³ In this part our main focus will be to discuss the chemistry related to complex **4** and its derivatives. The complex **4** is well known catalyst and particularly interesting because of chloro-bridged mode of bonding. In presence of other coordination molecules this complex undergoes cleavage of the bridged bonds and generates reactive unsaturated

species, which can be further stabilized and tuned by external ligands. The complex **4** is also commercially available and air and moisture stable (Scheme 5.1).

Scheme 5.1 Half-sandwich Complexes of Ruthenium

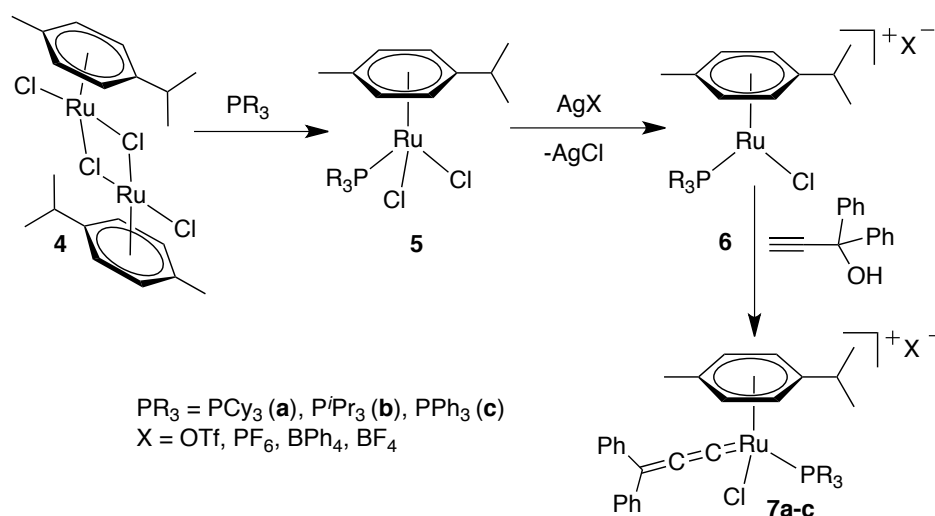


The half sandwich complexes are also called “Piano-stool complexes” for their analogous structure like piano-stool. Besides having a single cyclic polyhapto arene moiety the metal center in these complexes are surrounded by other monodentate or bidentate ligands. When three monodentate or one bidentate ligands along with one monodentate ligand encompasses the metal center, the geometry around the metal center becomes pseudo octahedral.² In rare cases the metal center also possess four monodentate ligands along with a single cyclic polyhapto ligand and leads to the capped pseudo octahedral geometry.⁴ The nature of coordinated arene moiety and monodentate or bidentate ligands influence greatly the reactivity and catalytic properties of these complexes. By changing the ligand environment around the metal center the structure-activity properties can be tuned.⁵ The coordinated η^n -arene moieties are inert towards substitution and reside as spectator ligand to protect the metal sites from one face and their further oxidation. The other coordination sites of the ruthenium center can be occupied by ligands having donor site embedded with N, O, S, P, Si, B etc.² A hydride ligand also can coordinate metal center to generate Ru–H species. The Ru–H species are particularly highly reactive in nature, and capable of exhibiting diverse catalytic activity.⁶ They are crucial intermediates in C–H activation, dehydrogenation, hydrogenation and hydroelementation reactions

such as hydrosilylation and hydroboration reactions of multiple bonds. Therefore these complexes link conceptually the classical Werner's coordination complexes and organometallic compounds as two different prototypical coordinative environments are combined in single mononuclear metal center. As a result, these complexes exhibit rich chemistry and ample scopes are available to develop this field further for their benign stoichiometric as well as catalytic transformations. Thus our present studies described in **PART B** will explore the catalysis based on half-sandwich ruthenium complexes.

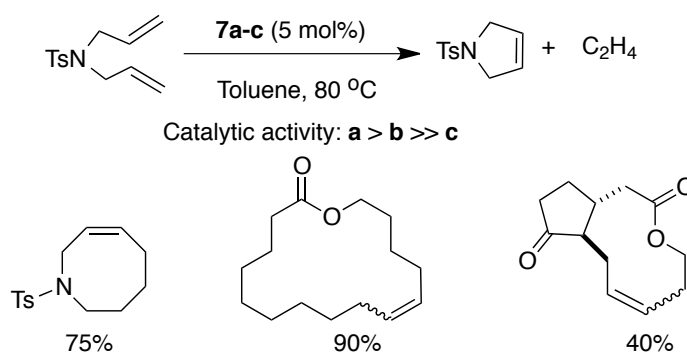
In recent years, one of the striking chemical transformations discovered is alkene metathesis reaction. The successful implementation of Grubbs's and Schrock's catalyst in ring closing and ring opening metathesis reaction prompted scientists worldwide to quest further for efficient catalysts in this topic. Dixneuf and coworkers disclosed very interesting example of ruthenium allenylidene complexes for efficient ring closing alkene metathesis reaction. The complexes can be prepared successfully by introducing a PCy₃ ligand in complex **4** to generate a half-sandwich phosphine coordinated Ru (II) complex **5**. Further, addition of silver salts lead to the formation of cationic ruthenium complexes, which upon treatment with prop-2-yn-1-ols activates the terminal alkyne motif to generate the corresponding ruthenium allenylidene complexes **7** (Scheme 5.2).⁷

Scheme 5.2: Preparation of the Ruthenium Allenylidene Catalyst Precursors



The catalytic activity of these complexes in ring closing metathesis revealed a strong correlation with the nature of the chosen phosphine ligand. Observations with ruthenium-based initiators disclosed the catalytic activity decreases in the order of $\text{PCy}_3 > \text{PPr}^i_3 \gg \text{PPh}_3$ (Scheme 5.2 and 5.3).⁸ As can be seen from the results compiled, these catalysts (**7a-c**) effectively employed in the construction of five membered and other larger ring size molecules, including macrocyclic and medium sized products. The isolated yields of the obtained products were found to be good to excellent and can be compared to those previously obtained using the Grubbs carbene complexes.

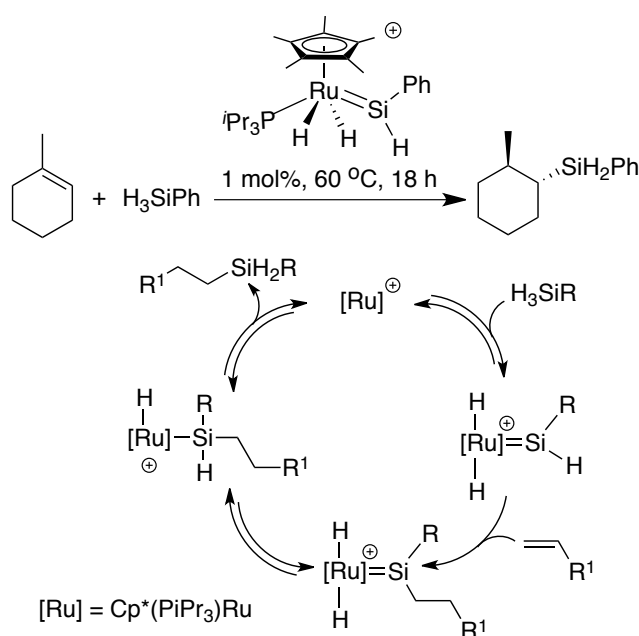
Scheme 5.3: Ring Closing Metathesis Using Ru-Allenylidene Catalysts



Hydrosilylation reaction is addition of silicon and hydrogen across a multiple bond, is

an important class of chemical transformation in organic synthesis to generate organosilicon compounds.⁹ The major reports for the hydrosilylation of alkenes features electron-rich transition metals such as platinum and rhodium, which typically proceed by “Chalk-Harrod” type mechanisms resulting in *cis* addition of the Si–H bond to a multiple bond.¹⁰ Don Tilley and coworkers described a different mechanism of alkene hydrosilylation based on transition metal silylene complexes,¹¹ in which a three-coordinated silicon center is bound to a metal center and further an unusual type of hydrosilylation proceeds by the concerted addition of the Si–H bond of the silylene across the multiple bond of the substrate to generate the corresponding hydrosilylated products (Scheme 5.4).

Scheme 5.4: Hydrosilylation of Alkenes by a Ruthenium Silylene Complex



NOTES AND REFERENCES

- (1) Wilkinson, G.; Rosenblum, M.; Whiting, M. C.; Woodward, R. B. *J. Am. Chem. Soc.* **1952**, *74*, 2125-2126.
- (2) (a) Consiglio, G.; Morandini, F. *Chem. Rev.* **1987**, *87*, 781-778. (b) Kumar, P.; Gupta, R. K.; Pandey, D. S. *Chem. Soc. Rev.*, **2014**, *43*, 707-733.
- (3) (a) Noyori, R.; Hashiguchi, S. *Acc. Chem. Res.*, **1997**, *30*, 97-102. b) Bennett, M. A. in *Comprehensive Organometallic Chemistry II*, ed. Shriver, D. S.; Bruce, M. I. Elsevier Science, Ltd., Oxford, 1995, vol. 7, pp. 549-602. c) Bozec, H. L.; Touchard, D.; Dixneuf, P. H. *Adv. Organomet. Chem.*, **1989**, *29*, 163-247. d) Moriarty, R. M.; Gill, U. S.; Ku, Y. Y. *J. Organomet. Chem.*, **1988**, *350*, 157-190.
- (4) Chatterjee, B.; Gunanathan. C. *Chem. Commun.*, **2014**, *50*, 888-890.
- (5) Habtemariam, A.; Melchart, M.; Fernandez, R.; Parsons, S.; Oswald, I. D. H.; Parkin, A.; Fabbiani, F. P. A.; Davidson, J. E.; Dawson, A.; Aird, R. E.; Jodrell, D. I.; Sadler, P. J.; *J. Med. Chem.*, **2006**, *49*, 6858-6868.
- (6) Arockiam, P. B.; Bruneau, C.; Dixneuf, P. H. *Chem. Rev.*, **2012**, *112*, 5879-5918.
- (7) (a) Furstner, A.; Picquet, M.; Bruneau, C.; Dixneuf, P. H. *Chem. Commun.* **1998**, 1315-1316. (b) Bruneau, C.; Dixneuf, P. H. *Angew. Chem. Int. Ed.* **2006**, *45*, 2176-2203.
- (8) (a) Stumpf, A. W.; Saive, E.; Demonceau, A.; Noels, A. F. *J. Chem., Soc. Chem. Commun.*, **1995**, 1127-1128. (b) Demonceau, A.; Stumpf, A. W.; Saive, E.; Noels, A. F. *Macromolecules*, **1997**, *30*, 3127-3136. (c) Hafner, A.; Mühlebach, A.; van der Schaaf, P. A. *Angew. Chem., Int. Ed. Engl.*, **1997**, *36*, 2121-2124.

(9) (a) Marciniak, B. *Silicon Chem.* **2002**, *1*, 155. (b) Brook, M. A. *Silicon in Organic, Organometallic, and Polymer Chemistry*; Wiley: New York, 2000. (c) Ojima, I.; Li, Z.; Zhu, J. *The Chemistry of Organic Silicon Compounds*, Wiley: Avon, 1998; Chapter 29.

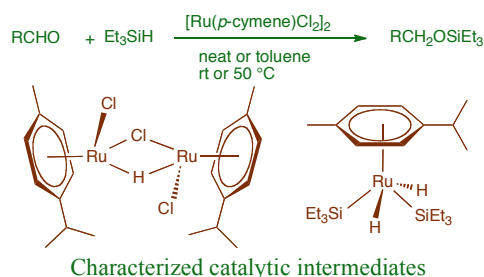
(10) (a) Chalk, A. J.; Harrod, J. F. *J. Am. Chem. Soc.* **1965**, *87*, 16-21. (b) Seitz, F.; Wrighton, M. S. *Angew. Chem., Int. Ed. Engl.* **1988**, *27*, 289-291. (c) Duckett, S. B.; Perutz, R. N. *Organometallics* **1992**, *11*, 90-98.

(11) Glaser, P. B.; Tilley, T. D. *J. Am. Chem. Soc.* **2003**, *125*, 13640-13641.

CHAPTER 6

Ruthenium Catalyzed Selective Hydrosilylation of Aldehydes

6.1 ABSTRACT



A chemoselective hydrosilylation method for aldehydes is developed using a ruthenium catalyst $[(\text{Ru}(\textit{p}\text{-cymene})\text{Cl}_2)_2]$ and triethylsilane; a mono hydride bridged dinuclear complex $[\{(\eta^6\text{-}\textit{p}\text{-cymene})\text{RuCl}\}_2(\mu\text{-H}-\mu\text{-Cl})]$ and a Ru(IV) mononuclear dihydride complex $[(\eta^6\text{-}\textit{p}\text{-cymene})\text{Ru}(\text{H})_2(\text{SiEt}_3)_2]$ are identified as potential intermediates in the reaction and the proposed catalytic cycle involves a 1,3-hydride migration.

6.2 INTRODUCTION

Hydrosilylation of carbonyl compounds is a valuable transformation in chemical synthesis as a single step operation serves on both reduction of carbonyl motifs and protection of resulting alcohols featuring high atom-economy. Catalytic hydrosilylation, which can be carried out under mild experimental conditions, is often used as a convenient alternative to hydrogenation reaction and is advantageous over those performed using the traditional and harsh reducing agents.¹ Alkoxy silanes function as useful synthetic intermediates, used for the synthesis of silicon-containing polymers, ceramic materials and thus produced in both small as well as large-scales.²

A number of transition metal complexes were reported to catalyze the hydrosilylation of carbonyl motifs.³⁻¹¹ However, known catalysts for hydrosilylation reactions are highly reactive and they invariably reduce a range of different functionalities. Thus, a synthetic method that can differentiate and catalyze a selective hydrosilylation of aldehydes using a simple, inexpensive catalyst would be valuable and have potential synthetic applications.^{12,13} Here, we report a chemoselective hydrosilylation of aldehydes under mild and neutral reaction conditions catalyzed by commercially available $[(\text{Ru}(p\text{-cymene})\text{Cl}_2)_2]$ **1**.

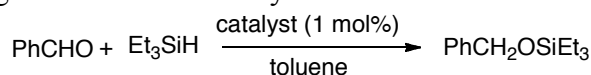
6.3 RESULTS AND DISCUSSIONS

A detailed investigation and optimization studies using the common ruthenium complexes and silanes revealed $[\text{Ru}(p\text{-cymene})\text{Cl}_2]_2$ **1** and triethylsilane as suitable catalyst and silane, respectively for hydrosilylation of aldehydes (Tables 6.1, 6.2 and 6.3). Interestingly, the reaction can be carried out under neat conditions or in toluene and benzyl(triethylsilyl)ether could be obtained in 95% yields from benzaldehyde using 1 mol % of **1** (Table 6.4).

At the outset various common and commercially available ruthenium complexes were explored to find out a suitable catalyst for the hydrosilylation of aldehydes using benzaldehyde as a benchmark substrate (Table 6.1). The initial screen of ruthenium complexes provided encouraging results (Entries 1-3). Although few ruthenium complexes were ineffective for the hydrosilylation of aldehydes (entries 4-6), moderate yields were obtained with complexes containing chloride ligands (entries 7-8). Out of all the complexes studied, the dinuclear Ru(II) complex, $[\text{Ru}(p\text{-cymene})\text{Cl}_2]_2$ (**1**) proved to be the optimal catalyst and provided the 95% yield of benzyl(triethylsilyl)ether (entry 9). Upon identifying suitable catalyst for

hydrosilylation of aldehydes, the reaction conditions were optimized further with $[\text{Ru}(p\text{-cymene})\text{Cl}_2]_2$ **1** at different temperatures and catalyst loadings (See, Table 6.2) and use of various silanes revealed the suitability of triethylsilane (See, Table 6.3).

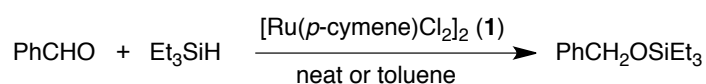
Table 6.1 Screening of Ruthenium Catalysts^a



Entry	Ru	Time (h)	Yield (%) ^b
1	$\text{RuCl}_3 \cdot 3\text{H}_2\text{O}$	36	25
2	$\text{Ru}(\text{CO})_3(\text{PPh}_3)_3$	36	52
3	$\text{Ru}_3(\text{CO})_{12}$	24	53
4	$[\text{Ru}(\text{CO})_2\text{Cl}_2]_n$	36	0
5	$\text{Ru}(\text{COD})\text{Cl}_2$	24	7
6	$\text{Ru}(\text{acac})_3$	36	9
7	$\text{RuCl}_2(\text{PPh}_3)_3$	36	68
8	$\text{RuHCl}(\text{CO})(\text{PPh}_3)_3$	11	85
9	$[\text{Ru}(p\text{-cymene})\text{Cl}_2]_2$	3	95
10	$\text{RuH}_2(\text{CO})(\text{PPh}_3)_3$	10	74

^aRuthenium complex (1 mol%), benzaldehyde (1 mmol), triethylsilane (1.3 mmol) and toluene (2 mL) were heated at 50 °C under nitrogen atmosphere. ^bYields of isolated product after column chromatography.

Despite taking 10 h for completion, $[\text{Ru}(p\text{-cymene})\text{Cl}_2]_2$ **1** catalyzed hydrosilylation reaction at room temperature provided 94% yields (Table 6.2, entry 1); lowering the catalyst load (0.5 mol %) and slightly increasing the temperature (50 °C) provided the product in 94% yield after 8 h (entry 2). Heating the reaction mixture at 50 °C with 1 mol % catalyst load yielded 95% of product after 3 h (entry 3). The reaction also effectively proceeded under solvent less condition and the corresponding silyl ether product was obtained in 94% (entry 4). Further, increase of temperature resulted in decrease of reaction time (2 h), however, product yield also decreased to 90% (entry 5).

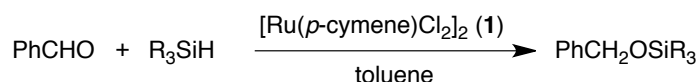
Table 6.2 Optimization of Reaction Conditions with $[\text{Ru}(p\text{-cymene})\text{Cl}_2]_2$ ^a

Entry	1 (mol%)	Temp. (°C)	Time (h)	Yield (%) ^b
1	1	25	10	94
2	0.5	50	8	94
3	1	50	3	95
4 ^c	1	50	3.5	94
5	1	75	2	90

^a $[\text{Ru}(p\text{-cymene})\text{Cl}_2]_2$ (1 mol%), benzaldehyde (1 mmol), triethylsilane (1.3 mmol) and toluene (2 mL) were reacted under nitrogen atmosphere. ^bYields of isolated product after column chromatography.

^cReaction carried out under neat conditions.

The next focus turned on towards search for suitable silane. Various hydrosilylated products were obtained upon reaction of benzaldehyde (1 equiv.) with silanes (1.3 equiv.) in the presence of $[\text{Ru}(p\text{-cymene})\text{Cl}_2]_2$ (1 mol %) (Table 6.3). Although, the silyl ether formed in all the reactions, the yields were lower than that of hydrosilylated product resulted from triethylsilane (Table 6.3).

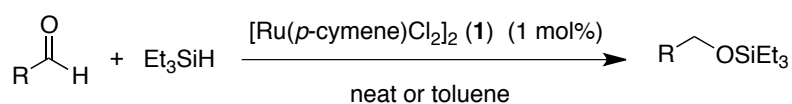
Table 6.3 Optimization of Silanes^a

Entry	Silane	Time (h)	Yield (%) ^b
1	Ph_3SiH	5	60
2	EtOMe_2SiH	3	83
3	$^i\text{Pr}_3\text{SiH}$	24	38
4 ^c	Et_2SiH_2	15	72 ^d
5 ^c	Ph_2SiH_2	15	35 ^e

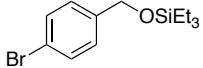
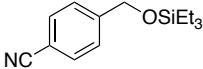
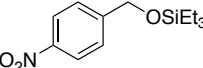
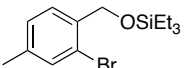
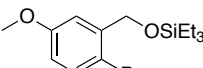
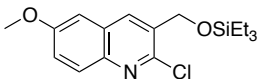
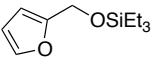
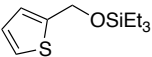
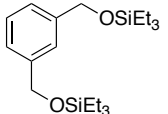
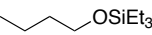
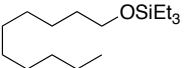
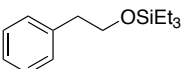
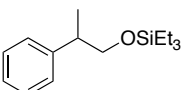
^a $[\text{Ru}(p\text{-cymene})\text{Cl}_2]_2$ (1 mol%), benzaldehyde (1 mmol), and silane (1.3 mmol) were heated at 50 °C under argon atmosphere and under neat conditions. ^bYields of isolated product after column chromatography. ^cReaction carried out under neat conditions. ^dCorresponding bis(benzyloxy)diethylsilane formed in 17% yields. ^eCorresponding bis(benzyloxy)diphenylsilane formed in 11% yields.

The substrate scope of hydrosilylation of an assortment of aldehydes using $[\text{Ru}(p\text{-cymene})\text{Cl}_2]_2$ **1** is investigated and summarized in Table 6.4. Silyl ether products are obtained in good yields with a range of substituents on aldehydes. Notably, aldehydes containing electron-releasing groups (entries 2-4) and electron withdrawing groups (entries 6-9), and both (entries 10-12) are tolerated and underwent facile hydrosilylation reactions. The heteroaromatic aldehydes such as furfuraldehyde and 2-thenaldehyde underwent hydrosilylation reactions under neat conditions (entries 13, 14). The dinuclear $[\text{Ru}(p\text{-cymene})\text{Cl}_2]_2$ **1** also catalyzed the hydrosilylation of aliphatic aldehydes at room temperature and under neat conditions provided silyl ether products in good yields (entries 16-19).

Table 6.4 Hydrosilylation of Aldehydes Catalyzed by $[\text{Ru}(p\text{-cymene})\text{Cl}_2]_2$ ^a



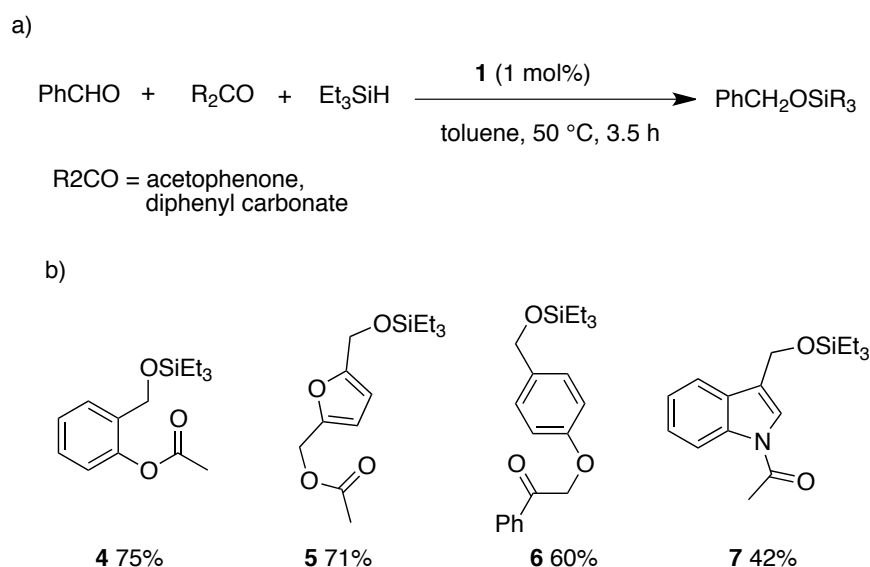
Entry	Silyl ethers	Time (h)	Yield (%) ^b
1 ^c		3.5	95
2 ^c		4.5	89
3		4.5	84
4		12	74
5		6	90
6 ^c		3.5	74

7 ^c		4.5	93
8		9	54
9		9	86
10		7	75
11		4.5	85
12		12	74
13 ^c		4.5	80
14 ^c		15	53
15		15	77
16 ^d		12	70
17 ^{c,d}		12	63
18 ^{c,d}		9	70
19 ^{c,d}		12	82

^aCatalyst [Ru(*p*-cymene)Cl₂]₂ (1 mol%), aldehyde (1 mmol), triethylsilane (1.3 mmol) and toluene (2 mL) were heated at 50 °C under argon atmosphere. ^bYields of isolated products after column chromatography. ^cReactions carried out under neat conditions. ^dReactions carried out at 25 °C. Analyses of reaction mixtures (¹H NMR, TLC) indicated the presence of unreacted aldehydes and products and no other side product is observed.

Furthermore, reaction of benzaldehyde with triethylsilane catalyzed by **1** was carried out in the presence of stoichiometrically equivalent amount of acetophenone and diphenyl carbonate (Scheme 6.1a). In both competition experiments hydrosilylation of benzaldehyde alone observed and benzyl triethylsilyl ether was isolated in 92% and 94% yields, respectively. Both acetophenone and diphenylcarbonate were quantitatively recovered. Similar chemoselectivity is observed in hydrosilylation of substrates containing aldehydes and a range of other functional groups (**4-7**, Scheme 6.1b). No hydrosilylation of ester or amide functionalities was observed under these conditions.¹¹

Scheme 6.1 Chemoselective Hydrosilylation of Aldehydes Catalyzed by [Ru(*p*-cymene)Cl₂]₂ **1**



To understand the reaction mechanism of this fundamental and interesting catalytic transformation, reaction of benzaldehyde with triethylsilane catalyzed by **1** was monitored by ¹H NMR, which indicated a first order kinetics (See, Figure 6.1) and formation of metal hydride intermediates during the catalysis.

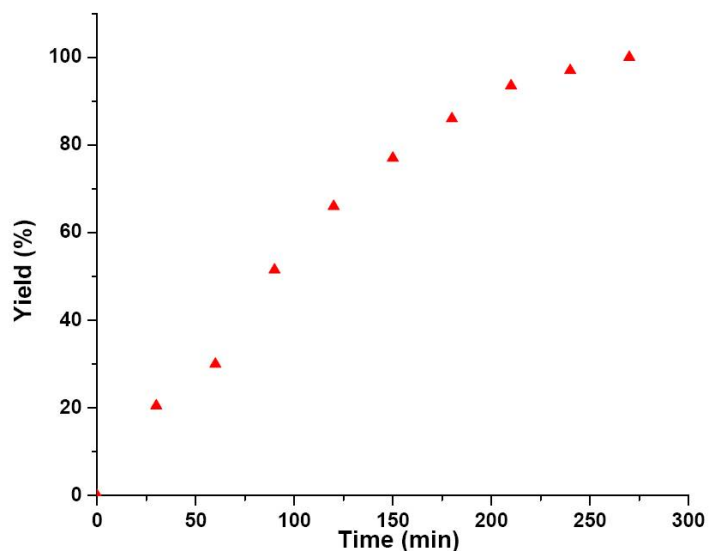


Figure 6.1 NMR monitoring of the reaction progress: benzyl triethylsilyl ether formation *vs.* time; benzene-d₆ solution of **1** and reactants (mesitylene is added as a reference) was heated at 50 °C.

A sharp singlet was observed at δ -10.18 ppm within 5 min of heating the reaction mixture. Over the time, intensity of this signal increased and then began to decrease after 30 min upon appearance of another singlet at δ -13.53 ppm (See, Figure 6.2).

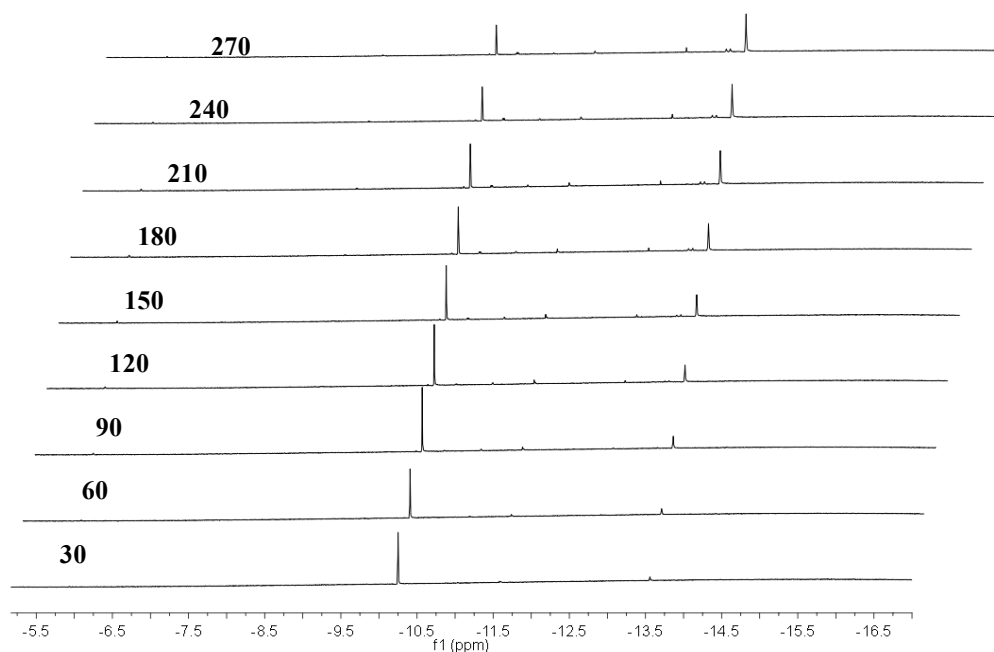
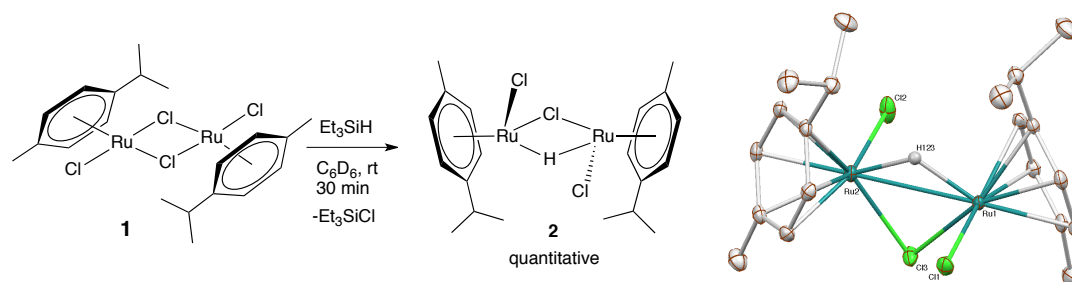


Figure 6.2 NMR study of the reaction progress (formation of hydride peaks at different time (min) interval).

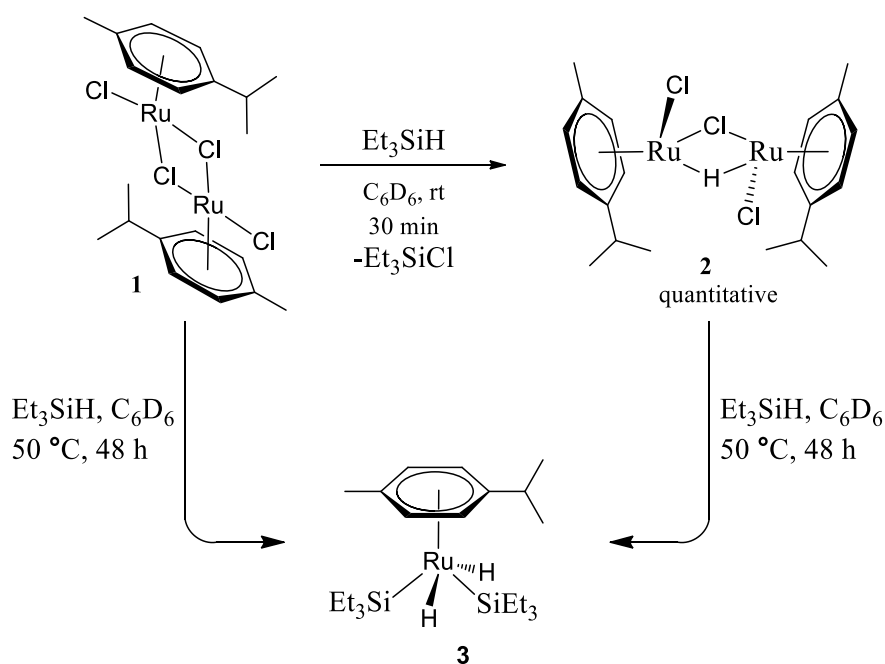
Both of these singlet signals remained in the spectra recorded further throughout the reaction. Stoichiometric reactions were performed in order to identify these metal hydride intermediates involved in the hydrosilylation of aldehydes. When $[\text{Ru}(p\text{-cymene})\text{Cl}_2]_2$ **1** was reacted with triethylsilane in benzene- d_6 at room temperature, a monohydrido bridged complex $[\{(\eta^6\text{-}p\text{-cymene})\text{RuCl}\}_2(\mu\text{-H-}\mu\text{-Cl})]$ **2** was obtained in quantitative yield (Scheme 6.2). The ‘bridged hydride’ in complex **2** displayed a singlet in ^1H NMR spectrum, which is attributable to the metal hydride signal observed at $\delta -10.18$ ppm during the catalysis. Suitable crystals were obtained from a toluene solution of **2** and the structure was unequivocally corroborated by single crystal X-ray analysis (Scheme 6.2).

Scheme 6.2 Synthesis and X-ray structure of $[\{(\eta^6\text{-}p\text{-cymene})\text{RuCl}\}_2(\mu\text{-H-}\mu\text{-Cl})]$ **2** (thermal ellipsoids drawn at 30% probability)



When a toluene solution of benzaldehyde, triethylsilane and **2** (1 mol %) was heated for 3 h the corresponding benzyl triethylsilyl ether was obtained in 95% yields, confirming the potential intermediacy of **2** in the reactions.¹⁵ Further, the metal hydride intermediate **3** that resonates a singlet at $\delta -13.53$ ppm was also independently prepared from both **1** and **2** and characterized as a mononuclear Ru(IV) dihydride complex $[(\eta^6\text{-}p\text{-cymene})\text{Ru}(\text{H})_2(\text{SiEt}_3)_2]$ **3** (Scheme 6.3).^{14,16} Isolated complex **3** also exhibited catalysis, indicating it's possible intermediacy in the catalytic cycle.¹⁷

Scheme 6.3 Synthesis of Complex $[(\eta^6\text{-}p\text{-cymene})\text{Ru}(\text{H})_2(\text{SiEt}_3)_2]$ (**3**) from **1** or **2**



The structure of **3** was also further confirmed by X-ray analysis of the single crystals obtained from hexane solution of **3**, which revealed capped pseudo-octahedral geometry around the metal center (Figure 6.3).

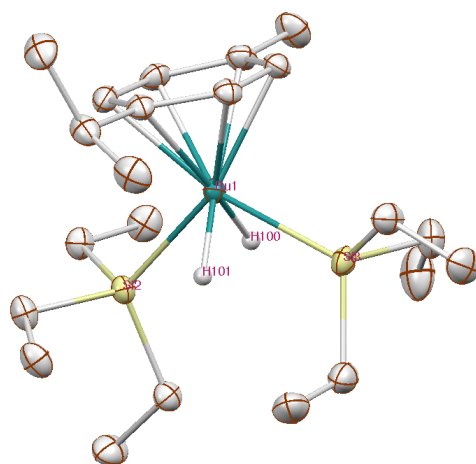
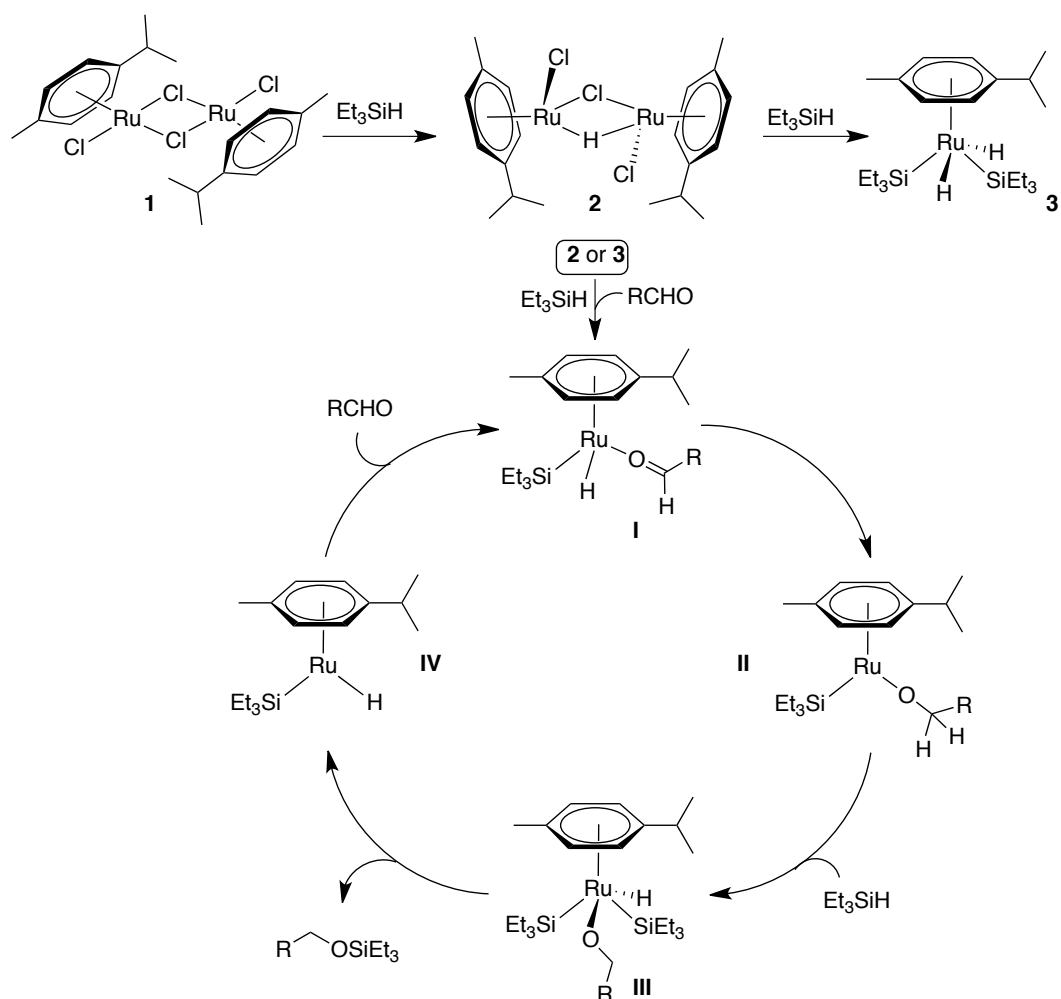


Figure 6.3 X-ray structure of **3** (thermal ellipsoids drawn at 30% probability)

On the basis of these observed data, a catalytic cycle for the hydrosilylation of aldehydes with silanes is proposed (Scheme 6.4). Either direct oxidative addition of triethylsilane¹⁸ on dinuclear Ru(II) **2** or reductive elimination of triethylsilane from intermediate **3** in the presence of aldehydes could produce the transient intermediate **I**, which undergoes 1,3-hydride migration from metal center to the carbonyl carbon leading to the reduction and concomitant formation of Ru(II) alkoxo intermediate **II**. Further oxidative addition of triethylsilane generates the Ru(IV) intermediate **III**. Coupling of silyl and alkoxo ligands on **III** by reductive elimination creates O–Si bonds and liberates silyl ethers providing Ru(II) intermediate **IV**. The coordination of aldehyde to **IV** regenerates **I** and closes the catalytic cycle.

Scheme 6.4 Proposed Catalytic Cycle for the Hydrosilylation of Aldehydes Catalyzed by $[\text{Ru}(p\text{-cymene})\text{Cl}_2]_2$ **1**



6.4 CONCLUSIONS

In conclusion, we have demonstrated a facile transformation for hydrosilylation of aldehydes using a commercially available dinuclear ruthenium complex $[\text{Ru}(p\text{-cymene})\text{Cl}_2]_2$ **1** as a catalyst. Using this novel catalytic method chemoselective hydrosilylation of aldehydes in the presence of other functionalities is also achieved. Potential intermediates $[(\eta^6\text{-}p\text{-cymene})\text{RuCl}]_2(\mu\text{-H}-\mu\text{-Cl})$ **2** and $[(\eta^6\text{-}p\text{-cymene})\text{Ru}(\text{H})_2(\text{SiEt}_3)_2]$ **3** involved in the reaction are identified and independently synthesized and characterized. The structures of **2** and **3** are solved by single crystal X-ray analyses. Proposed mechanism involves Ru(II)-Ru(IV) cycles and a 1,3-hydride migration that reduce the aldehyde at metal center.

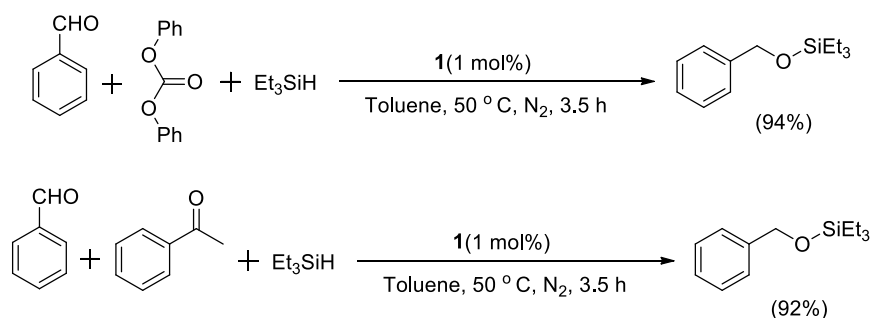
6.5 EXPERIMENTAL SECTION

General Experimental: All catalytic reactions were performed under nitrogen atmosphere. All stoichiometric reactions were performed in nitrogen atmosphere MBraun glove box. Chemicals were purchased from Acros, Sigma-Aldrich, Alfa-aesar, Himedia Chemicals and used without further purification. Dry solvents were prepared according to standard procedures. Ruthenium hydride intermediates [$\{(\eta^6\text{-}p\text{-cymene})\text{Ru}\}_2(\mu\text{-H}-\mu\text{-Cl})(\text{Cl})_2$] (**2**) and [$(\eta^6\text{-}p\text{-cymene})\text{Ru}(\text{H})_2(\text{SiEt}_3)_2$] (**3**) were prepared and isolated inside glove box. ^1H , ^{13}C spectra were recorded at Bruker AV-400 (^1H : 400 MHz, ^{13}C : 100.6 MHz). ^1H and $^{13}\text{C}\{^1\text{H}\}$ NMR chemical shifts were reported in ppm downfield from tetramethyl silane. Multiplicity is abbreviated as: s, Singlet; d, doublet; dd, doublet of doublet; t, triplet; q, quartet; dq, doublet of quartet; m, multiplet. Assignment of spectra was done based on one dimensional (dept-135) NMR techniques. IR Spectra were recorded in Perkin-Elmer FT-IR Spectrometer. Mass spectra were recorded on Bruker micrOTOF-Q II Spectrometer.

General Procedure for Catalytic Hydrosilylation of Aldehydes: Aldehyde (1 mmol), triethylsilane (1.3 mmol), $[\text{Ru}(p\text{-cymene})\text{Cl}_2]_2$ (1 mol %) [and toluene (2 mL), if aldehyde is in solid form] were taken in a closed flask equipped with a magnetic bar and the reaction mixture was heated at 50 °C. Progress of the reaction was monitored by TLC and ^1H NMR. Upon completion of the reaction, the resulting residue was chromatographed over silica-gel using 2% ethyl acetate/hexane mixture as eluent.

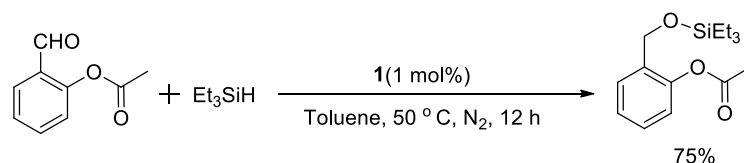
Procedure for Intermolecular Chemoselective Catalytic Hydrosilylation: Benzaldehyde (1 mmol), triethylsilane (1 mmol), diphenyl carbonate (1 mmol), $[\text{Ru}(p\text{-cymene})\text{Cl}_2]_2$ (1, 1 mol %) and toluene (2 mL) were taken in a closed flask equipped with a magnetic bar and the reaction mixture was heated at 50 °C. Progress of the reaction was monitored by TLC and ^1H NMR. Upon completion of the

reaction, the resulting residue was chromatographed over silica-gel using 2% ethyl acetate/hexane mixture as eluent. Similar experiment was also performed using acetophenone (1 mmol) as a competing substrate. Both unreacted acetophenone and diphenylcarbonate were quantitatively recovered.



Procedures for Intramolecular Chemoselective Catalytic Hydrosilylation:

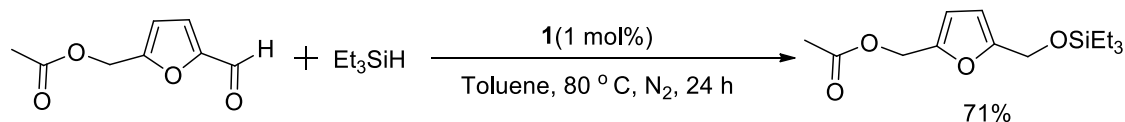
2-((Triethylsilyloxy)methyl)phenyl acetate (**4**):



2-formylphenyl acetate (1 mmol), triethylsilane (1 mmol), [Ru(*p*-cymene)Cl₂]₂ (1 mol %) and toluene (2 mL) were taken in a closed flask equipped with a magnetic bar and the reaction mixture was heated at 50 °C. Progress of the reaction was monitored by TLC and ¹H NMR. Upon completion of the reaction, the resulting residue was chromatographed over silica-gel using 2% ethyl acetate/hexane mixture as eluent. Colorless liquid. IR (DCM): 2955, 2877, 1767, 1487, 1456, 1369, 1206, 1175, 1079, 1010, 910, 789, 747 cm⁻¹. ¹H NMR (CDCl₃): δ 7.55 (d, *J* = 4 Hz, 1H, ArCH), 7.30-7.22 (m, *J* = 4 Hz, 2H, ArCH), 7.04 (d, *J* = 8 Hz, 1H, ArCH), 4.68 (s, 2H, OCH₂), 2.36 (s, 3H, CH₃), 0.99 (t, *J* = 8 Hz, 9 H, (SiCH₂CH₃)₃), 0.66 (q, *J* = 8 Hz, 6H, (SiCH₂CH₃)₃). ¹³C{¹H} NMR (CDCl₃): δ 169.15 (quat-C), 147.78 (quat-C), 133.24 (quat-C), 128.03 (CH), 127.98 (CH), 126.11 (CH), 121.91 (CH), 59.90 (OCH₂), 20.85

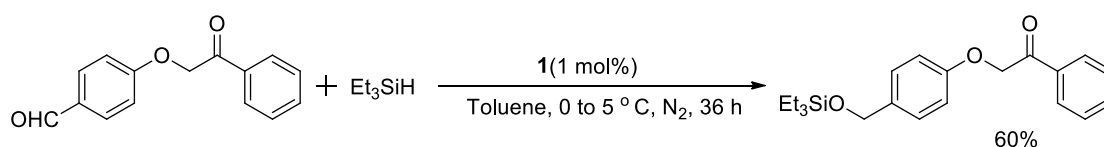
(CH₃), 6.81 (SiCH₂CH₃), 4.51 (SiCH₂CH₃). MS (ESI) m/z 281.15 (M)⁺. HR/MS: calcd (C₁₅H₂₅O₃Si)⁺ 281.1573. Found 281.1567.

5-((Triethylsilyloxy)methyl)furan-2-yl acetate (5):



(5-Formylfuran-2-yl)methyl acetate (1 mmol), triethylsilane (1 mmol), [Ru(*p*-cymene)Cl₂]₂ (1 mol %) and toluene (2 mL) were taken in a closed flask equipped with a magnetic bar and the reaction mixture was heated at 80 °C. Progress of the reaction was monitored by TLC and ¹H NMR. Upon completion of the reaction, the resulting residue was chromatographed over silica-gel using 2% ethyl acetate/hexane mixture as eluent. Colorless liquid. IR (DCM): 2955, 2877, 1741, 1413, 1377, 1237, 1066, 1017, 801, 742 cm⁻¹. ¹H NMR (CDCl₃): δ 6.32 (d, *J* = 2 Hz, 1H, ArCH), 6.20 (d, *J* = 2 Hz, 1H, ArCH), 5.01 (s, 2H, OCH₂), 4.61 (s, 2H, OCH₂), 2.05 (s, 3H, CH₃), 0.94 (t, *J* = 8 Hz, 9H, (SiCH₂CH₃)₃), 0.61 (q, *J* = 8 Hz, 6H, (SiCH₂CH₃)₃). ¹³C {¹H} NMR (CDCl₃): δ 170.71 (quat-C), 155.20 (quat-C), 149.08 (quat-C), 111.47 (CH), 108.39 (CH), 58.31 (OCH₂), 57.88 (OCH₂), 20.95 (CH₃), 6.73 (SiCH₂CH₃), 4.49 (SiCH₂CH₃). MS (ESI) m/z 284.14 (M)⁺. HR/MS: calcd (C₁₄H₂₄O₄Si)⁺ 284.1444. Found 284.1440.

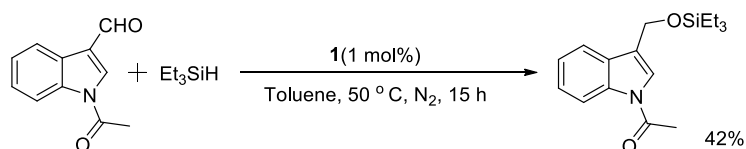
1-Phenyl-2-(4-(((triethylsilyl)oxy)methyl)phenoxy)ethanone (6):



4-(2-Oxo-2-phenylethoxy)benzaldehyde (1 mmol), triethylsilane (1 mmol), [Ru(*p*-cymene)Cl₂]₂ (1 mol %) and toluene (2 mL) were taken in a closed flask equipped with a magnetic bar and the reaction mixture was cooled to 0 to 5 °C. Progress of the

reaction was monitored by TLC and ^1H NMR. Upon completion of the reaction, the resulting residue was chromatographed over silica-gel using 2% ethyl acetate/hexane mixture as eluent (Corresponding product having hydrosilylation over both functional groups was also isolated in 6% yield). Colorless liquid. IR (DCM): 3061, 2925, 2856, 2360, 2340, 1699, 1598, 1507, 1217, 1177, 1086, 977, 823, 756, 689 cm^{-1} . ^1H NMR (CDCl_3): δ 8.00 (d, $J = 8$ Hz, 2H, ArCH), 7.61 (t, $J = 8$ Hz, 1H, ArCH), 7.50 (t, $J = 8$ Hz, 2H, ArCH), 7.25 (d, $J = 8$ Hz, 2H, ArCH), 6.91 (d, $J = 8$ Hz, 2H, ArCH), 5.26 (s, 2H, OCH_2), 4.66 (s, 2H, OCH_2), 0.96 (t, $J = 8$ Hz, 9 H, (silyl CH_2CH_3)₃), 0.63 (q, $J = 8$ Hz, 6H, (silyl CH_2CH_3)₃). $^{13}\text{C}\{^1\text{H}\}$ NMR (CDCl_3): δ 194.80 (quat-C), 157.35 (quat-C), 134.78 (quat-C), 134.71 (quat-C), 133.98 (CH), 128.96 (CH), 128.31 (CH), 127.93 (CH), 114.77 (CH), 71.16 (OCH_2), 64.39 (OCH_2), 6.91 (silyl CH_3), 4.63 (silyl CH_2). MS (ESI) m/z 357.18. HRMS: calcd ($\text{C}_{21}\text{H}_{29}\text{O}_3\text{Si}$)⁺ 357.1886. Found 357.1890.

1-(1H-Indol-1-yl)(3-(triethylsilyloxy)methyl)ethanone (7):



1-Acetyl-3-formyl indole (1 mmol), triethylsilane (1 mmol), $[\text{Ru}(p\text{-cymene})\text{Cl}_2]_2$ (1 mol%) and toluene (2 mL) were taken in a closed flask equipped with a magnetic bar and the reaction mixture was heated at 80 °C. Progress of the reaction was monitored by TLC and ^1H NMR. Upon completion of the reaction, the resulting residue was chromatographed over silica-gel using 4% ethyl acetate/hexane mixture as eluent. Faint yellow liquid. IR (DCM): 2955, 2876, 1711, 1607, 1451, 1385, 1329, 1220, 1240, 1124, 1090, 1061, 1016, 934, 746 cm^{-1} . ^1H NMR (CDCl_3): δ 8.42 (d, $J = 8$ Hz, 1H, ArCH), 7.54 (d, $J = 8$ Hz, 1H, ArCH), 7.35 (t, $J = 8$ Hz, 2H, ArCH), 7.27 (t, $J = 8$ Hz, 1H, ArCH), 4.88 (s, 2H, OCH_2), 2.61 (s, 3H, CH_3), 1.00 (t, $J = 8$ Hz, 9H,

(SiCH₂CH₃)₃, 0.69 (q, *J* = 8 Hz, 6H, (SiCH₂CH₃)₃). ¹³C{¹H} NMR(CDCl₃): δ 168.67 (quat-C), 136.34 (quat-C), 129.22 (quat-C), 125.46 (CH-C), 123.62 (CH), 123.13 (CH), 122.33 (CH), 119.29 (CH), 116.84 (quat-C), 57.71 (OCH₂), 24.08 (CH₃), 6.95 (SiCH₂CH₃), 4.59 (SiCH₂CH₃). MS (ESI) *m/z* 304.17 (M+1)⁺. HR/MS: calcd (C₁₇H₂₅NO₂Si)⁺ 304.1735. Found 304.1727.

Spectral Data of Silyl Ethers:

((Triethylsilyloxy)methyl)benzene¹⁹: Colorless liquid. IR (DCM): 2955, 2877, 1455, 1414, 1377, 1240, 1207, 1097, 1069, 1008, 809, 730, 696 cm⁻¹. ¹H NMR (CDCl₃): δ 7.38-7.25 (m, 5H, 5ArCH overlapped with solvent peak), 4.77 (s, 2H, OCH₂); 1.02 (t, *J* = 8 Hz, 9H, (SiCH₂CH₃)₃), 0.69 (q, *J* = 8 Hz, 6H, (SiCH₂CH₃)₃). ¹³C{¹H} NMR (CDCl₃): δ 141.46 (quat-C), 128.34 (CH), 126.96 (CH), 126.35 (CH), 64.86 (OCH₂), 6.91 (SiCH₂CH₃), 4.65 (SiCH₂CH₃). MS (ESI) *m/z* 222.14 (M)⁺. HR/MS: calcd (C₁₃H₂₂OSi)⁺ 222.1440. Found: 222.1434.

4-Methyl((triethylsilyloxy)methyl)benzene²⁰: Colorless liquid. IR (DCM): 3023, 2955, 2913, 2877, 1516, 1458, 1415, 1237, 1203, 1073, 1005, 803, 741, 688. cm⁻¹. ¹H NMR (CDCl₃): δ 7.25 (d, *J* = 8 Hz, 2H, ArCH), 7.16 (d, *J* = 8 Hz, 2H, ArCH), 4.72 (s, 2H, OCH₂), 2.36 (s, 3H, CH₃), 1.00 (t, *J* = 8 Hz, 9H, (SiCH₂CH₃)₃), 0.67 (q, *J* = 8 Hz, 6H, (SiCH₂CH₃)₃). ¹³C{¹H} NMR(CDCl₃): δ 138.44 (quat-C), 136.65 (quat-C), 129.02 (CH), 126.46 (CH), 64.78 (OCH₂), 21.24 (CH₃), 6.92 (SiCH₂CH₃), 4.66 (SiCH₂CH₃). MS (ESI) *m/z* 237.16 (M+1)⁺. HR/MS: calcd (C₁₄H₂₅OSi)⁺ 237.1675. Found: 237.1680.

4-Methoxy((triethylsilyloxy)methyl)benzene²¹: Colorless liquid. IR (DCM): 2955, 2910, 2876, 1613, 1513, 1463, 1376, 1310, 1246, 1170, 1088, 1038, 1008, 819, 741 cm⁻¹. ¹H NMR (CDCl₃): δ 7.28 (d, *J* = 8 Hz, 2H, ArCH), 6.89 (d, *J* = 8 Hz, 2H, ArCH), 4.69 (s, 2H, OCH₂), 3.82 (s, 3H, OCH₃), 1.00 (t, *J* = 8 Hz, 9H,

(SiCH₂CH₃)₃), 0.66 (q, *J* = 8 Hz, 6H, SiCH₂CH₃)₃). ¹³C{¹H} NMR(CDCl₃): δ 158.86 (quat-C), 133.59 (quat-C), 127.87 (CH), 113.76 (CH), 64.57 (OCH₂), 55.32 (OCH₃), 6.89 (SiCH₂CH₃), 4.64 (SiCH₂CH₃). MS (ESI) *m/z* 252.15 (M)⁺. HRMS: calcd (C₁₄H₂₄O₂Si)⁺ 252.1546. Found: 252.1541.

3,5-Dimethoxy((triethylsilyloxy)methyl)benzene: Colorless liquid. IR (DCM): 2955, 2877, 1599, 1462, 1430, 1240, 1205, 1155, 1065, 1015, 832, 743 cm⁻¹. ¹H NMR (CDCl₃): δ 6.52 (s, 1H, ArCH), 6.36 (s, 1H, ArCH), 4.70 (s, 2H, OCH₂), 3.79 (s, 2H, OCH₃), 1.00 (t, *J* = 2 Hz, 9H, (SiCH₂CH₃)₃), 0.67 (q, *J* = 2 Hz, 6H, (SiCH₂CH₃)₃). ¹³C{¹H} NMR (CDCl₃): δ 160.91 (CH), 144.07 (quat-C), 104.01 (CH), 99.13 (quat-C), 64.75 (OCH₂), 55.36 (OCH₃), 6.90 (SiCH₂CH₃), 4.63(SiCH₂CH₃). MS (ESI) *m/z* 283.16 (M+1)⁺. HRMS: calcd (C₁₅H₂₇O₃Si)⁺ 283.1729. Found 283.1724.

9-((Triethylsilyloxy)methyl)anthracene: Yellow solid. IR (DCM): 3053, 2951, 2875, 1623, 1502, 1476, 1454, 1412, 1382, 1345, 1239, 1072, 1009, 897, 868, 851, 822, 779, 732 cm⁻¹. ¹H NMR (CDCl₃): δ 8.46 (d, *J* = 8 Hz, (2+1)H, Overlapped with a singlet, ArCH), 8.03 (d, *J* = 8 Hz, 2H, ArCH), 7.58 (t, *J* = 8 Hz, 2H, ArCH), 7.50 (t, *J* = 8 Hz, 2H, ArCH), 5.69 (s, 2H, OCH₂), 1.04 (t, *J* = 8 Hz, 9H, (SiCH₂CH₃)₃), 0.75 (q, *J* = 8 Hz, 6H, (SiCH₂CH₃)₃). ¹³C{¹H} NMR (CDCl₃): δ 131.71 (quat-C), 131.55 (quat-C), 130.53 (quat-C), 129.10 (CH), 128 (CH), 125.96 (CH), 124.96 (CH), 124.60 (CH), 57.59 (OCH₂), 6.97 (SiCH₂CH₃), 4.72 (SiCH₂CH₃). MS (ESI) *m/z* 322.14 (M)⁺. HR/MS: calcd (C₁₇H₂₅ClNO₂Si)⁺ 322.1752. Found: 322.1749.

3-Bromo((triethylsilyloxy)methyl)benzene: Colorless liquid. IR (DCM): 2956, 2877, 1572, 1458, 1427, 1240, 1198, 1107, 1079, 1009, 814, 771, 744 cm⁻¹. ¹H NMR (CDCl₃): δ 7.51 (s, 1H, ArCH), 7.38 (d, *J* = 8 Hz, 1H, ArCH), 7.26 (d, *J* = 8 Hz, 1H, ArCH), 7.20 (t, *J* = 8 Hz, 1H, ArCH), 4.72 (s, 2H, OCH₂), 1.00 (t, *J* = 2 Hz, 9H,

(SiCH₂CH₃)₃, 0.68 (q, *J* = 2 Hz, 6H, (SiCH₂CH₃)₃). ¹³C{¹H} NMR (CDCl₃): δ 143.87 (quat-C), 130.09 (CH), 129.90 (CH), 129.29 (CH), 124.70 (CH), 122.56 (quat-C), 64.02 (OCH₂), 6.87 (SiCH₂CH₃), 4.58 (SiCH₂CH₃). MS (ESI) *m/z* 301.06 (M)⁺.HR/MS: calcd. (C₁₃H₂₂BrOSi)⁺ 301.0625. Found: 301.0618.

4-Bromo((triethylsilyloxy)methyl)benzene²²: Crystalline solid. IR (DCM): 2955, 2911, 2876, 1486, 1459, 1406, 1368, 1239, 1203, 1114, 1087, 1010, 798, 744 cm⁻¹. ¹H NMR (CDCl₃): δ 7.45 (d, *J* = 8 Hz, 2H, ArCH), 7.21 (d, *J* = 8 Hz, 2H, ArCH), 4.68 (s, 2H, OCH₂), 0.97 (t, *J* = 8 Hz, 9H, (SiCH₂CH₃)₃), 0.65 (q, *J* = 8Hz, 6H, (SiCH₂CH₃)₃). ¹³C{¹H} NMR (CDCl₃): δ 140.40 (quat-C), 131.30 (quat-C), 127.85 (CH), 120.67 (CH), 64.05 (OCH₂), 6.77 (SiCH₂CH₃), 4.50 (SiCH₂CH₃). MS (ESI) *m/z* 301.06 (M+1)⁺. HR/MS: calcd (C₁₃H₂₂BrOSi)⁺ 301.0623. Found: 301.0620.

4-Cyano((triethylsilyloxy)methyl)benzene: Colorless liquid. IR (DCM): 2956, 2877, 2229, 1610, 1458, 1414, 1376, 1240, 1207, 1092, 1017, 818, 743, 547 cm⁻¹. ¹H NMR (CDCl₃): δ 7.60 (d, *J* = 8 Hz, 2H, ArCH), 7.43 (d, *J* = 8 Hz, 2H, ArCH), 4.77 (s, 2H, OCH₂), 0.97 (t, *J* = 8 Hz, 9H, (SiCH₂CH₃)₃), 0.65 (q, *J* = 8 Hz, 6H, (SiCH₂CH₃)₃). ¹³C{¹H} NMR(CDCl₃): δ 146.97 (quat-C), 132.08 (CH), 126.40 (CH), 119.02 (quat-C), 110.62 (quat-C), 63.87 (OCH₂), 6.72 (SiCH₂CH₃), 4.42 (SiCH₂CH₃). MS (ESI) *m/z* 248.1 (M+1)⁺. HR/MS: calcd. (C₁₄H₂₂NOSi)⁺ 248.1472. Found: 248.1465.

4-Nitro((triethylsilyloxy)methyl)benzene: White solid. IR (DCM): 2957, 2878, 1603, 1520, 1345, 1241, 1203, 1099, 1014, 815, 736 cm⁻¹. ¹H NMR (CDCl₃): δ 8.18 (d, *J* = 8 Hz, 2H, ArCH), 7.49 (d, *J* = 8 Hz, 2H, ArCH), 4.82 (s, 2H, OCH₂), 0.98 (t, *J* = 8 Hz, 9H, (SiCH₂CH₃)₃), 0.67 (q, *J* = 8 Hz, 6 H, (SiCH₂CH₃)₃). ¹³C{¹H} NMR (CDCl₃): δ 149.05 (quat-C), 147.01 (quat-C), 126.36 (CH), 123.51 (CH), 63.71

(OCH₂), 6.71 (SiCH₂CH₃), 4.42 (SiCH₂CH₃). MS (ESI) m/z 268.13 (M+1)⁺. HR/MS: calcd (C₁₃H₂₂NO₃Si)⁺ 268.1369. Found: 268.1363.

2-Bromo-4-methyl((triethylsilyloxy)methyl)benzene: Colorless liquid. IR (DCM): 2954, 2875, 1606, 1458, 1238, 1207, 1101, 1032, 855, 816, 740 cm⁻¹. ¹H NMR (CDCl₃): δ 7.44 (d, *J* = 8 Hz, 1H, ArCH), 7.33 (s, 1H, ArCH), 7.13 (d, *J* = 8 Hz, 1H, ArCH), 4.72 (s, 2H, OCH₂), 2.32 (s, 3H, CH₃), 1.00 (t, *J* = 8Hz, 9H, (SiCH₂CH₃)₃), 0.68 (q, *J* = 8Hz, 6H, (SiCH₂CH₃)₃). ¹³C{¹H} NMR (CDCl₃): δ 138.22 (quat-C), 137.18 (quat-C), 132.51 (CH), 128.10 (CH), 127.52 (CH), 120.93 (quat-C), 64.16 (OCH₂), 20.68 (CH₃), 6.80 (SiCH₂CH₃), 4.49 (SiCH₂CH₃). MS (ESI) m/z 315.07 (M+1)⁺. HRMS: calcd. (C₁₃H₂₄BrOSi)⁺ 315.0781. Found: 315.0774.

2-Bromo-5-methoxy((triethylsilyloxy)methyl)benzene: Faint yellow liquid. IR (DCM): 2924, 2852, 1595, 1471, 1272, 1296, 1238, 1161, 1051, 1015, 916, 857, 804 cm⁻¹. ¹H NMR (CDCl₃): δ 7.37 (d, *J* = 8 Hz, 1H, ArCH), 7.19 (d, *J* = 4 Hz, 1H, ArCH), 6.67 (dd, *J* = 4 Hz, 1H, ArCH), 4.72 (s, 2H, OCH₂), 3.80 (s, 3H, OCH₃), 1.02 (t, *J* = 2 Hz, 9H, (SiCH₂CH₃)₃), 0.70 (q, *J* = 2Hz, 6H, (SiCH₂CH₃)₃). ¹³C{¹H} NMR (CDCl₃): δ 159.33 (quat-C), 141.59 (quat-C), 132.71(CH), 114.12 (CH), 113.20 (CH), 111.14 (quat-C), 64.34 (OCH₂), 55.52 (OCH₃), 6.94 (SiCH₂CH₃), 4.63 (SiCH₂CH₃). MS (ESI) m/z 331.07 (M+1)⁺. HRMS: calcd. (C₁₄H₂₄BrO₂Si)⁺ 331.0728. Found: 331.0723.

2-Chloro-6-methoxy((triethylsilyloxy)methyl)quinoline: Colorless liquid. IR (DCM): 2956, 2877, 1623, 1600, 1498, 1457, 1415, 1336, 1228, 1163, 1105, 1040, 910, 828, 745, 727 cm⁻¹. ¹H NMR (CDCl₃): δ 8.20 (s, 1H, ArCH), 7.89 (d, *J* = 8 Hz, 1H, ArCH), 7.33 (dd, *J* = 4 Hz, 1H, ArCH), 7.09 (d, *J* = 4 Hz, 1H, ArCH), 4.87 (s, 2H, OCH₂), 3.93 (s, 3H, OCH₃), 1.03 (t, *J* = 8 Hz, 9H, (SiCH₂CH₃)₃), 0.74 (q, *J* = 8 Hz, 6H, (SiCH₂CH₃)₃). ¹³C{¹H} NMR (CDCl₃): δ 158.25 (quat-C), 145.87 (quat-C),

142.70 (quat-C), 134.25 (CH), 133.38 (quat-C), 129.65 (CH), 128.75 (quat-C), 122.51 (CH), 105.33 (CH), 61.56 (OCH₂), 55.72 (OCH₃), 6.94 (SiCH₂CH₃), 4.57 (SiCH₂CH₃). MS (ESI) m/z 338.13 (M+1)⁺. HRMS: calcd (C₁₇H₂₅ClNO₂Si)⁺ 338.1343. Found: 338.1338.

2-((Triethylsilyloxy)methyl)furan: Colorless liquid. IR (DCM): 2956, 2913, 2877, 1455, 1368, 1239, 1206, 1095, 1033, 1016, 955, 793, 743, 699 cm⁻¹. ¹H NMR (CDCl₃): δ 7.37 (d, *J* = 4 Hz, 1H, ArCH), 6.31 (dd, *J* = 4 Hz, 1H, ArCH), 6.24 (t, *J* = 4 Hz, 1H, ArCH), 4.63 (s, 2H, OCH₂), 0.96 (t, *J* = 4 Hz, 9H, (SiCH₂CH₃)₃), 0.63 (q, *J* = 4 Hz, 6H, (SiCH₂CH₃)₃). ¹³C{¹H} NMR(CDCl₃): δ 154.34 (quat-C), 142.23 (CH), 110.32 (CH), 107.52 (CH), 57.81 (OCH₂), 6.76 (SiCH₂CH₃), 4.52 (SiCH₂CH₃). MS (ESI) m/z 212.12 (M)⁺. HR/MS: calcd (C₁₁H₂₀O₂Si)⁺ 212.1233. Found: 212.1231.

2-((Triethylsilyloxy)methyl)thiophene: Faint yellow liquid. IR (DCM): 2955, 2876, 1460, 1414, 1379, 1238, 1225, 1176, 1085, 1075, 1008, 829, 802, 742, 697 cm⁻¹. ¹H NMR (CDCl₃): δ 7.27 (dd, *J* = 1 Hz, 1H, ArCH), 6.99 (overlapped, 2H, ArCH), 4.93(s, 2H, OCH₂), 1.04 (t, *J* = 8 Hz, 9H, (SiCH₂CH₃)₃), 0.71 (q, *J* = 3 Hz, 6H, (SiCH₂CH₃)₃). ¹³C{¹H} NMR(CDCl₃): δ 145.05 (quat-C), 126.49 (CH), 124.70 (CH), 124.07 (CH), 60.35 (OCH₂), 6.75 (SiCH₂CH₃), 4.53 (SiCH₂CH₃). MS (ESI) m/z 229.10 (M+1)⁺. HRMS: calcd (C₁₁H₂₁OSSi)⁺ 229.1082. Found 229.1077.

1,3-Bis((triethylsilyloxy)methyl)benzene²³: Colorless liquid. IR (DCM): 2955, 2877, 1462, 1456, 1415, 1239, 1154, 1104, 1076, 1016, 824, 741 cm⁻¹. ¹H NMR (CDCl₃): δ 7.36-7.23 (m, 3H, ArCH), 4.77 (s, 2H, OCH₂), 1.02 (t, *J* = 8 Hz, 9H, (SiCH₂CH₃)₃), 0.69 (q, *J* = 8 Hz, 6H, (SiCH₂CH₃)₃). ¹³C{¹H} NMR (CDCl₃): δ 141.37 (CH), 128.20 (CH), 124.97 (quat-C), 124.21 (CH), 64.85 (OCH₂), 6.87 (SiCH₂CH₃), 4.62 (SiCH₂CH₃). MS (ESI) m/z 367.24 (M+1)⁺. HRMS: calcd (C₂₀H₃₉O₂Si₂)⁺ 367.2488. Found 367.2488.

((Triethylsilyloxy)butane²⁴: Colorless liquid. IR (DCM): 2956, 2877, 1459, 1415, 1238, 1098, 1015, 839, 780, 739 cm^{-1} . ^1H NMR (CDCl_3): δ 3.60 (t, $J = 6$ Hz, 2H, OCH_2), 1.53-1.48 (m, $J = 4$ Hz, 2H, CH_2), 1.38-1.26 (m, $J = 4$ Hz, 2H, CH_2), 0.96 (t, $J = 8$ Hz, 9H, $(\text{SiCH}_2\text{CH}_3)_3$), 0.91 (t, $J = 8$ Hz, 3H, CH_3), 0.59 (q, $J = 8$ Hz, 6H, $(\text{SiCH}_2\text{CH}_3)_3$). $^{13}\text{C}\{^1\text{H}\}$ NMR (CDCl_3): δ 62.83 (OCH_2), 35.22 (CH_3), 19.16 (CH_2), 14.06 (CH_2), 6.91 (SiCH_2CH_3), 4.59 (SiCH_2CH_3). MS (ESI) m/z 188.16 (M)⁺. HR/MS: calcd ($\text{C}_{10}\text{H}_{24}\text{OSi}$)⁺ 188.1596. Found 188.1600.

((Triethylsilyloxy)decane²⁵: Colorless liquid. IR (DCM): 2954, 2926, 1459, 1415, 1238, 1100, 1015, 797, 740 cm^{-1} . ^1H NMR (CDCl_3): δ 3.59 (t, $J = 8$ Hz, 2H, OCH_2), 1.51 (m, $J = 5$ Hz, 2H, CH_2), 1.27 (overlapped, 14H, CH_2), 0.96 (t, $J = 8$ Hz, 9H, $(\text{SiCH}_2\text{CH}_3)_3$), 0.88 (t, $J = 8$ Hz, 3H, CH_3), 0.59 (q, $J = 8$ Hz, 6H, $(\text{SiCH}_2\text{CH}_3)_3$). $^{13}\text{C}\{^1\text{H}\}$ NMR(CDCl_3): δ 63.16 (OCH_2), 33.11 (CH_2), 32.02 (CH_2), 29.82 (CH_2), 29.75 (CH_2), 29.65 (CH_2), 29.50 (CH_2), 26.01 (CH_2), 22.85 (CH_2), 14.24 (CH_3), 6.91 (SiCH_2CH_3), 4.60 (SiCH_2CH_3). MS (ESI) m/z 273.26 ($\text{M}+1$)⁺. HRMS: calcd ($\text{C}_{16}\text{H}_{36}\text{OSi}$)⁺ 273.2615. Found 273.2608.

1-Phenyl-1-((triethylsilyloxy)methyl)methane²⁶: Colorless liquid. IR (DCM): 2955, 2875, 1490, 1435, 1235, 1075, 1014, 931, 865, 723 cm^{-1} . ^1H NMR (CDCl_3): δ 7.27 (overlapped, 3H, ArCH), 7.19 (d, $J = 8\text{Hz}$, 2H, ArCH), 3.80 (t, $J = 8\text{Hz}$, 2H, OCH_2), 2.84 (t, $J = 8\text{Hz}$, 2H, CH_3), 0.93 (t, $J = 8\text{Hz}$, 9H, $(\text{SiCH}_2\text{CH}_3)_3$), 0.56 (q, $J = 8\text{Hz}$, 6H, $(\text{SiCH}_2\text{CH}_3)_3$). $^{13}\text{C}\{^1\text{H}\}$ NMR (CDCl_3): δ 139.17 (quat-C), 129.23 (CH), 128.39 (CH), 126.28 (CH), 64.38 (OCH_2), 39.83 (CH_3), 6.87 (SiCH_2CH_3), 4.54 (SiCH_2CH_3). MS (ESI) m/z 237.16 ($\text{M}+1$)⁺. HR/MS: calcd ($\text{C}_{14}\text{H}_{25}\text{OSi}$)⁺ 237.1675. Found 237.1669.

1-Phenyl-1-((triethylsilyloxy)methyl)ethane²⁷: Colorless liquid. IR (DCM): 3029, 2956, 2876, 1493, 1454, 1239, 1087, 1015, 830, 743, 699 cm^{-1} . ^1H NMR (CDCl_3): δ 7.32 (t, $J = 8$ Hz, 2H, ArCH), 7.23 (t, $J = 6$ Hz, 3H, ArCH), 3.68 (dq, $J = 48$ Hz, 2H,

OCH₂), 2.94 (m, *J* = 5 Hz, 1H, CH), 1.34 (d, *J* = 4 Hz, 3H, CH₃), 0.96 (t, *J* = 8 Hz, 9H, (SiCH₂CH₃)₃), 0.59 (q, *J* = 8 Hz, 6H, (SiCH₂CH₃)₃). ¹³C{¹H} NMR (CDCl₃): δ 144.66 (quat-C), 128.34 (CH), 127.65 (CH), 126.37 (CH), 69.13 (OCH₂), 42.72 (CH), 17.70 (CH₃), 6.86 (SiCH₂CH₃), 4.54 (SiCH₂CH₃). MS (ESI) *m/z* 251.18 (M+1)⁺. HR/MS: calcd (C₁₅H₂₇OSi)⁺ 251.1833. Found 251.1826.

Synthesis of Complex [(η⁶-*p*-cymene)Ru]₂(μ-H-μ-Cl)(Cl)₂ (2): To benzene-d₆ (1 mL) solution of [Ru(*p*-cymene)Cl₂]₂ (0.05 mmol) in a vial, triethylsilane (0.2 mmol) was added dropwise and the resulting mixture allowed to stir at room temperature for 30 min. The volume of dark red solution was reduced to one third and slow addition of cold pentane (2 mL) provided dark red precipitate. The solution was decanted and the precipitate was washed with a mixture of pentane and toluene. The resulted dark red complex was dried under vacuum for overnight (28 mg, quantitative yields). ¹H NMR (Benzene-d₆): δ 5.44 (d, *J* = 8 Hz, 2H, ArCH), 5.20 (d, *J* = 4 Hz, 2H, ArCH), 5.14 (d, *J* = 8 Hz, 2H, ArCH), 4.74 (d, *J* = 4 Hz, 2H, ArCH), 2.86 (m, *J* = 8 Hz, 2H, ^{*i*}PrCH), 1.95 (s, 6H, CH₃), 1.27 (d, *J* = 8 Hz, 6H, ^{*i*}PrCH₃), 1.18 (d, *J* = 8 Hz, 6H, ^{*i*}PrCH₃), -10.18(s, 1H, RuH). ¹³C{¹H} NMR (Benzene-d₆): δ 102.60 (quat-C), 97.64 (quat-C), 86.69 (ArCH), 83.34 (ArCH), 81.75 (ArCH), 81.50 (ArCH), 32.00 (^{*i*}PrCH), 24.05 (CH₃), 22.70 (CH₃), 19.92 (CH₃).

Synthesis of Complex [(η⁶-*p*-cymene)Ru(H)₂(SiEt₃)₂] (3):

To benzene-d₆ (1 mL) solution of either [Ru(*p*-cymene)Cl₂]₂ (1) or [(η⁶-*p*-cymene)Ru]₂(μ-H-μ-Cl)(Cl)₂ (2) (0.05 mmol), triethylsilane (0.4 mmol) was added dropwise and the resulting mixture in a sealed vial was heated to 50 °C for 48 h. Then the reaction mixture was cooled to room temperature and solvents are evaporated under reduced pressure. The resulted residue was dissolved in hexane and filtered through celite. The filtrate was dried under high vacuum to obtain a colorless solid (32

mg, 80% yield). IR (C₆D₆): 2016 cm⁻¹. ¹H NMR (Benzene-d₆): δ 5.19 (d, *J* = 8 Hz, 2H, ArCH), 5.14 (d, *J* = 8 Hz, 2H, ArCH), 2.27 (m, *J* = 8 Hz, 1H, ⁱPrCH), 1.84 (s, 3H, CH₃), 1.16 (t, *J* = 8 Hz, 18H, SiCH₂CH₃), 1.02 (d, *J* = 4 Hz, 6H, ⁱPrCH₃), 0.84 (q, *J* = 8 Hz, 12H, SiCH₂CH₃), -13.52 (s, 2H, RuH). ¹³C{¹H} NMR (Benzene-d₆): δ 120.22 (quat-C), 107.32 (quat-C), 94.36 (ArCH), 91.64 (ArCH), 32.68 (CH₃), 24.68 (CH₃), 20.56 (iPrCH), 14.50 (silyl CH₃), 9.75 (silyl CH₂).

Determination of the Molecular Structure of 2 and 3 in the Solid State by X-ray

Single Crystal Diffraction: Single crystals of complexes **2** and **3** suitable for X-ray analysis was obtained from solutions of toluene-pentane and hexane, respectively. Crystals suited for single crystal x-ray diffraction measurements were mounted on a glass fiber. Geometry and intensity data were collected with a Bruker SMART D8 goniometer equipped with an APEX CCD detector and with an Incoatec microsource (Mo-K α radiation, λ = 0.71073 Å, multilayer optics). Temperature was controlled using an Oxford Cryostream 700 instrument. Intensities were integrated with SAINT²⁸ and corrected for absorption with SADABS.²⁹ The structures were solved by direct methods and refined on F₂ with SHELXL-97.³⁰

Crystal Data of Complex [{}(η^6 -*p*-cymene)Ru]₂(μ -H- μ -Cl)(Cl)₂](2**):** C₂₀H₂₉Cl₃Ru₂, crystal dimensions: 0.24 x 0.15 x 0.10, *M* = 577.92, Orthorhombic with space group Pbc_a, *a* = 13.6640(6), *b* = 15.9211(7), *c* = 19.2494(9), α = 90°, β = 90°, γ = 90°, *V* = 4187.6(3) Å³, *Z* = 8, 2*q*_{max} = 61.26, ρ_{calcd} = 1.833 Mg/m³, *T* = 296(2) K, μ -(Mo_{K α}) = 0.71073, min/max transmission factors = 0.6153/0.7461, 72584 Reflections collected, 6414 unique (*R*₁ = 0.0195), *WR*₂ = 0.0447(all data). Residual electron density max/min = 0.626/-0.512 eÅ⁻³. The structure has been deposited at the CCDC data center and can be retrieved using the deposit number CCDC 932852.

Synthesis of Complex $[(\eta^6\text{-}p\text{-cymene})\text{Ru}(\text{H})_2(\text{SiEt}_3)_2](\mathbf{3})$: To benzene- d_6 (1 mL) solution of either $[\text{Ru}(p\text{-cymene})\text{Cl}_2]_2(\mathbf{1})$ or $[\{(\eta^6\text{-}p\text{-cymene})\text{Ru}\}_2(\mu\text{-H-}\mu\text{-Cl})(\text{Cl})_2](\mathbf{2})$ (0.05 mmol), triethylsilane (0.4 mmol) was added dropwise and the resulting mixture in a sealed vial was heated to 50 °C for 48 h. Then the reaction mixture was filtered through celite. The filtrate was dried under high vacuum to give a colorless solid (32 mg, 80% yield). IR(C_6D_6): 2016 cm^{-1} . ^1H NMR (Benzene- d_6): δ 5.19 (d, $J = 8$ Hz, 2H, ArCH), 5.14 (d, $J = 8$ Hz, 2H, ArCH), 2.27 (m, $J = 8$ Hz, 1H, $^i\text{PrCH}$), 1.84 (s, 3H, CH_3), 1.16 (t, $J = 8$ Hz, 18H, SiCH_2CH_3), 1.02 (d, $J = 4$ Hz, 6H, $^i\text{PrCH}_3$), 0.84 (q, $J = 8$ Hz, 12H, SiCH_2CH_3), -13.52 (s, 2H, RuH). $^{13}\text{C}\{^1\text{H}\}$ NMR (Benzene- d_6): δ 120.22 (quat-C), 107.32 (quat-C), 94.36 (ArCH), 91.64 (ArCH), 32.68 (CH_3), 24.68 (CH_3), 20.56 ($^i\text{PrCH}$), 14.50 (silyl CH_3), 9.75 (silyl CH_2).

Crystal Data of Complex $[(\eta^6\text{-}p\text{-cymene})\text{Ru}(\text{H})_2(\text{SiEt}_3)_2](\mathbf{3})$: $\text{C}_{22}\text{H}_{46}\text{Si}_2\text{Ru}_1$, crystal dimensions: 0.12 x 0.08 x 0.05, $M = 467.84$, Monoclinic with space group P21/C, $a = 16.4631(15)$, $b = 8.7200(8)$, $c = 17.7452(16)$, $\alpha = 90^\circ$, $\beta = 102.003^\circ(4)$, $\gamma = 90^\circ$, $V = 2491.8(4)\text{\AA}^3$, $Z = 4$, $2q_{\text{max}} = 61.22$, $\rho_{\text{calcd}} = 1.247 \text{ Mg/m}^3$, $T = 200(2) \text{ K}$, $\mu\text{-}(\text{Mo}_{\text{K}\alpha}) = 0.71073$, min/max transmission factors = 0.5565/0.7461, 44034 Reflections collected, 7598 unique ($R1 = 0.0299$), $WR2 = 0.0745$ (all data). Residual electron density max/min = 1.586/-1.009 $\text{e}\cdot\text{\AA}^{-3}$. CCDC 971350

6.6 NOTES AND REFERENCES

(1) For general reviews about hydrosilylation, see: (a) *Hydrosilylation: A Comprehensive Review on Recent Advances*, (Ed.: B. Marciniec), Springer, Heidelberg, 2009. (b) O. Riant, N. Mostefaï, J. Courmarcel. *Synthesis* 2004, 2943-2958.

(2) *The Chemistry of Organic Silicon Compounds*, Vol. 3 (Eds.: Z. Rappoport, Y. Apeloig) Wiley, New York, 2001.

(3) (a) Gregg, B. T.; Cutler, A. R. *J. Am. Chem. Soc.*, **1996**, *118*, 10069-10084.

(b) Cavanaugh, M. D.; Gregg, B. T.; Cutler, A. R. *Organometallics*, **1996**, *15*, 2764-2769. (c) Hanna, P. K.; Gregg, B. T.; Cutler, A. R. *Organometallics*, **1991**, *10*, 31-33.

(4) For iron catalyzed hydrosilylation reactions, see: (a) Li, H.; Castro, L. C. M.; Zheng, J.; Roisnel, T.; Dorcet, V.; Sortais, J. -B.; Darcel, C. *Angew. Chem. Int. Ed.* **2013**, *52*, 8045-8049. (b) Bøzier, D.; Venkanna, G. T.; Misal Castro, L. C.; Zheng, J.; Roisnel, T.; Sortais, J. -B.; Darcel, C. *Adv. Synth. Catal.*, **2012**, *354*, 1879-1884. (c) Zheng, J.; Misal Castro, L. C.; Roisnel, T.; Darcel, C.; Sortais, J. B. *Inorg. Chim. Acta*, **2012**, *380*, 301-307. (d) Misal Castro, L. C.; Bøzier, D.; Sortais, J. B.; Darcel, C. *Adv. Synth. Catal.*, **2011**, *353*, 1279-1284. (e) Bhattacharya, B.; Krause, J. A.; Guan, H. *Organometallics*, **2011**, *30*, 4720-4729. (f) Yang, J.; Don Tilley, T. *Angew. Chem. Int. Ed.*, **2010**, *49*, 10186-10188. (g) Shaikh, N. S.; Junge, K.; Beller, M. *Org. Lett.*, **2007**, *9*, 5429-5432. for reviews, see (h) Zhang, M.; Zhang, A. *Appl. Organomet. Chem.*, **2010**, *24*, 751-757. (i) Junge, K.; Schröder, K.; Beller, M. *Chem. Commun.*, **2011**, *47*, 4849-4859. (j) Jiang, F.; Bezier, D.; Sortais, J. B.; Darcel, C. *Adv. Synth. Catal.*, **2011**, *353*, 239-244. (k) Morris, R. H. *Chem. Soc. Rev.*, **2009**, *38*, 2282-2291.

(5) For nickel catalyzed hydrosilylation reactions, see: (a) Zheng, J.; Darcel, C.; Sortais, J. -B. *Catal. Sci. Technol.*, **2013**, *3*, 81-84. (b) Postigo, L.; Royo, B. *Adv. Synth. Catal.*, **2012**, *354*, 2613-2618. (c) Bheeter, L. P.; Henrion, M.; Brelot, L.; Darcel, C.; Chetcuti, M. J.; Sortais, J.; Ritleng, V. *Adv. Synth. Catal.*, **2012**, *354*, 2619-2624. (d) Kundu, S.; Brennessel, W. W.; Jones, W. D. *Inorg. Chem.*, **2011**,

50, 9443-9453. (e) Chakraborty, S.; Krause, J. A.; Guan, H. *Organometallics*, **2009**, *28*, 582-586. (f) Tran, B. L.; Pink, M.; Mindiola, D. J. *Organometallics*, **2009**, *28*, 2234-2243. (g) Fontaine, F. -G.; Nguyen, R. -V.; Zargarian, D. *Can. J. Chem.*, **2003**, *81*, 1299-1306. (h) Boudjouk, P.; Han, B. -H.; Jacobsen, J. R.; Hauck, B. J. *J. Chem. Soc. Chem. Commun.*, **1991**, 1424-1425. (i) Boudjouk, P.; Choi, S. -B.; Hauck, B. J.; Rajkumar, A. B. *Tetrahedron Lett.*, **1998**, *39*, 3951-3952.

(6) Lakshmi kantam, M.; Laha, S.; Yadav, J.; Likhar, P. R.; Sreedhar, B.; Jha, S.; Bhargava, S.; Udayakiran, M.; Jagadeesh. M. *Org. Lett.*, **2008**, *10*, 2979-2982.

(7) (a) Peterson, E.; Khalimon, A. Y.; Simionescu, R.; Kuzmina, L. G.; Howard, J. A. K.; Nikonov. G. I. *J. Am. Chem. Soc.*, **2009**, *131*, 908-909. (b) Fernandes, A. C.; Fernandes, R.; Romão, C. C.; Royo, B. *Chem. Commun.*, **2005**, 213-214.

(8) Dioumaev, V.K.; Bullock, R.M. *Nature*, **2000**, *424*, 530-532.

(9) (a) Smith, J. J. K.; Nolin, K. A.; Gunterman, H. P.; Toste, F. D. *J. Am. Chem. Soc.*, **2003**, *125*, 4056-4057. (b) Nolin, K. A.; Krumper, J. R.; Pluth, M. D.; Bergman, R. G.; Toste, F. D. *J. Am. Chem. Soc.*, **2007**, *129*, 14684-14696. (c) Du, G.; Fanwick, P. E.; Abu-omar, M. M. *J. Am. Chem. Soc.*, **2007**, *129*, 5180-5187. (d) Dong, H.; Berke, H. *Adv. Synth. Catal.* **2009**, *351*, 1783-1788. (e) Toh, C. K.; Sum, Y. N.; Fong, W. K.; Ang, S. G.; Fan, W. Y. *Organometallics*, **2012**, *31*, 3880-3887.

(10) (a) Cheng, C.; Brookhart, M. *J. Am. Chem. Soc.*, **2012**, *134*, 11304-11307. (b) Cheng, C.; Brookhart, M. *Angew. Chem. Int. Ed.*, **2012**, *51*, 9422-9424. (c) Park, S.; Brookhart, M. *Organometallics*, **2010**, *29*, 6057-6064.

(11) (a) Hydrosilylation of amides: (a) Li, B.; Sortais, J. -B.; Darcel. C.; *Chem. Commun.*, **2013**, *49*, 3691-3693. (b) Reeves, J. T.; Tan, Z.; Marsini, M. A.; Han,

Z. S.; Xu, Y.; Reeves, D. C.; Lee, H.; Lu, B. Z.; Senanayake, C. H. *Adv. Synth. Catal.*, **2013**, *355*, 47-52. (c) *Hydrosilylation of esters and amides*: Matsubara, K.; Iura, T.; Maki, T.; Nagashima, H. *J. Org. Chem.*, **2002**, *67*, 4985-4988; (d) *Hydrosilylation of esters*: (a) Reference 4a; (b) Igarashi, M.; Fuchikami, T. *Tetrahedron Lett.*, **2001**, *42*, 2149-2151.

(12) As far as we know, such chemoselective process is currently limited to only one reported example of dinuclear ruthenium carbonyl complex, which catalyzed the reaction under photolytic conditions. See, Do, Y.; Han, J.; Rhee, Y. H.; Park, J. *Adv. Synth. Catal.*, **2011**, *353*, 3363-3366.

(13) For catalytic hydrosilylation of aldehydes, see (a) for Fe: reference 4f; (b) for Au: Lantos, D.; Contel, M.; Sanz, S.; Bodor, A.; Horvath, I. T. *J. Organomet. Chem.*, **2007**, *692*, 1799-1805. (c) for Ag: Wile, B. M.; Stradiotto, M. *Chem. Commun.*, **2006**, 4104-4106. (d) Grubbs' 1st generation catalyst is reported to catalyse the hydrosilylation of aldehyde and ketones. See Maifeld, S. V.; Miller, R. L.; Lee, D. *Tetrahedron Lett.*, **2002**, *43*, 6363-6366.

(14) See Figure 6.16 and 6.17.

(15) The intermediate **2** could also be isolated from the reaction mixture upon completion of the reaction, which displayed identical spectral data as that of prepared complex **2**.

(16) A similar Ru(IV) complex containing trimethyl silyl ligands is reported. See, Djurovich, P. I.; Carroll, P. J.; Berry, D. H. *Organometallics*, **1994**, *13*, 2551.

(17) Similar to **3**, another intermediate complex containing bulkier triphenylsilane was also observed *in situ* by ¹H NMR. The mononuclear metal dihydride with triphenylsilane ligands resonated a characteristic hydride signal at -11.71 ppm.

- (18) Tuttle, T.; Wang, D.; Thiel, W.; Köhler, J.; Hofmann, M.; Weis, J. *Dalton Trans.*, **2009**, 5894-5901.
- (19) (a) Park, S.; Brookhart, M. *Organometallics*, **2010**, *29*, 6057-6064. (b) Du, G.; Abu-Omar, M. M. *Organometallics*, **2006**, *25*, 4920-4923. (c) Tran, B. L.; Pink, M.; Mindiola, D. J. *Organometallics*, **2009**, *28*, 2234-2243. (d) Ison, E. A.; Trivedi, E. R.; Corbin, R. A.; Abu-Omar, M. M. *J. Am. Chem. Soc.* **2005**, *127*, 15374-15375. (e) Gutsulyak, D. V.; Vyboishchikov, S. F.; Nikonov, G. I. *J. Am. Chem. Soc.*, **2010**, *132*, 5950-5951. (f) Ueno, M.; Yonemoto, M.; Hashimoto, M.; Wheatley, A. E. H.; Kondo, H. N.Y. *Chem. Commun.*, **2007**, 2264-2266. (g) Kim, S.; Kwon, M. S.; Park, J. *Tetrahedron Lett.*, **2010**, *51*, 4573-4575.
- (20) González, S. D.; Scott, N. M.; Nolan, S. P. *Organometallics*, **2006**, *25*, 2355-2358.
- (21) (a) Kennedy-Smith, J. J.; Nolin, K. A.; Gunterman, H. P.; Toste, F. D. *J. Am. Chem. Soc.*, **2003**, *125*, 4056-4057. (b) Kim, S.; Kwon, M. S.; Park, J. *Tetrahedron Lett.*, **2010**, *51*, 4573-4575.
- (22) Fernandes, A. C.; Fernandes, R.; Romão, C. C.; Royo, B. *Chem. Commun.*, **2005**, 213- 214.
- (23) Toh, C. K.; Sum, Y. N.; Fong, W. K.; Ang, S. G.; Fan, W. Y. *Organometallics*, **2012**, *31*, 3880-3887.
- (24) (a) Yang, J.; White, P. S.; Brookhart, M. *J. Am. Chem. Soc.*, **2008**, *130*, 17509-17518. (b) Park, S.; Brookhart, M. *Chem. Commun.*, **2011**, *47*, 3643-3645.
- (25) (a) Ito, H.; Watanabe, A.; Sawamura, M. *Org. Lett.*, **2005**, *7*, 1869-1871. (b) Ito, H.; Takagi, K.; Miyahara, T.; Sawamura, M.; *Org. Lett.*, **2005**, *7*, 3001-3004. (c) Ikawa, T.; Hattori, K.; Sajiki, H.; Hirota, K. *Tetrahedron*, **2004**, *60*, 6901-6911.

- (26) (a) González, S. D.; Scott, N. M.; Nolan, S. P. *Organometallics*, **2006**, *25*, 2355-2358. (b) Park, S.; Brookhart, M. *Chem. Commun.*, **2011**, *47*, 3643-3645. (c) Ito, H.; Takagi, K.; Miyahara, T.; Sawamura, M. *Org. Lett.*, **2005**, *7*, 3001-3004; (d) Park, J.; Jun, C. *Org. Lett.*, **2007**, *9*, 4073-4076.
- (27) (a) Rubio, M.; Campos, J.; Carmona, E. *Org. Lett.*, **2011**, *13*, 5236-5239. (b) Donga, H.; Berke, H. *Adv. Synth. Catal.*, **2009**, *351*, 1783-1788.
- (28) Bruker AXS, SAINT+, Program for Reduction of Data collected on Bruker CCD Area Detector Diffractometer V. 6.02. Bruker AXS Inc., Madison, Wisconsin, USA, 1999.
- (29) Bruker AXS, SADABS, Program for Empirical Absorption Correction of Area Detector Data V 2004/1, Bruker AXS Inc., Madison, Wisconsin, USA, 2004.
- (30) Sheldrick, G. M. *Acta Crystallogr.* **2008**, *A64*, 112-122.

NMR Spectra of Silyl ethers and intermediate complexes:
Figure 6.4 ^1H NMR spectrum of ((Triethylsilyloxy)methyl)benzene:

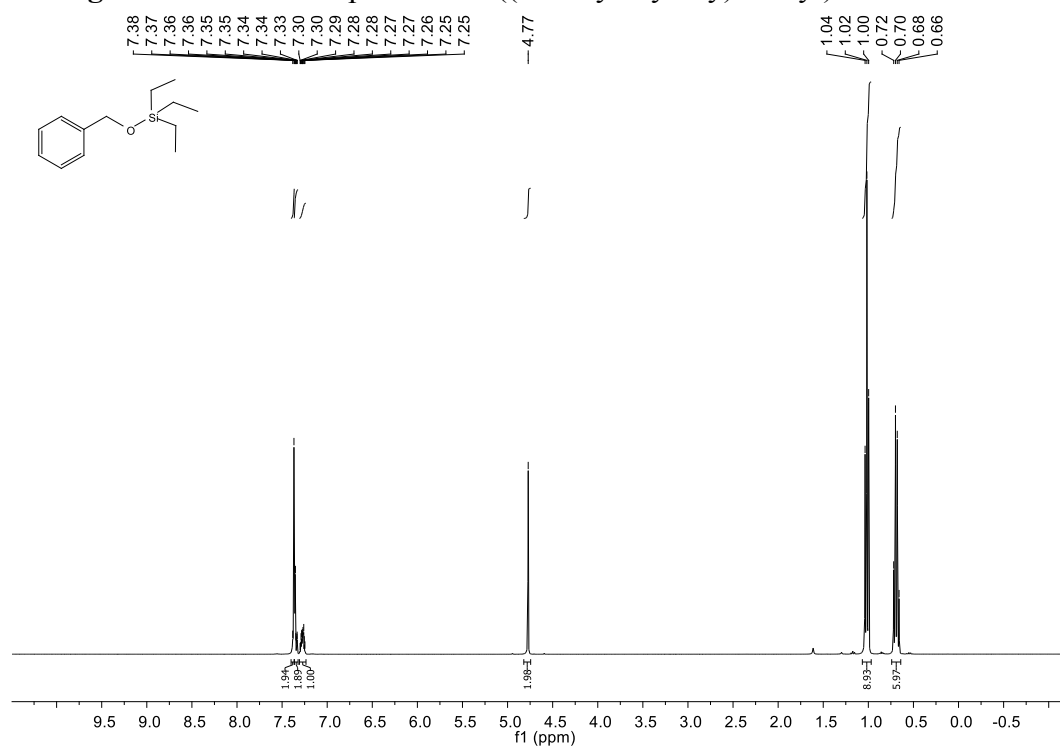


Figure 6.5 ^{13}C NMR spectrum of ((Triethylsilyloxy)methyl)benzene:

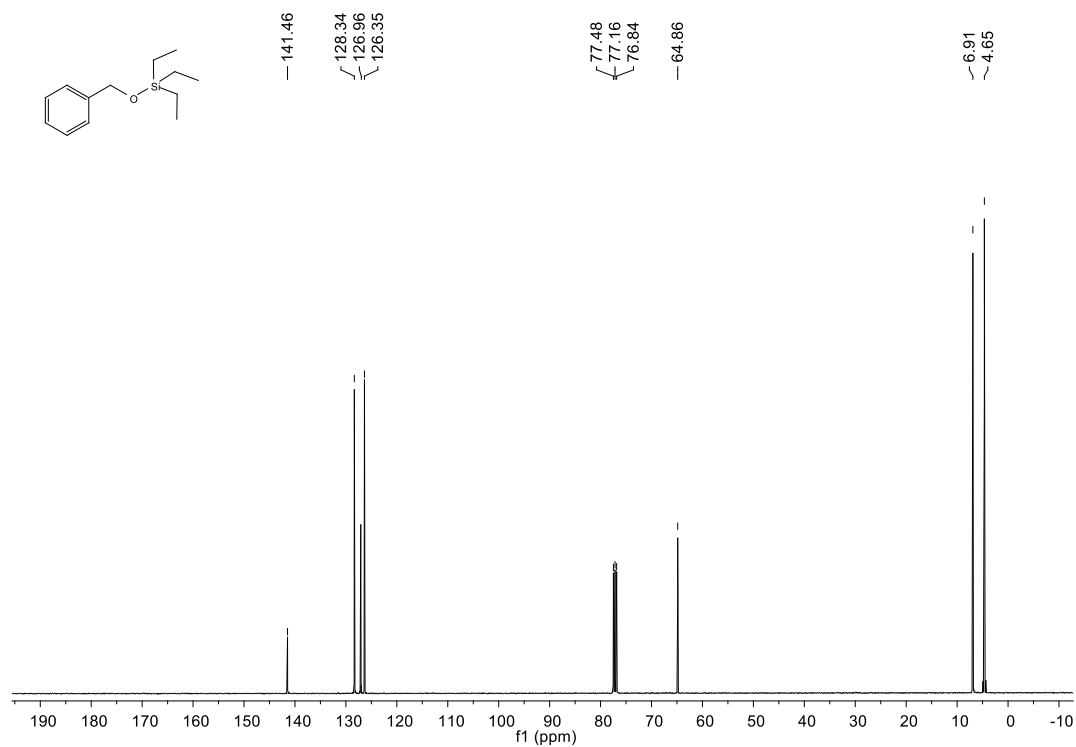


Figure 6.6 ^1H NMR spectrum of 9-((triethylsilyloxy)methyl)anthracene:

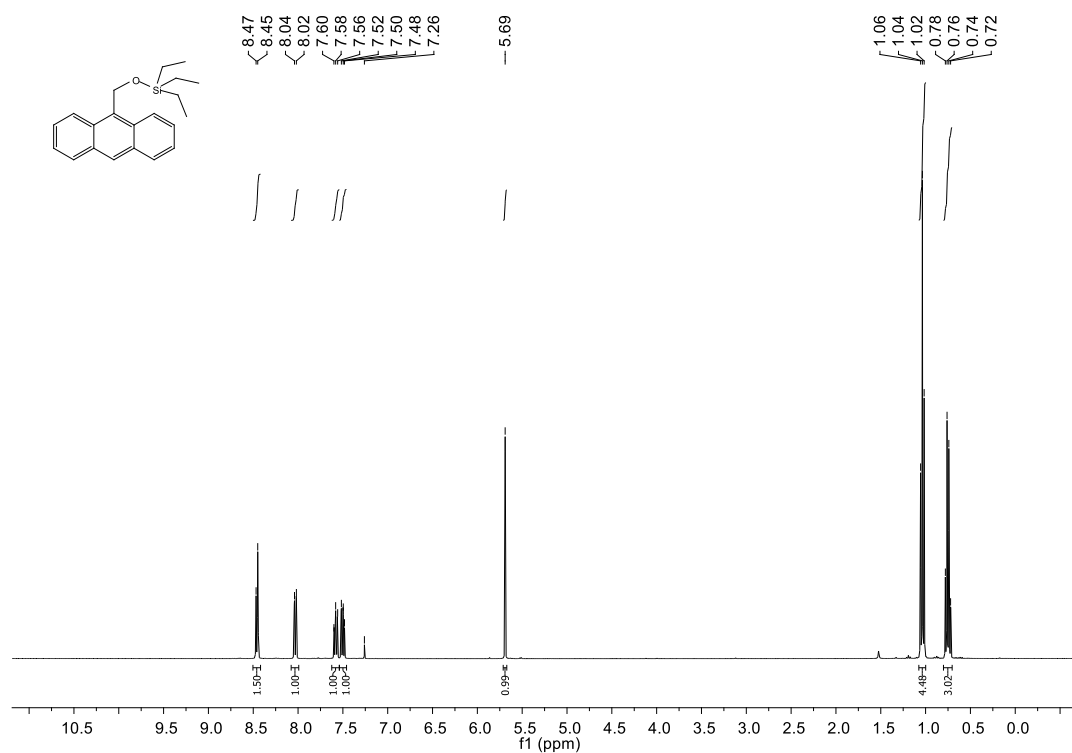


Figure 6.7 ^{13}C NMR spectrum of 9-((triethylsilyloxy)methyl)anthracene:

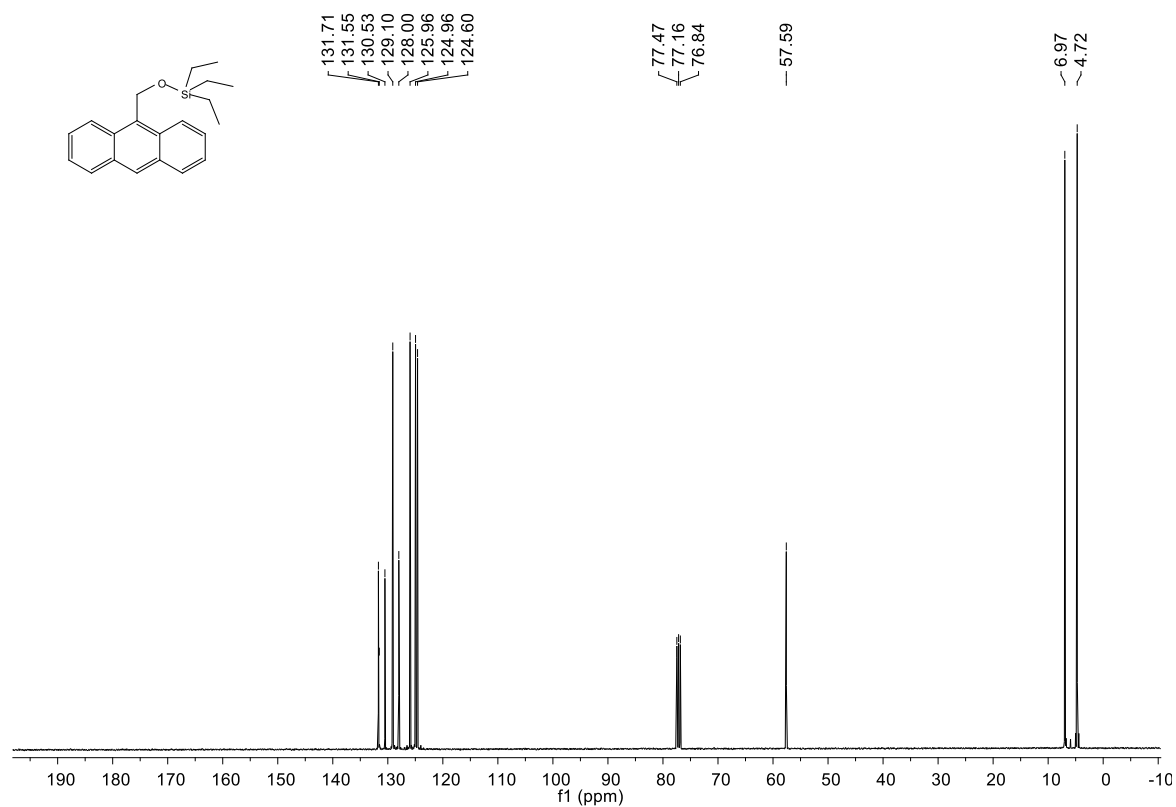


Figure 6.8 ^1H NMR spectrum of 5-((triethylsilyloxy)methyl)furan-2-yl acetate:

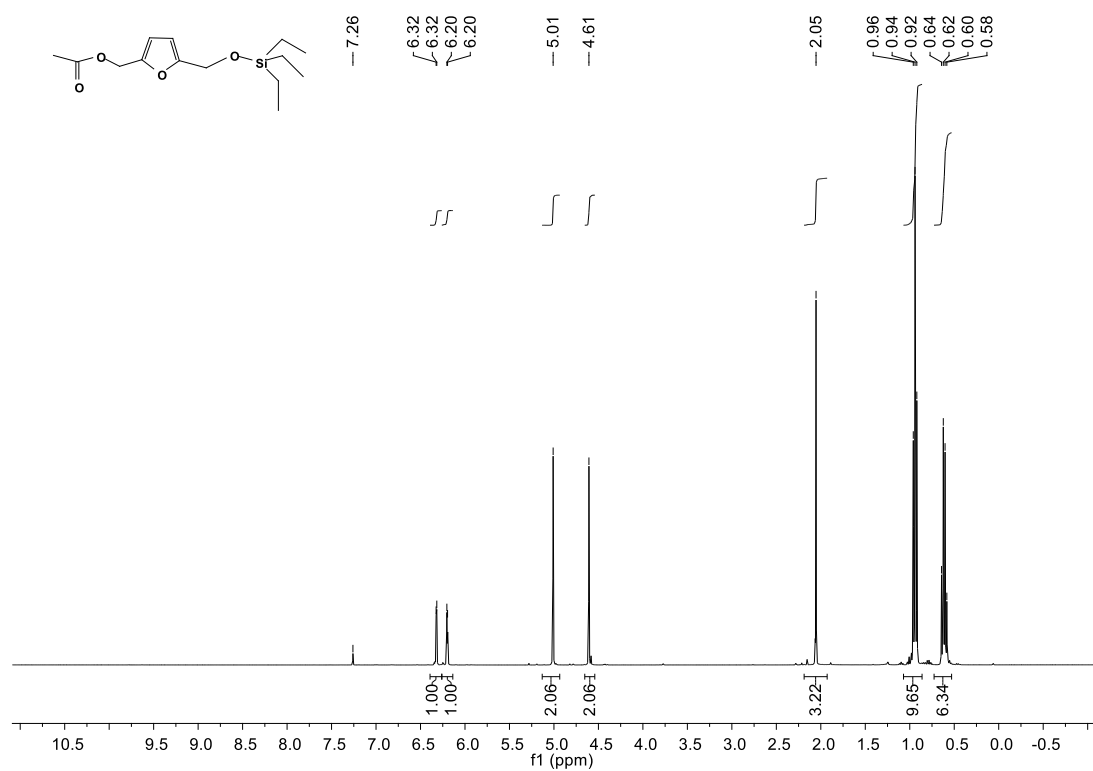


Figure 6.9 ^{13}C NMR spectrum of 5-((triethylsilyloxy)methyl)furan-2-yl acetate:

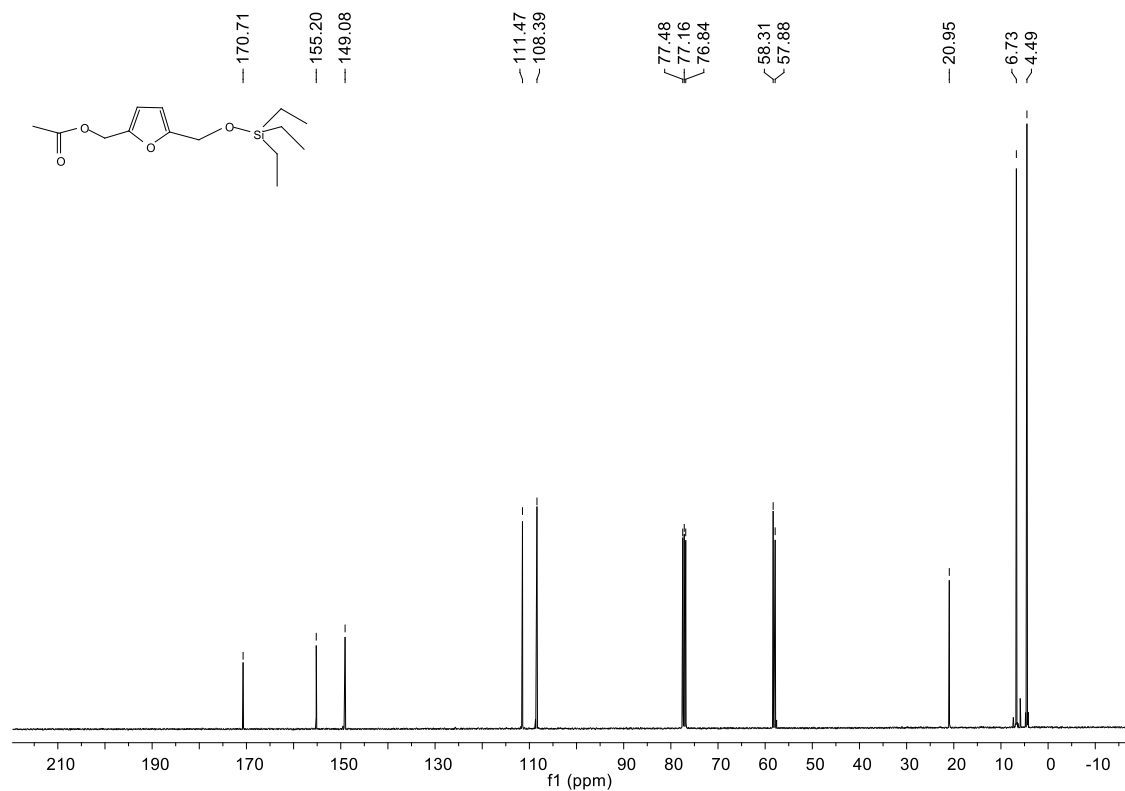


Figure 6.10 ^1H NMR spectrum of 1-(1H-indol-1-yl)(3-(triethylsilyloxy)methyl)ethanone:

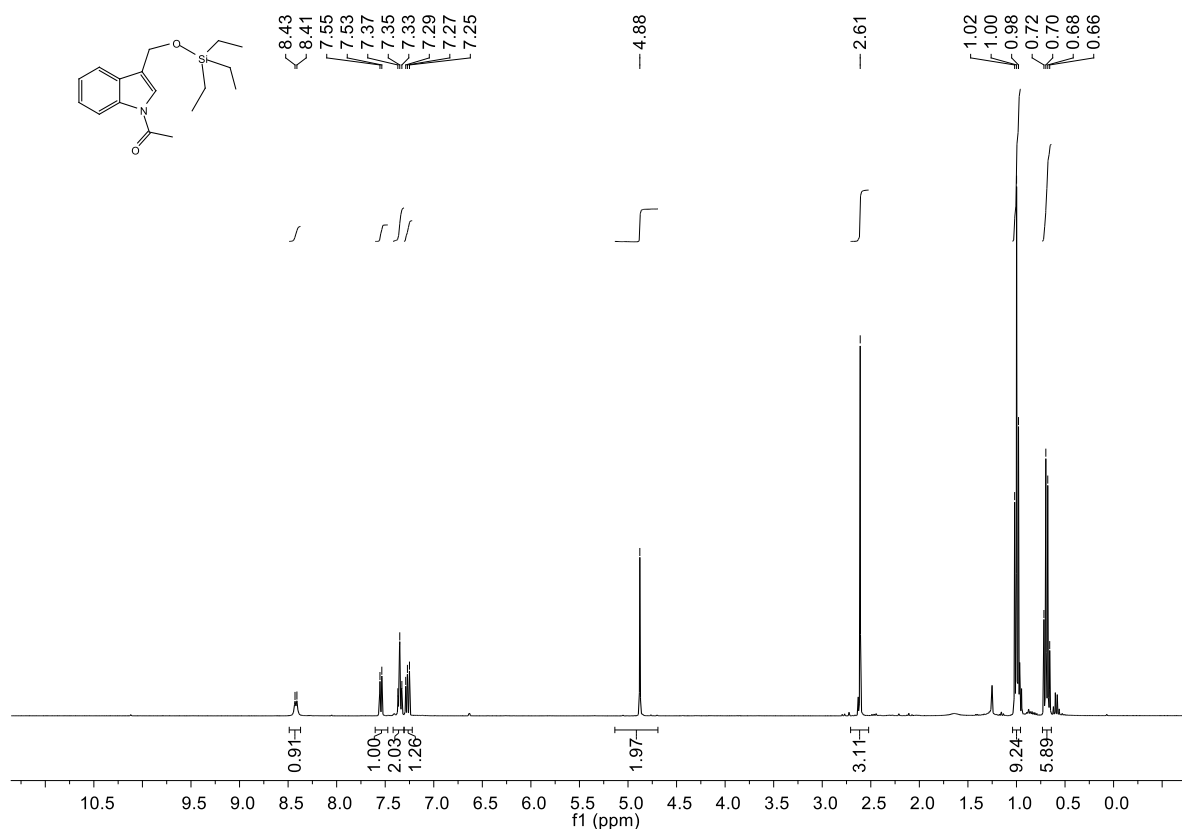


Figure 6.11 ^{13}C NMR spectrum of 1-(1H-indol-1-yl)(3-(triethylsilyloxy)methyl)ethanone:

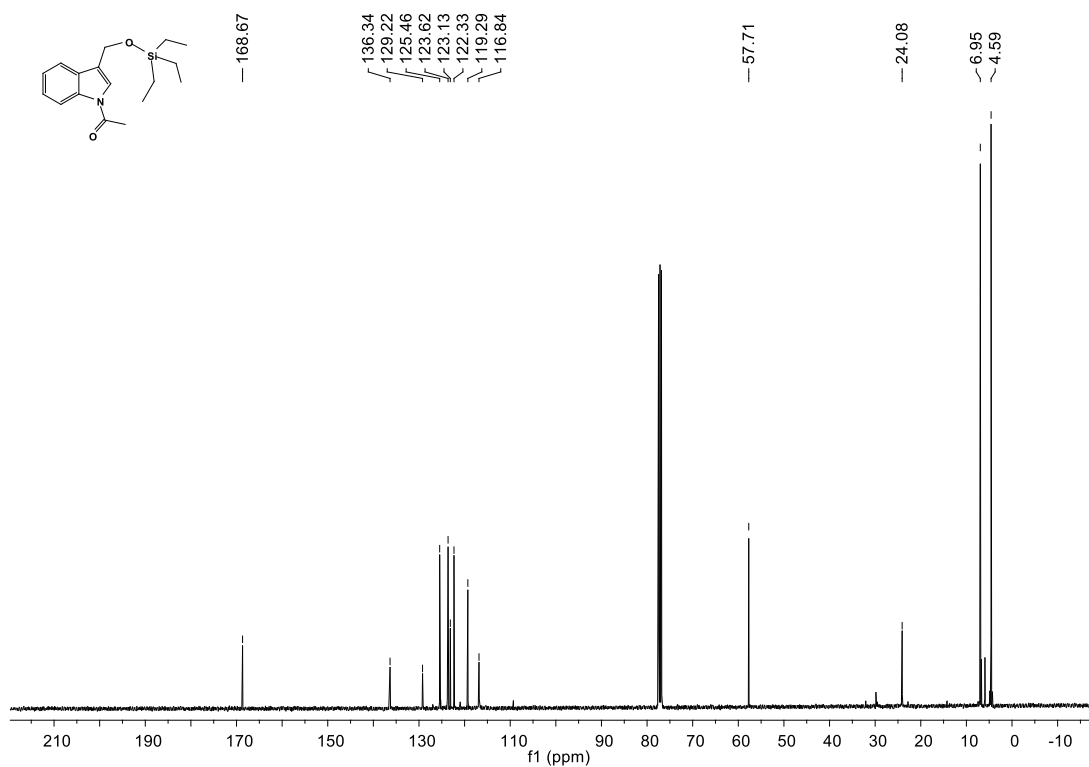


Figure 6.12 ^1H NMR spectrum of 1-phenyl-2-(4-(((triethylsilyl)oxy)methyl)phenoxy)ethanone:

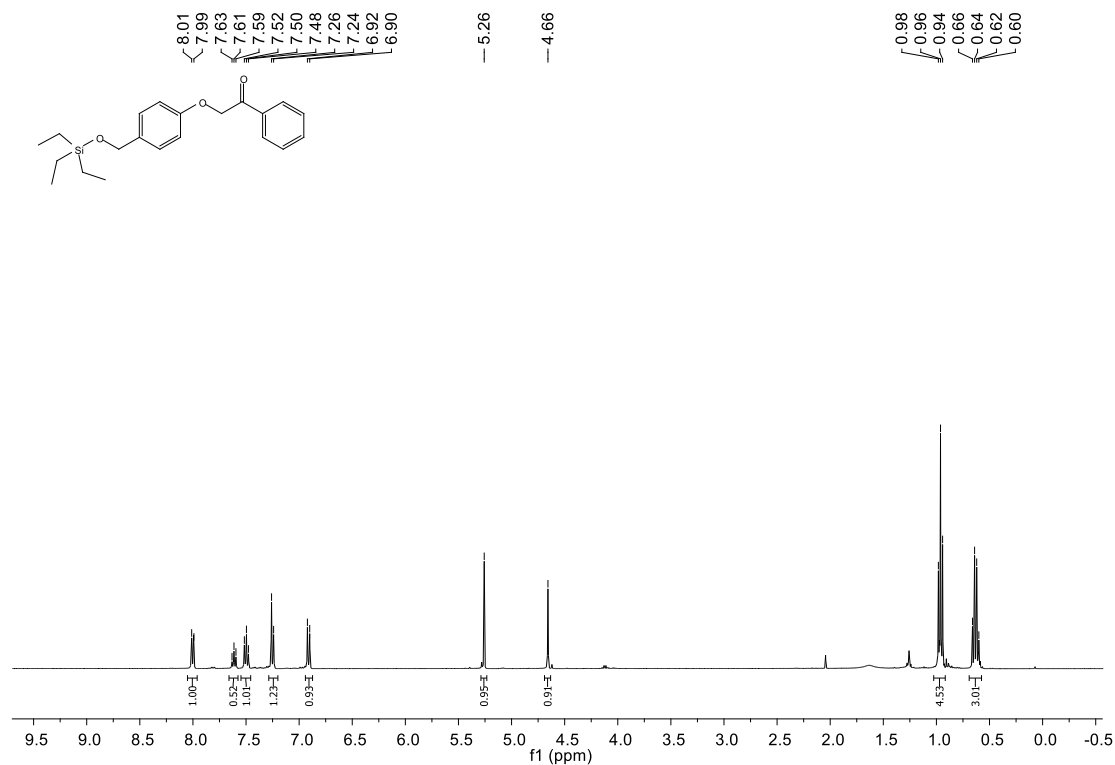


Figure 6.13 ^{13}C NMR spectrum of 1-phenyl-2-(4-(((triethylsilyl)oxy)methyl)phenoxy)ethanone:

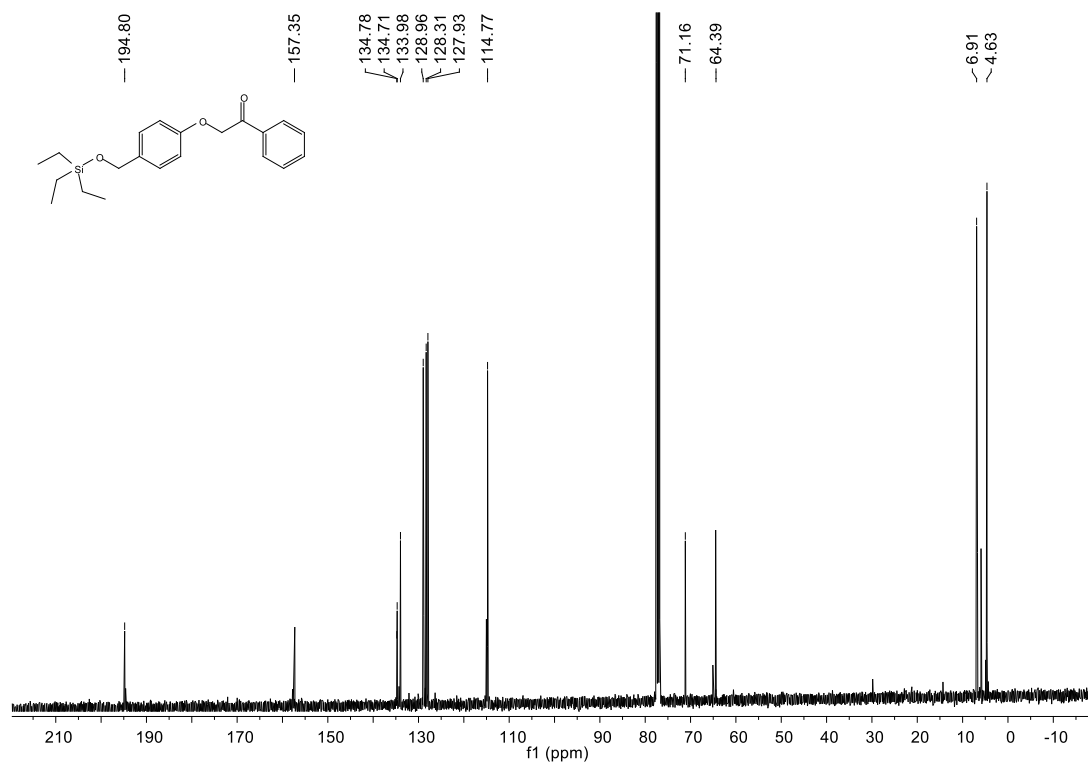


Figure 6.14 ^1H NMR spectrum of $[\{(\eta^6\text{-}p\text{-cymene})\text{Ru}\}_2(\mu\text{-H-}\mu\text{-Cl})(\text{Cl})_2](\mathbf{2})$:

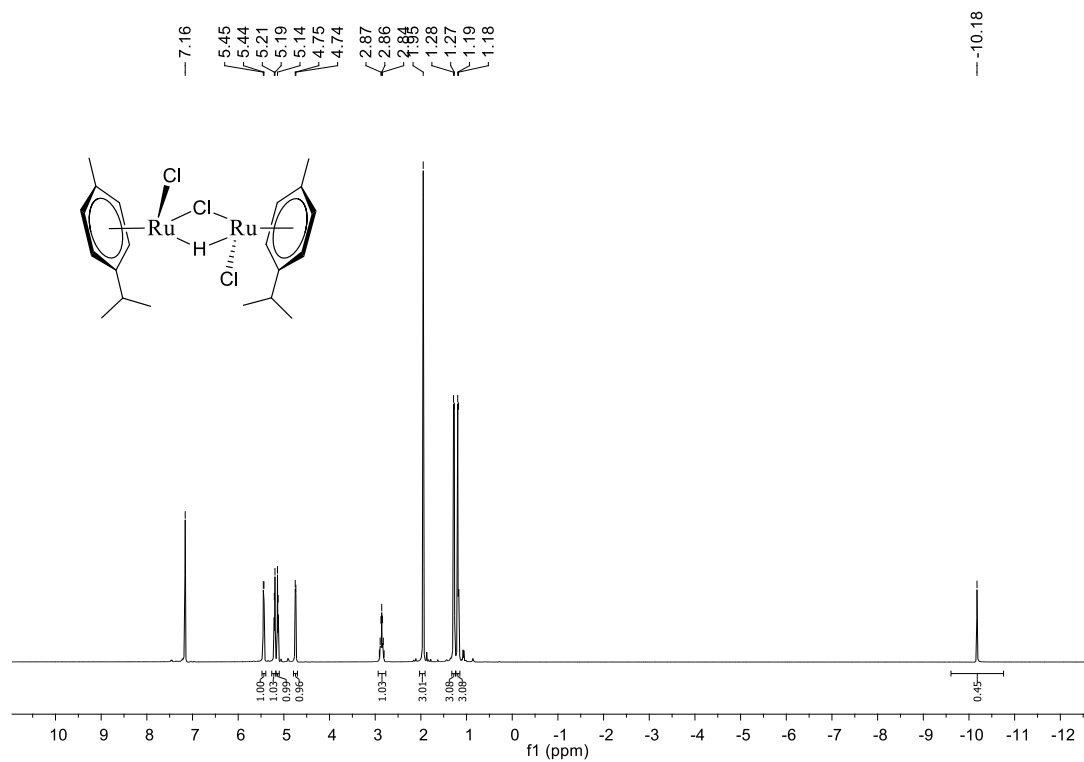


Figure 6.15 ^{13}C NMR spectrum of $[\{(\eta^6\text{-}p\text{-cymene})\text{Ru}\}_2(\mu\text{-H-}\mu\text{-Cl})(\text{Cl})_2](\mathbf{2})$:

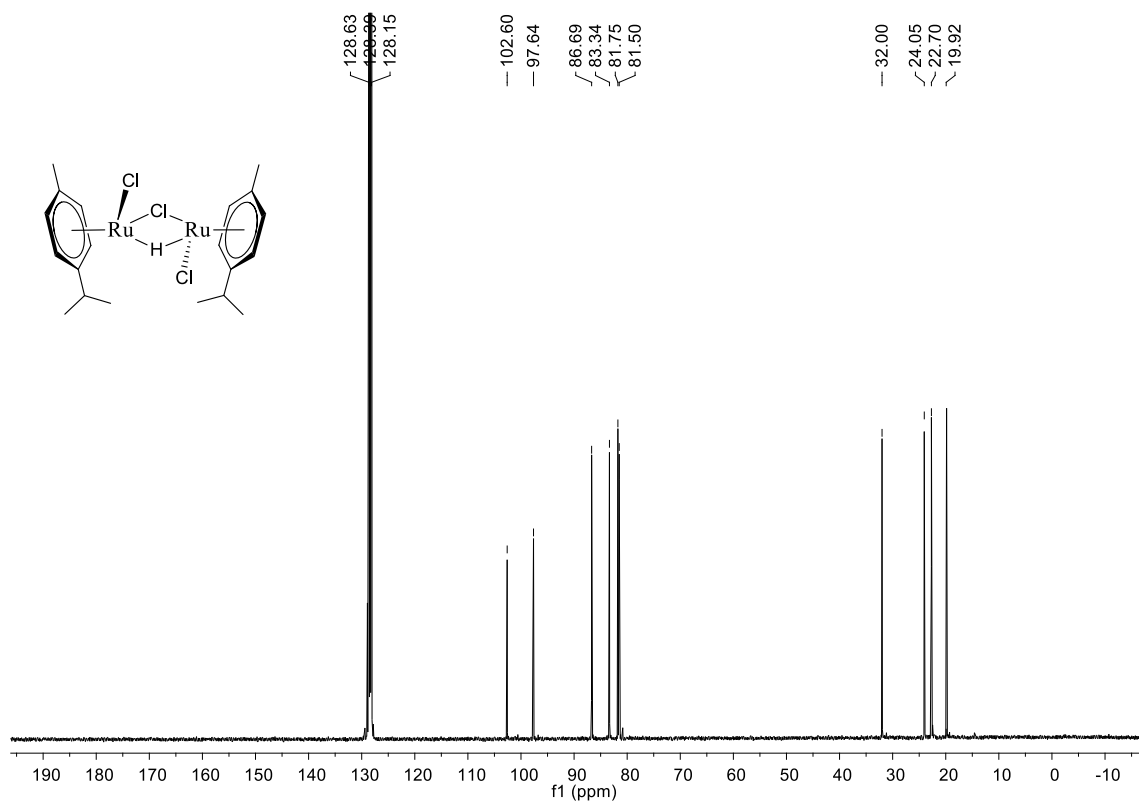


Figure 6.16 ^1H NMR spectrum of $[(\eta^6\text{-}p\text{-cymene})\text{Ru}(\text{H})_2(\text{SiEt}_3)_2]$ **3**:

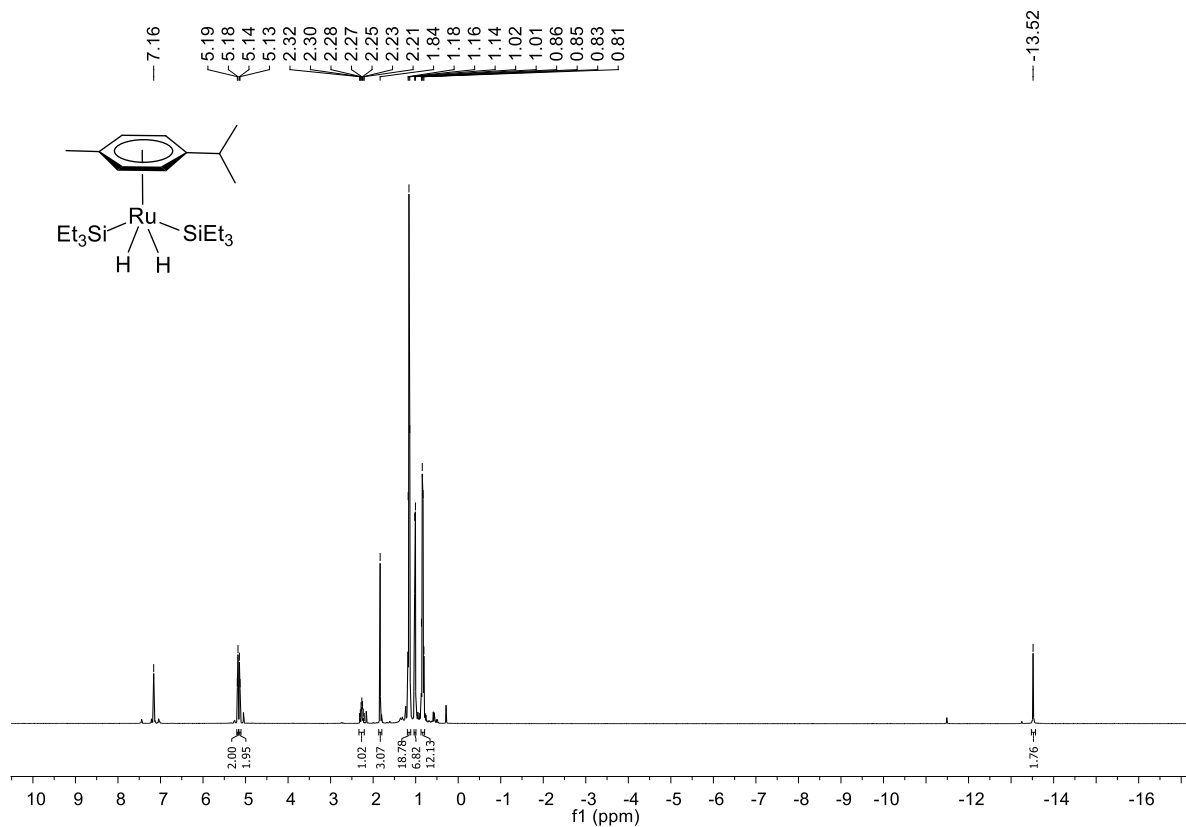
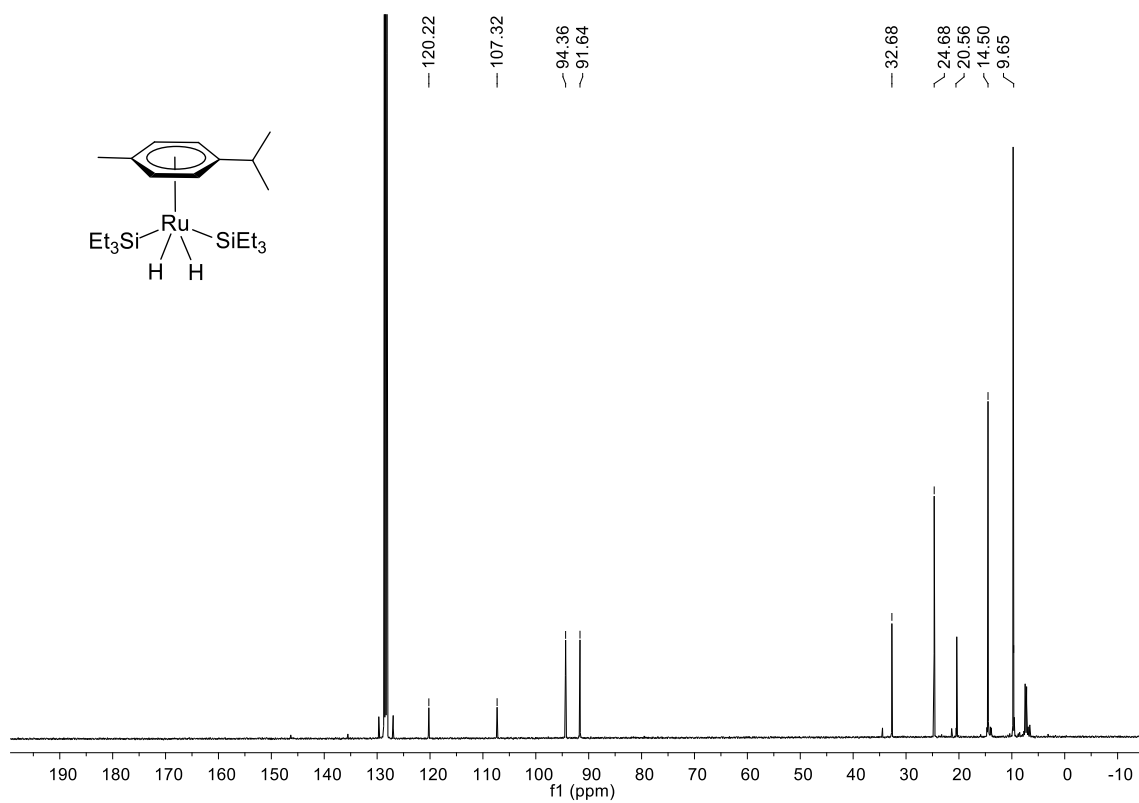


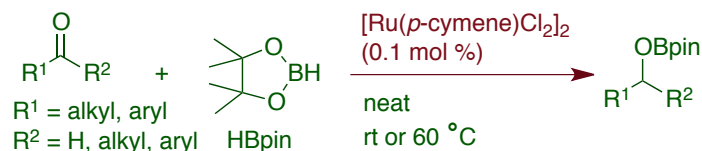
Figure 6.17 ^{13}C NMR spectrum of $[(\eta^6\text{-}p\text{-cymene})\text{Ru}(\text{H})_2(\text{SiEt}_3)_2]$ **3**:



CHAPTER 7

Ruthenium Catalyzed Selective Hydroboration of Carbonyl Compounds

7.1 ABSTRACT



Using the $[\text{Ru}(p\text{-cymene})\text{Cl}_2]_2$ (**1**) complex, catalytic hydroboration of aldehydes and ketones with pinacolborane under neat and mild conditions is described. At rt, chemoselective hydroboration of aldehydes over the ketones is also attained. Mechanistic studies confirmed the immediate formation of monohydrido bridged dinuclear complex $[\{(\eta^6\text{-}p\text{-cymene})\text{RuCl}\}_2(\mu\text{-H}-\mu\text{-Cl})]$ (**1b**) from the reaction of **1** with pinacolborane, which catalyzed the highly efficient hydroboration reactions. The catalytic cycle containing mononuclear Ru-H species and intramolecular 1,3-hydride transfer is postulated.

7.2 INTRODUCTION

Boronate esters are excellent synthetic surrogates in organic synthesis, and an assortment of chemical transformation is developed to incorporate them into organic substrates.^{1,2} The organoboronates are stable, nontoxic compounds and are thus preferred over the other organometallic compounds. Thus, a number of catalytic methods are employed for the synthesis of alkyl and vinyl boronates.^{2,3} Particularly, among metal-catalyzed reactions rhodium catalysts are extensively used in hydroboration.³ Use of ruthenium catalysts in hydroboration of alkenes resulted in either mixture of products⁴ or provided dehydrogenative vinyl boronates in addition to the hydroboration.⁵ Efficient conversion of carbonyl compounds into the corresponding alcohols is an important transformation in organic synthesis.⁶

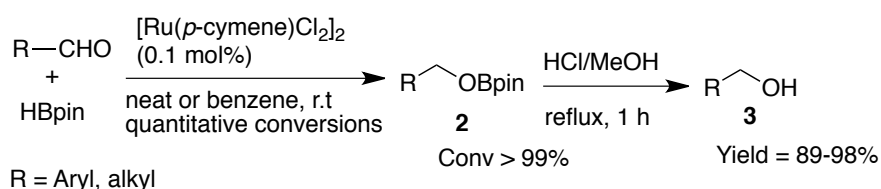
Transition metal complexes of molybdenum⁷ and titanium,⁸ and main group zinc complexes,⁹ are reported to catalyze the hydroboration of carbonyl compounds.¹⁰ While ruthenium catalyzed synthesis of organoboronates is well explored,^{4,5,11} its application in hydroboration of carbonyl compounds is limited to one interesting example, which is based on bifunctional catalysis.¹² Moreover, chemoselective hydroboration of aldehydes over ketones is a synthetically valuable and unknown transformation. Our interest in the hydroboration of carbonyl compounds emanated from the recently reported ruthenium catalyzed hydrosilylation reaction of aldehydes.¹³ Herein, we demonstrate highly efficient hydroboration of aldehydes and ketones and chemoselective hydroboration of aldehydes under mild conditions using the [Ru(*p*-cymene)Cl₂]₂ as a precatalyst.

7.2 RESULTS AND DISCUSSIONS

Initial studies focused on the hydroboration of aldehydes catalyzed by [Ru(*p*-cymene)Cl₂]₂ (**1**). Upon stirring a neat solution of benzaldehyde (1 mmol) and pinacolborane (1 mmol, HBpin = 4,4,5,5-tetramethyl-1,3,2-dioxaborolane) with complex **1** (0.1 mol %) at rt, hydroboration occurs rapidly to provide the PhCH₂OBpin. ¹H NMR analysis of the reaction mixture indicated the quantitative conversion of aldehydes in 4 h (TON > 990). Upon hydrolysis, benzyl alcohol was obtained in 92% yield after column chromatography (Scheme 7.1). Control experiments performed without a catalyst confirmed the absence of any significant hydroboration of aldehydes with pinacolborane at rt.^{14a} Further, a range of aromatic and aliphatic aldehydes were subjected to hydroboration with pinacolborane using [Ru(*p*-cymene)Cl₂]₂ (0.1 mol %). Aromatic aldehydes containing one or more electron-donating functional groups or both electron donating and withdrawing substituents required 4 to 4.5 h to provide the complete conversion of aldehydes.

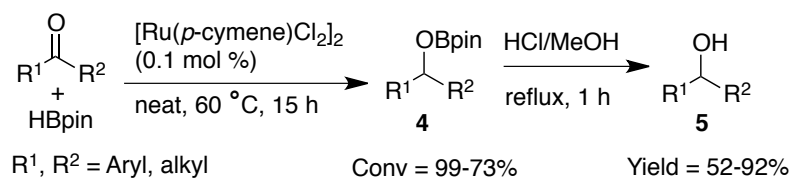
Aromatic aldehydes containing only electron-withdrawing functional groups and aliphatic aldehydes underwent fast hydroboration, and quantitative conversions of aldehydes (TON > 990) were observed within 3 h at rt. Reactions occur under neat conditions; solvent is used only for the solid aldehydes. Progress of the hydroboration reactions was monitored by TLC and ¹H NMR of the reaction mixture, which confirmed the quantitative conversion of aldehydes. Hydrolysis of the resulting boronate esters provided the corresponding alcohols in very high yields (Scheme 7.1).^{14b,c}

Scheme 7.1 Hydroboration of Aldehydes Catalyzed by [Ru(*p*-cymene)Cl₂]₂



Hydroboration of ketones using complex **1** required heating the reaction mixture at elevated temperature. When a neat solution of ketone, pinacolborane, and [Ru(*p*-cymene)Cl₂]₂ **1** (0.1 mol %) was heated at 60 °C, 60% to >99% conversion of ketones (TON: 600 to >990) to the corresponding boronate esters was observed by ¹H NMR analyses of the reaction mixtures. Boronate ester from the reaction of benzophenone and pinacolborane was isolated in 75% yield (Scheme 7.2) and characterized by single-crystal X-ray analysis (see Figure 7.1).¹⁵ Further hydrolysis of the boronate esters provides the secondary alcohols in good yields (Scheme 7.2). As observed in the case of aldehydes, both aliphatic and aryl ketones with different substituents are tolerated. The efficiency of this catalytic system^{14b,c} is remarkable when compared to the boron-substituted analogue of the Shvo's catalyst, which required 70 °C heating for 3 to 4.5 days at 4 mol % catalyst loading to provide moderate conversions.¹²

Scheme 7.2 [Ru(*p*-cymene)Cl₂]₂ Catalyzed Hydroboration of Ketones



The hydroboration of ketone was further unequivocally corroborated by single crystal X-ray analysis of 2-(2,2-diphenylethyl)-4,4,5,5-tetramethyl-1,3,2-dioxaborolane (Figure 7.1).

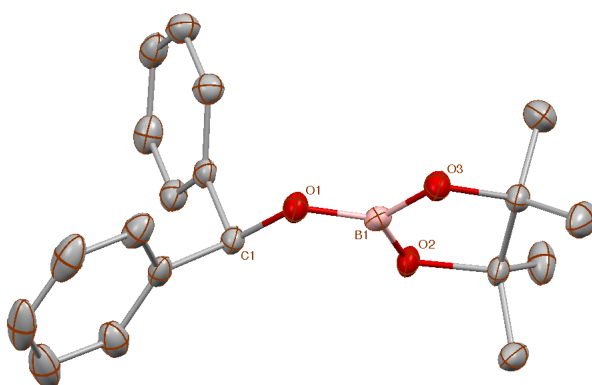
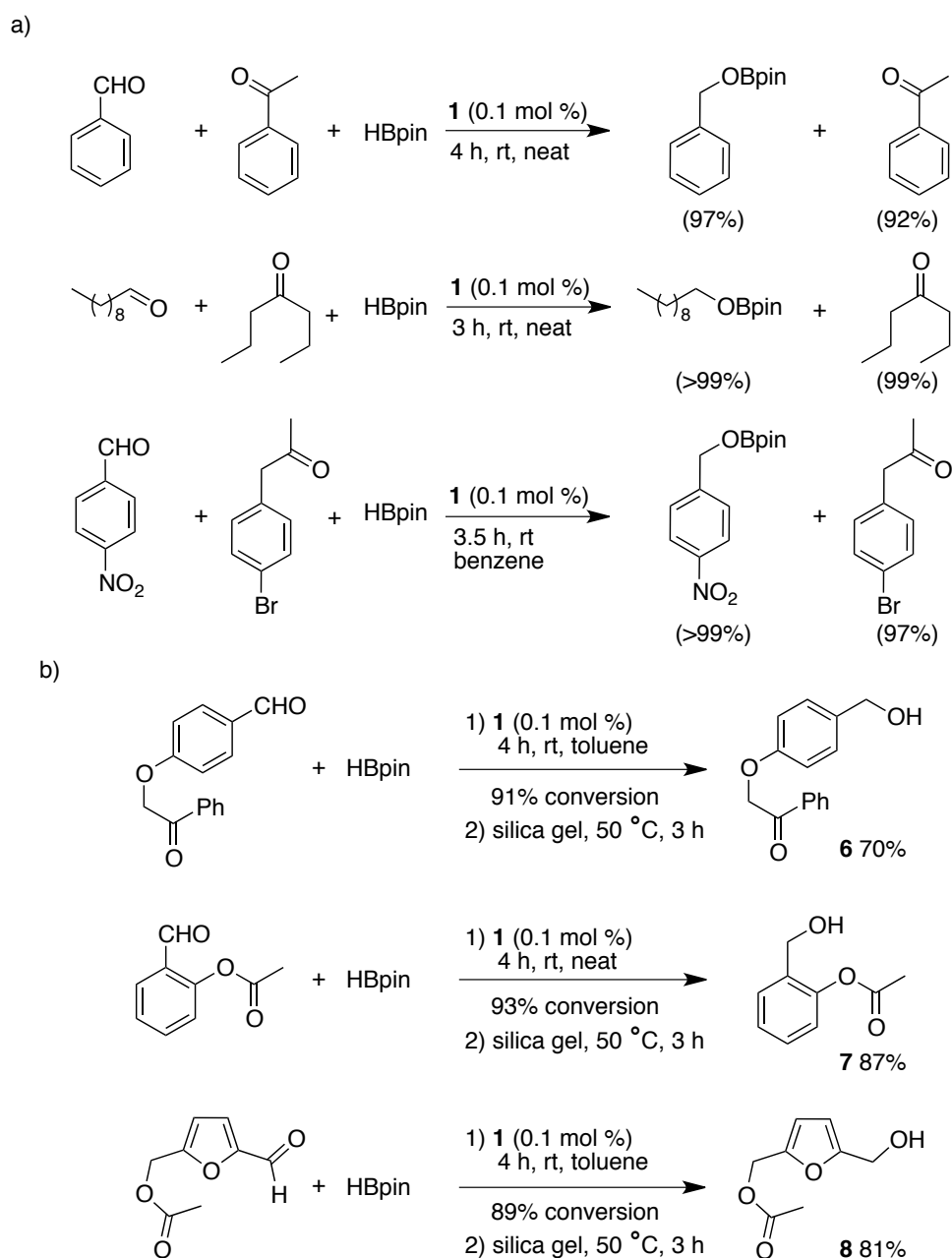


Figure 7.1 ORTEP diagram of 2-(2,2-diphenylethyl)-4,4,5,5-tetramethyl-1,3,2-dioxaborolane (thermal ellipsoids are drawn with 30% probability).

Further, using **1**, the challenging chemoselective hydroboration of aldehydes over the ketones is explored. Reaction of equimolar amounts of benzaldehyde, acetophenone, and pinacolborane were reacted together with **1** (0.1 mol %) under neat conditions, which resulted in 97% conversion of benzaldehyde in 4 h. ¹H NMR analysis indicated the presence of 92% of unreacted acetophenone in the reaction mixture. Similar chemoselectivity is also observed in competitive catalytic hydroboration reactions of 1-decanal over the 4-heptanone and *p*-nitro benzaldehyde over 1-(4-bromophenyl)propan-2-one (Scheme 7.3a). Aldehyde substrates that are embedded with functional groups such as ketones and esters also exhibited chemoselective hydroboration. 4-(2-Oxo-2-phenylethoxy)benzaldehyde, 2-formylphenyl acetate, and (5-formylfuran-2-yl)-methyl acetate were independently reacted with an equimolar

amount of pinacolborane and **1** (0.1 mol %) in toluene or under neat conditions at room temperature for 4 h. ¹H NMR analyses of these reaction mixtures indicated the chemoselective hydroboration of aldehydes over the other functional groups. The corresponding alcohols **6-8** were isolated in good yields after hydrolysis of the boronate esters, and characterization of the products confirmed further that ketone and ester motifs remain intact (Scheme 7.3b).

Scheme 7.3 Chemoselective Hydroboration of Aldehydes Catalyzed by [Ru(*p*-cymene)Cl₂]**1**



We previously prepared and characterized the structure of complex **1b** from the reaction of **1** with triethylsilane, as it was identified as a potential catalytic intermediate in the hydrosilylation of aldehydes.¹³

In situ monitoring of the reaction progress by ¹H NMR spectroscopy revealed the zero-order kinetics for the hydroboration of benzaldehyde (see Figure 7.2).

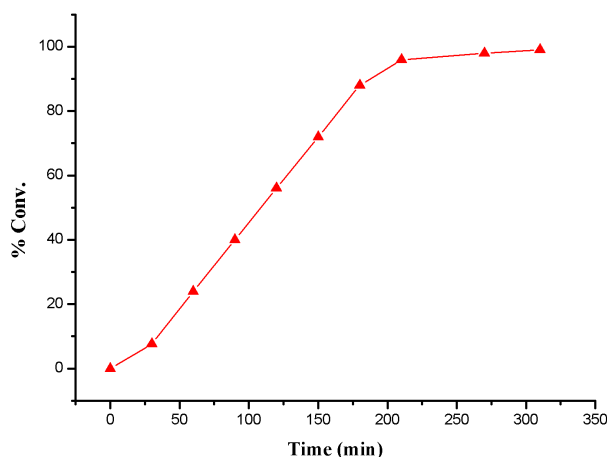
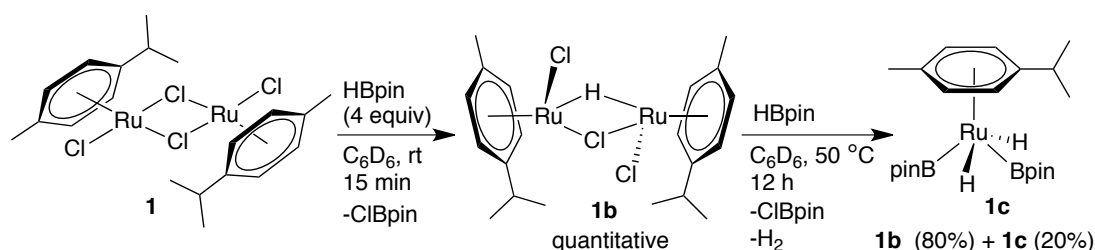


Figure 7.2 ¹H NMR monitoring of the reaction progress. Conversions (%) are determined from integration of ¹H NMR. Benzaldehyde (0.5 mmol), pinacolborane (0.5 mmol), catalyst (0.1 mol%) and benzene-d₆ were charged in a screw cap NMR tube and progress of the reaction is monitored by ¹H NMR spectroscopy at regular interval.

The hydride region in the ¹H NMR of the reaction mixture displayed a singlet resonance at $\delta_{\text{Ru-H}} = -10.18$ ppm immediately, and the observation is comparable to that of the hydrosilylation reaction catalyzed by **1**.¹³ Reaction of $[\text{Ru}(p\text{-cymene})\text{Cl}_2]_2$ **1** and pinacolborane (4 equiv) provided monohydrido bridged dinuclear ruthenium complex $[\{(\eta^6\text{-}p\text{-cymene})\text{RuCl}\}_2(\mu\text{-H}-\mu\text{-Cl})]$ **1b** at room temperature (Scheme 7.4). Interestingly, complex **1** reacts with pinacolborane (15 min) much faster than it reacts with triethylsilane (30 min) to provide complex **1b** quantitatively.¹⁶ Complexes **1** and **1b** also reacted further with triethylsilane and provided a mononuclear Ru(IV) dihydride complex $[(\eta^6\text{-}p\text{-cymene})\text{Ru}(\text{H})_2(\text{SiEt}_3)_2]$ ($\delta_{\text{Ru-H}} = -13.53$ ppm).¹³ Attempts

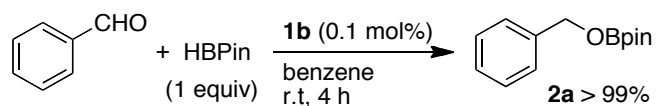
to prepare an analogous pinacolborane Ru(IV) dihydride complex from the prolonged reaction (12 h) of either complex **1** or **1b** with an excess of pinacolborane (4 to 8 equiv) at 50 °C provided a mixture of complexes **1b** and **1c** in the ratio 80:20, respectively.^{17,18} Efforts made to isolate complex **1c** from this reaction mixture proved to be unsuccessful. Hence, the structure of complex $[(\eta^6\text{-}p\text{-cymene})\text{Ru}(\text{H})_2(\text{Bpin})_2]$ ($\delta_{\text{Ru-H}} = -13.48$ ppm; $\delta_{\text{Ru-B}} 34.39$ ppm)⁵ **1c** is tentatively assigned based on the analogous silyl ruthenium dihydride complex $[(\eta^6\text{-}p\text{-cymene})\text{Ru}(\text{H})_2(\text{SiEt}_3)_2]$.^{13,19}

Scheme 7.4 Reaction of $[\text{Ru}(p\text{-cymene})\text{Cl}_2]_2$ **1** with Pinacolborane: Preparation of Intermediate **1b**



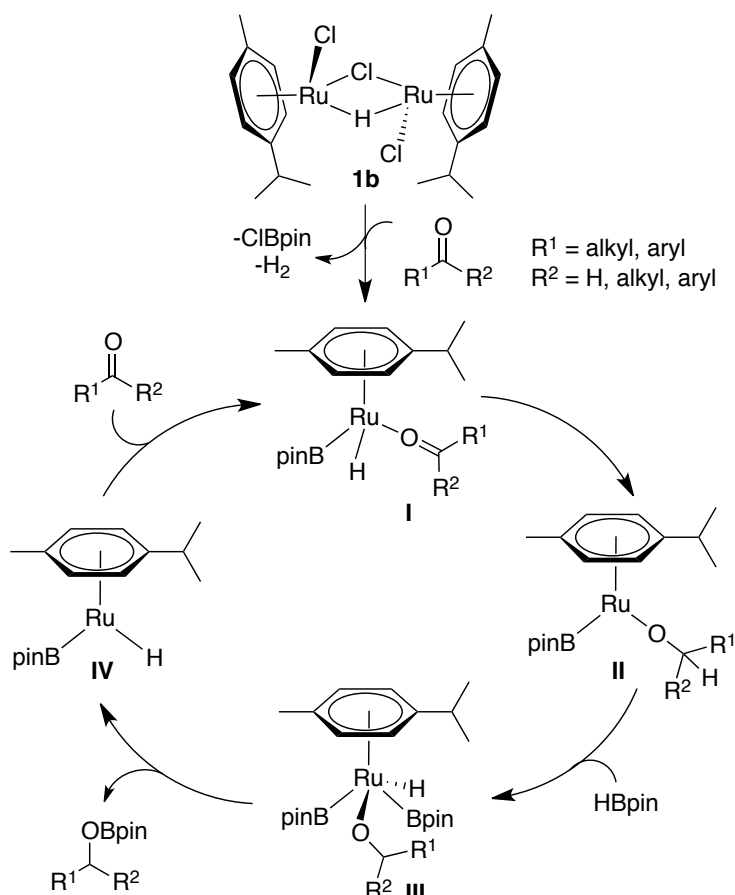
When isolated pure complex **1b** (0.1 mol %) was used as a catalyst in the hydroboration of benzaldehyde with pinacolborane, quantitative hydroboration was observed in 4 h, confirming the similar reactivity and efficiency as those of $[\text{Ru}(p\text{-cymene})\text{Cl}_2]_2$ **1** and thus indicating the potential intermediacy of **1b** in catalysis (Scheme 7.5). To ascertain any role of complex **1c** in catalysis,²⁰ hydroboration of benzaldehyde with pinacolborane was performed using 1 and 2 mol % loadings of **1**.²¹ Similarly, hydroboration of acetophenone with 1 mol % of **1** was also carried out and all the reactions were monitored by the ^1H NMR, which indicated that no hydride signal corresponding to **1c** ($\delta_{\text{Ru-H}} = -13.48$ ppm) appears in the reaction mixtures, thus confirming its non-involvement in the catalytic hydroboration of aldehydes and ketones.

Scheme 7.5 Catalytic Hydroboration by an Isolated Intermediate **1b** $[(\eta^6\text{-}p\text{-cymene})\text{RuCl}]_2(\mu\text{-H}-\mu\text{-Cl})$



On the basis of the above-mentioned observations, we postulate that under the experimental conditions intermediate **1b** reacts with pinacolborane upon splitting into monomeric [(*p*-cymene)RuHCl] and [(*p*-cymene)Ru(Cl)₂] complexes²² to provide Ru(II) intermediate **I**, which may involve the intermediacy of Ru (0) species and the B–H activation.²³ Reductions of carbonyl functional groups occur by an intramolecular 1,3-transfer of a “hydride” ligand to the “carbonyl” motif to provide **II**. Further, oxidative addition of pinacolborane to intermediate **II** results in formation of a Ru (IV) intermediate **III**, which reductively eliminates the boronate esters and generates **IV**. Coordination of the carbonyl compound to **IV** regenerates **I** to close a catalytic cycle (Scheme 7.6).

Scheme 7.6 Plausible Mechanism for the Hydroboration of Carbonyl Compounds



7.4 CONCLUSIONS

In conclusion, efficient hydroboration of aldehydes and ketones was achieved using the commercially available and economical ruthenium complex $[\text{Ru}(p\text{-cymene})\text{Cl}_2]_2$. At rt, chemoselective hydroboration of aldehydes is demonstrated. Mechanistic studies revealed that the reaction of pinacolborane with $[\text{Ru}(p\text{-cymene})\text{Cl}_2]_2$ provides $[\{(\eta^6\text{-}p\text{-cymene})\text{RuCl}\}_2(\mu\text{-H}-\mu\text{-Cl})]$ **1b**. Perhaps, further oxidative addition of pinacolborane may generate the catalytically active mononuclear Ru species. The catalytic cycle consists of 1,3-hydride transfer from the metal center to the carbonyl group, and reductive elimination of boronate esters from a Ru(IV) intermediate is postulated.

7.5 EXPERIMENTAL SECTION

General Experimental: All catalytic reactions were performed under nitrogen atmosphere. All stoichiometric reactions were performed in nitrogen atmosphere MBraun glove box. Chemicals were purchased from Acros, Sigma-Aldrich, Alfa-aesar and used without further purification. Dry solvents were prepared according to standard procedures. ^1H , ^{13}C spectra were recorded at Bruker AV-400 (^1H : 400 MHz, ^{13}C : 100.6 MHz). ^1H and $^{13}\text{C}\{^1\text{H}\}$ NMR chemical shifts were reported in ppm downfield from tetramethyl silane. Multiplicity is abbreviated as: s, Singlet; d, doublet; dd, doublet of doublet; t, triplet; q, quartet; dq, doublet of quartet; m, multiplet; br, broad. Assignment of spectra was done based on one dimensional (dept-135) NMR techniques. IR Spectra were recorded in Perkin-Elmer FT-IR Spectrometer. Mass spectra were recorded on Bruker micrOTOF-Q II Spectrometer.

General Procedure for Intermolecular Chemoselective Catalytic Hydroboration:

Aldehyde (1 mmol), pinacolborane (1 mmol), ketone (1 mmol), $[\text{Ru}(p\text{-cymene})\text{Cl}_2]_2$ (**1**, 0.1 mol%) [benzene (1 mL) for solid substrates] were taken in a PTFE screw capped reaction vial equipped with a magnetic bar and the reaction mixture was stirred at room temperature for 4 h. Reaction progress was monitored by ^1H NMR analyses, which clearly indicated the complete conversion of aldehydes to boronate esters and predominant presence of unreacted ketones.

General Procedure for Intramolecular Chemoselective Catalytic Hydroboration:

Substrate (1 mmol), pinacolborane (1 mmol), $[\text{Ru}(p\text{-cymene})\text{Cl}_2]_2$ (0.1 mol%) [toluene (1 mL) for solid substrate] were taken in a PTFE screw capped reaction vial equipped with a magnetic bar and the reaction mixture was stirred at room temperature for 4 h. Progress of the reaction was monitored by TLC and ^1H NMR. Upon completion of the reaction, silica gel (500 mg, 100-200 mesh) was added to the aliquot and stirred at 50 °C for 3 h. The reaction mixture was washed four times (3

mL) with 10% dilute HCl with vigorous shaking and extracted with ethyl acetate. The crude reaction mixture then purified by column chromatography over silica gel (100-200 mesh) and eluted by ethyl acetate/hexane (2:5) to get pure product.

Spectral Data of Chemoselective Hydroboration Products:

2-(4-(hydroxymethyl)phenoxy)-1-phenylethanone²⁴: Colorless liquid. IR (DCM): 3440, 2924, 1688, 1521, 1076, 824, 673 cm^{-1} . ^1H NMR (CDCl_3): δ 7.99 (d, $J = 4\text{ Hz}$, 2H, ArCH), 7.62 (t, $J = 8\text{ Hz}$, 1H, ArCH), 7.50 (t, $J = 8\text{ Hz}$, 2H, ArCH), 7.28 (d, $J = 8\text{ Hz}$, 2H, ArCH), 6.92 (d, $J = 8\text{ Hz}$, 2H, ArCH), 5.27 (s, 2H, OCH_2), 4.60 (s, 2H, OCH_2), 1.76 (s, 1H, OH). $^{13}\text{C}\{^1\text{H}\}$ NMR (CDCl_3): δ 194.61 (Carbonyl CO), 157.71 (quat-C), 134.65 (quat-C), 134.29 (quat-C), 134.05 (ArCH), 128.98 (ArCH), 128.79 (ArCH), 128.2 (ArCH), 114.98 (ArCH), 70.94 (OCH_2), 65.00 (OCH_2). MS (ESI) m/z 265.08 ($\text{M}+\text{Na}$)⁺.

2-(hydroxymethyl)phenyl acetate²⁵: Colorless liquid. IR (DCM): 3393, 1715, 1458, 1385, 1262, 1027, 757, 616 cm^{-1} . ^1H NMR (CDCl_3): δ 7.82 (s, 1H, OH), 7.25 (m, 2H, ArCH), 6.90 (m, 2H, ArCH), 5.13 (s, 2H, OCH_2), 2.08 (s, 3H, CH_3). $^{13}\text{C}\{^1\text{H}\}$ NMR (CDCl_3): δ 173.46 (quat-C, COO), 155.32 (quat-C), 131.81 (ArCH), 130.87 (ArCH), 121.80 (quat-C), 120.52 (ArCH), 117.25 (ArCH), 63.10 (OCH_2), 20.91 (CH_3). MS (ESI) m/z 189.05 ($\text{M}+\text{Na}$)⁺.

(5-(hydroxymethyl)furan-2-yl)methyl acetate²⁶: Colorless liquid. IR (DCM): 3445, 2926, 1734, 1375, 1243, 1021, 804 cm^{-1} . ^1H NMR (CDCl_3): δ 6.35 (d, $J = 4\text{ Hz}$, 1H, ArCH), 6.25 (d, $J = 4\text{ Hz}$, 1H, ArCH), 5.02 (s, 2H, OCH_2), 4.60 (s, 2H, OCH_2), 2.07 (s, 3H, CH_3), 1.86 (s, 1H, OH). $^{13}\text{C}\{^1\text{H}\}$ NMR (CDCl_3): δ 170.87 (quat-C, COO), 154.98 (quat-C), 149.51 (quat-C), 111.61 (ArCH), 108.76 (ArCH), 58.28 (OCH_2), 57.58 (OCH_2), 20.98 (CH_3). MS (ESI) m/z 193.05 ($\text{M}+\text{Na}$)⁺.

Synthesis of Complex $[\{\eta^6\text{-}p\text{-cymene}\}\text{Ru}\}_2(\mu\text{-H-}\mu\text{-Cl})(\text{Cl})_2](2)$: To benzene-d₆ (0.5 mL) in a screw-cap NMR tube, $[\text{Ru}(p\text{-cymene})\text{Cl}_2]_2$ (0.05 mmol, 32 mg), pinacolborane (0.2 mmol, 29 μl) was added and the resulting mixture was shaken occasionally at room temperature and monitored by ¹H NMR. After completion of the reaction the dark red solution was reduced to one third of its volume. Slow addition of cold pentane (2 mL) provided dark red precipitate. The solution was decanted and the precipitate was washed with a mixture of pentane and toluene. The resulted dark red complex was dried under vacuum for overnight (29 mg, quantitative yields). The spectral data of compound **2** were identical with our previously reported complex $[\{\eta^6\text{-}p\text{-cymene}\}\text{Ru}\}_2(\mu\text{-H-}\mu\text{-Cl})(\text{Cl})_2]$ prepared from the reaction of $[\text{Ru}(p\text{-cymene})\text{Cl}_2]_2$ and triethyl silane.¹³

Determination of the Molecular Structure of 2-(2,2-diphenylethyl)-4,4,5,5-tetramethyl-1,3,2-dioxaborolane in the Solid State by X-ray Single Crystal Diffraction: Single crystals of 2-(2,2-diphenylethyl)-4,4,5,5-tetramethyl-1,3,2-dioxaborolane suitable for X-ray analysis was obtained from a solution of dichloromethane. A single crystal suited for X-ray diffraction measurements was mounted on a glass fiber. Geometry and intensity data were collected with a Bruker SMART D8 goniometer equipped with an APEX CCD detector and with an Incoatec microsource (Mo-K α radiation, $\lambda = 0.71073 \text{ \AA}$, multilayer optics). Temperature was controlled using an Oxford Cryostream 700 instrument. Intensities were integrated with SAINT+²⁷ and corrected for absorption with SADABS.²⁸ The structure was solved by direct methods and refined on F^2 with SHELXL-97.^{29,30}

Crystal Data of 2-(2,2-diphenylethyl)-4,4,5,5-tetramethyl-1,3,2-dioxaborolane: C₁₉H₂₃BO₃ crystal dimensions: 0.33 \times 0.27 \times 0.21, $M=310.18$, monoclinic with space group P21/n, $a = 6.4137(5)$, $b = 29.2081(19)$, $c = 9.2715(6)$, $\alpha = 90^\circ$, $\beta = 101.425^\circ(4)$,

$\gamma = 90^\circ$, $V = 1702.4(2)\text{\AA}^3$, $Z = 4$, $2\theta_{\text{max}} = 56.67$, $\rho_{\text{calcd}} = 1.210 \text{ Mg/m}^3$, $T = 100\text{K}$, $\mu(\text{MoK}\alpha) = 0.079 \text{ mm}^{-1}$, min/max transmission factors = 0.0538/0.0350, 28255 Reflections collected, 4247 unique ($R1 = 0.0425$), $WR2 = 0.1049$ (all data). Residual electron density max/min = 0.27/-0.22 $\text{e}\cdot\text{\AA}^{-3}$. The structure has been deposited at the CCDC data center and can be retrieved using the deposit number CCDC 1418431.

7.6 NOTES AND REFERENCES

- (1) (a) *Boronic Acids. Preparation and Applications in Organic Synthesis and Medicine*; Hall, D. G., Ed.; 2nd ed.; Wiley-VCH: Weinheim, 2011. (b) Crudden, C. M.; Edwards, D. *Eur. J. Org. Chem.* **2003**, 4695-4712. (c) Ramachandran, P. V.; Brown, H. C. *Recent Advances in Borane Chemistry. Organoboranes for Synthesis*; ACS Symp. Ser. 783; American Chemical Society: Washington, DC, 2001. (d) *Contemporary Boron Chemistry*; Davidson, M. G., Wade, K., Marder, T. B., Hughes, A. K., Eds.; Royal Society of Chemistry: Cambridge, 2000 (e) Matteson, D. S. *Tetrahedron* **1998**, *54*, 10555-10607. (f) Pelter, A.; Smith, K.; Brown, H. C. *Borane Reagents*; Academic Press, London, 1988. (g) Brown, H. C.; Kramer, G. W.; Levy, A. B.; Midland, M. M. *Organic Syntheses via Boranes*; Wiley-Interscience: New York, 1975; Vol. 1.
- (2) (a) Lennox, A. J.; Lloyd-Jones, G. C. *Chem. Soc. Rev.* **2014**, *43*, 412-443. (b) Suzuki, A. *J. Organomet. Chem.* **1999**, *576*, 147-168. (c) Miyaura, N.; Suzuki, A. *Chem. Rev.* **1995**, *95*, 2457-2483. (d) Matteson, D. S. *Chem. Rev.* **1989**, *89*, 1535-1551.
- (3) (a) Carroll, A.-M.; O'Sullivan, T. P.; Guiry, P. J. *Adv. Synth. Catal.* **2005**, *347*, 609-631. (b) Beletskaya, I.; Pelter, A. *Tetrahedron* **1997**, *53*, 4957-5026. (c) Burgess, K.; Ohlmeyer, M. J. *Chem. Rev.* **1991**, *91*, 1179-1191.

- (4) Burgess, K.; Jaspars, M. *Organometallics* **1993**, *12*, 4191-4200.
- (5) (a) Caballero, A.; Sabo-Etienne, S. *Organometallics* **2007**, *26*, 1191-1195. (b) Montiel-Palma, V.; Lumbierres, M.; Donnadiou, B.; Sabo-Etienne, S.; Chaudret, B. *J. Am. Chem. Soc.* **2002**, *124*, 5624-5625.
- (6) (a) Cho, B. T. *Chem. Soc. Rev.* **2009**, *38*, 443-452. (b) Togni, A.; Grützmacher, H. *Catalytic Heterofunctionalization*; Wiley- VCH: Weinheim, 2001. (c) Magano, J.; Dunetz, J. R. *Org. Process Res. Dev.* **2012**, *16*, 1156-1184.
- (7) Khalimon, A. Y.; Farha, P.; Kuzmina, L. G.; Nikonov, G. I. *Chem. Commun.* **2012**, *48*, 455-457.
- (8) (a) Oluyadi, A. A.; Ma, S. -H.; Muhoro, C. N. *Organometallics* **2013**, *32*, 70-78. (b) Sarvary, I.; Almqvist, F.; Frejd, T. *Chem. Eur. J.* **2001**, *7*, 2158-2166. (c) Almqvist, F.; Torstensson, L.; Gudmundsson, A.; Frejd, T. *Angew. Chem. Int. Ed. Engl.* **1997**, *36*, 376-377. (d) Giffels, G.; Dreisbach, C.; Kragl, U.; Weigerding, M.; Waldmann, H.; Wandrey, C. *Angew. Chem. Int. Ed. Engl.* **1995**, *34*, 2005-2006. (e) Lindsley, C. W.; DiMare, M. *Tetrahedron Lett.* **1994**, *35*, 5141-5144.
- (9) (a) Lummis, P. A.; Momeni, M. R.; Lui, M. W.; McDonald, R.; Ferguson, M. J.; Miskolzie, M.; Brown, A.; Rivard, E. *Angew. Chem. Int. Ed.* **2014**, *53*, 9347-9351. (b) Roh, S.-G.; Yoon, J. U.; Jeong, J. H. *Polyhedron* **2004**, *23*, 2063-2067. (c) Locatelli, M.; Cozzi, P. G. *Angew. Chem. Int. Ed.* **2003**, *42*, 4928-4930. (d) Locatelli, M.; Cozzi, P. G. *Angew. Chem. Int. Ed.* **2003**, *42*, 4928-4930. (f) Roh, S.-G.; Park, Y.-C.; Park, D.-K.; Kim, T.-J.; Jeong, J. H. *Polyhedron* **2001**, *20*, 1961-1965. (g) Bandini, M.; Cozzi, P. G.; Angelis, M. D.; Umani-Ronchi, A. *Tetrahedron Lett.* **2000**, *41*, 1601-1605.
- (10) Chong, C. C.; Kinjo, R. *ACS Catal.* **2015**, *5*, 3238-3259.

- (11) Gunanathan, C.; Hölscher, M.; Pan, F.; Leitner, W. *J. Am. Chem. Soc.* **2012**, *134*, 14349-14352.
- (12) Clark and co-workers reported the boron-substituted analogue of Shvo catalyst for the reductive borylation reactions that required elevated temperatures, 2 to 4 mol % catalyst and prolonged reaction time. See Koren-Selfridge, L.; Londino, H. N.; Vellucci, J. K.; Simmons, B. J.; Casey, C. P.; Clark, T. B. *Organometallics* **2009**, *28*, 2085-2090.
- (13) Chatterjee, B.; Gunanathan, C. *Chem. Commun.*, **2014**, *50*, 888-890.
- (14) Uncatalyzed hydroboration occurs at C=C multiple bonds in the presence of carbonyl functionalities. (a) Kabalka, G. W.; Yu, S.; Li, N. -S. *Tetrahedron Lett.* **1997**, *38*, 5455-5458. (b) Kaithal, A.; Chatterjee, B.; Gunanathan, C. *Org. Lett.* **2015**, *17*, 4790-4793. (c) Kaithal, A. *M.Sc Thesis*, NISER Bhubaneswar, **2016**.
- (15) CCDC 1418431.
- (16) Reaction of complex **1** with 0.5 equivalent of pinacolborane in C₆D₆ was carried out in NMR tube. Complete formation of complex **1b** and ClBpin (observed by ¹¹B NMR, $\delta = 27.9$ ppm) required 5 h at room temperature.
- (17) Attempts made to increase the amount of complex **1c** formations under different conditions failed. In the reaction mixtures ¹H NMR spectra, multiple signals appeared in the metal-hydride region designating the decomposition of intermediate complexes.
- (18) ¹¹B NMR spectrum of this reaction mixture displayed signals corresponds to HBpin ($\delta = 28.4$ ppm), ClBpin ($\delta = 27.9$ ppm) and a singlet at $\delta = 34.39$ ppm, which confirmed the presence of Ru-Bpin species. This boron chemical shift is comparable to that other Ru-Bpin complexes reported in the literature; see reference 5.
- (19) [Cp*Rh(H)₂(Bpin)₂] and [Cp*Ir(H)₂(Bpin)₂] are reported and the corresponding Rh^V-H and Ir^V-H signals appeared at $\delta -11.9$ ppm and $\delta -15.8$ ppm, respectively. (a)

For rhodium complex, see Hartwig, J. F.; Cook, K. S.; Hapke, M.; Incarvito, C. D.; Fan, Y.; Webster, C. E.; Hall, M. B. *J. Am. Chem. Soc.* **2005**, *127*, 2538-2552. (b) For iridium complex, see Kawamura, K.; Hartwig, J. F. *J. Am. Chem. Soc.* **2001**, *123*, 8422-8423.

(20) Ru(IV) dihydride complex $[(\eta^6\text{-}p\text{-cymene})\text{Ru}(\text{H})_2(\text{SiEt}_3)_2]$ catalyzed the hydrosilylation albeit in slower rate than complexes **1** and **1b**.

(21) Interestingly, with 1 and 2 mol % loads of **1**, hydroboration occurred rapidly to provide 80% and 89% conversion of benzaldehyde (^1H NMR), respectively, within 5 min. In both conditions, reaction completed within 30 min.

(22) However, ^1H NMR studies of the reaction mixture could not confirm the formation of these monomers. Only the presence of Ru–H corresponds to complex **1b** was observed during and upon completion of the catalytic reaction, indicating that it could also be a resting state for the catalytically active species.

(23) B–H activation by PNP ruthenium pincer complex was recently reported. See Anaby, A.; Butschke, B.; Ben-David, Y.; Shimon, L. J. W.; Leitun, G.; Feller, M.; Milstein, D. *Organometallics* **2014**, *33*, 3716-3726.

(24) Chandrasekhar, S.; Shrinidhi, A. *Synth. Commun.* **2014**, *44*, 2051-2056.

(25) Nishimura, R. H. V.; Murie, V. E.; Soldi, R. A.; Clososki, G. C. *Synthesis* **2015**, *47*, 1455-1460.

(26) Fotso, S.; Maskey, R. P.; Schroeder, D.; Ferrer, A. S.; Gruen-Wollny, I.; Laatsch, H. *J. Nat. Prod.*, **2008**, *71*, 1630-1633.

(27) Bruker AXS, SAINT+, Program for Reduction of Data collected on Bruker CCD Area Detector Diffractometer V. 6.02. Bruker AXS Inc., Madison, Wisconsin, USA, 1999.

- (28) Bruker AXS, SADABS, Program for Empirical Absorption Correction of Area Detector Data V 2004/1, Bruker AXS Inc., Madison, Wisconsin, USA, 2004.
- (29) Sheldrick, G. M. *Acta Crystallogr.* **2008**, *A64*, 112-122.
- (30) Dolomanov, O. V.; Bourhis, L. J.; Gildea, R. J.; Howard, J. A. K.; Puschmann, H. J. *Appl. Crystallogr.* **2009**, *42*, 339-341.

NMR Spectra of Alcohols:

Figure 7.3 ^1H NMR of 2-(hydroxymethyl)phenyl acetate:

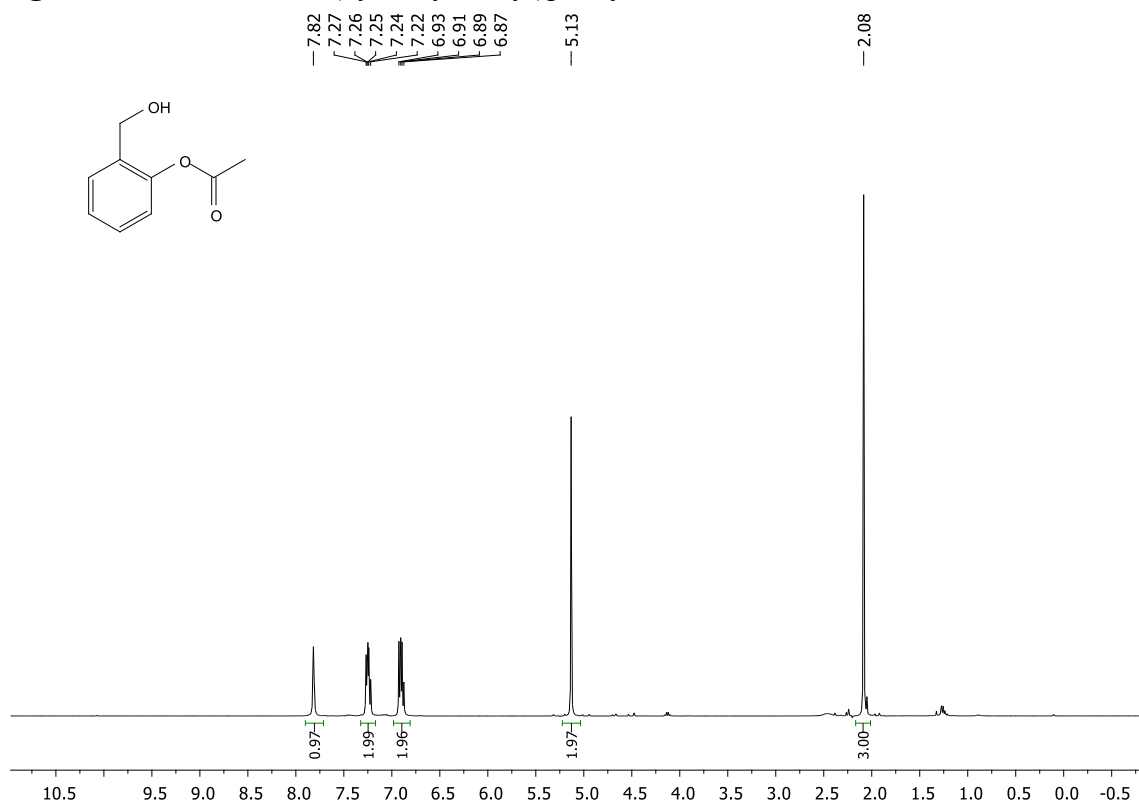


Figure 7.4 ^{13}C NMR of 2-(hydroxymethyl)phenyl acetate:

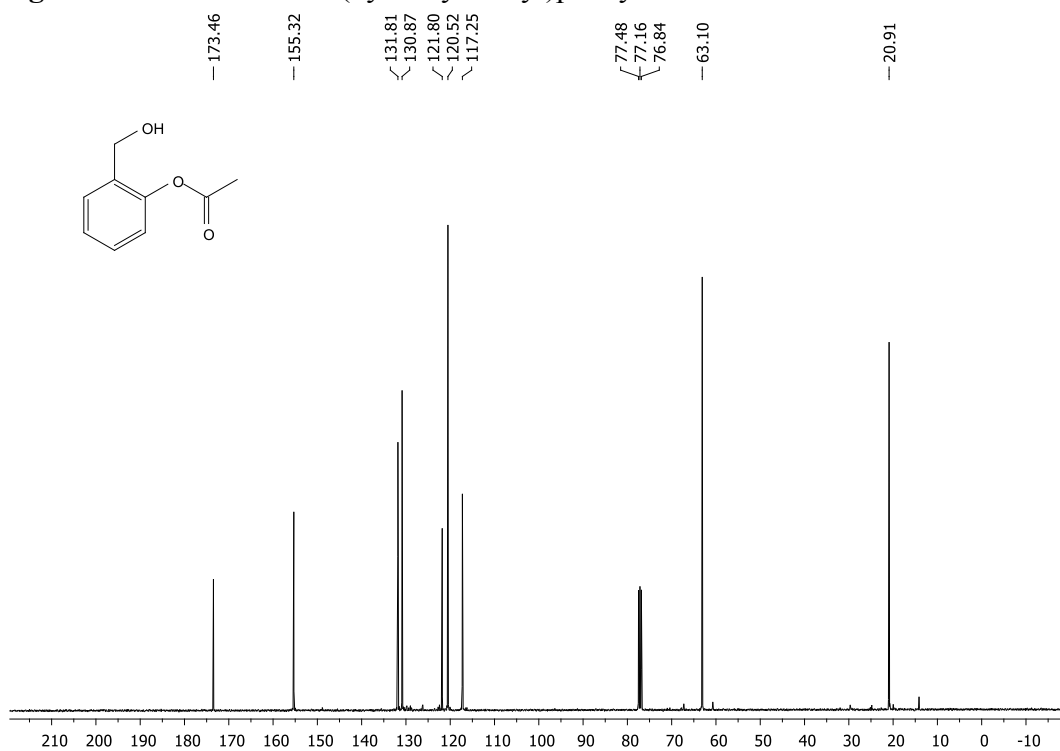


Figure 7.5 ^1H NMR of (5-(hydroxymethyl)furan-2-yl)methyl acetate:

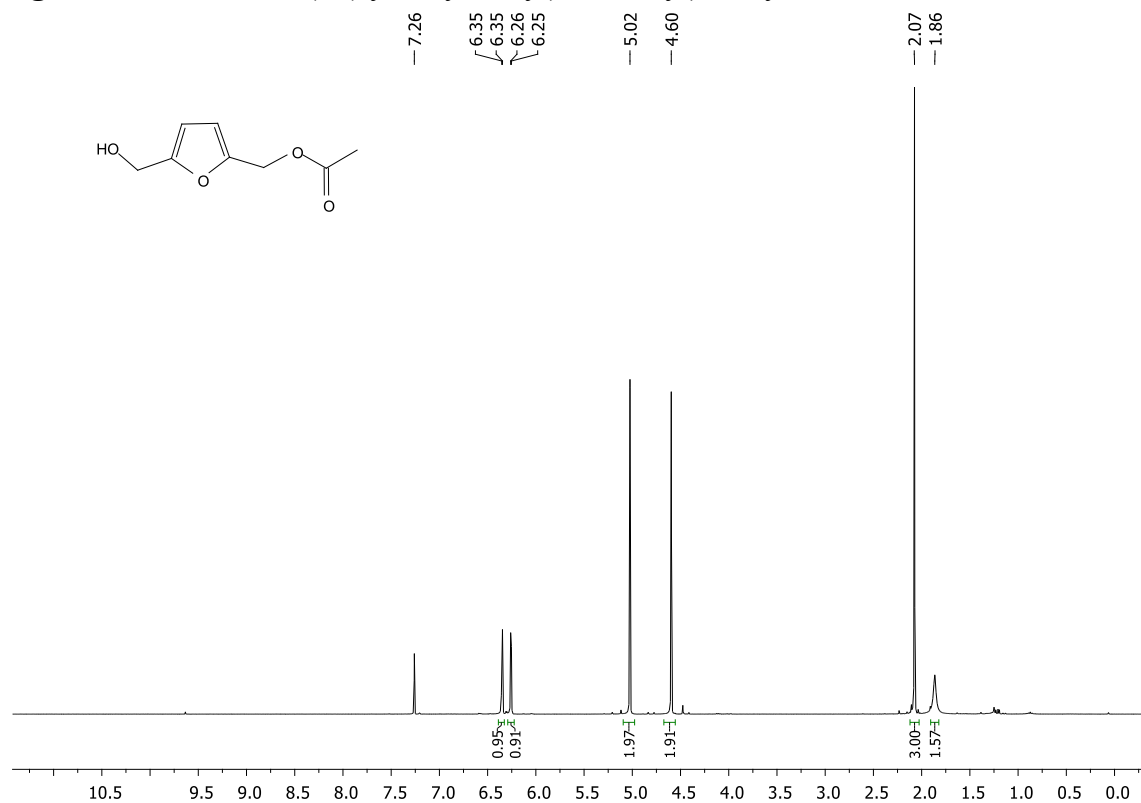


Figure 7.6 ^{13}C NMR of (5-(hydroxymethyl)furan-2-yl)methyl acetate:

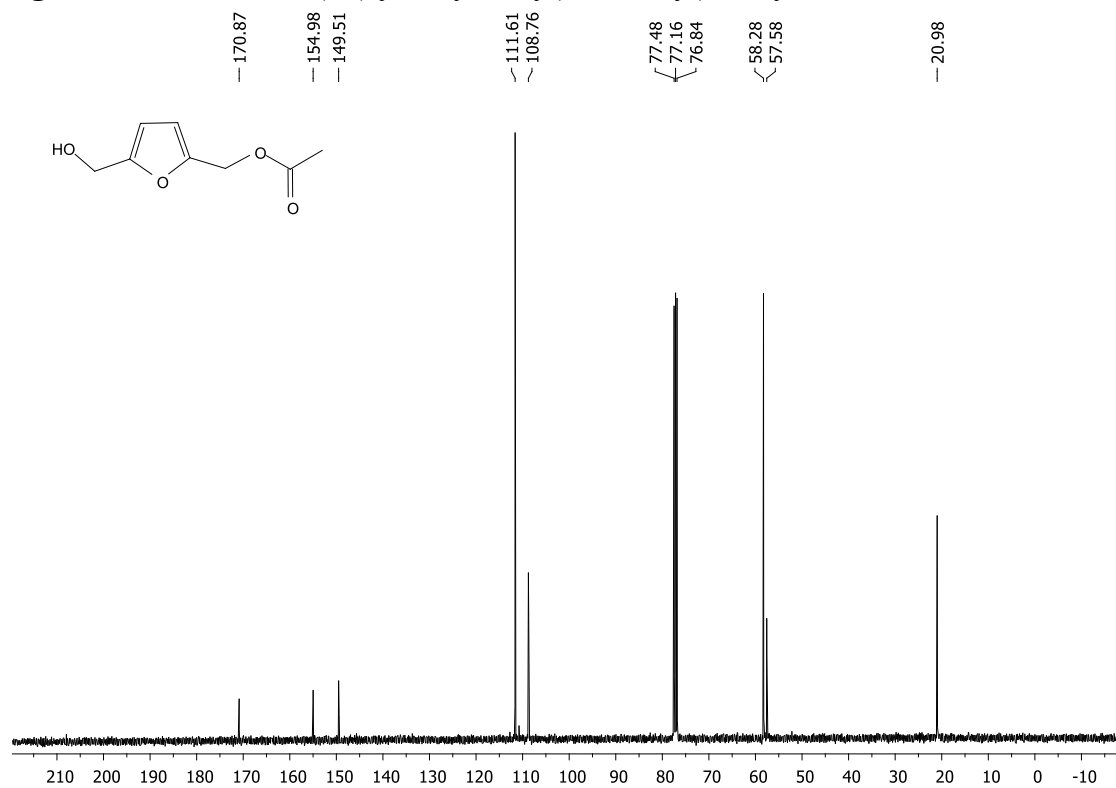


Figure 7.7 ^1H NMR of 2-(4-(hydroxymethyl)phenoxy)-1-phenylethanone:

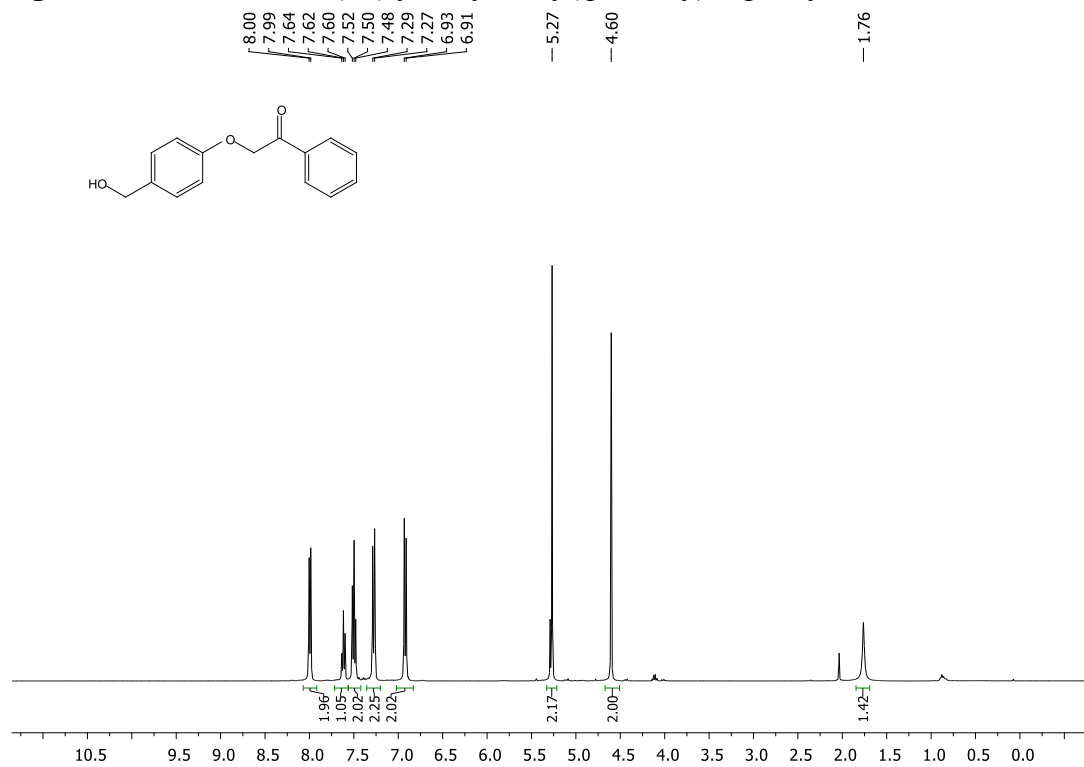


Figure 7.8 ^{13}C NMR of 2-(4-(hydroxymethyl)phenoxy)-1-phenylethanone:

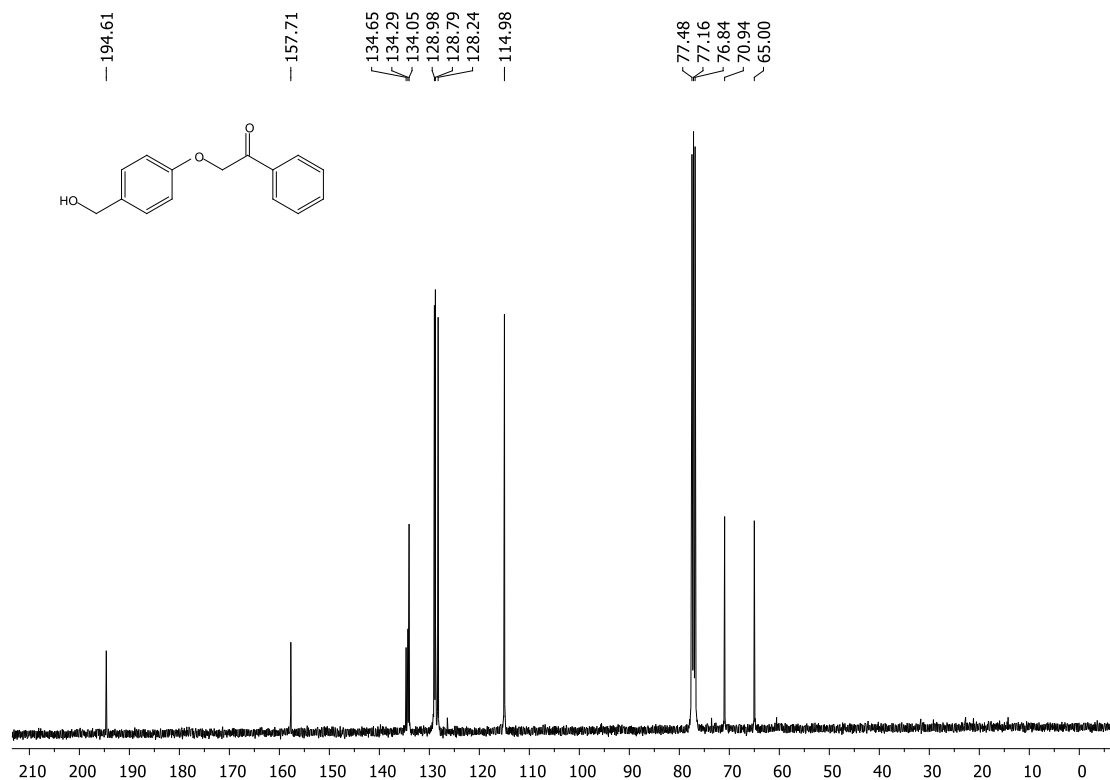
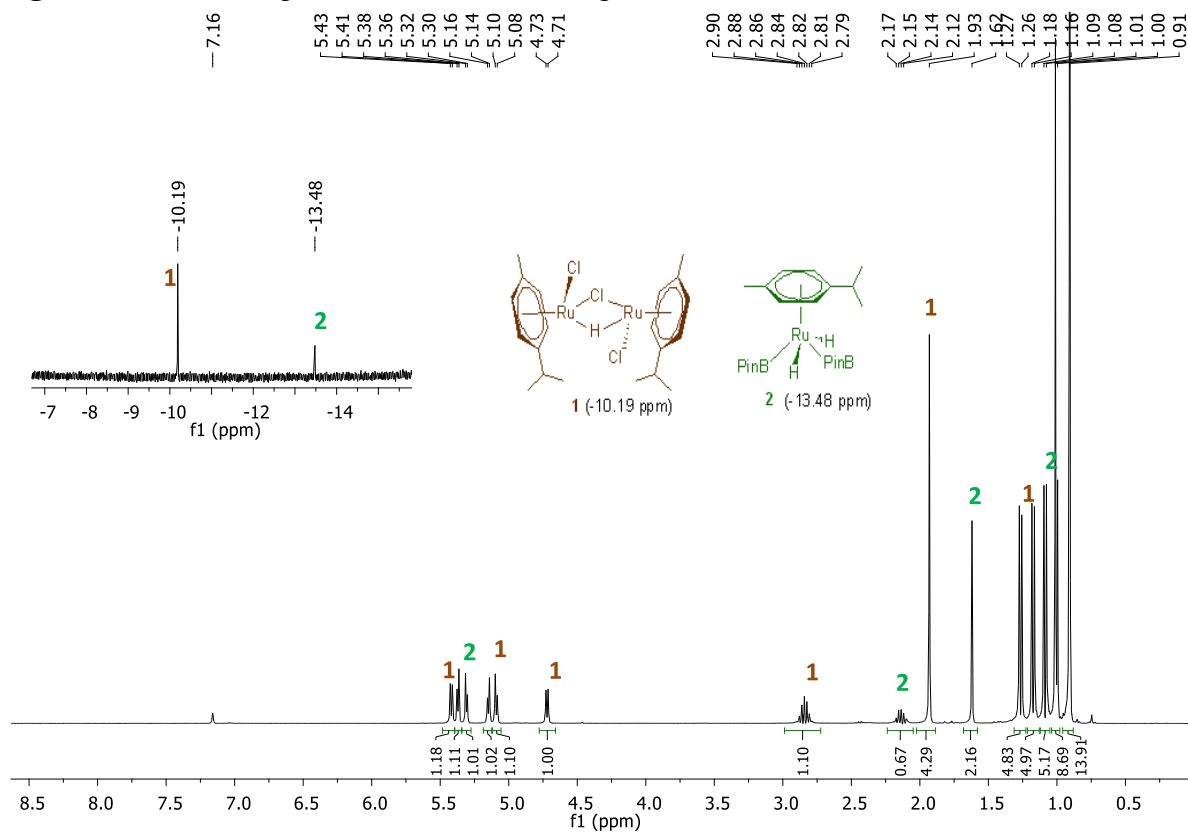


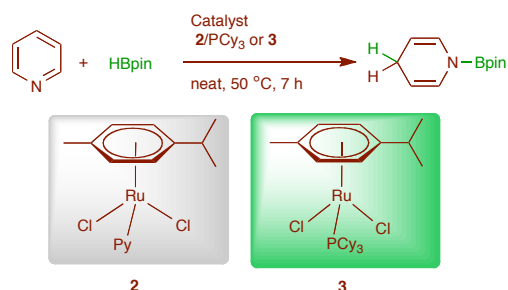
Figure 7.9 ^1H NMR spectrum: mixture of complexes **2** and **3**



CHAPTER 8

Ruthenium-Catalyzed Regioselective 1,4-Hydroboration of Pyridines

8.1 ABSTRACT



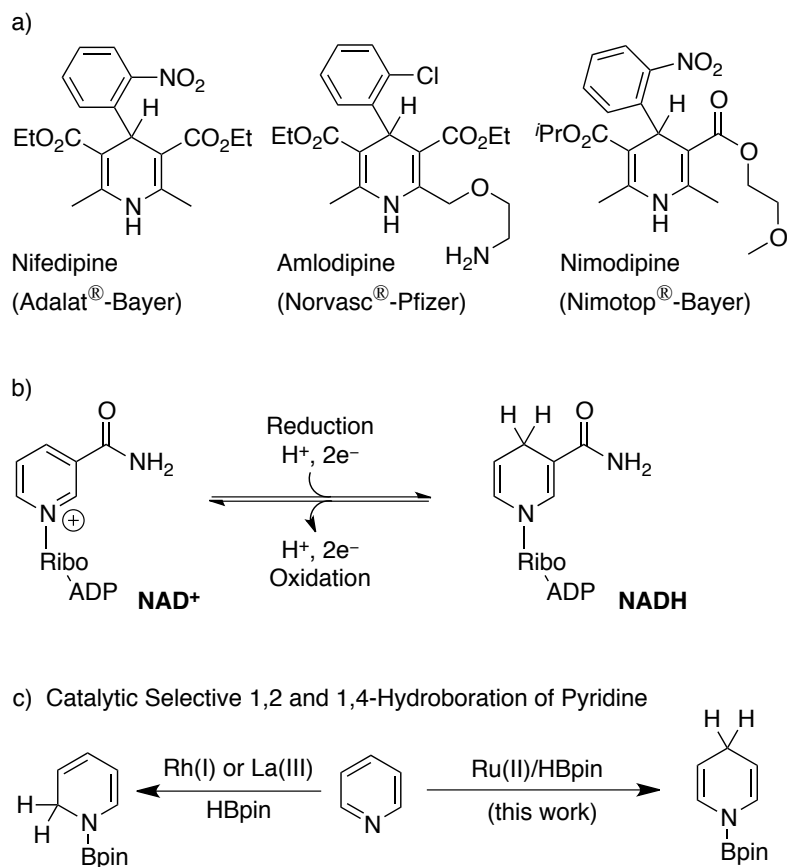
Simple ruthenium precursor $[\text{Ru}(\text{p-cymene})\text{Cl}_2]_2$ **1** catalyzed regioselective 1,4-dearomatization of pyridine derivatives using pinacolborane is reported. Two catalytic intermediates, $[\text{Ru}(\text{p-cymene})\text{Cl}_2\text{Py}]$ **2** and $[\text{Ru}(\text{p-cymene})\text{Cl}_2(\text{PCy}_3)]$ **3**, involved in this process are identified, independently synthesized, characterized, and further used directly as an effective catalysts; two more catalytic intermediates $[\text{Ru}(\text{p-cymene})\text{Cl}_2(\text{Py})(\text{PCy}_3)]$ **4** and $[\text{Ru}(\text{p-cymene})(\text{H})\text{Cl}(\text{Py})(\text{PCy}_3)]$ **5** are identified in solution. Complex **5** is the active catalytic intermediate. An intramolecular selective 1,5-hydride transfer in **5** leading to the regioselective 1,4-hydroboration of pyridine compounds is proposed.

8.2 INTRODUCTION

1,4-Dihydropyridines are prevalent in nature and are also commercially available, as they possess pharmacological applications such as Ca^{2+} channel blockers, and for cardiovascular diseases they are the most used drugs. For example, nifedipine, amlodipine, and nimodipine are essential medicines and used for the treatment of various ailments (Scheme 8.1a).¹ In general, around 92% of the drug candidates possesses nitrogen containing cycles. The NAD^+/NADH redox couple undergoes

dearomatization/aromatization of pyridine motifs and plays an important role in biological systems² (Scheme 8.1b), and 1,4-dihydropyridines are also widely used as reducing agents in organocatalysis.³ Selective synthesis of dihydropyridines from pyridine is a fundamental and challenging transformation,⁴ which is conventionally performed using an excessive amount of alkali metals or metal-hydrides leading to a mixture of 1,2- and 1,4-dihydropyridines.^{5,6} Strategies toward the selective synthesis of dihydropyridines from pyridines are more limited.⁷ While the direct catalytic hydrogenation resulted in over-reduction of pyridines to piperidines,⁸ hydrosilylation,⁹ silaboration,¹⁰ phosphinoboration,¹¹ and hydroboration allow their selective synthesis. Hill reported the pioneering catalytic hydroboration of pyridines using a Mg(II) complex, which led to the formation of both 1,2- and 1,4-hydroboration products.¹² Harder and co-workers found that dinuclear Mg(II) complexes provide selective 1,2-hydroboration of pyridine; however, catalytic hydroboration resulted in regioisomeric mixtures.¹³ The same group also demonstrated stoichiometric 1,2-reduction of pyridines using Ca(II) complexes.¹⁴ The groups of Suginome¹⁵ and Marks¹⁶ developed Rh(I) and La(III) catalyzed elegant hydroboration of pyridine in which insertion of the pyridine C–N bond into the M–H bond provided selective 1,2-hydroboration (Scheme 8.1c). Ru(II)-catalyzed selective 1,4-hydrosilylation of pyridine was reported by the groups of Nikonov^{9c} and Oestreich.^{9d} However, selective catalytic 1,4-hydroboration of pyridine remains a challenge and limited to a recent report in which a frustrated Lewis pair from bulky organoborane and pyridine resulted in 1,4-hydroboration of pyridines.¹⁷ The above-mentioned lead studies and our interest in developing efficient hydroboration reactions¹⁸ guided us to investigate transition metal catalyzed selective 1,4-hydroboration of pyridines.

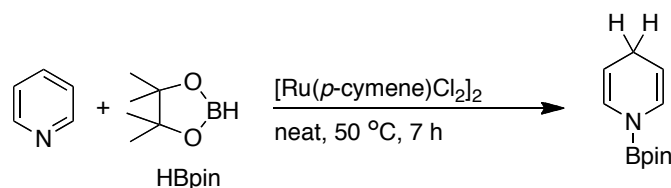
Scheme 8.1 1,4-Dihydropyridines: Applications, Role in Nature and Recent Advances in Synthesis of 1,2-Dihydropyridines



8.3 RESULTS AND DISCUSSIONS

The detailed optimization studies with several ruthenium complexes revealed $[Ru(p\text{-cymene})Cl_2]_2$ **1** as the optimum catalyst for regioselective 1,4-hydroboration of pyridine (Table 8.1).¹⁹

Table 8.1 Optimization of Reaction Condition Using $[\text{Ru}(p\text{-cymene})\text{Cl}]_2\text{Cl}_2$ as a Catalyst^a

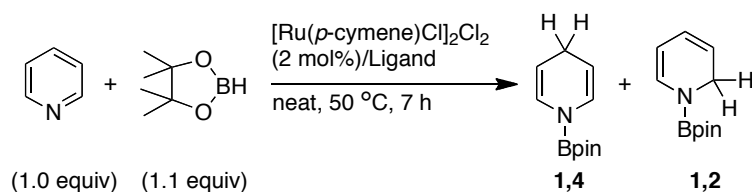


Entry	Cat. (mol%)	HBpin (mmol)	Time (h)	Temp. (°C)	Yield (%) ^b
1	1	1	20	50	55
2	1	1	20	100	50
3	1	1.2	20	r.t	36
4	1	1.2	7	75	30
5	1	1.1	7	50	55
6	2	1.02	7	50	71
7	3	1.1	7	50	81

^apyridine (1 mmol), pinacolborane, and catalyst are heated. ^bBased on ¹H NMR analysis.

Further improvement was made possible by the use of phosphine ligands. Tricyclohexyl phosphine (PCy_3) is found to be the most suitable ligand (Table 8.2). Upon using 2 equiv of ligand PCy_3 (4 mol %, 1 equiv. per Ru) with respect to **1** (2 mol %), an efficient 1,4-hydroboration was observed (97% yield) with complete regioselectivity (Table 8.2, entry 4).

Table 8.2 Optimization of Experimental Conditions for 1,4-Hydroboration of Pyridine



Entry	Cat. (mol %)	ligand (mol %)	Yield (%) ^a	1,4:1,2 ratio ^a
1	1	PPh_3 (2)	28	72:28

2	1	PCy ₃ (2)	74	100:0
3	1.5	PCy ₃ (3)	82	100:0
4	2	PCy ₃ (4)	97	100:0
5	2	(Ad) ₂ PBn (4)	62	100:0

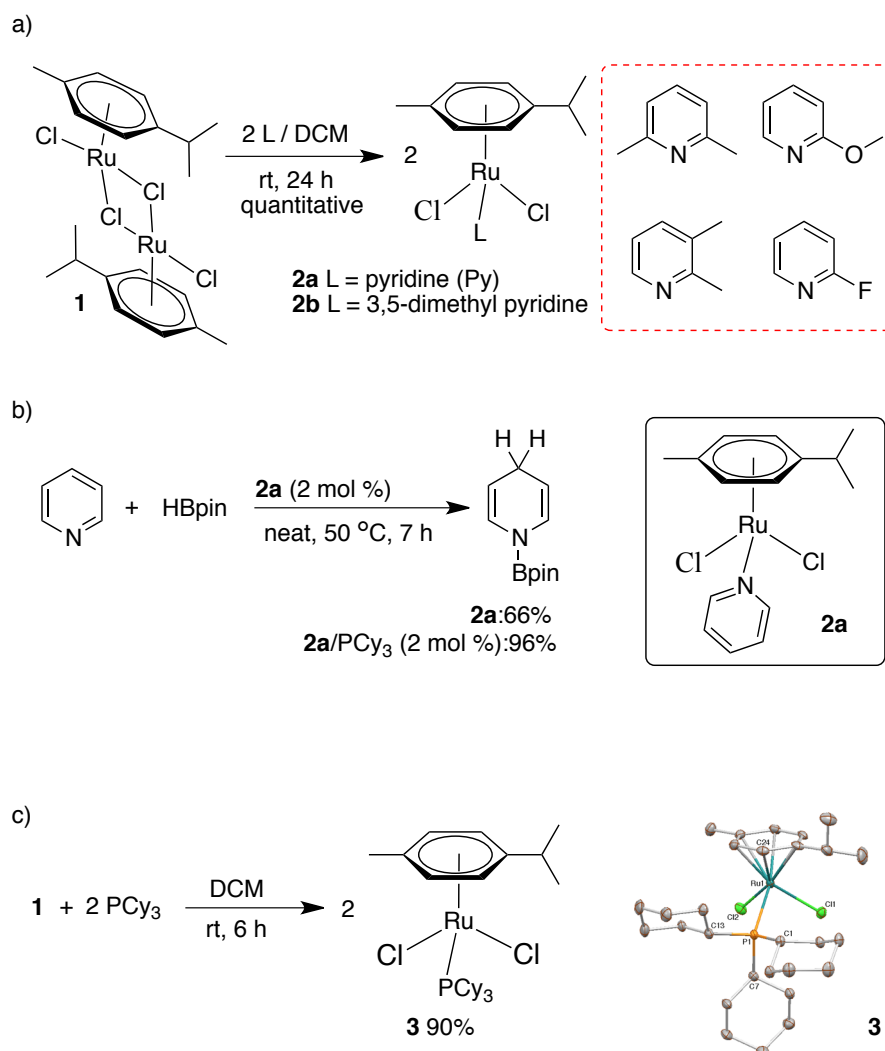
^aBased on ¹H NMR analysis of the reaction mixture.

In an attempt to identify the intermediates involved in the hydroboration of pyridines, complex **1** was reacted independently with pyridine and 3,5-dimethylpyridine, which resulted in quantitative formation of mononuclear complexes **2a** and **2b** (Scheme 8.2a). However, when complex **1** was reacted with 2-methoxypyridine, 2-fluoropyridine, 2,6-lutidine, and 2,3-dimethylpyridine, no such mononuclear complexes were formed. Interestingly, when isolated complex **2a** was used as a catalyst (2 mol %), hydroboration of pyridine was observed in 66% yield, indicating the possible involvement of complex **2a** in catalysis (Scheme 8.2b). Notably, 2, 2,3- and 2,6-substituted pyridines, which failed to provide coordination complexes (Scheme 8.2a) with **1** were subjected to catalytic hydroboration [**1** (2 mol %)/PCy₃ (4 mol %)] and no reaction was observed in all these substrates emphasizing that *prior pyridine coordination to ruthenium center is an essential requirement for the occurrence of catalysis*.

Upon the reaction of complex **2a** (2 mol %) together with PCy₃ (2 mol %) an efficient regioselective hydroboration was observed and *N*-boryl-1,4-dihydropyridine was obtained in 96% yield, further eliciting the interest in the phosphine coordinated intermediate complex. When Ru dimer complex **1** was reacted with PCy₃ (2 equiv; 1 equiv per Ru), phosphine-ligated mononuclear ruthenium complex **3** formed (90% yield).²⁰ Complex **3** exhibited a ³¹P NMR singlet signal at δ 25.92 ppm, and its structure is unequivocally corroborated by single-crystal X-ray analysis, which displayed pseudo-octahedral geometry around the metal center (Scheme 8.2c).

Complex **3** is a suitable catalyst for the regioselective 1,4-hydroboration of pyridines.

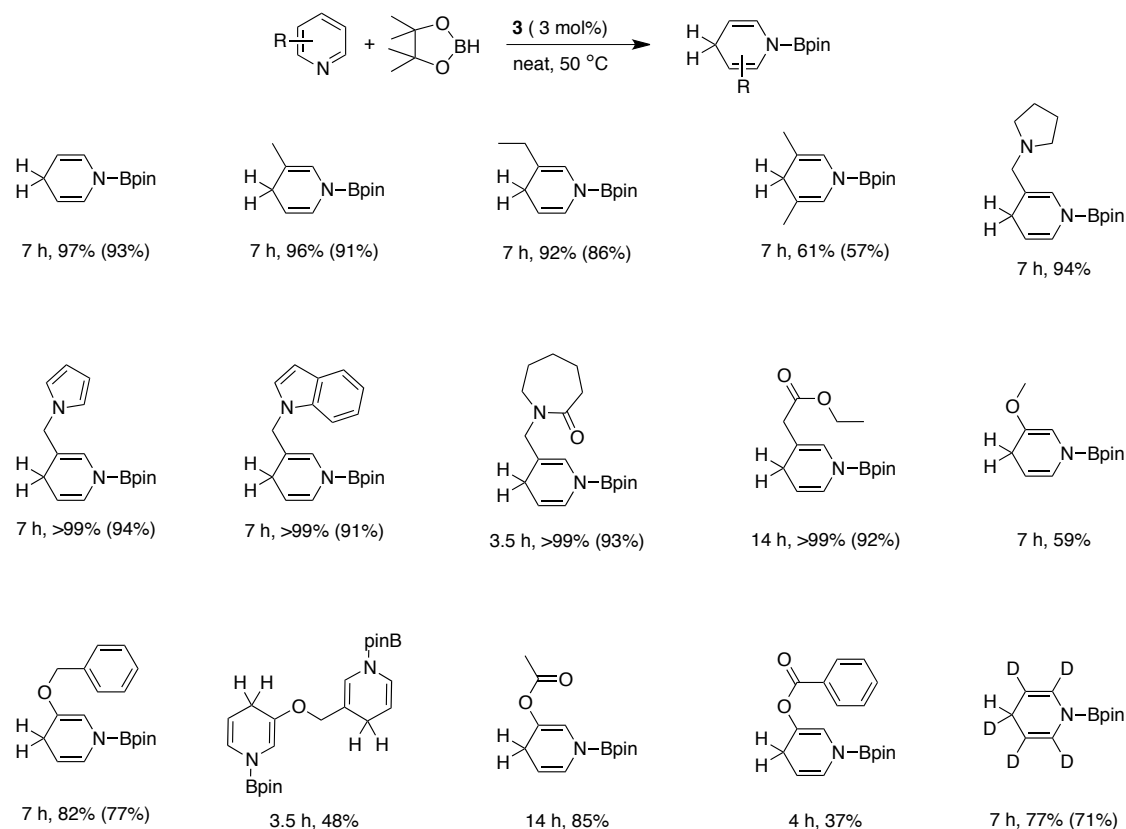
Scheme 8.2 Preparation of Intermediates **2** and **3** Involved in the 1,4-Hydroboration of Pyridines



Upon using **3** (3 mol %) as a catalyst, regioselectively *N*-boryl-1,4-dihydropyridine was obtained in 97% yield, confirming the potential involvement of complex **3** in catalysis (Scheme 8.3). Notably, use of added ligand is no longer required. Using complex **3** as a catalyst, regioselective 1,4-hydroboration was explored for the different pyridines, which indicated that a wide range of 3-substitution on pyridine is tolerated (Scheme 8.3). An assortment of 3-substituted pyridines undergoes regioselective 1,4-hydroboration with good to excellent yields. Alkyl, aryl, heteroaryl,

ester, amine, amide, alkoxy, and acyloxy functional groups are well tolerated in this ruthenium catalyzed reaction. Remarkably, 3,5-dimethylpyridine and 3-methoxypyridine, which were not compatible with an organoborane catalyzed reaction,¹⁷ undergoes ruthenium catalyzed 1,4-hydroboration to provide the corresponding products in moderate yields (Scheme 8.3), highlighting the potential of this transformation. Moreover, quantitative product formation was observed for several 3-substituted pyridine compounds. Interestingly, with 3-(pyridin-3-ylmethoxy)pyridine successful bis-1,4-hydroboration occurred. As observed in mechanistic studies various 2-substituted pyridines (*vide infra*) do not undergo a hydroboration reaction attributable to steric hindrance and is in agreement with the reactivity of organolanthanides in the catalytic 1,2-hydroboration of pyridines.¹⁶ 4-Methylpyridine also failed to undergo ruthenium catalyzed 1,4-hydroboration.

Scheme 8.3 Ruthenium Catalyzed Regioselective 1,4-Hydroboration of Pyridines^a

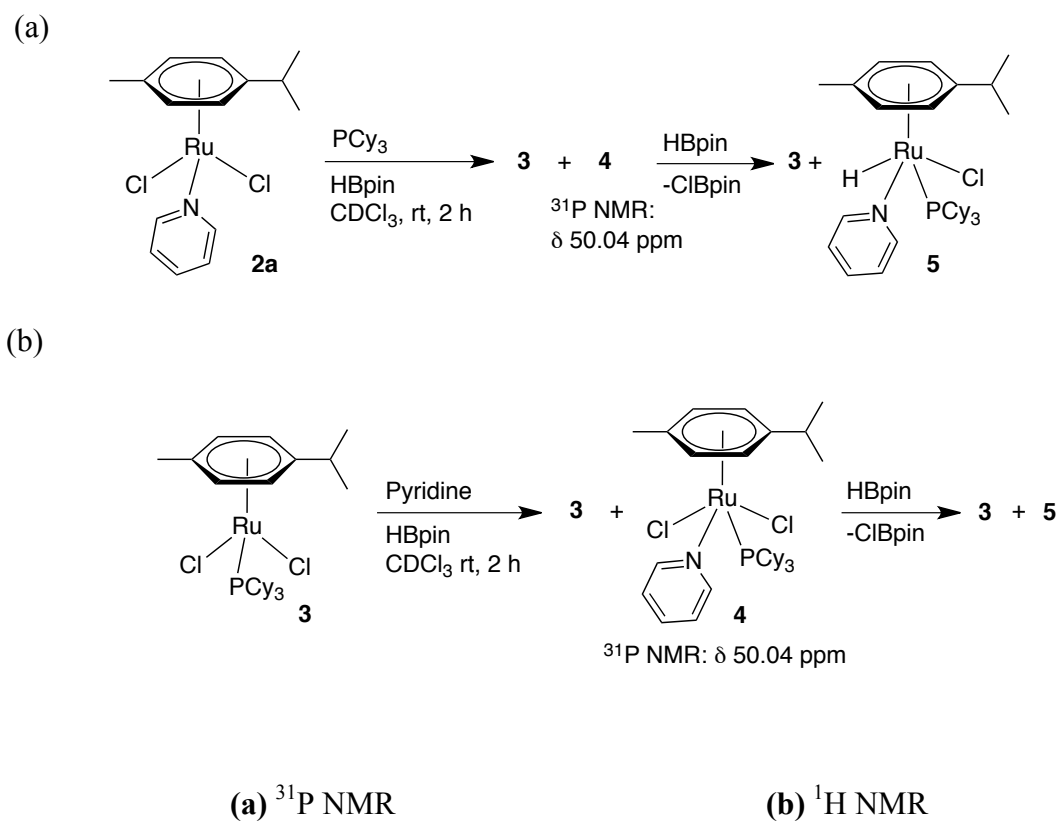


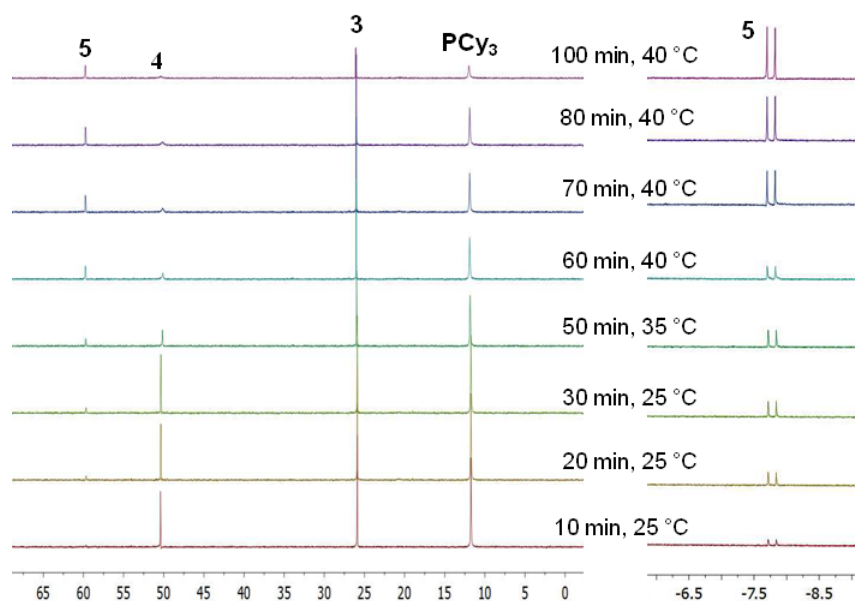
^asubstrate (1 mmol), pinacolborane (1.1 mmol), catalyst **3** (3 mol %) are heated at 50 °C under neat conditions. Yields are based on ¹H NMR analysis of the reaction mixture. ^bIsolated yields. ^cDCM (0.5 mL) is added as either substrate or reaction mixture is not homogeneous. ^d2.1 equiv. of pinacolborane is used. ^eAnisole is used as internal standard.

Mechanistic insights were deciphered by performing a series of elementary reactions and in situ monitoring of both stoichiometric and catalytic reactions (Figure 8.1). Reaction of **2a** with PCy₃ and HBpin and reaction of **3** with pyridine and HBpin resulted in formation of the same intermediates **4** and **5** in solution, which displayed characteristic singlet signals at δ 50.04 ppm and δ 59.66 ppm in ³¹P NMR, respectively (Scheme 8.4a, b). As both reactions progressed, the intensity of complex **4** decreased upon the rise of a singlet signal at δ 59.66 ppm in ³¹P NMR together with

increasing intensity of a doublet at $\delta -7.88$ ppm ($J_{\text{PH}} = 48.0$ Hz) in ^1H NMR confirming the complex **5** is a monohydride ruthenium complex.²¹ ^{11}B NMR of both reaction mixtures confirmed the formation of ClBpin ($\delta 27.09$ ppm). Further, the equimolar reaction of complex **2a** and HBpin was incomplete after 1 h. Upon use of 5 equiv. of HBpin, complete conversion of ligated pyridine on **2a** occurred and resulted in quantitative formations of N-boryl-1,4 dihydropyridine and monohydride bridged dinuclear complex $[\{(\eta^6\text{-}p\text{-cymene})\text{-RuCl}\}_2(\mu\text{-H-}\mu\text{-Cl})]$ **6** (Scheme 8.4c).^{18,22} To ascertain any role of complex **6** in catalysis, the regioselective 1,4-hydroborations of pyridine catalyzed by complexes **2** and **3** (3 mol %)²³ were monitored using ^1H NMR, which confirmed the formation and presence of only monohydride complex **5** throughout the catalysis in both experiments.²⁴

Scheme 8.4 Stoichiometric Experiments, *in situ* Observation of Intermediates and Reaction Progress





(c)

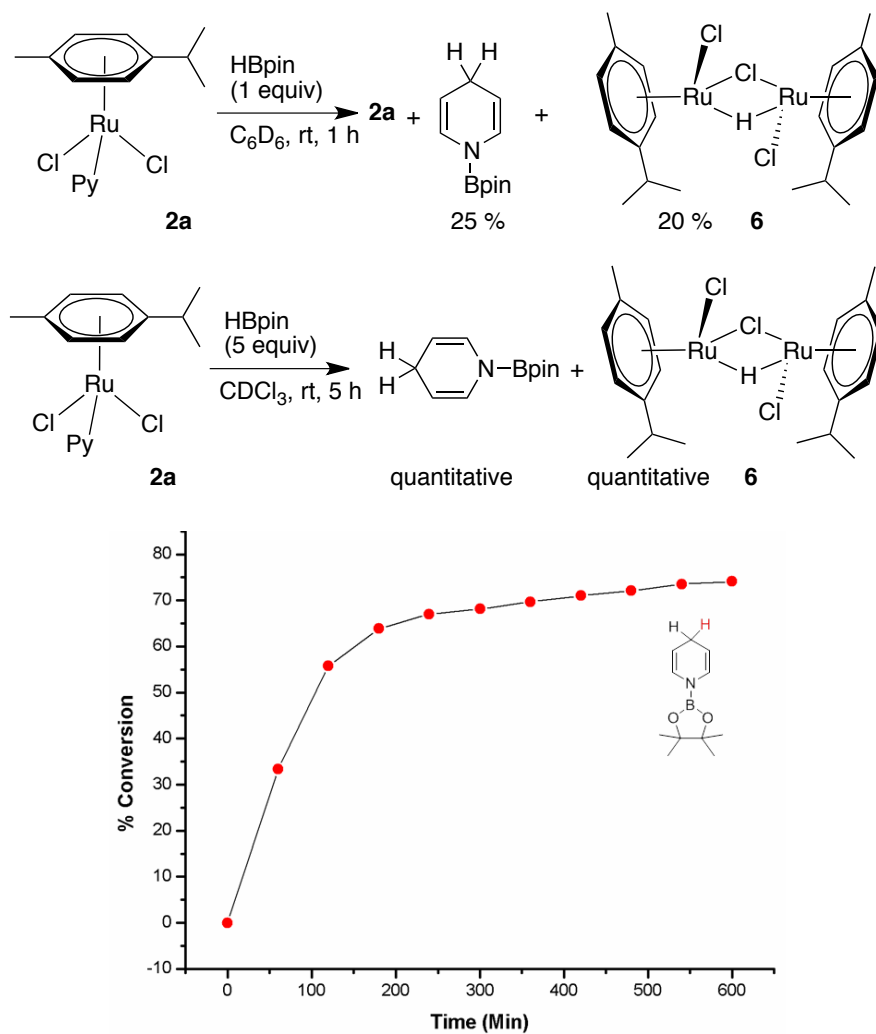
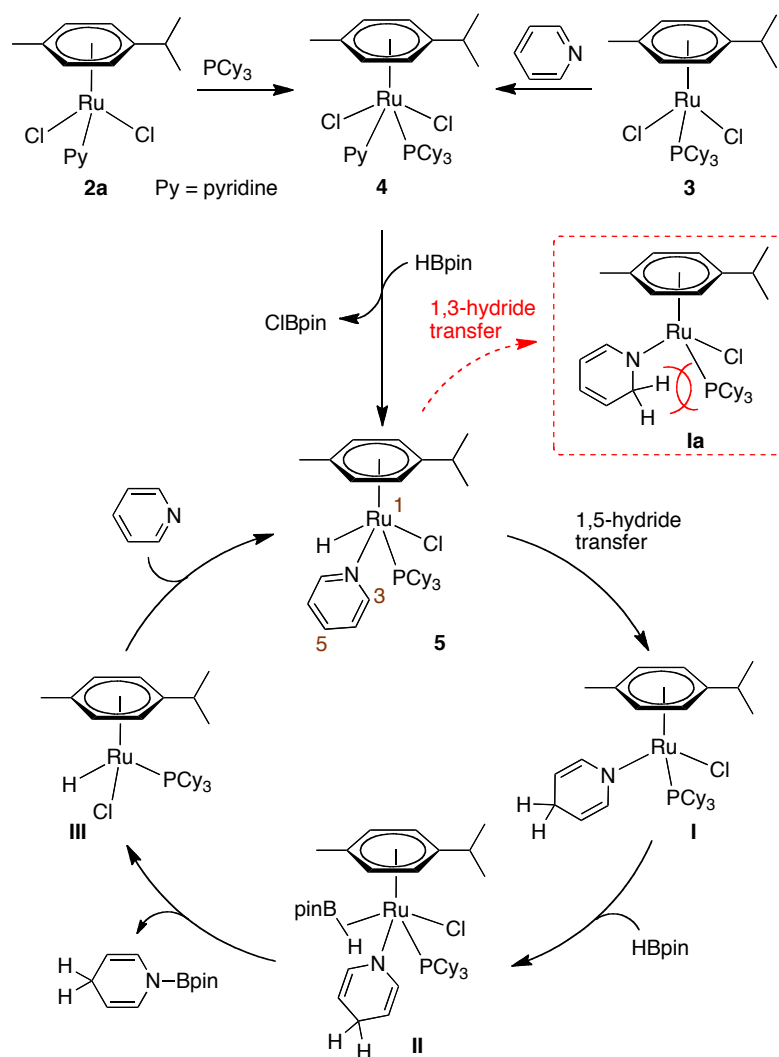


Figure 8.1 NMR monitoring of the reaction progress. Pyridine (0.25 mmol), pinacolborane (0.275 mmol), catalyst **3** (0.0075 mmol) and CD_2Cl_2 were charged in a

screw cap NMR tube and monitored by ^1H NMR spectroscopy at regular interval. % Conversion is determined from integration of ^1H NMR.

On the basis of the above-mentioned experimental observations, a catalytic cycle is proposed as depicted in Scheme 8.5. Reaction of **2a** with PCy_3 or reaction of **3** with pyridine leads to the common intermediate **4**, which upon reaction with HBpin generates Ru–H complex **5** (as observed in Scheme 8.4a, b). Remarkably, in complex **5**, 1,5-hydride transfer prevails over the 1,3-hydride transfer. Perhaps, the steric hindrance between the “ $\text{sp}^3\text{-CH}_2$ ” of the amide ligand at the ortho-position in **1a** that will arise upon 1,2-addition on the pyridine motif and other ligands on the metal center and the electronic factors might be preventing the commonly observed 1,3-hydride transfer.^{18,21,25} Notably, no hydroboration reaction was observed with 2-substituted pyridines under these conditions. Thus, intramolecular “1,5-hydride transfer” to the pyridine ligand coordinated at the metal center in **5** leads to the regioselective 1,4-hydroboration of pyridine and amide ligated Ru(II) intermediate **I**. Reaction of HBpin with **I** results in coordination complex **II**, and the subsequent transmetalation of amide ligand provides regioselective pyridine 1,4-hydroboration product and unobserved intermediate **III**. Coordination of pyridine to **III** regenerates the intermediate complex **5** to close the catalytic cycle. Catalytically active intermediate **5** persisted in the reaction mixture throughout the catalysis as observed by ^1H and ^{31}P NMR analyses.

Scheme 8.5 Proposed Reaction Mechanism for the Regioselective 1,4-Hydroboration of Pyridines



8.4 CONCLUSIONS

In summary, an efficient regioselective 1,4-hydroboration of pyridine compounds were demonstrated using well-defined transition metal catalysts. Stoichiometric experiments and in situ spectral studies allowed identification of the reaction intermediates 2-5. Intermediates **2** and **3** are independently synthesized, characterized, and further used in catalysis. Phosphine ligated complex **3** turned out to be the optimal catalyst for the regioselective 1,4-hydroboration of pyridines. Solvent is required only when the substrate is solid or the reaction mixture turns inhomogeneous; otherwise catalysis proceeded very well under solventless conditions. Supported by the experimental observations, a mechanism is postulated

involving in situ generation of mononuclear Ru–H complex **5**, which undergoes an intramolecular 1,5-hydride transfer leading to the regioselective 1,4-hydroboration of pyridines.

8.5 EXPERIMENTAL SECTION

General Experimental: All catalytic reactions were performed under nitrogen atmosphere. All stoichiometric reactions were performed in nitrogen atmosphere MBraun glove box. Pinacolborane, tricyclohexylphosphine, and $[\text{RuCl}_2(p\text{-cymene})]_2$ were bought from Sigma-Aldrich. All chemicals were purchased from Acros, Sigma-Aldrich, Alfa-aesar, Himedia Chemicals and used without further purification. Dry solvents were prepared according to standard procedures. ^1H , ^{13}C spectra were recorded at Bruker AV-400 (^1H : 400 MHz, ^{13}C : 100.6 MHz, ^{31}P : 162 MHz, ^{11}B : 96.3 MHz). ^1H and $^{13}\text{C}\{^1\text{H}\}$ NMR chemical shifts were reported in ppm downfield from tetramethyl silane. Multiplicity is abbreviated as: s, Singlet; d, doublet; dd, doublet of doublet; t, triplet; q, quartet; dq, doublet of quartet; m, multiplate; br, broad. Assignment of spectra was done based on one-dimensional (dept-135) NMR techniques. Mass spectra were recorded on Bruker micrOTOF-Q II Spectrometer.

Synthesis of Pyridine Derivatives:

1-(Pyridin-3-ylmethyl)-1*H*-indole²⁶: In an oven dried 25 mL RB flask indole (3 mmol, 351.45 mg) was dissolved in 5 mL of DMF under nitrogen atmosphere. This solution was transferred via cannula to another flask containing DMF (2 mL) solution of sodium hydride (55% in mineral oil, pre-washed with dry hexane) (9 mmol, 393 mg) under ice-cold condition and the solution was stirred for 30 minutes. To this solution, 3-(chloromethyl)pyridine hydrochloride (3 mmol, 492.09 mg) dissolved in 8 mL of DMF was slowly added under ice-cold condition and then the reaction mixture was allowed to warm to room temperature and stirred for 12 h. Upon completion, the

reaction mixture was poured into ice-cold water and extracted with dichloromethane. The combined organic layers were dried over anhydrous sodium sulphate and evaporated under reduced pressure. The crude reaction mixture was purified by column chromatography. ^1H NMR (CDCl_3): δ 8.52 (s, 2H, ArCH), 7.76 (d, 1H, $J = 8$ Hz, ArCH), 7.25-7.27 (m, 2H, ArCH), 7.20-7.24 (m, 2H, ArCH), 7.04-7.08 (m, 2H, ArCH), 6.65 (d, 1H, $J = 4$ Hz, ArCH), 5.13 (s, 2H, CH_2). $^{13}\text{C}\{^1\text{H}\}$ NMR (CDCl_3): δ 148.59 (ArCH), 147.88 (ArCH), 135.69 (quat-C), 134.03 (ArCH), 132.79 (quat-C), 128.49 (quat-C), 127.68 (ArCH), 123.26 (ArCH), 121.62 (ArCH), 120.81 (ArCH), 119.49 (ArCH), 109.19 (ArCH), 101.87 (ArCH), 46.95 (CH_2).

3-(Pyrrolidin-1-ylmethyl)pyridine²⁷: In an oven dried 25 mL RB flask pyrrolidine (3 mmol, 250.42 μl) was dissolved in 5 mL of DMF under nitrogen atmosphere. This solution was transferred via cannula to another flask containing DMF (2 mL) solution of sodium hydride (55% in mineral oil, pre-washed with dry hexane) (9 mmol, 393 mg) and stirred under ice-cold condition for 30 minutes. To this solution, 3-(chloromethyl)pyridine hydrochloride (3 mmol, 492.09 mg) dissolved in 8 mL of DMF was slowly added under ice-cold condition and then the reaction mixture was allowed to warm to room temperature and stirred for 12 h. Upon completion, the reaction mixture was poured into ice-cold water and extracted with dichloromethane. The combined organic layers were dried over sodium sulphate and evaporated under reduced pressure. The crude reaction mixture was purified by column chromatography. ^1H NMR (CDCl_3): δ 8.54 (d, 1H, $J = 1.6$ Hz, ArCH), 8.48-8.49 (m, 1H, ArCH), 7.68 (d, 1H, $J = 8$ Hz, ArCH), 7.22-7.26 (m, 1H, ArCH), 3.62 (s, 2H, CH_2), 2.50-2.53 (m, 4H, CH_2), 1.77-1.80 (m, 4H, CH_2). $^{13}\text{C}\{^1\text{H}\}$ NMR (CDCl_3): δ 150.08 (ArCH), 148.35 (ArCH), 136.39 (ArCH), 134.59 (quat-C), 123.20 (ArCH), 57.69 (CH_2), 54.00 (CH_2), 23.38 (CH_2).

1-(Pyridin-3-ylmethyl)azepan-2-one: In an oven dried 25 mL RB flask caprolactam (3 mmol, 339 mg) was dissolved in 5 mL of DMF under nitrogen atmosphere and added via syringe to another flask containing sodium hydride (55% in mineral oil) (9 mmol, 393 mg) and stirred under ice-cold condition for 30 minutes. This solution was transferred via cannula to another flask containing DMF (2 mL) solution of sodium hydride (55% in mineral oil, pre-washed with dry hexane) (9 mmol, 393 mg) under ice-cold condition and the solution was stirred for 30 minutes. To this solution, 3-(chloromethyl)pyridine hydrochloride (3 mmol, 492.09 mg) dissolved in 8 mL of DMF was slowly added under ice-cold condition and then the reaction mixture was allowed to warm to room temperature and stirred for 12 h. Upon completion, the reaction mixture was poured into ice-cold water and extracted with dichloromethane. The combined organic layers were dried over sodium sulphate and evaporated under reduced pressure. The crude reaction mixture was purified by column chromatography. ^1H NMR (CDCl_3): δ 8.48-8.50 (m, 2H, ArCH), 7.60-7.62 (m, 1H, ArCH), 7.21-7.24 (m, 1H, ArCH), 4.56 (s, 2H, CH_2), 3.27-3.29 (m, 2H, CH_2), 2.56-2.57 (br m, 2H, CH_2), 1.67-1.68 (br m, 4H, CH_2), 1.47 (br s, 2H, CH_2). $^{13}\text{C}\{^1\text{H}\}$ NMR (CDCl_3): δ 175.73 (CO), 149.03 (ArCH), 148.48 (ArCH), 135.61 (ArCH), 133.31 (quat-C), 123.27 (ArCH), 48.87 (CH_2), 48.51 (CH_2), 36.69 (CH_2), 29.49 (CH_2), 27.89 (CH_2), 23.00 (CH_2).

3-(Benzyloxy)pyridine²⁸: In an oven dried 25 mL RB flask 3-hydroxypyridine (5 mmol, 475 mg) was dissolved in 5 mL of DMF under nitrogen atmosphere. This solution was transferred via cannula to another flask containing DMF (2 mL) solution of sodium hydride (55% in mineral oil, pre-washed with dry hexane) (10 mmol, 436 mg) and stirred under ice-cold condition for 30 minutes. To this solution, benzyl bromide (5 mmol, 593.7 μl) was dissolved in 8 mL of DMF was slowly added under

ice-cold condition and then the reaction mixture was allowed to warm to room temperature and stirred for 12 h. Upon completion, the reaction mixture was poured into ice-cold water and extracted with dichloromethane. The combined organic layers were dried over sodium sulphate and evaporated under reduced pressure. The crude reaction mixture was purified by column chromatography. ^1H NMR (CDCl_3): δ 8.42 (d, 1H, $J = 4$ Hz, ArCH), 8.25 (d, 1H, $J = 4$ Hz, ArCH), 7.33-7.44 (m, 5H, ArCH), 7.18-7.26 (m, 2H, ArCH), 5.09 (s, 2H, CH_2). $^{13}\text{C}\{^1\text{H}\}$ NMR (CDCl_3): δ 154.83 (quat-C), 142.22 (ArCH), 138.25 (ArCH), 136.09 (quat-C), 128.62 (ArCH), 128.19 (ArCH), 127.43 (ArCH), 123.78 (ArCH), 121.42 (ArCH), 70.17 (CH_2).

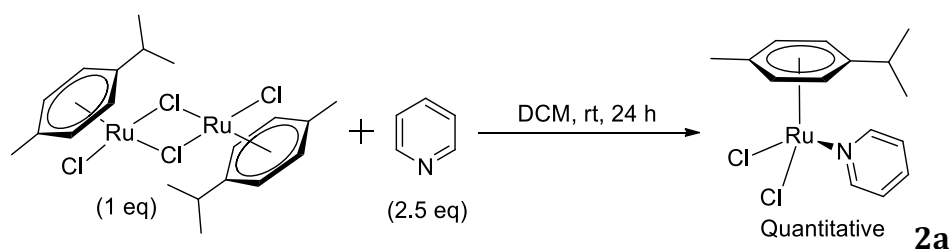
3-(Pyridin-3-ylmethoxy)pyridine²⁹: In an oven dried 25 mL RB flask 3-hydroxypyridine (3 mmol, 285 mg) was dissolved in 5 mL of DMF under nitrogen atmosphere. This solution was transferred via cannula to another flask containing DMF (2 mL) solution of sodium hydride (55% in mineral oil, pre-washed with dry hexane) (10 mmol, 436 mg) and stirred under ice-cold condition for 30 minutes. To this solution, 3-(chloromethyl)pyridine hydrochloride (3 mmol, 492.09 mg) was dissolved in 8 mL of DMF was slowly added under ice-cold condition and then the reaction mixture was allowed to warm to room temperature and stirred for 12 h. Upon completion, the reaction mixture was poured into ice-cold water and extracted with dichloromethane. The combined organic layers were dried over sodium sulphate and evaporated under reduced pressure. The crude reaction mixture was purified by column chromatography. ^1H NMR (CDCl_3): δ 8.65 (br s, 1H, ArCH), 8.56- 8.57 (m, 1H, ArCH), 8.36 (m, 1H, ArCH), 8.21-8.23 (m, 1H, ArCH), 7.73-7.75 (m, 1H, ArCH), 7.27-7.32 (m, 1H, ArCH), 7.18-7.24 (m, 2H, ArCH), 5.09 (s, 2H, CH_2). $^{13}\text{C}\{^1\text{H}\}$ NMR (CDCl_3): δ 154.22 (quat-C), 149.31 (ArCH), 148.61 (ArCH), 142.33

(ArCH), 137.83 (ArCH), 135.05 (ArCH), 131.48 (quat-C), 123.67 (ArCH), 123.29 (ArCH), 121.18 (ArCH), 67.45 (CH₂).

Pyridin-3-yl benzoate³⁰: In an oven dried 25 mL RB flask 3-hydroxypyridine (5.26 mmol, 500 mg) and sodium hydroxide (5.77 mmol, 231 mg) was dissolved in 8 mL of THF under nitrogen atmosphere and stirred at room temperature for 1 h. To this solution, benzoyl chloride (5.26 mmol, 608 μ l) dissolved in 8 mL of THF and added drop wise and the reaction mixture was allowed to stir at room temperature for 10 h. After completion of the reaction the solvent was evaporated and the resulted residue was dissolved in water and extracted using dichloromethane. The combined organic layers were dried over sodium sulphate and evaporated under reduced pressure. The resulting crude reaction mixture was purified by column chromatography. ¹H NMR (CDCl₃): δ 8.57 (br s, 1H, ArCH), 8.48-8.49 (m, 1H, ArCH), 8.14 (d, 2H, $J = 4$ Hz, ArCH), 7.57-7.59 (m, 2H, ArCH), 7.42-7.45 (m, 2H, ArCH), 7.29-7.32 (m, 1H, ArCH). ¹³C{¹H} NMR (CDCl₃): δ 164.34 (CO), 147.54 (quat-C), 146.39 (ArCH), 143.04 (ArCH), 133.82 (ArCH), 130.02 (ArCH), 129.63 (quat-C), 129.53 (ArCH), 128.49 (ArCH), 123.89 (ArCH).

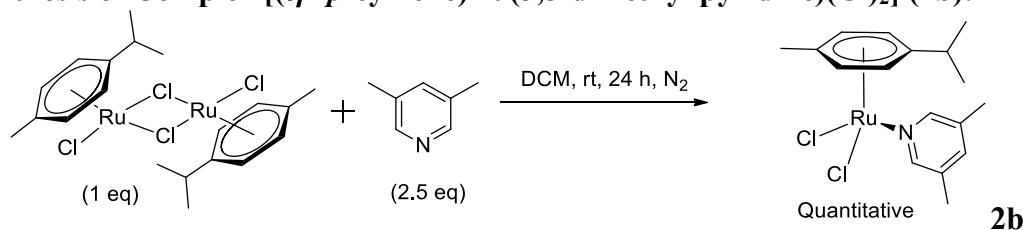
General Procedure for Screening of Ru-Catalysts: To a PTFE screw capped reaction vial with a magnetic bead pyridine (1 mmol, 80 μ l), pinacolborane (1.02 mmol, 146 μ l) and ruthenium catalyst (1 mol%) were added under nitrogen atmosphere. The reaction mixture was stirred for 7 h in a pre-heated oil bath of 50 °C and further analyzed by ¹H NMR spectroscopy.

Synthesis of Complex $[(\eta^6\text{-}p\text{-cymene})\text{Ru}(\text{Cl})_2(\text{pyridine})](\mathbf{2a})$:



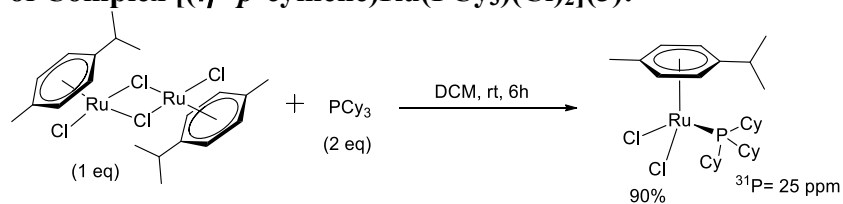
In a screw cap scintillation vial $[\text{Ru}(p\text{-cymene})\text{Cl}_2]_2$ (0.08 mmol, 50 mg) was dissolved in dichloromethane (2 mL). To this solution pyridine (0.2 mmol, 16 μL) dissolved in dichloromethane (0.5 mL) was added drop wise and the resulted mixture allowed to stir at room temperature for 24 h. The volume of dark red solution was reduced to one third and slow addition of hexane (2 mL) provided yellow precipitate. The solution was decanted and the precipitate was washed with hexane (3 x 1 mL). The resulted yellow complex was dried under vacuum (62 mg, quantitative yield). ^1H NMR (CDCl_3): δ 9.03 (d, 2H, ArCH), 7.73 (t, 1H, ArCH), 7.31 (t, $J = 8\text{Hz}$, 2H, ArCH), 5.44 (d, $J = 8\text{Hz}$, 2H, ArCH), 5.22 (d, $J = 8\text{ Hz}$, 2H, ArCH), 2.99 (m, 1H, $J = 8\text{Hz}$, $^i\text{PrCH}_3$), 2.09 (s, 3H, CH_3), 1.31 (d, 6H, CH_3). $^{13}\text{C}\{^1\text{H}\}$ NMR (CDCl_3): δ 154.79 (ArCH), 137.67 (ArCH), 124.58 (ArCH), 103.34 (quat-C), 97.07 (quat-C), 82.76 (ArCH), 82.19 (ArCH), 30.57 ($^i\text{PrCH}_3$), 22.21 (CH_3), 18.17 (CH_3). HRMS (EI) m/z calcd for $\text{C}_{15}\text{H}_{20}\text{Cl}_2\text{NRu}$: ($\text{M}+\text{H}^+$) 386.0016, found: 386.0009.

Synthesis of Complex $[(\eta^6\text{-}p\text{-cymene})\text{Ru}(\text{3,5-dimethyl pyridine})(\text{Cl})_2]$ (**2b**):



To a dichloromethane (1 mL) solution of $[\text{Ru}(p\text{-cymene})\text{Cl}_2]_2$ (0.032 mmol, 20 mg) in a vial, 3,5-dimethyl pyridine (0.8 mmol, 10 μL) was added drop wise after dissolving in dichloromethane (0.5 mL) and the resulted mixture was allowed to stir at room temperature for 24 h. The volume of dark red solution was reduced to one third and slow addition of hexane (2 mL) provided yellow-orange precipitate. The solution was decanted and the precipitate was washed with hexane (3 x 1 mL). The resulted yellow-orange complex was dried under vacuum (26 mg, quantitative yield). ^1H NMR (CDCl_3): δ 8.63 (s, 2H, ArCH), 7.32 (s, 1H, ArCH), 5.41 (d, 2H, $J = 8\text{Hz}$, ArCH), 5.18 (d, 2H, $J = 8\text{Hz}$, ArCH), 2.93 (m, 1H, $J = 4\text{ Hz}$, $^i\text{PrCH}$), 2.27 (s, 6H, CH_3), 2.05 (s, 3H, CH_3), 1.28 (d, 6H, $J = 8\text{Hz}$, $^i\text{PrCH}_3$). $^{13}\text{C}\{^1\text{H}\}$ NMR (CDCl_3): δ 152.34 (ArCH), 139.20 (quat-C), 133.97 (ArCH), 103.33 (quat-C), 97.29 (quat-C), 83.11 (ArCH), 82.18 (ArCH), 43.60 ($^i\text{PrCH}$), 30.73 ($^i\text{PrCH}_3$), 22.41 (CH_3), 18.40 (CH_3). HRMS (EI) m/z calcd for $\text{C}_{17}\text{H}_{24}\text{Cl}_2\text{NRu}$: ($\text{M}+\text{H}^+$): 414.0329, found: 414.0322.

Synthesis of Complex $[(\eta^6\text{-}p\text{-cymene})\text{Ru}(\text{PCy}_3)(\text{Cl})_2]$ (**3**):



In a screw cap scintillation vial $[\text{Ru}(p\text{-cymene})\text{Cl}_2]_2$ (0.08 mmol, 50 mg), tricyclohexylphosphine (0.179 mmol, 50 mg) and dichloromethane (2 mL) were added and the resulted reaction mixture was allowed to stir at room temperature for 6 h. The volume of dark red solution was reduced to one third and slow addition of cold

hexane (2 mL) provided red color precipitate. The solution was decanted and the precipitate was washed with hexane (3 x 1 mL). The resulted red complex was dried under vacuum for overnight (84 mg, 90%). ^1H NMR (CDCl_3): δ 5.55 (s, 4H, ArCH), 2.82 (m, 1H, $J = 8$ Hz, $^i\text{PrCH}$), 2.39 (m, 3H, $J = 12$ Hz, CyCH), 2.11 (br, 9H, CH_2), 1.78 (br, 9H, CH_2), 1.43 (m, 7H, $J = 12$ Hz, CH_2), 1.27 (br, 16H, CH_2). $^{13}\text{C}\{^1\text{H}\}$ NMR (CDCl_3): δ 107.15 (ArCH), 94.57 (ArCH), 88.54 (quat-C), 84.11 (quat-C), 36.11(CH_2), 35.93 (CH_2), 30.72 ($^i\text{PrCH}$), 29.92 (CH_2), 27.81 (CH_2), 27.71 (CH_2), 26.66 (CH_2), 22.63 (CH_3), 18.02 (CH_3). $^{31}\text{P}\{^1\text{H}\}$ NMR (CDCl_3): δ 25.92. HRMS (EI) m/z calcd for $\text{C}_{28}\text{H}_{48}\text{Cl}_2\text{PRu}$: ($\text{M}+\text{H}^+$) 587.1914, found: 587.1921.

Determination of the Molecular Structure of 3 in the Solid State by X-ray single Crystal Diffraction: Single crystals of complex **3** suitable for X-ray analysis were obtained from a solution of acetone and hexane. The crystal was mounted on a glass fiber. Geometry and intensity data were collected with a Bruker SMART D8 goniometer equipped with an APEX CCD detector and with an Incoatec microsource (Mo-K α radiation, $\lambda = 0.71073$ Å, multilayer optics). Temperature was controlled using an Oxford Cryostream 700 instrument. Intensities were integrated with SAINT+³¹ and corrected for absorption with SADABS.³² The structure was solved by direct methods and refined on F^2 with SHELXL-97.^{33,34}

Crystal Data of Complex $\text{Ru}(p\text{-cymene})\text{Cl}_2(\text{PCy}_3)$: $\text{C}_{31}\text{H}_{53}\text{Cl}_2\text{OPRu}$, crystal dimensions: $0.3 \times 0.26 \times 0.21$, $M = 644.67$, triclinic with space group P-1 (no. 2), $a = 9.7477(5)$ Å, $b = 10.3507(6)$ Å, $c = 15.9213(9)$ Å, $\alpha = 85.117(3)^\circ$, $\beta = 82.715(3)^\circ$, $\gamma = 80.032(3)^\circ$, $V = 1566.08(15)$ Å³, $Z = 2$, $T = 100$ K, $2\theta_{\text{max}} = 51.52$, $\rho_{\text{calcd}} = 1.367$ g/cm³, μ (MoK α) = 0.744 mm⁻¹. 16268 Reflections collected, 5911 unique ($R1 = 0.0431$), $WR2 = 0.0928$ (all data). The structure has been deposited at the CCDC data center and can be retrieved using the deposit number CCDC 1444045.

General Procedure for Regioselective 1,4-Hydroboration of Pyridine

Derivatives: Pyridine derivative (1 mmol), pinacolborane (1.1 mmol), Ru complex (3 mol%) [DCM (0.5 ml) for solid substrates] were charged in a PTFE screw capped reaction vial with a magnetic bead under nitrogen atmosphere. The reaction mixture was allowed to stir at 50 °C. Progress of the reaction was monitored using ^1H NMR. Reactions were stopped after completion indicated by disappearance of pyridine compound's aromatic (*ArCH*) protons and appearance of a new CH_2 peak upon selective 1,4-hydroboration. The reaction mixture then passed through a pad of celite and the filtrate was concentrated under reduced pressure. These products are highly air and moisture sensitive. All experimental procedures were carried out under nitrogen atmosphere and NMR samples were prepared under the nitrogen atmosphere glove-box by using dry CDCl_3 .

Spectral Data of 1,4-Dihydropyridines:

1-(4,4,5,5-Tetramethyl-1,3,2-dioxaborolan-2-yl)-1,4-dihydropyridine (7a)³⁵:

Colorless viscous liquid. Yield (192 mg, 93%). ^1H NMR (CDCl_3): δ 6.17-6.19 (m, 2H, alkene-*CH*), 4.59-4.62 (m, 2H, alkene-*CH*), 2.85-2.87 (m, 2H, CH_2), 1.22 (s, 12H, CH_3). $^{13}\text{C}\{^1\text{H}\}$ NMR (CDCl_3): δ 127.15 (alkene-*CH*), 102.44 (alkene-*CH*), 83.46 (quat-C), 24.69 (CH_3), 22.39 (CH_2). $^{11}\text{B}\{^1\text{H}\}$ NMR (CDCl_3): δ 23.29 (s, N-*Bpin*). HRMS (EI) m/z calcd for $\text{C}_{11}\text{H}_{18}\text{BNO}_2$: (M^+) 207.1431, found: 207.1439.

3-Methyl-1-(4,4,5,5-tetramethyl-1,3,2-dioxaborolan-2-yl)-1,4-dihydropyridine

(7b)¹: Light yellow viscous liquid. Yield (201 mg, 91%). ^1H NMR (CDCl_3): δ 6.24 (d, 1H, $J = 12\text{Hz}$, alkene-*CH*), 6.03 (s, 1H, alkene-*CH*), 4.62-4.65 (m, 1H, alkene-*CH*), 2.75 (br s, 2H, CH_2), 1.52 (s, 3H, CH_3), 1.23 (s, 12H, CH_3). $^{13}\text{C}\{^1\text{H}\}$ NMR (CDCl_3): δ 126.61 (alkene-*CH*), 121.36 (alkene-*CH*), 110.65 (quat-C), 101.75 (alkene-*CH*), 83.38 (quat-C), 28.06 (CH_2), 24.69 (CH_3), 20.78 (CH_3). $^{11}\text{B}\{^1\text{H}\}$ NMR

(CDCl₃): δ 23.30 (s, N-*Bpin*). HRMS (EI) m/z calcd for C₁₂H₁₉BNO₂: (M-H⁺) 220.1509, found: 220.1513.

3-Ethyl-1-(4,4,5,5-tetramethyl-1,3,2-dioxaborolan-2-yl)-1,4-dihydropyridine (7c):

Yellow viscous liquid. Yield (202 mg, 86%). ¹H NMR (CDCl₃) δ 6.22 (d, 1H, J = 8 Hz, alkene-*CH*), 6.04 (s, 1H, alkene-*CH*), 4.65 (m, 1H, alkene-*CH*), 2.78 (s, 2H, CH₂), 1.86 (quat, 2H, J = 8Hz, CH₂), 1.23 (s, 12H, CH₃), 0.98 (t, 3H, J = 8 Hz, CH₃). ¹³C{¹H} NMR (CDCl₃): δ 126.74 (alkene-*CH*), 120.63 (alkene-*CH*), 115.93 (quat-*C*), 101.86 (alkene-*CH*), 83.37 (quat-*C*), 28.09 (CH₂), 25.91 (CH₂), 24.70 (CH₃), 11.78 (CH₃). ¹¹B{¹H} NMR (CDCl₃): δ 23.32 (s, N-*Bpin*). HRMS (EI) m/z calcd for C₁₃H₂₁BNO₂: (M-H⁺) 234.1665, found: 234.1655.

3,5-Dimethyl-1-(4,4,5,5-tetramethyl-1,3,2-dioxaborolan-2-yl)-1,4-

dihydropyridine (7d): Yellow viscous liquid. Yield (134 mg, 57%). ¹H NMR (CDCl₃): δ 6.02 (s, 2H, alkene-*CH*), 2.58 (s, 2H, CH₂), 1.51 (s, 6H, CH₃), 1.19 (s, 12H, CH₃). ¹³C{¹H} NMR (CDCl₃): δ 120.83 (alkene-*CH*), 109.67 (alkene-*CH*), 83.08 (quat-*C*), 33.64 (CH₂), 24.52 (CH₃), 20.34 (CH₃). ¹¹B{¹H} NMR (CDCl₃): δ 23.30 (s, N-*Bpin*). HRMS (EI) m/z calcd for C₁₃H₂₁BNO₂: (M-H⁺) 234.1665, found: 234.1654.

3-(Pyrrolidin-1-ylmethyl)-1-(4,4,5,5-tetramethyl-1,3,2-dioxaborolan-2-yl)-1,4-

dihydropyridine (7f): (data inferred from reaction mixture NMR spectra) ¹H NMR (CDCl₃): δ 6.18-6.20 (m, 2H, alkene-*CH*), 4.68-4.70 (m, 1H, alkene-*CH*), 2.86 (br s, 4H, pyr-CH₂ and CH₂), 2.42 (br s, 4H, CH₂), 1.73 (br s, 4H, CH₂), 1.23 (s, 12H, CH₃). ¹³C{¹H} NMR (CDCl₃): δ 126.46 (alkene-*CH*), 123.63 (alkene-*CH*), 112.79 (quat-*C*), 102.66 (alkene-*CH*), 83.44 (quat-*C*), 61.33 (CH₂), 54.14 (CH₂), 26.48 (CH₂), 24.69 (CH₃), 23.57 (CH₂). ¹¹B{¹H} NMR (CDCl₃): δ 22.47 (s, N-*Bpin*). HRMS (EI) m/z calcd for C₁₆H₂₇BN₂O₂: (M⁺) 290.2166, found: 290.2175.

3-((1H-Pyrrol-1-yl)methyl)-1-(4,4,5,5-tetramethyl-1,3,2-dioxaborolan-2-yl)-1,4-dihydropyridine (7g): Brown viscous liquid. Yield (269 mg, 94%). ¹H NMR (CDCl₃): δ 6.66 (m, 2H, alkene-CH), 6.34 (s, 1H, alkene-CH), 6.20 (d, 1H, *J* = 8 Hz, alkene-CH), 6.13 (m, 2H, alkene-CH), 4.64-4.67 (m, 1H, alkene-CH), 4.28 (s, 2H, CH₂), 2.61 (br s, 2H, CH₂), 1.27 (s, 12H, CH₃). ¹³C{¹H} NMR (CDCl₃): δ 126.29 (alkene-CH), 125.22 (alkene-CH), 120.68 (alkene-CH), 110.49 (quat-C), 108.04 (alkene-CH), 102.46 (alkene-CH), 83.75 (quat-C), 54.35 (CH₂), 24.70 (CH₃), 23.98 (CH₂). ¹¹B{¹H} NMR (CDCl₃): δ 23.29 (s, N-*Bpin*). HRMS (EI) *m/z* calcd for C₁₆H₂₃BN₂O₂: (M⁺) 286.1853, found: 286.1842.

1-((1-(4,4,5,5-Tetramethyl-1,3,2-dioxaborolan-2-yl)-1,4-dihydropyridin-3-yl)methyl)-1H-indole (7h): Yellow-brown viscous liquid. Yield (306 mg, 91%). ¹H NMR (CDCl₃): δ 7.63 (d, 1H, *J* = 8 Hz, ArCH), 7.42 (d, 1H, *J* = 8 Hz, ArCH), 7.21 (t, 1H, *J* = 8 Hz, ArCH), 7.15 (d, 1H, *J* = 4 Hz, ArCH), 7.08-7.12 (m, 1H, ArCH), 6.50 (br s, 1H, ArCH), 6.46 (br s, 1H, alkene-CH), 6.20 (d, 1H, *J* = 8 Hz, alkene-CH), 4.60-4.63 (m, 1H, alkene-CH), 4.55 (s, 2H, CH₂), 2.59 (br s, 2H, CH₂), 1.28 (s, 12H, CH₃). ¹³C{¹H} NMR (CDCl₃): δ 136.61 (quat-C), 128.85 (quat-C), 127.80 (ArCH), 126.36 (alkene-CH), 125.30 (ArCH), 121.42 (ArCH), 120.94 (ArCH), 119.33 (alkene-CH), 110.04 (quat-C), 109.71 (ArCH), 102.35 (alkene-CH), 101.28 (ArCH), 83.79 (quat-C), 50.97 (CH₂), 24.73 (CH₃), 24.24 (CH₂). ¹¹B{¹H} NMR (CDCl₃): δ 23.36 (s, N-*Bpin*). HRMS (EI) *m/z* calcd for C₂₀H₂₄BN₂O₂: (M-H⁺): 335.1931, found: 335.1928.

1-((1-(4,4,5,5-Tetramethyl-1,3,2-dioxaborolan-2-yl)-1,4-dihydropyridin-3-yl)methyl)azepan-2-one (7i): Yellow viscous liquid. Yield (309 mg, 93%). ¹H NMR (CDCl₃): δ 6.13-6.17 (m, 2H, alkene-CH), 4.62- 4.65 (m, 1H, alkene-CH), 3.82 (s, 2H, CH₂), 3.22- 3.25 (m, 2H, CH₂), 2.69 (br s, 2H, CH₂), 2.48- 2.51 (m, 2H, CH₂),

1.64-1.68 (m, 4H, CH_2), 1.55-1.58 (m, 2H, CH_2), 1.21 (s, 12H, CH_3). $^{13}C\{^1H\}$ NMR ($CDCl_3$): δ 176.17 (CO), 126.30 (alkene-CH), 125.02 (alkene-CH), 110.15 (quat-C), 102.43 (alkene-CH), 83.59 (quat-C), 51.00 (CH_2), 47.19 (CH_2), 37.40 (CH_2), 30.13 (CH_2), 28.21 (CH_2), 24.61 (CH_3), 24.17 (CH_2), 23.65 (CH_2). $^{11}B\{^1H\}$ NMR ($CDCl_3$): δ 23.38 (s, N-*Bpin*). HRMS (EI) m/z calcd for $C_{18}H_{28}BN_2O_3$: ($M-H^+$): 331.2193, found: 331.2204.

Ethyl-2-(1-(4,4,5,5-tetramethyl-1,3,2-dioxaborolan-2-yl)-1,4-dihydropyridin-3-yl)acetate (7j): Yellow viscous liquid. Yield (270 mg, 92%). 1H NMR ($CDCl_3$): δ 6.16-6.19 (m, 2H, alkene-CH), 4.63-4.66 (m, 1H, alkene-CH), 4.09-4.14 (m, 2H, CH_2), 2.83 (br s, 4H, pyr- CH_2 and CH_2), 1.25 (t, 3H, $J = 4$ Hz, CH_3), 1.22 (s, 12H, CH_3). $^{13}C\{^1H\}$ NMR ($CDCl_3$): δ 171.68 (CH_2COOEt), 126.27(alkene-CH), 125.35 (alkene-CH), 107.26 (alkene-CH), 101.99 (alkene-CH), 83.51 (quat-C), 60.56 (CH_2), 40.79 (CH_2), 26.08 (CH_2), 24.63 (CH_3), 14.32 (CH_3). $^{11}B\{^1H\}$ NMR ($CDCl_3$): δ 23.39 (s, N-*Bpin*). HRMS (EI) m/z calcd for $C_{15}H_{23}BNO_4$: ($M-H^+$): 292.1720, found: 292.1711.

3-Methoxy-1-(4,4,5,5-tetramethyl-1,3,2-dioxaborolan-2-yl)-1,4-dihydropyridine (7k): (data inferred from reaction mixture NMR spectra) 1H NMR ($CDCl_3$): δ 6.20 (d, 1H, $J = 8$ Hz, alkene-CH), 5.71 (s, 1H, alkene-CH), 4.62-4.65 (m, 1H, alkene-CH), 3.52 (s, 3H, CH_3), 2.92 (m, 2H, CH_2), 1.20 (s, 12H, CH_3). $^{13}C\{^1H\}$ NMR ($CDCl_3$): δ 137.39 (quat-C), 126.27 (alkene-CH), 102.27 (alkene-CH), 100.32 (alkene-CH), 83.20 (quat-C), 54.31 (CH_3), 26.33 (CH_2), 24.41 (CH_3). $^{11}B\{^1H\}$ NMR ($CDCl_3$): δ 23.21 (s, N-*Bpin*). HRMS (EI) m/z calcd for $C_{12}H_{20}BNO_3$: (M^+) 237.1536, found: 237.1549.

3-(Benzyloxy)-1-(4,4,5,5-tetramethyl-1,3,2-dioxaborolan-2-yl)-1,4-dihydropyridine (7l): Yellow viscous liquid. Yield (241 mg, 77%). 1H NMR

(CDCl₃): δ 7.38-7.28 (m, 5H, ArCH), 6.27 (d, 1H, $J = 8$ Hz, alkene-CH), 5.92 (s, 1H, alkene-CH), 4.50 (s, 2H, CH₂), 4.73-4.59 (m, 1H, alkene-CH), 3.05 (m, 2H, CH₂), 1.24 (s, 12H, CH₃). ¹³C{¹H} NMR (CDCl₃): δ 139.59 (quat-C), 137.36 (Olefinic-C), 128.54 (ArCH), 127.91 (ArCH), 127.86 (Olefinic-C), 126.47 (ArCH), 103.84 (Olefinic-C), 100.91 (Olefinic-C), 83.47 (quat-C), 69.29 (OCH₂), 26.71 (CH₂), 24.70 (CH₃). ¹¹B{¹H} NMR (CDCl₃): δ 23.42 (s, N-Bpin). HRMS (EI) m/z calcd for C₁₈H₂₄BNO₃: (M⁺) 313.1849, found: 313.1841.

1-(4,4,5,5-Tetramethyl-1,3,2-dioxaborolan-2-yl)-3-((1-(4,4,5,5-tetramethyl-1,3,2-dioxaborolan-2-yl)-1,4-dihydropyridin-3-yl)methoxy)-1,4-dihydropyridine (7m): (data inferred from reaction mixture NMR spectra) ¹H NMR (CDCl₃): δ 6.36 (m, 1H, alkene-CH), 6.21 (dd, 1H, $J = 8$ Hz, 1H), 6.02 (m, 1H, alkene-CH), 4.89-4.91 (m, 2H, alkene-CH), 4.61- 4.65 (m, 1H, alkene-CH), 4.55- 4.59 (m, 1H, alkene-CH), 3.75 (s, 2H, CH₂), 2.74-2.76 (m, 4H, CH₂), 1.22 (s, 24H, CH₃). ¹³C{¹H} NMR (CDCl₃): δ 126.34 (quat-C), 125.10 (alkene-CH), 121.14 (alkene-CH), 110.26 (quat-C), 109.20 (alkene-CH), 101.43 (alkene-CH), 99.83 (alkene-CH), 83.12 (quat-C), 83.08 (quat-C), 48.05 (CH₂), 30.03 (CH₂), 27.80 (CH₂), 24.92 (CH₃), 24.75 (CH₃). ¹¹B{¹H} NMR (CDCl₃): δ 23.63 (s, N-Bpin). HRMS (EI) m/z calcd for C₂₃H₃₆B₂N₂O₅: (M⁺): 442.2810, found: 442.2797.

1-(4,4,5,5-Tetramethyl-1,3,2-dioxaborolan-2-yl)-1,4-dihydropyridin-3-yl acetate (7n): (data inferred from reaction mixture NMR spectra) ¹H NMR (CDCl₃): δ 6.26 (s, 1H, alkene-CH), 6.17 (d, 1H, $J = 8$ Hz, alkene-CH), 4.68-4.72 (m, 1H, alkene-CH), 3.05 (m, 2H, CH₂), 2.09 (s, 3H, CH₃), 1.22 (s, 12H, CH₃). ¹³C{¹H} NMR (CDCl₃): δ 169.63 (CO), 131.13 (quat-C), 126.13 (alkene-CH), 118.74 (alkene-CH), 101.96 (alkene-CH), 83.76 (quat-C), 25.77 (CH₂), 24.65 (CH₃), 20.90 (CH₂). ¹¹B{¹H} NMR

(CDCl₃): δ 23.04 (s, N-*Bpin*). HRMS (EI) m/z calcd for C₁₃H₂₀BNO₄: (M⁺) 265.1485, found: 265.1481.

1-(4,4,5,5-Tetramethyl-1,3,2-dioxaborolan-2-yl)-1,4-dihydropyridin-3-yl

benzoate (7o): (data inferred from reaction mixture NMR spectra) ¹H NMR (CDCl₃): δ 7.52-7.57 (m, 5H, ArCH), 6.42 (s, 1H, alkene-CH), 6.23 (d, 1H, alkene-CH), 4.75-4.77 (m, 1H, alkene-CH), 3.19 (br s, 2H, CH₂), 1.24 (s, 12H, CH₃). ¹³C{¹H} NMR (CDCl₃): δ 164.76 (CO), 137.93 (ArCH), 133.52 (ArCH), 130.11 (ArCH), 128.58 (alkene-CH), 126.19 (alkene-CH), 118.93 (alkene-CH), 102.11 (alkene-CH), 100.19 (alkene-CH), 83.81 (quat-C), 25.94 (CH₂), 24.76 (CH₃). ¹¹B{¹H} NMR (CDCl₃): δ 23.46 (s, N-*Bpin*). HRMS (EI) m/z calcd for C₁₈H₂₂BNO₄: (M⁺) 327.1642, found: 327.1654.

1-(4,4,5,5-Tetramethyl-1,3,2-dioxaborolan-2-yl)-1,4-dihydropyridine-d5 (7p):

Yellow viscous liquid. Yield (151 mg, 71%). ¹H NMR (CDCl₃): δ 2.86 (s, 1H, CH), 1.26 (s, 12H, CH₃). ¹³C{¹H} NMR (CDCl₃): δ 126.80 (t, alkene-CH), 101.82 (t, alkene-CH), 83.41 (quat-C), 24.66 (CH₃), 21.69 (t, CH₂). ¹¹B{¹H} NMR (CDCl₃): δ 23.21 (s, N-*Bpin*). HRMS (EI) m/z calcd for C₁₁H₁₃D₅BNO₂: (M⁺): 212.1744, found: 212.1751.

Determination of the Rate Equation:

Kinetic measurements were carried out by NMR scale reactions with constant concentration of pinacolborane (0.5 mmol, 73 μ l), pyridine (0.5 mmol, 40 μ l) and varying catalyst concentrations (graph a), constant concentration of pinacolborane (0.5 mmol, 73 μ l), catalyst (3 mol %, 0.3 $\times 10^{-5}$ mol) and varying pyridine concentrations (graph b), constant concentration of pyridine (0.5 mmol, 40 μ l), catalyst (3 mol %, 0.3 $\times 10^{-5}$ mol) and varying pinacolborane concentrations (graph c). The data for the kinetic analysis was obtained by integration of ¹H NMR. The

concentrations of the product and starting material were determined from integration of characteristic peak in ^1H NMR of pyridine ($\alpha\text{-CH}$) and 1,4-dihydropyridine ($\alpha\text{-CH}$). Rate of the reaction was determined from the slope (m) by using equation 1.

$$[\text{Product}] = m \times t \quad (\text{equation 1})$$

Overall rate equation for the hydroboration of pyridine:

$$d[\text{P}]/dt = K_{\text{obs}} [\text{catalyst}]^1 [\text{HBpin}]^1 [\text{Py}]^X \quad X = 1-0$$

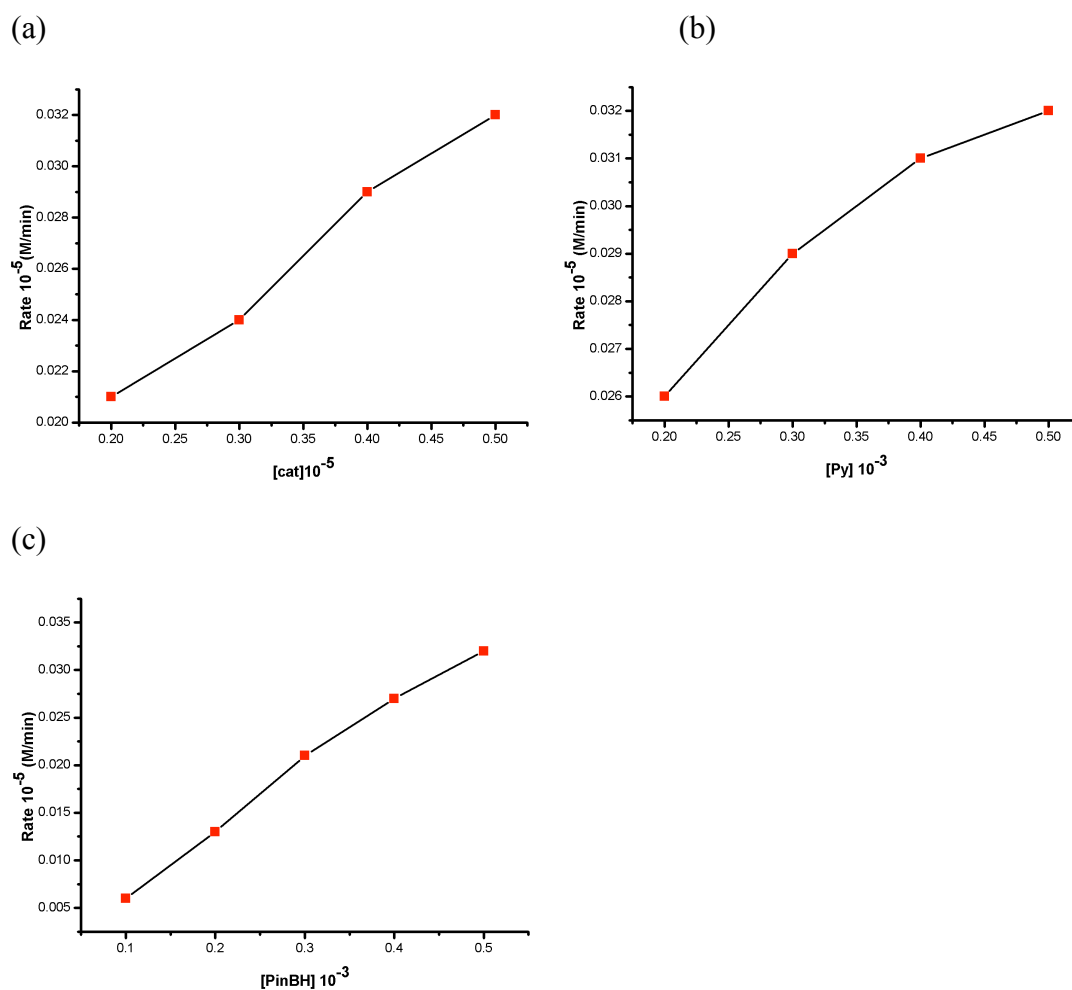


Figure 8.2 (a) Plot of rate (M/min) Vs. [cat] (1^{st} order). (b) Plot of rate (M/min) Vs. [Pyridine] (1^{st} order at low pyridine concentration but tends to Zero order at higher pyridine concentration). (c) Plot of rate (M/min) Vs. [PinBH] (1^{st} order).

8.6 NOTES AND REFERENCES

- (1) (a) Cozzi, P.; Carganico, G.; Fusar, D.; Grossoni, M.; Menichincheri, M.; Pinciroli, V.; Tonani, R.; Vaghi, F.; Salvati, P. *J. Med. Chem.* **1993**, *36*, 2964-2972. (b) Kumar, P. P.; Stotz, S. C.; Paramashivappa, R.; Beedle, A. M.; Zamponi, G. W.; Rao, A. S. *Mol. Pharm.* **2002**, *3*, 649-658. (c) López-Arrieta, J. M.; Birks, J. *Cochrane Database Syst. Rev.* **2002**, *3* CD000147. (d) Lavilla, R. *J. Chem. Soc., Perkin Trans. 1*, **2002**, 1141-1156.
- (2) Pollak, N.; Dölle, C.; Ziegler, M. *Biochem. J.* **2007**, *402*, 205-218.
- (3) Ouellet, S. G.; Walji, A. M.; MacMillan, D. W. C. *Acc. Chem. Res.* **2007**, *40*, 1327-1339.
- (4) (a) Eisner, U.; Kuthan, J. *Chem. Rev.* **1972**, *72*, 1-42. (b) Stout, D. M.; Meyers, A. I. *Chem. Rev.* **1982**, *82*, 223-243. (c) Keay, J. G. *Comprehensive Organic Synthesis*: Trost, B. M.; Fleming, I., Eds; Vol. 8, Pergamon, 1991. (d) Edraki, N.; Mehdipour, A. R.; Khoshneviszadeh, M.; Miri, R. *Drug Discovery Today* 2009, *14*, 1058-1066. (e) Bull, J. A.; Mousseau, J. J.; Pelletier, G.; Charette, A. B. *Chem. Rev.* **2012**, *112*, 2642-2713.
- (5) (a) Birch, A. J.; Karakhamor, E. A. *J. Chem. Soc., Chem. Commun.* **1975**, 480-481. (b) Olah, G. A.; Hunadi R. J. *J. Org. Chem.* **1981**, *46*, 715-718. (c) Donohoe, T. J.; McRiner, A. J.; Sheldrake, P. *Org. Lett.* **2000**, *2*, 3861-3863. (d) Danishefsky, S.; Cavanaugh, R. *J. Am. Chem. Soc.* **1968**, *90*, 520-521. (e) Danishefsky, S.; Cain P.; Nagel, A. *J. Am. Chem. Soc.* **1975**, *97*, 380-387. (f) Danishefsky, S.; Cain, P. *J. Org. Chem.* **1975**, *40*, 3606-3608. (g) Danishefsky, S.; Cain, P. *J. Steroid Biochem.* **1975**, *6*, 177-181.
- (6) (a) Comins, D.; Abdullah, A. H. *J. Org. Chem.* **1984**, *49*, 3392-3394. (b) Sundberg, R. J.; Hamilton, G.; Trindle, C. *J. Org. Chem.* **1986**, *51*, 3672-3677.

- (7) Katritzky, A. R.; Taylor, R. *Adv. Heterocycl. Chem.* **1990**, *47*, 1-467.
- (8) (a) Adkins, H.; Kuick, L. F.; Farlow, M.; Wojcik, B. *J. Am. Chem. Soc.* **1934**, *56*, 2425-2428. (b) Freifelder, M.; Stone, G. R. *J. Org. Chem.* **1961**, *26*, 3805-3808. (c) Lunn, G.; Sansone, E. B. *J. Org. Chem.* **1986**, *51*, 513-517. (d) Takasaki, M.; Motoyama, Y.; Higashi, K.; Yoon, S.-H.; Mochida, I.; Nagashima, H. *Chem. Asian J.* **2007**, *2*, 1524-1533. (e) Buil, M. L.; Esteruelas, M. A.; Niembro, S.; Olivan, M.; Orzechowski, L.; Pelayo, C.; Vallribera, A. *Organometallics* **2010**, *29*, 4375-4383. (f) Freifelder, M. *Practical Catalytic Hydrogenation*. Wiley Inter Science, 1971. (g) Glorius, F. *Org. Biomol. Chem.* **2005**, *3*, 4171-4175.
- (9) (a) Hao, L.; Harrod, J. F.; Lebus, A. -M.; Mu, Y.; Shu, R.; Samuel, E.; Woo, H. -G. *Angew. Chem. Int. Ed.* **1998**, *37*, 3126-3129. (b) Harrod, J. F.; Shu, R.; Woo, H. G.; Samuel, E. *Can. J. Chem.* **2001**, *79*, 1075-1085. (c) Gutsulyak, D. V.; van der Est, A.; Nikonov, G. I. *Angew. Chem. Int. Ed.* **2011**, *50*, 1384-1387. (d) Königs, C. D. F.; Klare, H. F. T.; Ostreich, M. *Angew. Chem. Int. Ed.* **2013**, *52*, 10076-10079.
- (10) Oshima, K.; Ohmura, T.; Suginome, M. *J. Am. Chem. Soc.* **2011**, *133*, 7324-7327.
- (11) Daley, E. N.; Vogels, C. M.; Geier, S. J.; Decken, A.; Doherty, S.; Westcott, S. A. *Angew. Chem. Int. Ed.* **2015**, *54*, 2121-2125.
- (12) Arrowsmith, M.; Hill, M. S.; Hadlington, T.; Kociok-Köhn, G. *Organometallics* **2011**, *30*, 5556-5559.
- (13) Intemann, J.; Lutz, M.; Harder, S. *Organometallics* **2014**, *33*, 5722-5729.
- (14) Intemann, J.; Bauer, H.; Pahl, J.; Maron, L.; Harder, S. *Chem. Eur. J.* **2015**, *21*, 11452-11461.
- (15) Oshima, K.; Ohmura, T.; Suginome, M. *J. Am. Chem. Soc.* **2012**, *134*, 3699-3702.

- (16) Dudnik, A. S.; Weidner, V. L.; Motta, A.; Delferro, M.; Marks, T. J. *Nat. Chem.* **2014**, *6*, 1100-1107.
- (17) Fan, X.; Zheng, J.; Li, Z. H.; Wang, H. *J. Am. Chem. Soc.* **2015**, *137*, 4916-4919.
- (18) Kaithal, A.; Chatterjee, B.; Gunanathan, C. *Org. Lett.* **2015**, *17*, 4790-4793.
- (19) (a) Kaithal, A.; Chatterjee, B.; Gunanathan, C. *Org. Lett.* **2016**, *18*, 3402-3405.
(b) Kaithal, A. M.Sc Thesis, NISER, Bhubaneswar, 2016 (May).
- (20) Martin, M. A.; Smith, A. K. *J. Chem. Soc., Dalton Trans.* **1974**, 233-241.
- (21) See Figure 8.3 and 8.4.
- (22) Chatterjee, B.; Gunanathan, C. *Chem. Commun.* **2014**, *50*, 888-890.
- (23) First order kinetics is observed for the regioselective 1,4-hydroboration of pyridine using catalyst **3**. See Figure 8.1.
- (24) No hydride signal at δ -10.2 ppm that corresponds to complex **6** was observed. See ref. 18 and 21.
- (25) ¹H NMR kinetic experiments at 50 °C indicated that the rate law is first order with [3], [HBpin], and [Py]. However, at a higher concentration (0.8 to 1 equiv) of pyridine, the rate approached being zero order. See ref 20.
- (26) Edwin, G. P.; Cristian, O.; Dominik, F.; Jhon, J.L.; Guibeth, L. M.; Ricardo, A. T.; Hugo, R. A. *Med. Chem. Commun.*, **2013**, *4*, 1166-1170.
- (27) Jiashou, W.; Huajiang, J.; Dingben, C.; Jianfen, S.; Datong, Z.; Jing, X.; Qizhong, Z. *Synlett*, **2014**, *25*, 539-542.
- (28) Gary, M. N.; Barry, R. H.; Andrew, D. C.; Timothy, W. G.; Benjamin, E. P.; Gill, M. L. *Tetrahedron Lett.*, **2013**, *54*, 4518-4521.
- (29) Moetaz, I. A.; Geoffrey, R. B.; Lindsay, A. S. *J. Heterocycl. Chem.*, **1985**, *22*, 319-20.
- (30) Nicole, A. L.; Jennifer, A. L. *Eur. J. Org. Chem.*, **2015**, *25*, 5546-5553.

- (31) Bruker AXS, SAINT⁺, *Program for Reduction of Data collected on Bruker CCD Area Detector Diffractometer V. 6.02*. Bruker AXS Inc., Madison, Wisconsin, USA, 1999.
- (32) Bruker AXS, SADABS, *Program for Empirical Absorption Correction of Area Detector Data V 2004/1*, Bruker AXS Inc., Madison, Wisconsin, USA, 2004.
- (33) G. M. Sheldrick, *Acta Crystallogr.* **2008**, *A64*, 112-122.
- (34) Dolomanov, O. V.; Bourhis, L. J.; Gildea, R. J.; Howard, J. A. K.; Puschmann, H. J. *Appl. Crystallogr.*, **2009**, *42*, 339-341.
- (35) Fan, X.; Zheng, J.; Li, Z. H.; Wang, H. *J. Am. Chem. Soc.*, **2015**, *137*, 4916-4919.

^1H and ^{13}C NMR spectra of the Reaction Mixture and isolated 1,4 dihydropyridines

Figure 8.3 Stacked ^{31}P NMR spectra of the stoichiometric reaction of **2a**, PCy_3 , and pinacolborane:

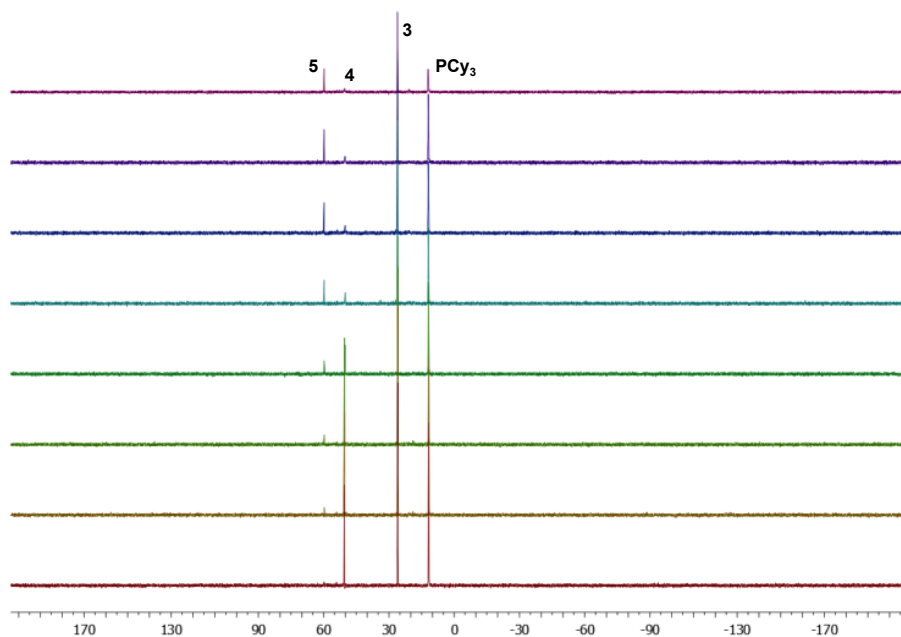


Figure 8.4 Stacked ^1H NMR spectra (hydride region) of the stoichiometric reaction of **2a**, PCy_3 , and pinacolborane:

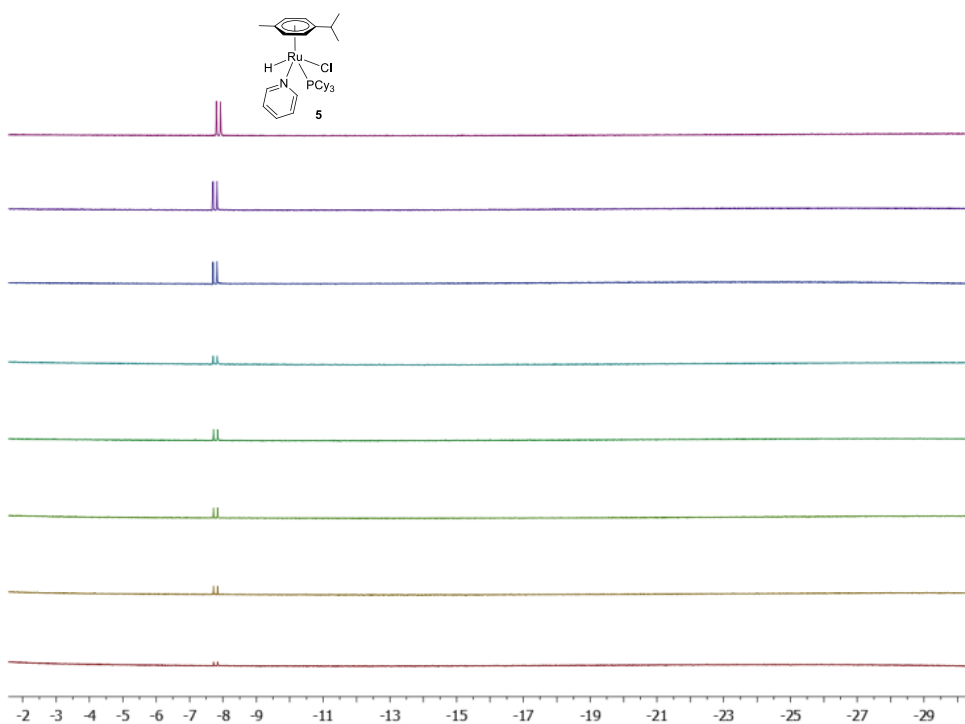


Figure 8.5 ^1H NMR spectra of isolated 1-(4,4,5,5-tetramethyl-1,3,2-dioxaborolan-2-yl)-1,4-dihydropyridine (**7a**):

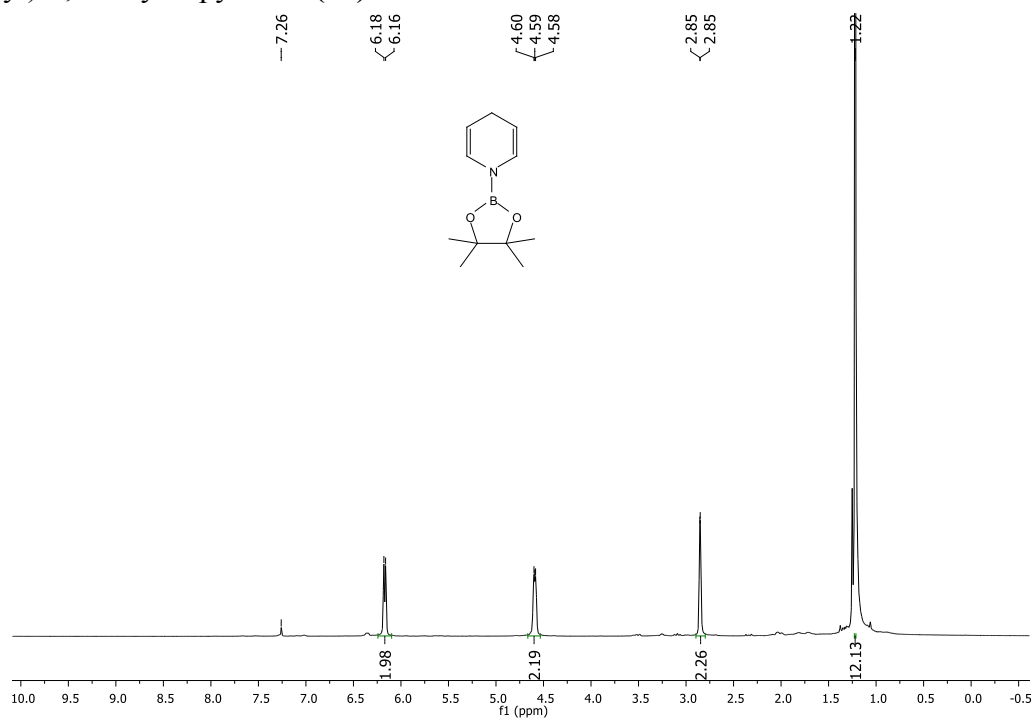


Figure 8.6 ^{13}C NMR spectra of isolated 1-(4,4,5,5-tetramethyl-1,3,2-dioxaborolan-2-yl)-1,4-dihydropyridine (**7a**):

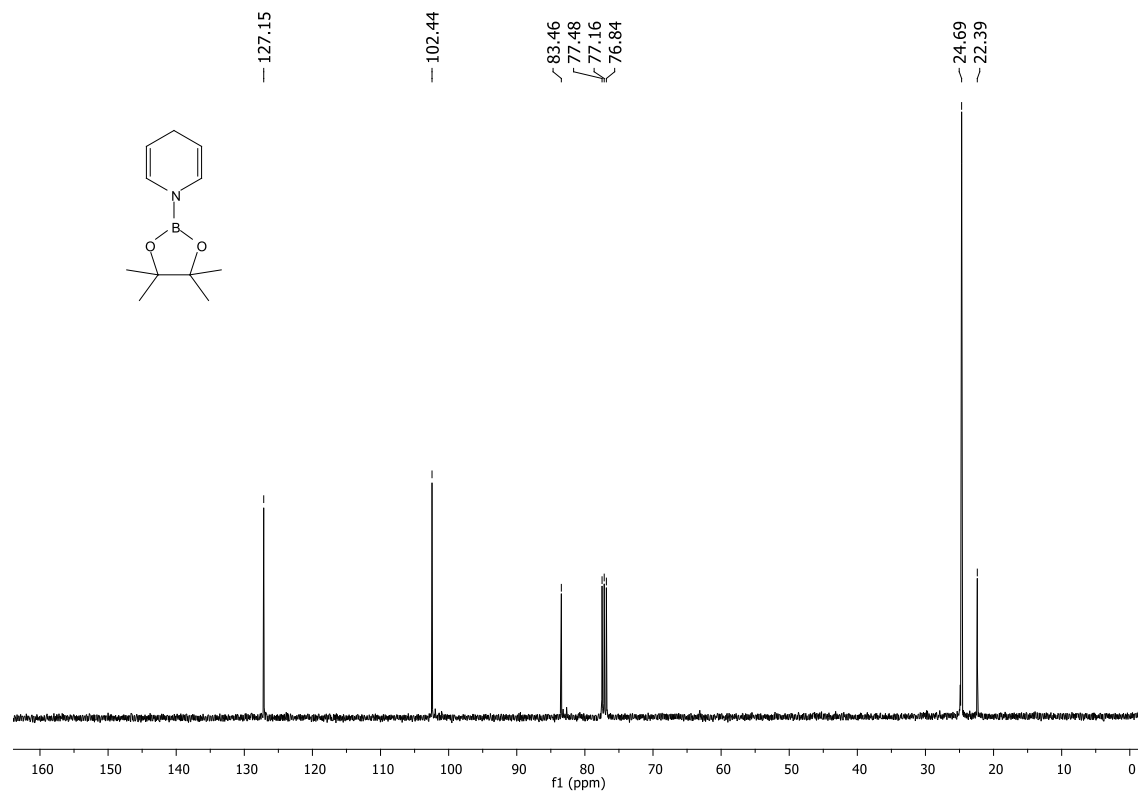


Figure 8.7 ^1H NMR spectra of isolated 3-methyl-1-(4,4,5,5-tetramethyl-1,3,2-dioxaborolan-2-yl)-1,4-dihydropyridine (**7b**):

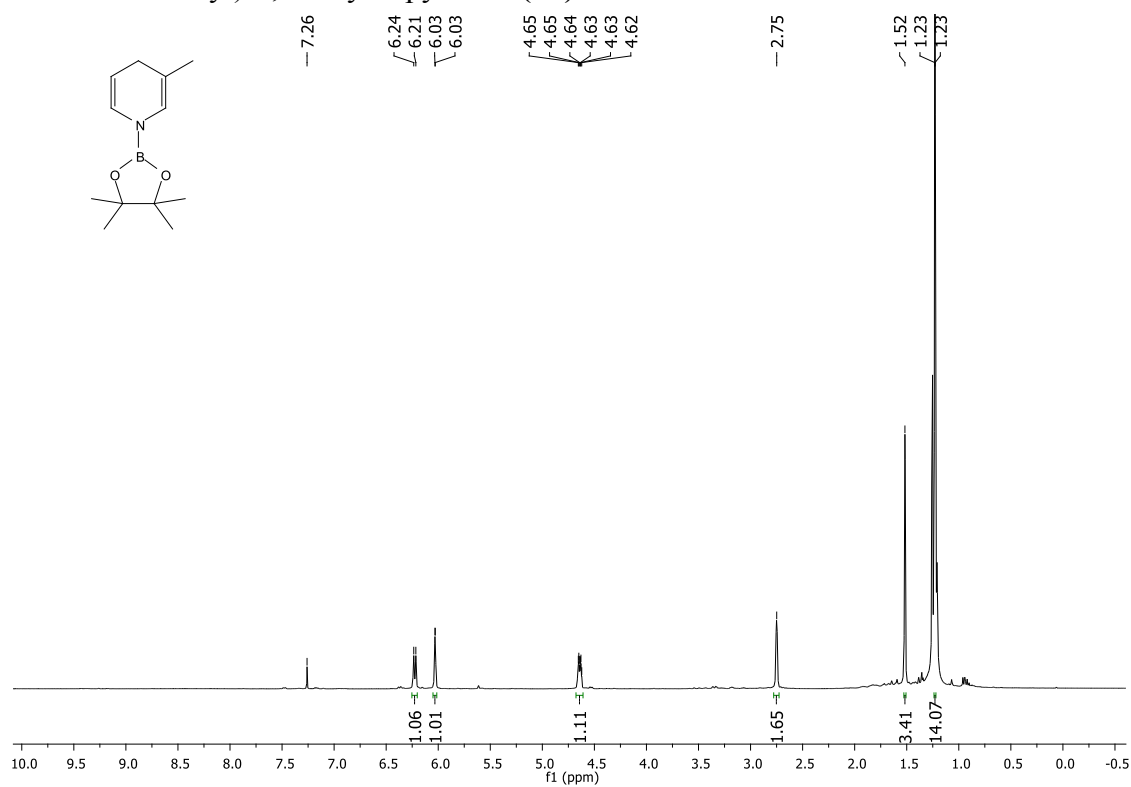
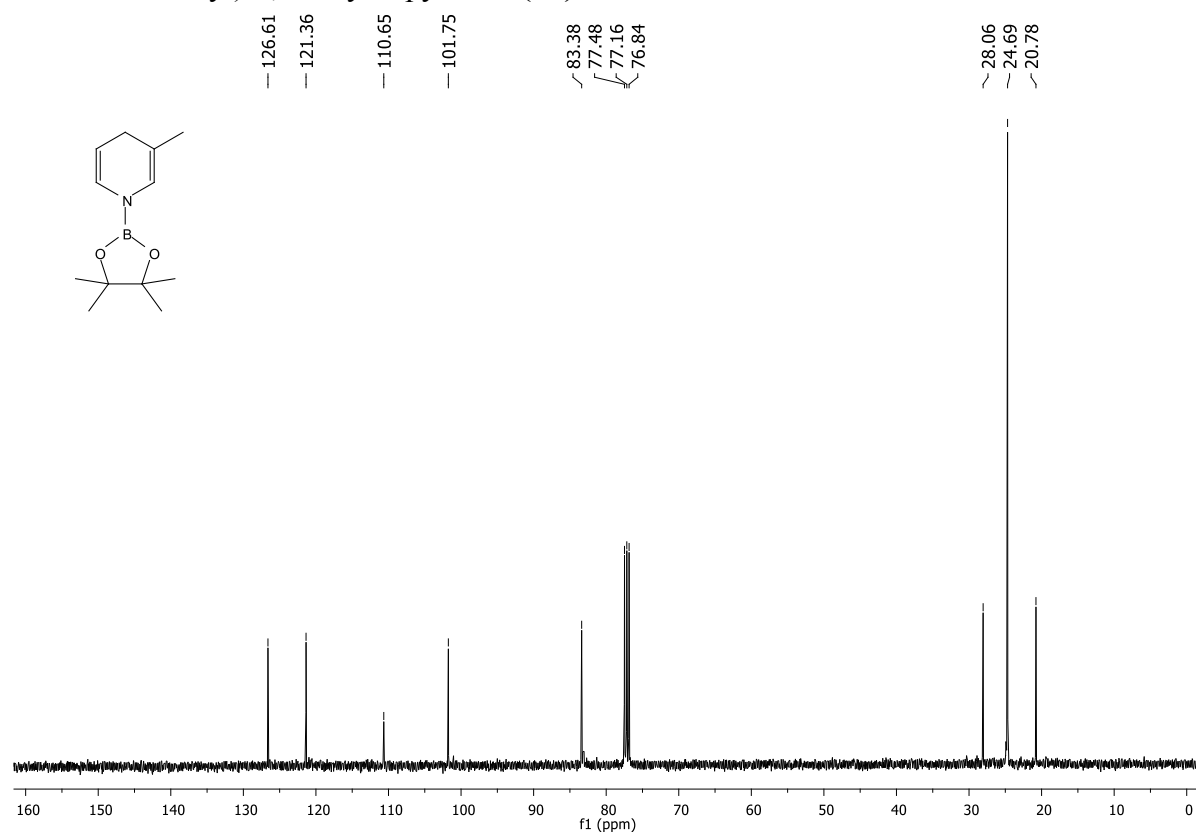


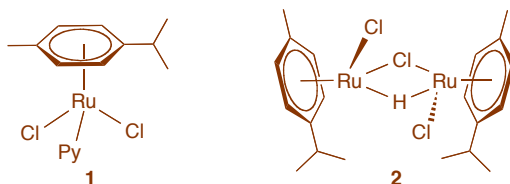
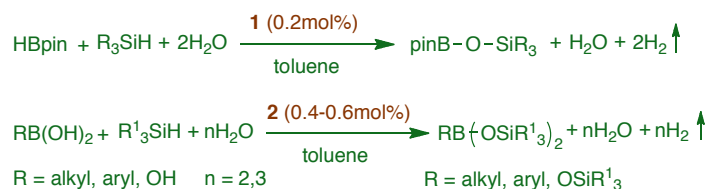
Figure 8.8 ^{13}C NMR spectra of isolated 3-methyl-1-(4,4,5,5-tetramethyl-1,3,2-dioxaborolan-2-yl)-1,4-dihydropyridine (**7b**):



CHAPTER 9

Ruthenium Catalyzed Multicomponent Synthesis of Borasiloxanes

9.1 ABSTRACT



We describe the selective atom economical synthesis of borasiloxanes using a multi-component approach directly from the one-pot ruthenium catalyzed reaction of boranes, silanes and water.

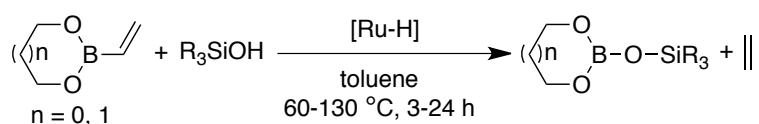
9.2 INTRODUCTION

Boron and silicon compounds have found extensive applications in synthetic, medicinal and material chemistry.¹ Borasiloxanes are used in functional inorganic material synthesis as they possess inherent molecular properties such as high stability providing resistance to heat and chemical reactions.² Borasiloxanes form cages, act as bifunctional molecules and used as polymeric sensor for amines.³ The conventional synthetic methods comprise the reaction of hydroxyborane with silane derivatives or the reaction of silanol with borane derivatives leading to the formation of borasiloxanes.⁴ Such conventional synthesis of silane and borane derivatives⁵ requires stoichiometric reagents, tedious experimental conditions and work up, which make the ultimate synthesis of borasiloxanes multi-step. To alleviate these problems, two catalytic

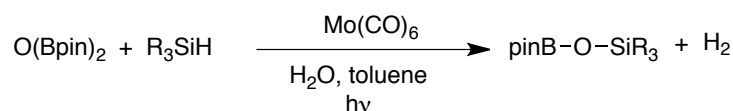
methods were developed in recent times for the synthesis of borasiloxanes.^{6,7} Marciniec reported the pioneering coupling of vinylboronates with silanol (Scheme 9.1a).⁶ Nakazawa and coworkers have disclosed a remarkable metal carbonyl complex catalyzed photolytic synthesis of borasiloxanes (Scheme 9.1b).⁷ However, synthesis of borasiloxanes from borane, silane and water in a direct multicomponent pathway is desirable, highly atom economical, and remains a challenge (Scheme 9.1c). Recently, we have reported the ruthenium-catalyzed chemoselective hydrosilylation⁸ of aldehydes, and hydroboration⁹ of carbonyl compounds, nitriles, imines and pyridines. Here in this chapter we present the ruthenium-catalyzed selective synthesis of borasiloxanes directly from boranes, silanes and water. This efficient catalytic process proceeds with the liberation of molecular hydrogen and water and generates no waste.

Scheme 9.1 Recent Advances in the Synthesis of Borasiloxanes

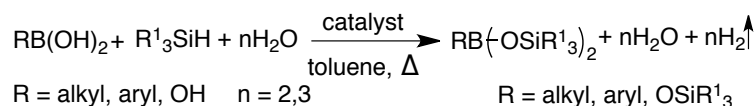
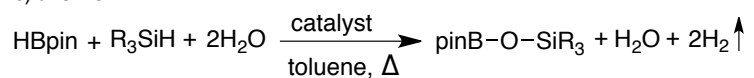
a) Coupling of Vinylborate with Silane (Marciniec)



b) Coupling of Bisboryloxide with Silane (Nakazawa)



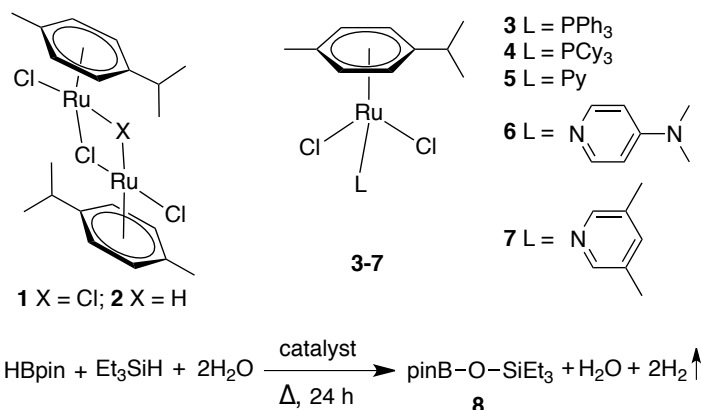
c) this work



9.3 RESULTS AND DISCUSSIONS

Catalyst screening embarked on $[(Ru(p\text{-cymene})Cl_2)_2]$ **1**. Thus, reaction mixture of **1** (0.5 mol%), pinacolborane (1 mmol), triethylsilane (1 mmol) and water (3 mmol) in toluene (2 mL) were stirred at room temperature for 2 h and then heated to 100 °C for 24 h, which provided borasiloxanes in 57% isolated yield (entry 1, Table 9.1); similar reaction at 125 °C provided the product in 63% yield (entry 2). Despite the product formation in poor yields, the result indicated that the elegant catalytic coupling of boranes, silanes and water directly to borasiloxanes is indeed feasible. Next, the monohydrido bridged dinuclear complex $[(\eta^6\text{-}p\text{-cymene})RuCl]_2(\mu\text{-H-}\mu\text{-Cl})$ **2**, was used as a catalyst leading to the formation of the borasiloxanes in 80% yield (entry 3). In an attempt to develop further efficient catalyst, mononuclear ruthenium complexes were explored.^{9b} While PPh_3 ligated ruthenium catalyst **3** (0.2 mol%) provided 50% yield (entry 4), electron-rich PCy_3 coordinated catalyst **4** provided borasiloxanes in 10% yield (entry 5), perhaps due to strongly bound phosphine ligands encumber further reaction at the metal center. Thus, labile pyridine ligated complex **5** was prepared and used as a catalyst in different solvent and temperatures (entries 6-9), which provided poor to moderate yields. However, upon using toluene as a solvent and increasing the reaction temperature to 100 °C and 125 °C, borasiloxane was obtained in 88% and 96% yields, respectively (entries 10-11). Further, catalysts **6** and **7** provided 29% and 80% yields, respectively (entries 12-13). Control experiment provided unreacted silane and hydroxyborane implying the catalyst is essential for successful formation of products (entry 14, Table 9.1). Thus, pyridine ligated complex **5** is preferred as the most suitable catalyst for the synthesis of borasiloxanes.

Table 9.1 Screening of Catalysts and Reaction Conditions for the Selective Synthesis of Borasiloxanes^a



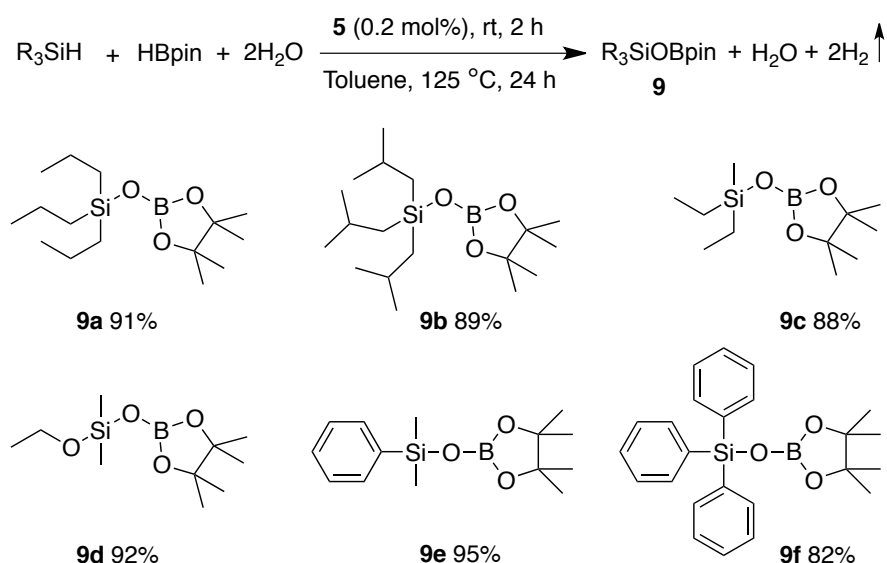
Entry	Catalyst (mol %)	Solvent	Temp. (°C)	pinBOSiEt ₃ (% yield) ^b
1	1 (0.5)	toluene	100	57
2	1 (0.5)	toluene	125	63
3	2 (0.2)	toluene	125	80
4	3 (0.2)	toluene	100	50
5	4 (0.2)	toluene	125	10
6	5 (0.2)	toluene	80	80
7	5 (0.2)	toluene	rt	-
8	5 (0.2)	CH ₃ CN	80	-
9	5 (0.2)	THF	80	15
10	5 (0.2)	toluene	100	88
11	5 (0.2)	toluene	125	96
12	6 (0.2)	toluene	100	29
13	7 (0.2)	toluene	100	80
14 ^c	-	toluene	125	-

^aCatalyst, pinacolborane (1 mmol), silane (1 mmol), degassed water (3 mmol) and solvent (2 mL) were stirred at room temperature for 2 h and then heated at indicated temperature for 24 h.

^bYield of isolated product. ^cControl experiment without catalyst.

The formation of silanol was highly efficient with catalyst **5** and the evolution of dihydrogen at room temperature was observed during the reaction progress.¹⁰ Upon reaction with H₂O, pinacolborane produced hydroxyborane quantitatively with concomitant liberation of dihydrogen, which also occurred at room temperature. The condensation reaction of silanol and hydroxyboranes was realized upon heating the reaction mixture at 125 °C to accomplish the formation of borasiloxanes selectively, overcoming the self-condensation due to the formation of stronger B–O–Si bond.^{3,11} Thus, applying the optimized condition, the substrate scope (alkyl, alkoxy and aryl silanes) was investigated and found that the complex **5** is highly effective in synthesis of a wide-range of borasiloxanes (**9a-f**) from boranes, silanes and water (Scheme 9.2).

Scheme 9.2 Synthesis of Borasiloxanes

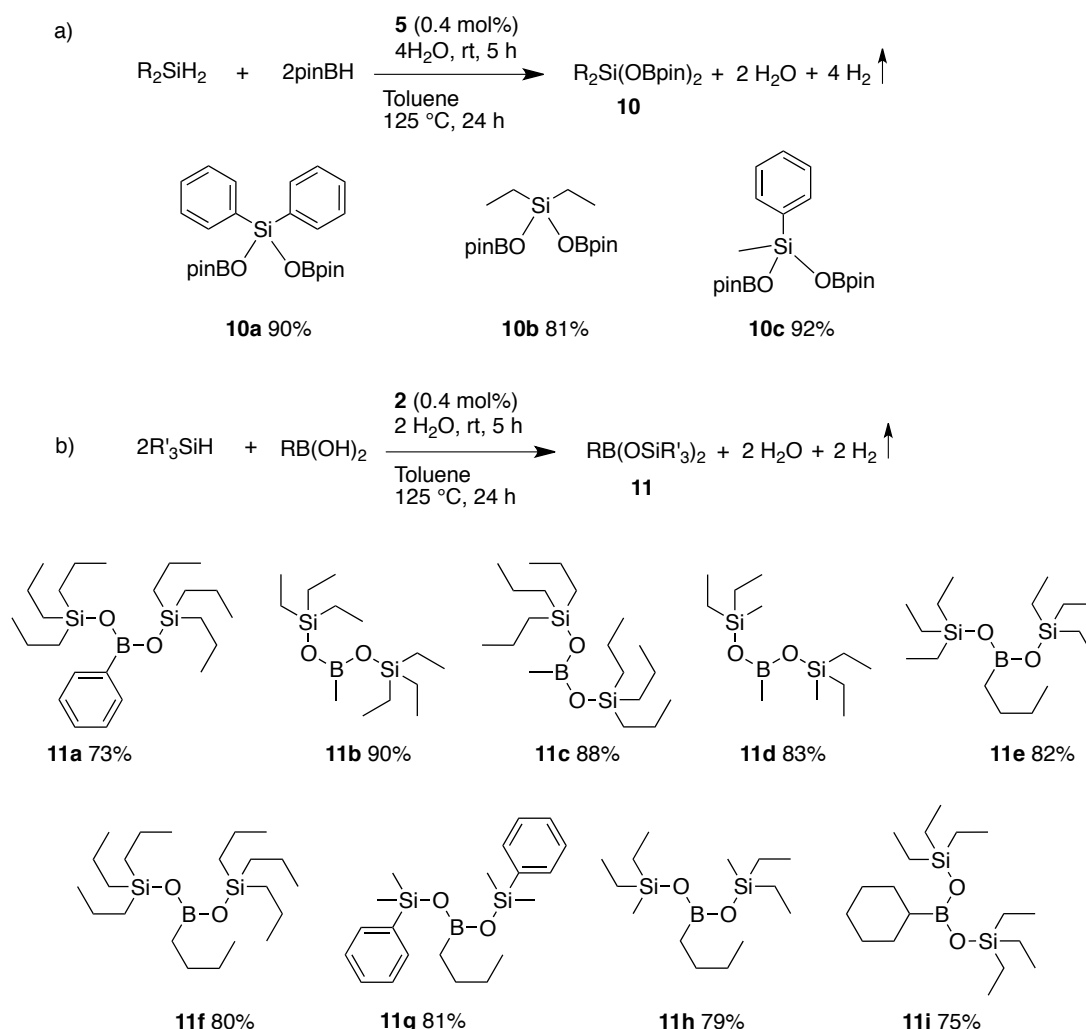


Silane (1 mmol), borane (1 mmol), catalyst **5** (0.2 mol%), degassed water (3 mmol) and toluene (2 mL) were stirred at room temperature for 2 h and then heated to 125 °C for 24 h. Yield corresponds to isolated pure products.

Scope of this direct coupling reaction was explored with disubstituted silanes. Diphenylsilane, diethylsilane, and methylphenylsilane exhibited efficient

reactivity and provided the corresponding (diboryl)siloxanes (**10a-c**) in excellent yields (Scheme 9.3a). Further, we envisaged the reaction between boronic acids and silanes. Unexpectedly under the optimized condition, catalyst **5** provided the expected products in poor yields. However, upon using **2** as a catalyst, reactions occurred effectively and an assortment of aryl and alkyl boronic acids underwent facile reaction with various silanes to provide a range of (disilyl)boroxanes (**11a-i**) in good to excellent yields (Scheme 9.3b).

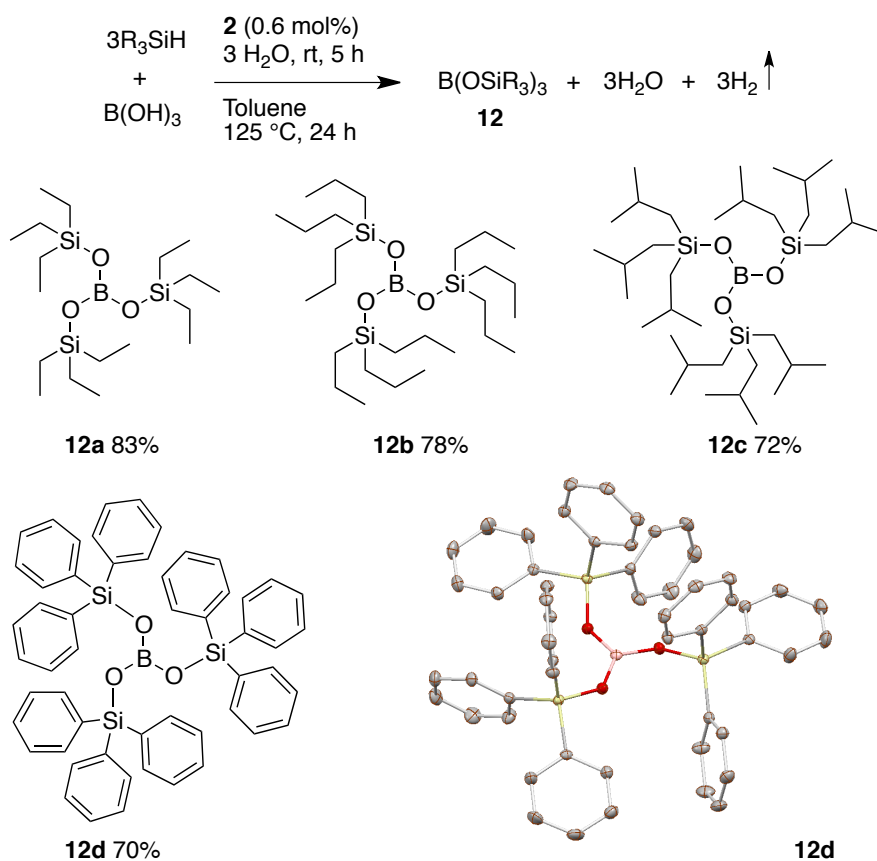
Scheme 9.3 Synthesis of (Diboryl)siloxanes and (Disilyl)boroxanes



Substrates, catalyst (0.4 mol%), degassed water (10 mmol, 180 μ l) and solvent (2 mL) were stirred at room temperature for 5 h and then heated to 125 $^\circ$ C for 24 h. Yield corresponds to isolated pure compounds.

When boric acid was subjected to the **2** catalyzed borasiloxane formation with different silanes (3 equiv.) and H₂O (10 equiv.), the corresponding tris(trialkylsilyl)borate products (**12a-d**) were isolated in good yields. Similarly, triphenylsilane also led to the formation of tris(triphenylsilyl) borate **12d** in 70% yield (Scheme 9.4); unexpectedly, a minor amount (10%) of 1,1,1,3,3,3-hexaphenyldisiloxane **13** also formed in this reaction. Further, the structure of tris(triphenylsilyl) borate (**12d**) was unequivocally corroborated by single crystal X-ray analysis (Scheme 9.4).

Scheme 9.4 Synthesis of Borasiloxanes Using Boric Acid



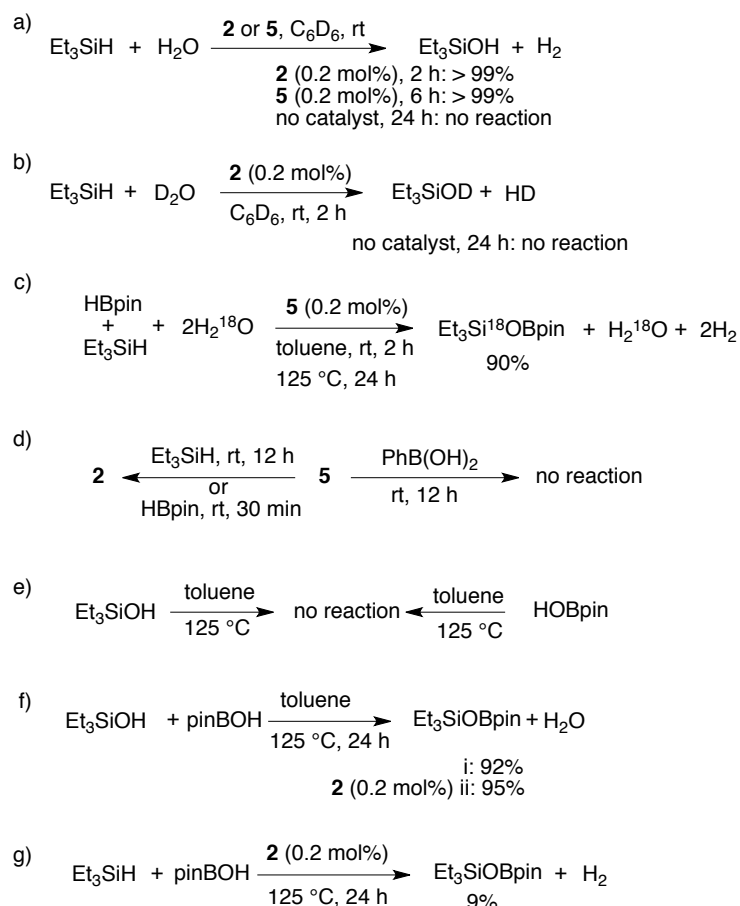
Crystal structure of tris(triphenylsilyl) borate **12d**. 1,1,1,3,3,3-hexaphenyldisiloxane **13** also co-crystallized along with **12d**, which is removed for clarity.

Series of elementary reactions, labelling studies and in situ monitoring of both catalytic and stoichiometric experiments allowed us to understand the sequence of reactions, choice of catalysts (**2** and **5**) and the reaction mechanism involved in this multi-component process (Scheme 9.5). When the independent reactions of triethylsilane, water with catalysts **2** and **5** (both 0.2 mol% in benzene-d₆, rt) were monitored by ¹H NMR, quantitative triethylsilanol formation¹³ was observed after 2 h and 6 h, respectively (Scheme 9.5a). ¹H NMR spectra of both reaction mixtures indicated that **2** (δ -10.18 ppm) is the major catalytic species present in solution; however, a minor hydride signal was observed at δ -11.54 ppm (1:10 for **2** and 1:8 for **5**, major signal being **2**).¹³ Monitoring the reaction of triethylsilane and D₂O catalyzed by **2** (0.2 mol%), formation of HD (t, ²J_{HD} = 48.0 Hz) was observed in the ¹H NMR (Scheme 9.5b). Control experiments revealed the necessity of catalyst in the silanol formation step (Scheme 9.5a and 9.5b). Further, oxygen labelled water (H₂¹⁸O) was used and the corresponding ¹⁸O labelled borasiloxane was isolated in 90% yield. The presence of labelled oxygen in the product was identified by the mass spectroscopy [(m/z = 299.1521 (M+K)⁺], which confirmed water as the source of oxygen atom (Scheme 9.5c) in the products.

Stoichiometric experiments were performed with complex **5** and triethylsilane or pinacolborane, which confirmed the formation of complex **2** (monitored by ¹H NMR, δ_{Ru-H} -10.18 ppm).^{8,9} However, the generation of **2** from **5** in presence of triethylsilane was sluggish and reaction completed after 12 h, whereas the reaction was much faster in presence of pinacolborane and complete formation of **2** occurred within 30 min. On contrary, complex **5** didn't react with phenylboronic acid and no formation of complex **2** was observed

(Scheme 9.5d). These observations confirm that **2** is the true catalyst involved in the reactions of pinacolborane as well (Scheme 9.2 and 9.3a). However, the relatively less reactivity of **2** (see Table 9.1) over catalyst **5** is not fully understood at this stage; perhaps the liberated pyridine from **5** (upon formation of **2**) act as a weak base and influences the condensation reaction.^{15,16} As the formation of complex **2** from **5** occurs on a diminished rate in silane, when boronic and boric acids (with them **5** do not react, see Scheme 9.5d) are used as boryl partners, catalyst **5** resulted in poor yields, whereas direct use of catalyst **2** provided good reactivity. Silanol and hydroxyboranes were independently heated at 125 °C in toluene for 24 h, which resulted in no reaction as observed by ²⁹Si and ¹¹B NMR, respectively in addition to ¹H NMR (Scheme 9.5e), which confirmed that there occur no self-condensations. The cross-condensation between silanol and hydroxyboranes proceeded with remarkable selectivity. The reaction of isolated triethylsilanol and hydroxyborane, provided the corresponding borasiloxane in 92% yield (Scheme 9.5f). The cross-condensation reaction was also performed with catalyst **2** (0.2 mol%), which provided 95% borasiloxane, indicating the insignificant effect of catalyst in cross-condensation reactions. Further, Reaction of isolated hydroxyboranes and triethylsilane was performed in the presence of catalyst **2**, which afforded the corresponding borasiloxane in only 9% yield and excluded the possibility of dehydrogenative coupling (Scheme 9.5g).

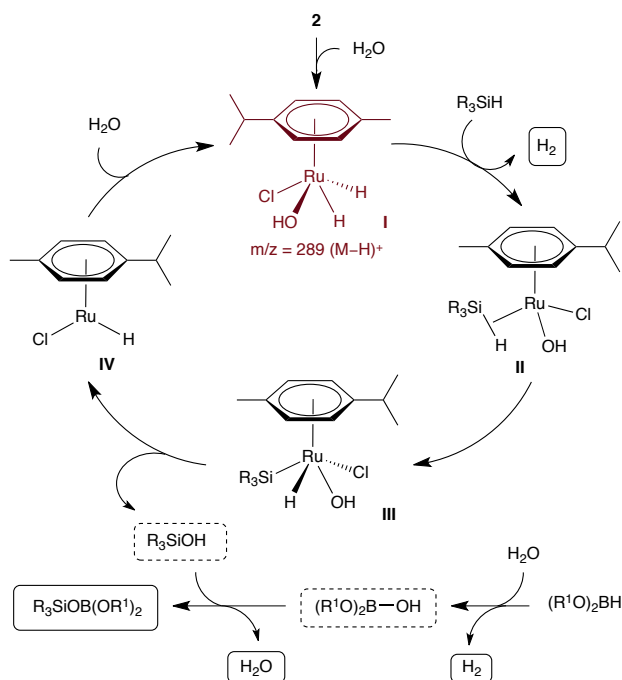
Scheme 9.5 Mechanistic Studies



On the basis of above experiments, a plausible mechanism is proposed for the synthesis of borasiloxanes catalyzed by **2** (Scheme 9.6). The complex **2** undergoes oxidative addition with water¹⁷ to form a Ru(IV) intermediate **I**, which reacts with silane to generate coordination complex **II** by liberating a molecule of hydrogen. Further oxidative addition of silane^{8,13} provide Ru(IV) intermediate **III** from which silyl and hydroxyl ligands undergo reductive elimination to deliver silanol and Ru(II) intermediate **IV**, which reacts further with water to close a catalytic cycle. Hydroxyborane formed from the reaction of pinacolborane and water undergoes condensation reaction with catalytically generated silanol and results in borasiloxane and water (Scheme 9.6). The

electrospray ionization mass spectrometric (ESI-MS) analysis of the reaction mixture of **2** with H₂O was performed in which **I** ($m/z = 289$ (M-H)⁺) was observed, indicating the involvement of intermediate **I** in the catalytic cycles.¹⁴

Scheme 9.6 Proposed Mechanism for the Formation of Borasiloxanes



9.4 CONCLUSIONS

In conclusion, an effective protocol for the selective synthesis of borasiloxanes catalyzed by simple ruthenium catalysts is demonstrated. High atom-economy, selectivity, catalytic efficiency, abundant and cheap resources, benign by products (water and molecular hydrogen) makes this method highly attractive for synthesis of borosiloxane materials.

9.5 EXPERIMENTAL SECTION

General Experimental: All manipulations were carried out using standard Schlenk line and glove box techniques under nitrogen atmosphere. Chemicals were purchased from Acros, Sigma-Aldrich, Alfa-aesar, and were used without further purification. Dry solvents were prepared according to standard procedures. ^1H , ^{13}C , ^{11}B and ^{29}Si spectra were recorded at Bruker AV-400 (^1H : 400 MHz, ^{13}C : 100.6 MHz, ^{11}B : 128 MHz, ^{29}Si : 79 MHz). ^1H , $^{13}\text{C}\{^1\text{H}\}$ NMR chemical shifts were reported in ppm downfield from tetramethyl silane. Multiplicity is abbreviated as: s, singlet; d, doublet; t, triplet; q, quartet; br, broad. Assignment of spectra was done based on one dimensional (dept-135) NMR technique. IR spectra were recorded on Bruker FTIR spectrometer. Mass spectra were recorded on Bruker micrOTOF-Q II Spectrometer.

Synthesis of Ruthenium Complexes: The complex **1** was bought from Sigma-Aldrich. Ruthenium complex **2** was prepared by following the procedure described in **chapter 6** and the ruthenium complexes **4**, **5** and **7** were prepared by following the procedure described in **chapter 8**.

Synthesis of $[\text{Ru}(\eta^6\text{-}p\text{-cymene})\text{Cl}_2(\text{PPh}_3)]$ (3**):** To a dichloromethane (2 mL) solution of $[\text{Ru}(p\text{-cymene})\text{Cl}_2]_2$ (0.08 mmol, 50 mg) taken in a vial, triphenylphosphine (0.16 mmol, 42 mg) was added and the resulting mixture was allowed to stir at room temperature for 24 h. The volume of dark red solution was reduced to one third. Upon slow addition of hexane (2 mL), orange precipitate was formed. The solution was decanted and the precipitate washed with hexane (1 mL) for three times. The resulted orange complex **3** was dried under vacuum (85 mg, yield 92%). ^1H NMR (CDCl_3): δ 7.85-7.80 (m, 6H, ArCH), 7.39-7.32 (m, 9H, ArCH), 5.19 (d, $J = 4$ Hz, 2H, ArCH), 4.99 (d, $J = 4$ Hz, 2H, ArCH), 2.84 (m, $J = 4$ Hz, ^1H , $^i\text{PrCH}$), 1.86 (s, 3H, CH_3), 1.09 (d, $J = 8$ Hz, 6H, $^i\text{PrCH}_3$). $^{13}\text{C}\{^1\text{H}\}$ NMR (CDCl_3): δ

134.30 (ArCH), 133.62 (quat-C), 130.20 (ArCH), 127.91 (ArCH), 111.11 (quat-C), 95.97 (quat-C), 89.11 (ArCH), 87.16 (ArCH), 30.25 (ⁱPrCH), 21.89 (ⁱPrCH₃), 17.77 (CH₃). HRMS (EI) m/z calcd for C₂₈H₃₀Cl₂PRu: 569.0506 (M+H)⁺, found: 569.0523.

Synthesis of [Ru(η^6 -*p*-cymene)Cl₂(*N,N*-dimethylpyridin-4-amine)] (6): To a dichloromethane (2 mL) solution of [Ru(*p*-cymene)Cl₂]₂ (0.08 mmol, 50 mg) taken in a vial, *N,N*-dimethylpyridin-4-amine (0.16 mmol, 19.5 mg) was added and the resulting mixture was allowed to stir at room temperature for 24 h. The volume of dark red solution was reduced to one third. Upon slow addition of hexane (2 mL), the product was precipitated as yellow solid. The solution was decanted and the precipitate washed with hexane (1 mL) for three times. The resulted complex was dried under vacuum (63 mg, yield 90%). ¹H NMR (CDCl₃): δ 8.38 (t, *J* = 4 Hz, 2H, ArCH), 6.38 (d, *J* = 8 Hz, 2H, ArCH), 5.37 (d, *J* = 4 Hz, 2H, ArCH), 5.15 (d, *J* = 4 Hz, 2H, ArCH), 2.95 (s, 6H, NCH₃), 2.91 (m, *J* = 4 Hz, 1H, ⁱPrCH), 2.05 (s, 3H, CH₃), 1.26 (d, *J* = 8 Hz, 6H, ⁱPrCH₃). ¹³C{¹H} NMR (CDCl₃): δ 154.33 (quat-C), 153.18 (ArCH), 107.35 (ArCH), 102.69 (quat-C), 96.85 (quat-C), 82.76 (ArCH), 81.76 (ArCH), 39.25 (NCH₃), 30.59 (ⁱPrCH), 22.33 (ⁱPrCH₃), 18.33 (CH₃). HRMS (EI) m/z calcd for C₁₇H₂₅Cl₂N₂Ru: 429.0438 (M+H)⁺, found: 429.0460.

General Procedure for the Synthesis of *mono*-Borasiloxanes: To an oven dried Schlenk-tube, silane (1mmol), borane (1 mmol), [Ru(*p*-cymene)Cl₂(pyridine)] **5** (0.002 mmol) and toluene (2 mL) were added under nitrogen atmosphere. Degassed water (3 mmol, 54 μ l) was added to the reaction mixture. The reaction mixture was allowed to stir for 2 h at room temperature (for the formation of silanol and hydroxyborane). Then the Schlenk-tube was immersed into a pre-heated oil bath of 125 °C and stirred for 24 h. After cooling the reaction mixture to room temperature, the solvent was evaporated under vacuum and the product was extracted with hexane

(2mL x 3). Combined hexane solution was filtered through a short plug of Celite and the filtrate was evaporated under reduced pressure to obtain mono-borasiloxanes products.

Spectral Data of *mono*-Borasiloxanes:

Triethyl((4,4,5,5-tetramethyl-1,3,2-dioxaborolan-2-yl)oxy)silane:⁷ Colorless liquid. Yield: 247 mg (96 %). IR (DCM): 2978, 2934, 1475, 1451, 1327, 1142, 981, 850, 672 cm⁻¹. ¹H NMR (CDCl₃): δ 1.22 (s, 12H, PinB-CH₃), 0.94 (t, *J* = 8 Hz, 9H, (SiCH₂CH₃)₃), 0.62 (q, *J* = 6 Hz, 6H, (SiCH₂CH₃)₃). ¹³C{¹H} NMR (CDCl₃): δ 82.10 (quat-C), 24.67 (PinB-CH₃), 6.58 (SiCH₂CH₃), 5.53 (SiCH₂CH₃). ¹¹B{¹H} NMR (CDCl₃): 20.37 (br. s).

Tripropyl((4,4,5,5-tetramethyl-1,3,2-dioxaborolan-2-yl)oxy)silane:⁷ Colorless liquid. Yield: 273 mg (91 %). IR (DCM): 2975, 2891, 1457, 1389, 1291, 1039, 971, 854, 650 cm⁻¹. ¹H NMR (CDCl₃): δ 1.37 (m, *J* = 8 Hz, 6H, (SiCH₂CH₂CH₃)₃), 1.21 (s, 12H, PinB-CH₃), 0.94 (t, *J* = 8 Hz, 9H, (SiCH₂CH₃)₃), 0.62 (t, *J* = 8 Hz, 6H, (SiCH₂CH₃)₃). ¹³C{¹H} NMR (CDCl₃): δ 82.08 (quat-C), 24.68 (PinB-CH₃), 18.34 (SiCH₂CH₂CH₃)₃, 17.44 (SiCH₂CH₃), 16.62 (SiCH₂CH₃). ¹¹B{¹H} NMR (CDCl₃): 20.20 (br. s).

Triisobutyl((4,4,5,5-tetramethyl-1,3,2-dioxaborolan-2-yl)oxy)silane: Colorless liquid. Yield: 304 mg (89 %). IR (DCM): 2954, 2911, 1443, 1359, 1270, 1009, 946, 891, 751 cm⁻¹. ¹H NMR (CDCl₃): δ 1.74 (m, *J* = 6 Hz, 3H, (SiCH₂CH(CH₃)₂)₃), 1.24 (s, 12H, PinB-CH₃), 0.92 (d, *J* = 4 Hz, 18H, (SiCH₂CH(CH₃)₂)₃), 0.56 (m, *J* = 4 Hz, 6H, (SiCH₂CH(CH₃)₂)₃). ¹³C{¹H} NMR (CDCl₃): δ 83.17 (quat-C), 26.00 ((SiCH₂CH(CH₃)₂)₃), 25.45 ((SiCH₂CH(CH₃)₂)₃), 24.52 ((SiCH₂CH(CH₃)₂)₃), 23.09 (PinB-CH₃). ¹¹B{¹H} NMR(CDCl₃): 20.54 (br. s). HRMS (EI) *m/z* calcd for C₁₈H₃₉BO₃Si: 342.2762 (M)⁺, found: 342.2765.

Diethyl(methyl)((4,4,5,5-tetramethyl-1,3,2-dioxaborolan-2-yl)oxy)silane:

Colorless liquid. Yield: 214 mg (88 %). IR (DCM): 2941, 2917, 1419, 1345, 1259, 1039, 951, 857, 681 cm^{-1} . ^1H NMR (CDCl_3): δ 1.23 (s, 12H, PinB- CH_3), 0.95 (t, $J = 8$ Hz, 6H, (SiCH_2CH_3)₃), 0.60 (q, $J = 6$ Hz, 4H, (SiCH_2CH_3)₃), 0.11 (s, 3H, SiCH_3). $^{13}\text{C}\{^1\text{H}\}$ NMR (CDCl_3): δ 81.94 (quat-C), 24.49 (PinB- CH_3), 7.14 (CH_3), 6.39 (CH_2), -3.59 (CH_3). $^{11}\text{B}\{^1\text{H}\}$ NMR (CDCl_3): 20.45 (br. s). HRMS (EI) m/z calcd for $\text{C}_{11}\text{H}_{25}\text{BO}_3\text{Si}$: 244.1666 (M)⁺, found: 244.1670.

Ethoxydimethyl((4,4,5,5-tetramethyl-1,3,2-dioxaborolan-2-yl)oxy)silane:

Colorless liquid. Yield: 226 mg (92 %). IR (DCM): 2972, 2920, 1446, 1344, 1309, 1262, 1057, 956, 806, 678 cm^{-1} . ^1H NMR (CDCl_3): δ 1.22 (s, 12H, PinB- CH_3), 0.16-0.08 (m, 11H, SiOCH_2 , $\text{SiOCH}_2\text{CH}_3$ and 2SiCH_3). $^{13}\text{C}\{^1\text{H}\}$ NMR (CDCl_3): δ 82.26 (quat-C), 24.73 (PinB- CH_3), 1.07 (OCH_2CH_3), 0.98 (2SiCH_3), 0.30 (SiOCH_2). $^{11}\text{B}\{^1\text{H}\}$ NMR (CDCl_3): 20.27 (br. s). HRMS (EI) m/z calcd for $\text{C}_{10}\text{H}_{23}\text{BO}_4\text{Si}$: 246.1459 (M)⁺, found: 246.1465.

Dimethyl(phenyl)((4,4,5,5-tetramethyl-1,3,2-dioxaborolan-2-yl)oxy)silane:⁷

Colorless liquid. Yield: 264 mg (95 %). IR (DCM): 3010, 2959, 1434, 1357, 1278, 1047, 956, 875, 751, 679 cm^{-1} . ^1H NMR (CDCl_3): δ 7.63 (m, 2H, ArCH), 7.37 (m, 3H, ArCH), 1.24 (s, 12H, PinB- CH_3), 0.45 (s, 6H, ($\text{Si}(\text{CH}_3)_2$)). $^{13}\text{C}\{^1\text{H}\}$ NMR(CDCl_3): δ 133.28 (ArCH), 129.63 (ArCH), 129.24 (quat-C), 127.80 (ArCH), 82.38 (quat-C), 24.68 (PinB- CH_3), -0.11 (SiCH_3). $^{11}\text{B}\{^1\text{H}\}$ NMR(CDCl_3): 20.94 (br. s).

Triphenyl((4,4,5,5-tetramethyl-1,3,2-dioxaborolan-2-yl)oxy)silane:⁷ White solid.

Yield: 329 mg (82 %), mp 194-195 °C. IR (DCM): 3041, 2954, 1444, 1378, 1261, 1021, 843, 625 cm^{-1} . ^1H NMR (CDCl_3): δ 7.61 (d, $J = 8$ Hz, 6H, ArCH), 7.42 (m, 9H, ArCH), 1.31 (s, 12H, PinB- CH_3). $^{13}\text{C}\{^1\text{H}\}$ NMR (CDCl_3): δ 135.93 (ArCH), 133.45

(quat-C), 129.93 (ArCH), 128.17 (ArCH), 83.30 (quat-C), 24.61 (PinB-CH₃). ¹¹B{¹H} NMR (CDCl₃): 21.09 (br. s).

General Procedure for the Synthesis of (Diboryl)siloxanes: To an oven dried Schlenk-tube silane (1mmol), borane (2 mmol), [(η^6 -*p*-cymene)Ru(Cl)₂(pyridine)] **5** (0.004 mmol) and toluene (2 mL) were added under nitrogen atmosphere. Degassed water (10 mmol, 180 μ l) was added to the reaction mixture and stirred for 5 h at room temperature (for the formation of silanol and hydroxyborane). Then the Schlenk-tube was immersed into a pre-heated oil bath of 125 °C and stirred for 24 h. After cooling of the reaction mixture to room temperature, the solvent was evaporated under vacuum and the product was extracted with hexane (2mL x 3, if the product is not soluble in hexane then hexane/ether solution is used for extraction). Combined hexane solution was filtered through a short plug of celite and the filtrate was evaporated under reduced pressure to obtain (diboryl)siloxanes.

Spectral Data of (Diboryl)siloxanes:

Diphenylbis((4,4,5,5-tetramethyl-1,3,2-dioxaborolan-2-yl)oxy)silane:^{6b} Colorless liquid. Yield: 421 mg (90 %). IR (DCM): 3011, 2975, 1401, 1354, 1031, 971, 754, 672 cm⁻¹. ¹H NMR (CDCl₃): δ 7.67-7.65 (m, 4H, ArCH), 7.44-7.35 (m, 6H, ArCH), 1.27 (s, 12H, PinB-CH₃), 1.24 (s, 12H, PinB-CH₃). ¹³C{¹H} NMR (CDCl₃): δ 134.68 (ArCH), 134.56 (ArCH), 130.49 (ArCH), 128.04 (quat-C), 83.29 (quat-C), 82.91 (quat-C), 24.68 (PinB-CH₃), 24.66 (PinB-CH₃). ¹¹B{¹H} NMR (CDCl₃): 20.60 (br. s).

Diethylbis((4,4,5,5-tetramethyl-1,3,2-dioxaborolan-2-yl)oxy)silane:⁷ Colorless liquid. Yield: 301 mg (81 %). IR (DCM): 2944, 2879, 1415, 1371, 1263, 1051, 1005, 951, 873, 625 cm⁻¹. ¹H NMR (CDCl₃): δ 1.19 (s, 24H, PinB-CH₃), 0.93 (t, 6H, *J* = 8 Hz, (SiCH₂CH₃)₃), 0.64 (q, 4H, *J* = 8 Hz, (SiCH₂CH₃)₃). ¹³C{¹H} NMR (CDCl₃): δ

82.29 (quat-C), 24.62 (PinB-CH₃), 6.01 (SiCH₂CH₃)₃, 5.95 (SiCH₂CH₃)₃. ¹¹B{¹H} NMR (CDCl₃): 20.43 (br. s).

Methyl(phenyl)bis((4,4,5,5-tetramethyl-1,3,2-dioxaborolan-2-yl)oxy)silane:

Colorless liquid. Yield: 373 mg (92 %). IR (DCM): 3021, 2977, 2891, 1432, 1387, 1046, 978, 891, 734, 669 cm⁻¹. ¹H NMR (CDCl₃): δ 7.71-7.61 (m, 2H, ArCH), 7.42-7.28 (m, 3H, ArCH), 1.27 (s, 12H, PinB-CH₃), 1.23 (s, 12H, PinB-CH₃), 0.50 (s, 3H, SiCH₃). ¹³C{¹H} NMR (CDCl₃): δ 134.98 (quat-C), 133.73 (ArCH), 130.23 (ArCH), 127.70 (ArCH), 83.26 (quat-C), 82.60 (quat-C), 24.70 (PinB-CH₃), 24.63 (PinB-CH₃), -1.67 (SiCH₃). ¹¹B{¹H} NMR (CDCl₃): 20.17 (br. s). HRMS (EI) m/z calcd for C₁₉H₃₂B₂O₆Si: 406.2154 (M)⁺, found: 406.2156.

General Procedure for the Synthesis of (Disilyl)boroxanes: To an oven dried Schlenk-tube silane (2 mmol), boronic acid (1 mmol), [$\{(\eta^6\text{-}p\text{-cymene})\text{RuCl}\}_2(\mu\text{-H-}\mu\text{-Cl})$] **2** (0.004 mmol) and toluene (2 mL) were added under nitrogen atmosphere. Degassed water (10 mmol, 180 μl) was added under nitrogen atmosphere and the reaction mixture was allowed to stir for 5 h for the complete formation of silanol and hydroxyborane. The Schlenk-tube was then immersed into a pre-heated oil bath at 125 °C and stirred for 24 h. After the reaction mixture was cooled to rt, the solvent was evaporated under vacuum and the product was extracted with hexane (2mL x 3, if the product is not soluble in hexane then hexane/ether solution is used for extraction). Organic layers were combined, filtered through a short plug of celite and the filtrate was evaporated under reduced pressure to obtain (disilyl)boroxanes in good yield.

Spectral Data of (Disilyl)boroxanes:

Bis(tripropylsilyl) phenylboronate:¹⁸ Colorless liquid. Yield: 316 mg (73 %). IR (DCM): 3011, 2972, 2897, 1447, 1359, 1041, 1019, 954, 751, 658 cm^{-1} . ^1H NMR (CDCl_3): δ 7.87 (d, 2H, $J = 8$ Hz, ArCH), 7.50-7.44 (m, 3H, ArCH), 1.55 (m, 12H, $(\text{SiCH}_2\text{CH}_2\text{CH}_3)_3$), 1.11 (t, 18H, $J = 8$ Hz $(\text{SiCH}_2\text{CH}_2\text{CH}_3)_3$), 0.85 (m, 12H, $(\text{SiCH}_2\text{CH}_2\text{CH}_3)_3$). $^{13}\text{C}\{^1\text{H}\}$ NMR (CDCl_3): δ 135.81 (ArCH), 132.85 (ArCH), 128.14 (ArCH), 18.36 $((\text{SiCH}_2\text{CH}_2\text{CH}_3)_3)$, 18.18 $((\text{SiCH}_2\text{CH}_2\text{CH}_3)_3)$, 14.15 $((\text{SiCH}_2\text{CH}_2\text{CH}_3)_3)$. $^{11}\text{B}\{^1\text{H}\}$ NMR (CDCl_3): 29.75 (br. s).

Bis(triethylsilyl) methylboronate: Colorless liquid. Yield: 259 mg (90 %). IR (DCM): 2956, 2889, 1411, 1368, 1016, 967, 773, 677 cm^{-1} . ^1H NMR (CDCl_3): δ 0.95 (t, $J = 8$ Hz, 18H, $(\text{SiCH}_2\text{CH}_3)_3$), 0.61 (q, $J = 6$ Hz, 12H, $(\text{SiCH}_2\text{CH}_3)_3$), 0.21 (s, 3H, CH_3). $^{13}\text{C}\{^1\text{H}\}$ NMR (CDCl_3): δ 6.81 $((\text{SiCH}_2\text{CH}_3)_3)$, 5.81 $((\text{SiCH}_2\text{CH}_3)_3)$, 5.62 (BCH_3). $^{11}\text{B}\{^1\text{H}\}$ NMR (CDCl_3): 29.34 (br. s). HRMS (EI) m/z calcd for $\text{C}_{13}\text{H}_{33}\text{BO}_2\text{Si}_2$: 288.2112 (M)⁺, found: 288.2117.

Bis(tripropylsilyl) methylboronate: Colorless liquid. Yield: 327 mg (88 %). IR (DCM): 2951, 2893, 1441, 1375, 1044, 971, 852, 769, 671 cm^{-1} . ^1H NMR (CDCl_3): δ 1.35 (m, 12H, $(\text{SiCH}_2\text{CH}_2\text{CH}_3)_3$), 0.98 (t, 18H, $J = 8$ Hz, $(\text{SiCH}_2\text{CH}_2\text{CH}_3)_3$), 0.60 (t, 12H, $J = 8$ Hz, $(\text{SiCH}_2\text{CH}_2\text{CH}_3)_3$), 0.19 (s, 3H, BCH_3). $^{13}\text{C}\{^1\text{H}\}$ NMR (CDCl_3): δ 18.48 $((\text{SiCH}_2\text{CH}_2\text{CH}_3)_3)$, 17.87 $(\text{SiCH}_2\text{CH}_2\text{CH}_3)_3$, 17.70 (BCH_3), 16.87 $((\text{SiCH}_2\text{CH}_2\text{CH}_3)_3)$. $^{11}\text{B}\{^1\text{H}\}$ NMR (CDCl_3): 29.45 (br. s). HRMS (EI) m/z calcd for $\text{C}_{19}\text{H}_{45}\text{BO}_2\text{Si}_2$: 372.3051 (M)⁺, found: 372.3054.

Bis(diethyl(methyl)silyl) methylboronate: Colorless liquid. Yield: 215 mg (83 %). IR (DCM): 2944, 2895, 1417, 1372, 1101, 1032, 975, 851, 749, 678 cm^{-1} . ^1H NMR (CDCl_3): δ 0.94 (t, 12H, $J = 8\text{Hz}$, $(\text{SiCH}_2\text{CH}_3)_3$), 0.58 (q, 8H, $J = 6\text{Hz}$, $(\text{SiCH}_2\text{CH}_3)_3$), 0.10 (s, 3H, BCH_3), 0.07 (s, 6H, SiCH_3). $^{13}\text{C}\{^1\text{H}\}$ NMR (CDCl_3): δ 29.86 (BCH_3),

7.43 ((SiCH₂CH₃)₃), 6.78 ((SiCH₂CH₃)₃), -3.38 (SiCH₃). ¹¹B{¹H} NMR (CDCl₃): 29.57 (br. s). HRMS (EI) m/z calcd for C₁₁H₂₉BO₂Si₂: 260.1799 (M)⁺, found: 260.1805.

Bis(triethylsilyl) butylboronate: Colorless liquid. Yield: 270 mg (82 %). IR (DCM): 2954, 2876, 1459, 1317, 1237, 1004, 972, 844, 726 cm⁻¹. ¹H NMR (CDCl₃): δ 1.37-1.25 (m, 6H, CH₂), 0.95 (t, *J* = 8 Hz, 18H, (SiCH₂CH₃)₃), 0.88 (q, *J* = 8 Hz, 3H, CH₃), 0.60 (q, *J* = 6 Hz, 12H, (SiCH₂CH₃)₃). ¹³C{¹H} NMR (CDCl₃): δ 27.37 (CH₃), 25.63 (CH₂), 14.22 (CH₂), 6.84 (CH₂), 6.78 (CH₂), 5.91 (CH₃). ¹¹B{¹H} NMR (CDCl₃): 30.12 (br. s). HRMS (EI) m/z calcd for C₁₆H₃₉BO₂Si₂: 330.2582 (M)⁺, found: 330.2585.

Bis(tripropylsilyl) butylboronate: Colorless liquid. Yield: 331 mg (80 %). IR (DCM): 2951, 2885, 1448, 1367, 1033, 876, 744, 681 cm⁻¹. ¹H NMR (CDCl₃): δ 1.41-1.32 ((m, 16H, (SiCH₂CH₂CH₃)₃ and BCH₂CH₂CH₂CH₃)), 0.96 (t, *J* = 8 Hz, 18H, (SiCH₂CH₂CH₃)₃), 0.87 (t, *J* = 6 Hz, 3H, BCH₂CH₂CH₂CH₃), 0.67-0.58 (m, 14H, SiCH₂CH₂CH₃)₃ and BCH₂CH₂CH₂CH₃). ¹³C{¹H} NMR (CDCl₃): δ 27.34 (BCH₂), 25.62 (BCH₂), 18.51 (SiCH₂), 18.44 (BCH₃), 17.97 (SiCH₃), 16.88 (SiCH₂), 14.21 (BCH₃). ¹¹B{¹H} NMR (CDCl₃): 30.25 (br. s). HRMS (EI) m/z calcd for C₂₂H₅₁BO₂Si₂: 414.3521 (M)⁺, found: 414.3523.

Bis(dimethyl(phenyl)silyl) butylboronate: Colorless liquid. Yield: 299 mg (81 %). IR (DCM): 3110, 2967, 2877, 1445, 1397, 1276, 1042, 1019, 978, 762, 681 cm⁻¹. ¹H NMR (CDCl₃): δ 7.66-7.57 (m, 4H, ArCH), 7.44-7.39 (m, 6H, ArCH), 1.42-1.27 (m, 4H, BCH₂), 0.49-0.39 (m, 14H, BCH₂ and SiCH₃), 0.15 (m, 3H, BCH₃). ¹³C{¹H} NMR (CDCl₃): δ 138.99 (quat-C), 133.13 (ArCH), 129.38 (ArCH), 127.74 (ArCH), 26.93 (BCH₂), 25.43 (BCH₂), 14.02 (BCH₂), 0.89 (BCH₃), 0.20 (SiCH₃). ¹¹B{¹H} NMR (CDCl₃): 30.25 (br. s).

NMR (CDCl₃): 30.45 (br. s). HRMS (EI) m/z calcd for C₂₀H₃₁BO₂Si₂: 370.1956 (M)⁺, found: 370.1959.

Bis(diethyl(methyl)silyl)butylboronate: Colorless liquid. Yield: 238 mg (79 %). IR (DCM): 2951, 2896, 1452, 1381, 1039, 1011, 865, 731, 689 cm⁻¹. ¹H NMR (CDCl₃): δ 1.35-1.25 (m, 6H, BCH₂), 0.94 (t, 12H, *J* = 8 Hz, SiCH₂CH₃), 0.86 (t, 3H, *J* = 8 Hz, BCH₂CH₂CH₂CH₃), 0.58 (q, 8H, *J* = 6 Hz, SiCH₂CH₃), 0.08 (s, 6H, SiCH₃). ¹³C{¹H} NMR (CDCl₃): δ 27.26 (BCH₂), 27.01 (BCH₂), 25.60 (BCH₂), 14.16 (BCH₃), 7.70 (SiCH₂), 6.78 (SiCH₃), -3.00 (SiCH₃). ¹¹B{¹H} NMR (CDCl₃): 30.19 (br.s). HRMS (EI) m/z calcd for C₁₄H₃₅BO₂Si₂: 302.2269 (M)⁺, found: 302.2273.

Bis(triethylsilyl) cyclohexylboronate: Colorless liquid. Yield: 267 mg (75 %). IR (DCM): 2947, 2891, 1437, 1378, 1041, 1020, 976, 861, 677 cm⁻¹. ¹H NMR (CDCl₃): δ 1.33-1.22 (m, 11H, CyCH₂), 0.94 (t, 18H, *J* = 8 Hz, SiCH₂CH₃), 0.59 (q, 12H, *J* = 8 Hz, SiCH₂CH₃). ¹³C{¹H} NMR (CDCl₃): δ 34.35 (CyCH₂), 30.84 (CyCH), 25.93 (CyCH₂), 24.24 (CyCH₂), 6.78 (SiCH₃), 5.71 (SiCH₃). ¹¹B{¹H} NMR (CDCl₃): 29.79 (br. s). HRMS (EI) m/z calcd for C₁₈H₄₁BO₂Si₂: 356.2738 (M)⁺, found: 356.2742.

General Procedure for the Synthesis of Tris(trisilyl) Borate from Boric Acid: To an oven dried schlenk-tube silane (3mmol), boric acid (1 mmol, 60 mg), [$\{(\eta^6\text{-}p\text{-cymene})\text{RuCl}\}_2(\mu\text{-H}-\mu\text{-Cl})$] **2** (0.006 mmol) and toluene (2 mL) were added under nitrogen atmosphere. Degassed water (10 mmol, 180 μl) was added and the reaction mixture was allowed to stir for 5 h at room temperature for the complete formation of silanol. Then the schlenk-tube was immersed into a pre-heated oil bath at 125 °C and stirred for 24h. After the reaction mixture was cooled to rt, the solvent was evaporated under vacuum and the product was extracted with hexane (2mL x 3, if the product is not soluble in hexane then hexane/ether solution is used for the extraction). Organic

layers were combined, filtered through a short plug of celite and the filtrate was evaporated under reduced pressure to obtain tris(trisilyl) borate.

Spectral Data of Tris(trisilyl)borates:

Tris(triethylsilyl) borate:¹⁹ Colorless liquid. Yield: 335 mg (83 %). IR (DCM): 2949, 2895, 1441, 1376, 1036, 978, 871, 756, 679 cm^{-1} . ^1H NMR (CDCl_3): δ 0.95 (t, 27H, $J = 8$ Hz, SiCH_2CH_3), 0.60 (q, 18H, $J = 8$ Hz, SiCH_2CH_3). $^{13}\text{C}\{^1\text{H}\}$ NMR (CDCl_3): δ 6.80 (SiCH_2CH_3), 5.63 (SiCH_2CH_3). $^{11}\text{B}\{^1\text{H}\}$ NMR (CDCl_3): 21.17 (br. s). HRMS (EI) m/z calcd for $\text{C}_{18}\text{H}_{45}\text{BO}_3\text{Si}_3$: 404.2770 (M^+), found: 407.2772.

Tris(tripropylsilyl) borate: Colorless liquid. Yield: 413 mg (78 %). IR (DCM): 2948, 2891, 1437, 1391, 1044, 971, 876, 683 cm^{-1} . ^1H NMR (CDCl_3): δ 1.41-1.32 (m, 18H, $\text{SiCH}_2\text{CH}_2\text{CH}_3$), 0.96 (t, 27H, $J = 8$ Hz, $\text{SiCH}_2\text{CH}_2\text{CH}_3$), 0.59 (t, 18H, $J = 8$ Hz, $\text{SiCH}_2\text{CH}_2\text{CH}_3$). $^{13}\text{C}\{^1\text{H}\}$ NMR (CDCl_3): δ 18.53 ($\text{SiCH}_2\text{CH}_2\text{CH}_3$), 17.70 ($\text{SiCH}_2\text{CH}_2\text{CH}_3$), 16.85 ($\text{SiCH}_2\text{CH}_2\text{CH}_3$). $^{11}\text{B}\{^1\text{H}\}$ NMR (CDCl_3): 21.43 (br. s). HRMS (EI) m/z calcd for $\text{C}_{27}\text{H}_{63}\text{BO}_3\text{Si}_3$: 530.4178 (M^+), found: 530.4180.

Tris(triisobutyl) borate: Colorless liquid. Yield: 473 mg (72 %). IR (DCM): 2948, 2899, 1437, 1378, 1260, 1041, 981, 765, 673 cm^{-1} . ^1H NMR (CDCl_3): δ 1.82-1.72 (m, 9H, $^i\text{PrCH}$), 0.95 (d, $J = 4$ Hz, 54H, $^i\text{PrCH}_3$), 0.59 (d, $J = 4$ Hz, 18H). $^{13}\text{C}\{^1\text{H}\}$ NMR (CDCl_3): δ 26.11 ($^i\text{PrCH}_3$), 25.56 ($^i\text{PrCH}$), 23.19 (SiCH_2). $^{11}\text{B}\{^1\text{H}\}$ NMR (CDCl_3): 21.36 (br. s). HRMS (EI) m/z calcd for $\text{C}_{36}\text{H}_{81}\text{BO}_3\text{Si}_3$: 656.5587 (M^+), found: 656.5587.

Tris(triphenylsilyl)borate: Colorless liquid. Yield: 585 mg (70 %), mp 210-211 $^\circ\text{C}$. IR (DCM): 3015, 2956, 2894, 1444, 1271, 1039, 975, 861, 774, 669 cm^{-1} . ^1H NMR (CDCl_3): δ 7.68 (t, 18H, $J = 4$ Hz, ArCH), 7.52-7.44 (m, 27H, ArCH). $^{13}\text{C}\{^1\text{H}\}$ NMR (CDCl_3): δ 136.00 (ArCH), 133.51 (quat-C), 130.00 (ArCH), 128.21 (ArCH).

$^{11}\text{B}\{^1\text{H}\}$ NMR(CDCl_3): 21.68 (br. s). HRMS (EI) m/z calcd for $\text{C}_{54}\text{H}_{45}\text{BO}_3\text{Si}_3$: 836.2770 (M)⁺, found: 836.2771.

Determination of the Molecular Structure of 8 in the Solid State by X-ray Single Crystal Diffraction: Single crystals of compound **8** suitable for X-ray analysis was obtained from the solution of hexane and ether. A suitable crystal was mounted on a glass fiber. The geometry and intensity data were collected using Bruker SMART D8 goniometer equipped with an APEX CCD detector and an Incoatec microsource (Mo- $\text{K}\alpha$ radiation, $\lambda = 0.71073 \text{ \AA}$, multilayer optics). Temperature was controlled using an Oxford Cryostream 700 instrument. Intensities were integrated with SAINT⁺²⁰ and corrected for absorption with SADABS.²¹ The structure was solved by direct methods and refined on F2 with SHELXL-97.²²

Crystal Data: $2(\text{C}_{54}\text{H}_{45}\text{BO}_3\text{Si}_3)$, $\text{C}_{36}\text{H}_{30}\text{OSi}_2$, crystal dimensions: $0.25 \times 0.21 \times 0.19$, monoclinic with space group P121/c, $a = 18.8982(9)(7) \text{ \AA}$, $b = 18.8982(9) \text{ \AA}$, $c = 28.7167(14) \text{ \AA}$, $\alpha = 90^\circ$, $\beta = 90^\circ$, $\gamma = 120^\circ$, $V = 8881.9(10) \text{ \AA}^3$, $Z = 3$, $T = 100 \text{ K}$, $2\theta_{\text{max}} = 30.22$, $\rho_{\text{calcd}} = 1.239 \text{ g/cm}^3$, $\mu(\text{MoK}\alpha) = 0.150 \text{ mm}^{-1}$. min/max transmission factors = 0.4100/0.7461, 3662 Reflections collected, 3203 unique ($R_1 = 0.0475$), $WR_2 = 0.1197$ (all data). The structure has been deposited at the CCDC data center and can be retrieved by using the number CCDC **1483484**.

Detection of Hydrogen Evolution During Silanol Formation by Labeling

Experiment with D_2O :

In a screw cap NMR tube triethylsilane (0.25 mmol, 40 μl), catalyst **2** (0.0005 mmol, 0.3 mg), D_2O (0.25 mmol, 5 μl) and C_6D_6 (0.4 mL) were taken under nitrogen atmosphere and monitored by ^1H NMR spectroscopy at room temperature for 2 h.

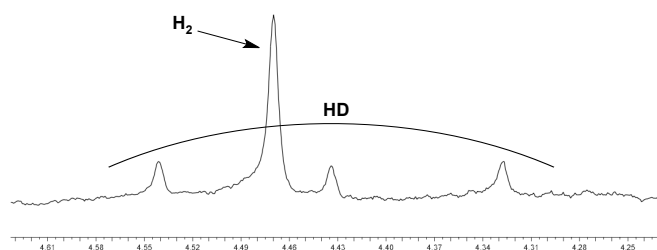
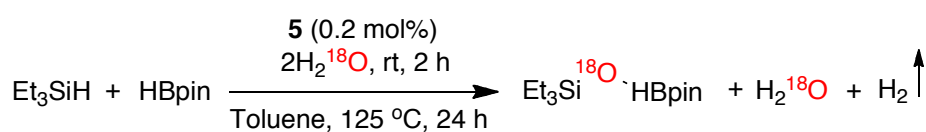


Figure 9.1 ^1H NMR spectrum of labeling experiment with D_2O (H_2 and HD region).

ESI-MS Analysis by Using Labeled Water (H_2^{18}O) to Verify Oxygen Source in Borasiloxane:



To an oven dried Schlenk-tube, triethylsilane (1mmol, 159 μl), pinacolborane (1 mmol, 145 μl), $[\text{Ru}(\text{p-cymene})\text{Cl}_2(\text{pyridine})]$ **5** (0.002 mmol) and toluene (2 mL) were added under nitrogen atmosphere. Degassed labeled water H_2^{18}O (3 mmol, 60 μl) was added and the reaction mixture was stirred for 2 h for the complete formation of $\text{Et}_3\text{Si}^{18}\text{OH}$ and $\text{PinB}^{18}\text{OH}$. The Schlenk-tube was then immersed into a pre-heated oil bath at 125 $^\circ\text{C}$ and heated for 24 h. After the completion of the reaction, the solvent was evaporated under vacuum and the product was extracted with hexane (2mL X 3 times). Combined hexane solution was filtered through a short plug of celite and the filtrate was evaporated under reduced pressure to produce borasiloxane. Mass spectrum was recorded on Bruker micrOTOF-Q II Spectrometer by positive tune low mode method. (EI) m/z 299.15 ($\text{M}+\text{K}$) $^+$. HRMS: Calcd $[\text{C}_{12}\text{H}_{27}\text{SiB}^{(16}\text{O})_2^{18}\text{OK}]$: 299.1501, found 299.1521.

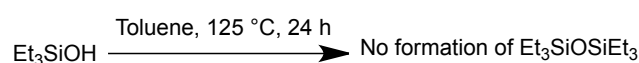
Experiments to Comprehend Condensation Mechanism:

Verification of the Formation of B–O–B Bond (Homocondensation Product):



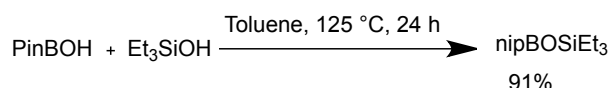
To an oven dried Schlenk-tube, hydroxypinacolborane (1 mmol) and toluene (2 mL) were added under nitrogen atmosphere then the Schlenk-tube was immersed into a pre-heated oil bath of 125 °C and stirred for 24 h. After completion of the reaction, the solvent was evaporated under vacuum and the product was washed with hexane (2mL X 3). The white solid obtained was dried under vacuum which provided the hydroxypinacolborane quantitatively.

Verification of the Formation of Si–O–Si Bond (Homocondensation Product):



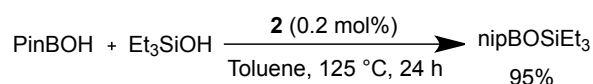
To an oven dried Schlenk-tube, triethylsilanol (1 mmol) and toluene (2 mL) were added under nitrogen atmosphere then the Schlenk-tube was immersed into a pre-heated oil bath of 125 °C and stirred for 24 h. After completion of the reaction, the solvent was evaporated under vacuum and the product was extracted with hexane (2mL X 3). Combined hexane solution was filtered through a short plug of celite and the filtrate was evaporated under reduced pressure, which provided the triethylsilanol quantitatively.

Condensation Reaction of Hydroxypinacolborane and Triethylsilanol:



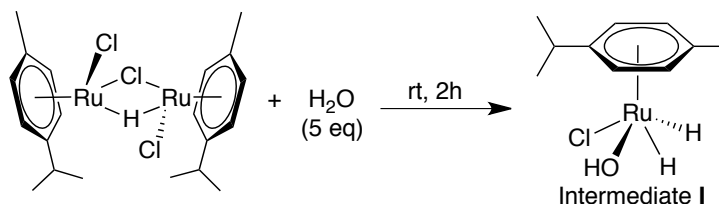
To an oven dried Schlenk-tube, hydroxypinacolborane (1 mmol), triethylsilanol (1 mmol) and toluene (2 mL) were added under nitrogen atmosphere then the Schlenk-tube was immersed into a pre-heated oil bath at 125 °C and stirred for 24 h. After completion of the reaction, the solvent was evaporated under vacuum and the product was extracted with hexane (2mL X 4). Combined hexane solution was filtered through a short plug of celite and the filtrate was evaporated under reduced pressure to obtain borasiloxane.

Interpretation of Catalyst's Role on Condensation Reaction:



To an oven dried Schlenk-tube, hydroxypinacolborane (1 mmol), triethylsilanol (1 mmol), [$\{(\eta^6\text{-}p\text{-cymene})\text{RuCl}\}_2(\mu\text{-H}-\mu\text{-Cl})$] **2** (0.002 mmol) and toluene (2 mL) were added under nitrogen atmosphere then the Schlenk-tube was immersed into a pre-heated oil bath at 125 °C and stirred for 24 h. Upon heating the reaction mixture turned black in 15 minutes and Ru-black particles appeared in solution. After completion of the reaction, the solvent was evaporated under vacuum and the product was extracted with hexane (2mL X 4). Combined hexane solution was filtered through a short plug of celite and the filtrate was evaporated under reduced pressure to obtain borasiloxane.

ESI-MS Analysis to Observe Intermediate I:



To a scintillation reaction vial, monohidrido bridged ruthenium intermediate **2** (10 mg, 0.017 mmol), degassed water (1.5 μl , 0.085 mmol) and 1,4-dioxane (50 μl) as solvent were added and stirred for 2h. The resulting reaction mixture then passed through small plug of celite under nitrogen atmosphere. Mass spectrum was recorded on Bruker micrOTOF-Q II Spectrometer.

Figure 9.2 Mass spectrum (Intermediate I): $\text{C}_{36}\text{H}_{60}\text{B}_3\text{NO}_7\text{Ru}$: $(\text{M}-\text{H})^+$ 289.0 (Theoretical)

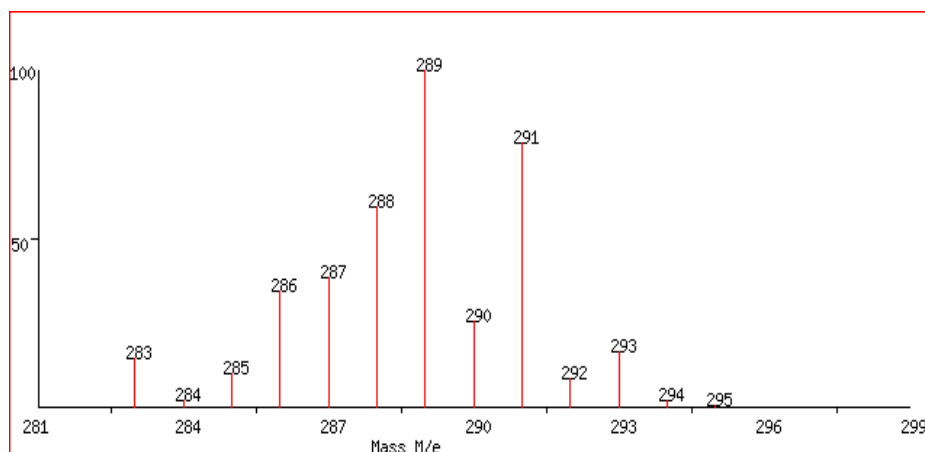
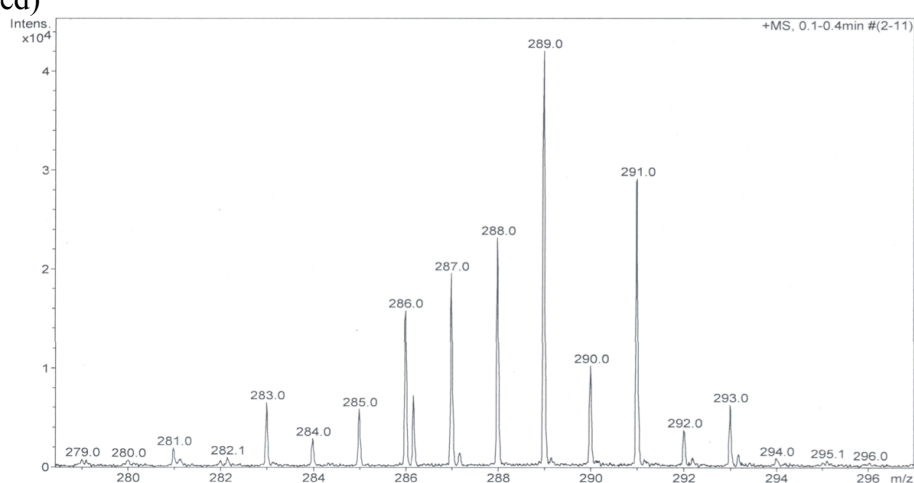


Figure 9.3 Mass spectrum (Intermediate I): $C_{36}H_{60}B_3NO_7Ru$: $(M-H)^+$ 289.0 (obtained)



9.6 NOTES AND REFERENCES

(1) (a) Hall, D. G. (Ed.). *Boronic Acids: Preparation and Applications in Organic Synthesis, Medicine and Materials*. 2nd edn, Wiley-VCH, Weinheim, 2011. (b) Hosmane, N. S. (Ed.). *Boron Science: New Technology and Applications* CRC press, Florida, 2012. (c) Davidson, M. G.; Hughes, A. K.; Marder, T. B.; Wade, K. (Eds.) *Contemporary Boron Chemistry* RSC, Cambridge, 2000.

(2) (a) Neville, L. A.; Spalding, T. R.; Ferguson, G. *Angew. Chem., Int. Ed.* **2000**, *39*, 3598-3601. (b) Fujinami, T; Mehta, M. A.; Sugie, K.; Mori, K. *Electrochim. Acta.* **2000**, *45*, 1181-1186. (c) Rees, W. S.; *CVD of Nonmetals* VCH, New York, 1996. (d) Foucher, D. A.; Lough, A. J.; Manners, I. *Inorg. Chem.* **1992**, *31*, 3034-3043. (e) Soraru, G. D.; Dallabona, N.; Gervais, C.; Babonneau, F. *Chem. Mater.* **1999**, *11*, 910-

919. (f) Wang, Q.; Fu, L.; Hu, X.; Zhang, Z.; Xie, Z. *J. Appl. Polym. Sci.* **2006**, *99*, 719-724. (g) Peña-Alonso, R.; Mariotto, G.; Gervais, C.; Babonneau, F.; Soraru, G. D. *Chem. Mater.* **2007**, *19*, 5694-5702.
- (3) Liu, W.; Pink, M.; Lee, D. *J. Am. Chem. Soc.* **2009**, *131*, 8703-8707.
- (4) (a) Makarova, E. A.; Shimizu, S.; Matsuda, A.; Luk'yanets, E. A.; Kobayashi, N. *Chem. Commun.* **2008**, 2109-2111. (b) Andrianov, K. A.; Vasil'eva, T. V. *Chem. Abstr.* **1968**, *69*, 87069. (c) Pascu, M.; Ruggi, A.; Scopelliti, R.; Severin, K. *Chem. Commun.* **2013**, *49*, 45-47. (d) Ferguson, G.; Lawrence, S. E.; Neville, L. A.; O'Leary, B. J.; Spalding, T. R. *Polyhedron* **2007**, *26*, 2482-2492. (e) Zhao, Z.; Cammidge, A. N.; Cook, M. J. *Chem. Commun.* **2009**, 7530-7532. (f) Furdala, K. L.; Oliver, A. G.; Hollander, F. J.; Tilley, T. D. *Inorg. Chem.* **2003**, *42*, 1140-1150.
- (5) (a) Masaoka, S.; Banno, T.; Ishikawa, M. *J. Organomet. Chem.* **2006**, *691*, 174-181. (b) Kanth, J. V. B.; Brown, H. C. *J. Org. Chem.* **2001**, *66*, 5359-5365. (c) Bates, T. F.; Dandekar, S. A.; Longlet, J. J.; Wood, K. A.; Thomas, R. D. *J. Organomet. Chem.* **2000**, *595*, 87-92.
- (6) (a) Marciniak, B.; Walkowiak, J. *Chem. Commun.* **2008**, 2695-2697. (b) Frackowiak, D.; Walkowiak, J.; Hreczycho, G.; Marciniak, B. *Eur. J. Inorg. Chem.* **2014**, 3216-3220.
- (7) Ito, M.; Itazaki, M.; Nakazawa, H. *J. Am. Chem. Soc.* **2014**, *136*, 6183-6186.
- (8) Chatterjee, B.; Gunanathan, C. *Chem. Commun.* **2014**, *50*, 888-890.
- (9) (a) Kaithal, A.; Chatterjee, B.; Gunanathan, C. *Org. Lett.* **2015**, *17*, 4790-4793. (b) Kaithal, A.; Chatterjee, B.; Gunanathan, C. *Org. Lett.* **2016**, *18*, 3402-3405. (c) Kaithal, A.; Chatterjee, B.; Gunanathan, C. *J. Org. Chem.* **2016**, *81*, 11153-11161.
- (10) (a) Jeon, M.; Han, J.; Park, J. *ACS Catal.* **2012**, *2*, 1539-1549. (b) Tan, S. T.; Kee, J. W.; Fan, W. Y. *Organometallics* **2011**, *30*, 4008-4013. (c) Lee, Y.; Seomoon, D.;

Kim, S.; Han, H.; Chang, S.; Lee, P. H. *J. Org. Chem.* **2004**, *69*, 1741-1743. (d) Lee, M.; Ko, S.; Chang, S. *J. Am. Chem. Soc.*, **2000**, *122*, 12011-12012. (e) Ojima, Y.; Yamaguchi, K.; Mizuno, N. *Adv. Synth. Catal.* **2009**, *351*, 1405-1411.

(11) Spalding, T. R.; O'Leary, B. J.; Neville, L.; Ferguson, G. in Ref. 1c, pp. 92-95.

(12) As the reaction proceeded, ¹H NMR signal corresponds to Si-H ($\delta = 3.67$ ppm, multiplet) disappeared and a singlet signal $\delta = 2.05$ ppm, corresponds to Si-OH emerged.

(13) This minor intermediate complex remains elusive to isolation and further characterization. However, the previously observed [Ru(H)₂(SiEt₃)₂(η^6 -*p*-cymene)] complex ($\delta -13.53$ ppm) was not involved in this reaction. See Ref. 8.

(14) See figure 9.2 and 9.3.

(15) (a) Fioravanti, S.; Pellacani, L.; Tardella, P. A.; Vergari, M. C. *Org. Lett.* **2008**, *10*, 1449-1451. (b) Crombie, L.; Ponsford, R. *J. Chem. Soc.* **1971**, 788-795.

(16) Upon heating a toluene solution of triethylsilanol and hydroxyborane in the presence of pyridine (4 mol%), 50% borasiloxane formation was observed in 4 h, indicating influence of pyridine in this condensation reaction.

(17) (a) Chatterjee, B.; Gunanathan, C. *Org. Lett.* **2015**, *17*, 4794-4797. (b) Gunanathan, C.; Milstein, D. *Acc. Chem. Res.* **2011**, *44*, 588-602. (c) Gunanathan, C.; Milstein, D. *Chem. Rev.* **2014**, *114*, 12024-12087.

(18) Abel, E. W.; Singh, A. *J. Chem. Soc.* **1959**, 690-693.

(19) J. A. Gerbec, *Process for Synthesis of Hybrid Siloxy Derived Resins and Cross Linked Networks Therefrom*, US 2014/0142242 A1, May 22, 2014.

(20) Bruker AXS, SAINT⁺, *Program for Reduction of Data collected on Bruker CCD Area Detector Diffractometer V. 6.02*. Bruker AXS Inc., Madison, Wisconsin, USA, 1999.

(21) Bruker AXS, SADABS, *Program for Empirical Absorption Correction of Area Detector Data V 2004/1*, Bruker AXS Inc., Madison, Wisconsin, USA, 2004.

(22) G. M. Sheldrick, *Acta Crystallogr.* 2008, **A64**, 112-122

^1H and ^{13}C NMR spectra of borasiloxanes:

Figure 9.4 ^1H NMR spectrum of triethyl((4,4,5,5-tetramethyl-1,3,2-dioxaborolan-2-yl)oxy)silane:

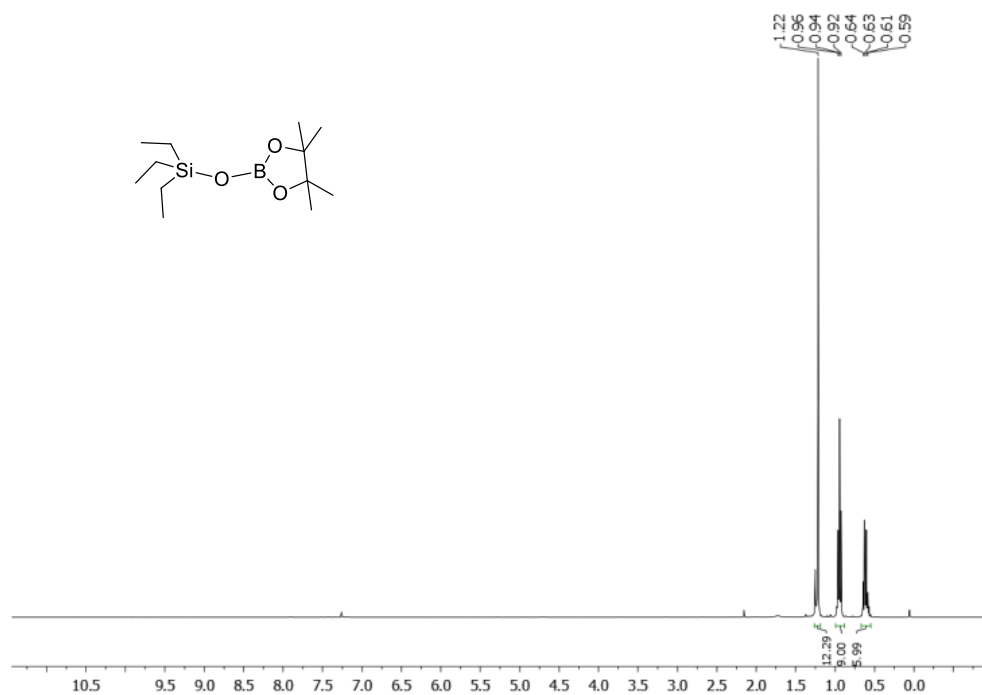


Figure 9.5 ^{13}C NMR spectrum of triethyl((4,4,5,5-tetramethyl-1,3,2-dioxaborolan-2-yl)oxy)silane:

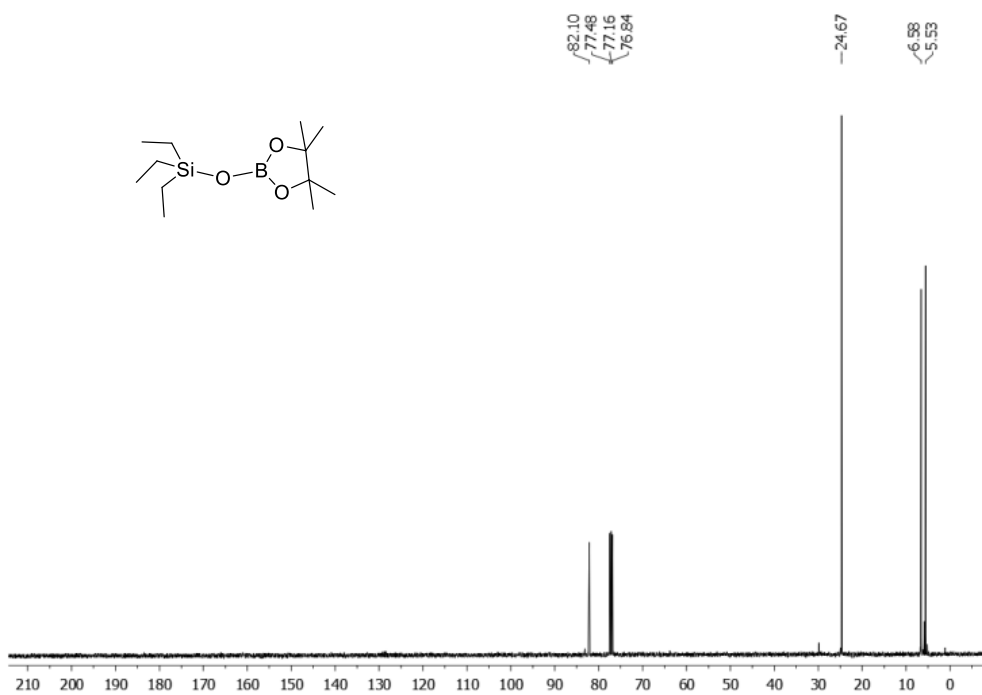


Figure 9.6 ^1H NMR spectrum of bis(triethylsilyl) methylboronate:

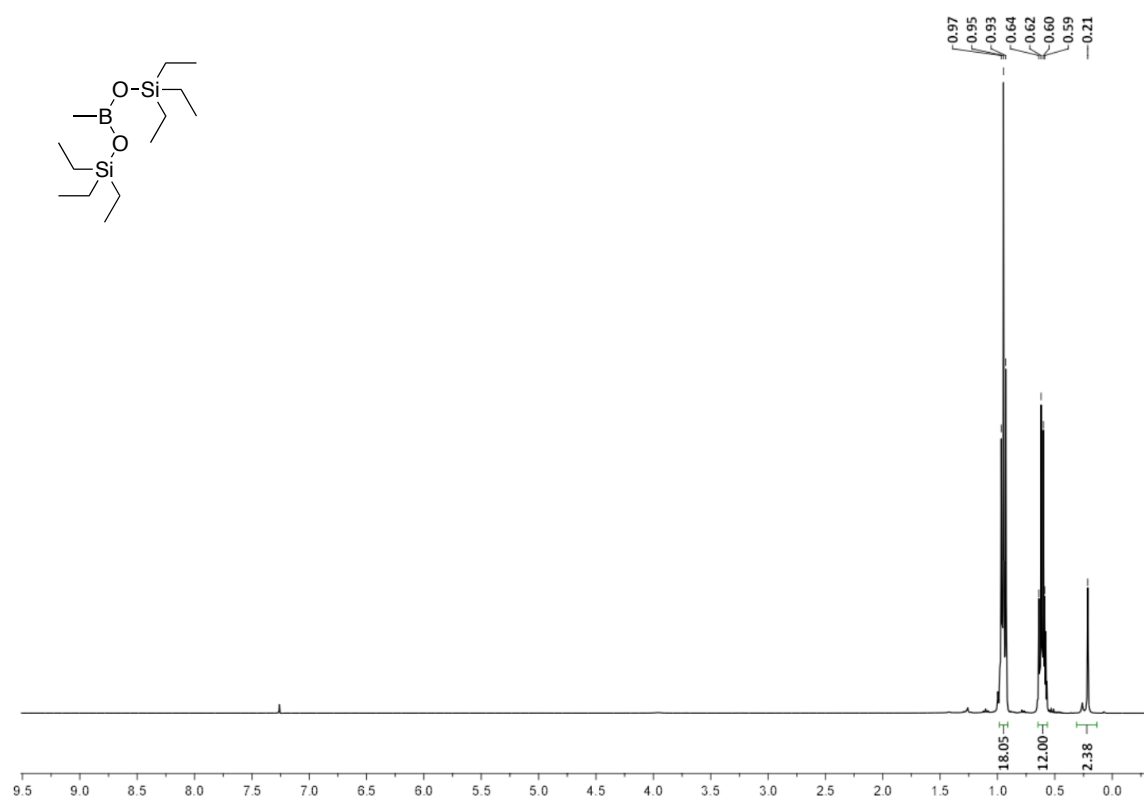


Figure 9.7 ^{13}C NMR spectrum of bis(triethylsilyl) methylboronate:

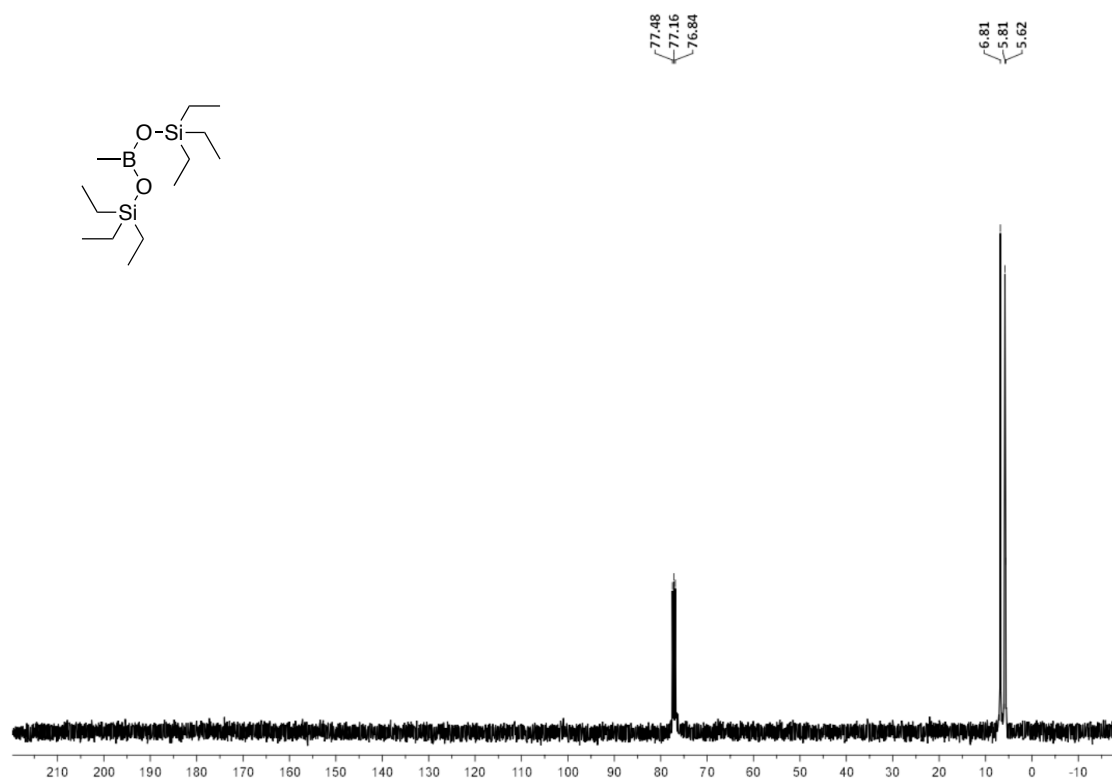


Figure 9.8 ^1H NMR spectrum of tris(tripropylsilyl) borate:

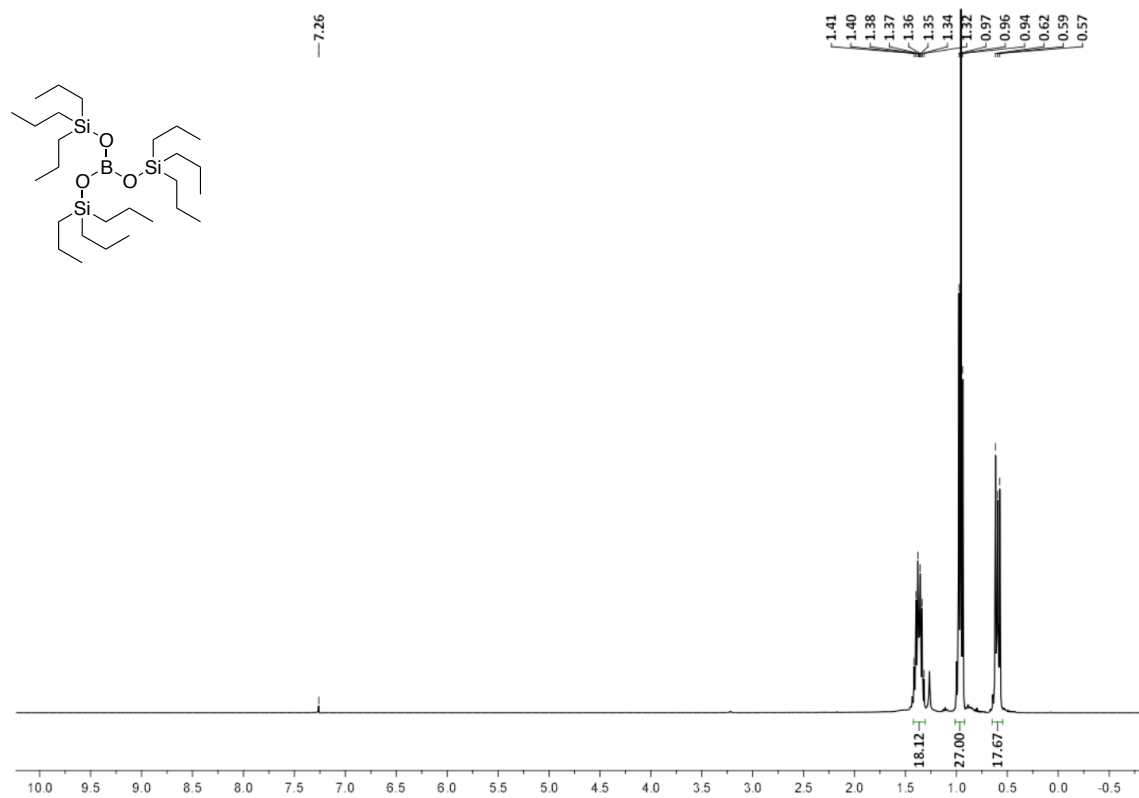
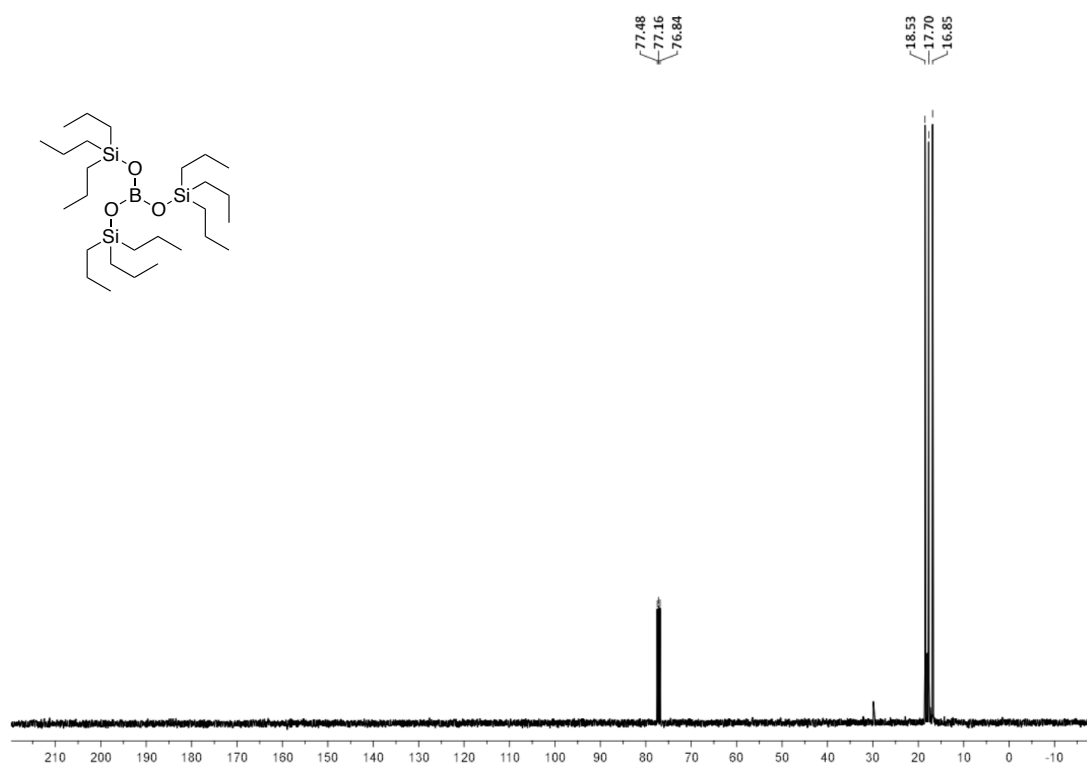


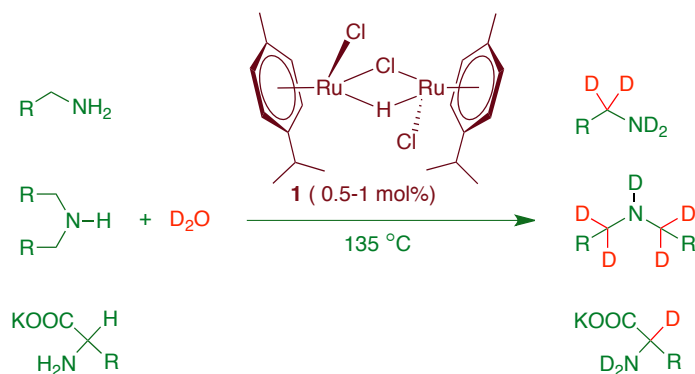
Figure 9.9 ^{13}C NMR spectrum of tris(tripropylsilyl) borate:



CHAPTER 10

Selective α -Deuteration of Amines and Amino Acids Using D_2O

10.1 ABSTRACT



Monohydrido-bridged ruthenium complex $[\{(\eta^6\text{-}p\text{-cymene})RuCl\}_2(\mu\text{-}H\text{-}\mu\text{-}Cl)]$ catalyzes (catalyst load: 0.5-1 mol %) α -selective deuteration of primary and secondary amines, amino acids, and drug molecules using deuterium oxide (D_2O) as a deuterium source. Mechanistic investigations revealed $N\text{-}H$ activation of amines, which was also established by single-crystal X-ray analysis of an intermediate. β -Hydride elimination on amide ligand results in formation of imine ligated ruthenium intermediate and subsequent 1,3-deuteride migrations to imine ligand leading to the selective deuteration at the $\alpha\text{-}CH_2$ protons of amine functionality is proposed.

10.2 INTRODUCTION

Selective deuteration of organic compounds is one of the important transformations in chemical synthesis, as deuterated organic compounds find widespread applications as NMR solvents, mechanistic probe in chemical and biological processes, biologically active compounds, and pharmaceuticals.¹ Deuterated organic compounds are uniquely suited as internal standards for quantitative LC-MS/MS analysis of life science samples.² Organic light-emitting diodes and optical fibers for high-speed telecommunication systems are also derived from them.³ Deuteration of the reactive

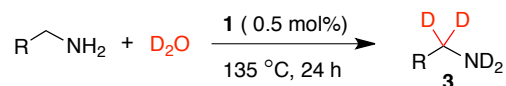
site repressed the undesired reaction pathways due to a kinetic isotopic effect, which was assimilated in the total synthesis of norzoanthamine.⁴ When the metabolism of drugs involves cleavage of C–H bonds, deuteration of those covalently bound hydrogen atoms can provide an improved metabolomics profile and prevent formation of toxic metabolites.⁵ Isotopically labeled drug candidates play a crucial role in understanding the metabolic profile of drug molecules and their toxicity assessment.⁶ Thus, direct catalytic deuteration of these target molecules by C–H activation⁷ is a highly desired protocol. From this perspective, deuteration of amines and amino acids gains significant importance, as around 92% of the drug candidates are nitrogen-containing compounds. Rhodium and ruthenium catalysts are well explored for the synthesis of deuterated amines.⁸ However, catalytic methods reported for the deuteration of primary and secondary amines essentially employ very limited high molecular weight non-functionalized amines and suffer from harsh reaction conditions, low labeling, and poor selectivity.⁹ Ruthenium-catalyzed deuteration of primary and secondary amines was reported to occur under a high-pressure setup (3 mol % of catalyst, 150 °C, and 10 atm).^{9a} Deuteration of secondary amines using a high load of ruthenium complexes (33.33 mol %, 150 °C) in DMSO-d₆ /D₂O (5:1) medium together with DMF as cosolvent was also reported.^{9b} Selective α,β -deuteration of tertiary amines was achieved by using Shvo's catalyst (5–10 mol %, 150 °C).¹⁰ Recently, polymer-supported ruthenium nanoparticle catalyzed α -deuteration of amines¹¹ using deuterium gas (1–2 bar D₂) as a deuterium source was revealed in which only 40% deuteration occurred on primary amines. α -Selective deuteration of amino acids remains a challenge, and it has been scarcely studied.^{1,12} Sajiki and co-workers reported a heterogeneous Pd/C–H₂ /D₂O catalytic system that required prolonged heating at high temperature (160 °C, 48 h) for the moderate

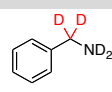
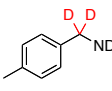
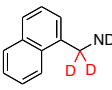
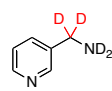
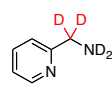
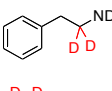
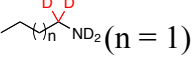
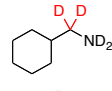
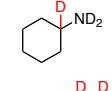
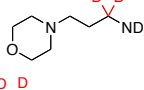
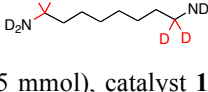
deuteration at the α -position of 1-phenylalanine.¹³ α -Deuterated glycine and its derivatives are often synthesized in multistep synthetic procedures (up to 9 synthetic steps) involving imine formation¹⁴ or bislactim ether formation.¹⁵ Recently, we reported the ruthenium pincer complex catalyzed selective deuteration of alcohols and terminal alkynes.¹⁶ Herein, we report a monohydrido-bridged dinuclear complex [$\{\eta^6\text{-p-cymene}\text{RuCl}\}_2(\mu\text{-H}-\mu\text{-Cl})$] (**1**) catalyzed¹⁷ facile selective α -deuteration of amines and amino acids using deuterium oxide as a deuterium source.

10.3 RESULTS AND DISCUSSIONS

At the outset, we performed the deuteration of benzylamine using complex **1** (0.5 mol %) in D₂O (0.4 mL) at 135 °C for 24 h and found excellent deuterium incorporation (95%) at sp³- α -CH₂ protons. Reducing the catalyst load to 0.2 mol % led to the partial deuterium incorporation (55%). Thus, an assortment of primary amines was subjected to this catalytic deuteration using 0.5 mol % of **1**, which resulted in efficient deuteration at their α -CH₂ positions. Arylmethylamines (entries 1-3, Table 10.1), 2-picolylamine, and 3-picolylamine provided facile deuteration at the α -CH₂ position (entries 4 and 5), despite the fact that 2-picolylamine is well known for its coordination ability with ruthenium.¹⁸ A series of linear aliphatic amines displayed facile deuteration selectively at α -CH₂ (entries 6-13). When Cyclohexylmethylamine and cyclohexylamine were reacted (entries 14 and 15), 77% and 70% deuteration were obtained, respectively, in their α -CH₂ positions. Octane-1,8-diamine exhibited efficient deuteration at both α -CH₂ positions. Notably, no detectable deuteration at β -CH₂ position is observed in these acyclic amines and diamines (entries 11-17, Table 10.1).

Table 10.1 Selective α -Deuteration of Primary Amines^a



entry	product	deuteration (%) ^b	D _n ^c	
1		3a	95	1.9
2		3b	75	1.5
3		3c	81	1.62
4		3d	95	1.9
5		3e	95	1.9
6 ^d		3f	80:4	1.68
7		3g	57	1.14
8 ^d	(n = 2)	3h	90:9	1.98
9 ^d	(n = 3)	3i	91:6	1.94
10 ^d	(n = 4)	3j	92:2	1.88
11	(n = 5)	3k	91	1.82
12	(n = 9)	3l	80	1.6
13	(n = 15)	3m	91	1.82
14		3n	77	1.54
15 ^e		3o	70	0.7
16 ^f		3p	85	1.7
17 ^{g,h}		3q	81	3.24

^aPrimary amine (0.5 mmol), catalyst **1** (0.0025 mmol, 0.5 mol %) and D₂O (0.4 mL, 20 mmol) were charged in a scintillation vial and heated to 135 °C. ^bCalculated from the integration of residual signals in ¹H NMR spectra. Maximum theoretical % of deuteration is 95.23%. ^cAverage number of catalytically exchanged deuterium atoms per molecule (excluding the labile heteroatom-H protons). ^dMinor amount (2-9%) of β-deuteration is also occurred. ^eMaximum theoretical % deuterium incorporation is 96.38%. ^fReaction carried out at 150 °C. ^g1 mol % catalyst **1** is used. ^hMaximum theoretical % deuterium incorporation is 90.90%.

Secondary amines were tested in catalytic selective deuteration using 1 mol % of **1**

(Table 10.2). Interestingly, when *N*-methyl-*N*-benzylmethylamine was subjected to catalysis, deuteration occurred only at *N*-methyl protons. Surprisingly, *N*-benzylic “CH₂” protons remained unaffected (entry 1, Table 10.2). Dibutylamine showed 71% deuterium incorporation (entry 2). When dihexylamine and cyclic secondary amines were examined, efficient deuteration at both α -positions occurred and provided products with high D content (D_n: 3.0-6.8) (entries 3-6). Piperazine was deuterated over all α -CH₂ positions (entry 7, Table 10.2). Unlike Shvo’s catalyst, complex **1** was not effective in deuteration of tertiary amines, indicating different reactivity.¹⁰

Table 10.2 Selective α -Deuteration of Secondary Amines^a

entry	product	deuteration (%) ^b	D _n ^c
1 ^d		95	2.85
2 ^e		71	2.84
3 ^{e,f}		89	3.56
4 ^{e,f}		75	3.0
5 ^e		79	3.16
6 ^{f,g}		85	6.8
7 ^{f,g,h}		83	6.64

^{a,b,c}As shown in footnote of Table 10.1 (catalyst **1** (0.005 mmol, 1 mol %) is used). Maximum theoretical % of deuteration: ^d95.23%; ^e94.11%; ^f88.88%. ^g0.01 mmol of **1** is used. ^hReaction carried out at 150 °C and 1,4-dioxane (80 μ l) used as internal standard.

As complex **1** turned out to be the most efficient catalyst for the selective α -

deuteration of primary and secondary amines, we further envisaged expanding its scope to the labeling of biologically active molecules and amino acids. When L-phenylalanine was tested no significant deuterium incorporation was observed, perhaps attributable to the dilapidation of Ru-hydride catalyst **1** in the presence of carboxylic acid functionality. To circumvent this setback, reactions were carried out with the potassium salt of L-phenylalanine (preneutralized with 1 equiv. of KOH), and 84% α -deuteration was observed (entry 1, Table 10.3). The control experiment carried out with base (1 equiv) and without catalyst led to only 17% deuteration (entry 2). A series of proteinogenic, highly useful essential amino acids¹⁹ were subjected to catalysis by **1** using deuterium oxide. Tyrosine exhibited only 40% deuteration due to low solubility (entry 3). Glycine exhibited 89% α -deuterium incorporation (entry 4). Alanine also showed 71% deuterium incorporation (entry 5). Hydroxy functionality containing serine showed facile H/D exchange chemoselectively at α -CH₂ of amines, where α -CH₂ related to alcohol functionality^{16a} remains unaffected (entry 6), offering further opportunity for selective deuteration toward amines α -CH₂ by catalyst **1**. Embedded with sulfur heteroatom, methionine displayed efficient H/D exchange at the α -CH₂ of amine (entry 7, Table 10.3). Further, moderate to excellent deuteration occurred on isoleucine, aspartic acid, methyl ester of serine, valine, and cyclic amino acid proline (entries 8-12). Notably, the β -deuteration is observed only on linear acyclic primary amines such as pentyl-, hexyl-, heptyl-, and phenethylamines (2-9%). On other primary amines, primary diamines, secondary amines, and amino acids no such β -deuteration is observed, indicating the high selectivity of this method for the α -deuteration of amine functionalities.

Table 10.3 Selective α -Deuteration of Amino acids^a

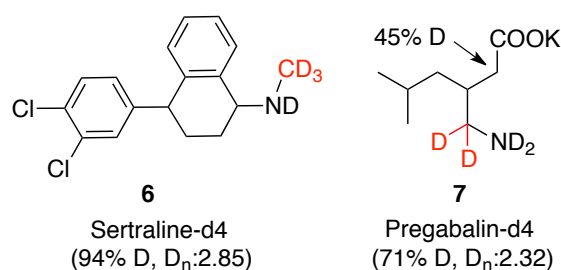
entry	product		deuteration (%) ^b	D _n ^c
1		5a	84	0.84
2 ^d		5a	17	0.17
3 ^e		5b	40	0.4
4 ^{e,f}		5c	89	1.78
5		5d	71	0.71
6 ^e		5e	86	0.86
7		5f	70	0.7
8		5g	50	0.5
9		5h	73	0.73
10 ^e		5i	93	0.93
11		5j	80	0.8
12 ^{e,g}		5k	80, 50	1.8

^aAmino acid (0.5 mmol), KOH (0.5 mmol), and D₂O (0.6 mL, 30 mmol) were charged in a scintillation vial and stirred for 30 minutes at rt. Then catalyst **1** (0.005 mmol, 1 mol %) in 1,4-dioxane (stock solution) was added and heated to 135 °C for 36 h. ^bCalculated from the integration of residual signals in ¹H NMR spectra. Maximum theoretical % deuterium incorporation is 97.56%. ^cAverage number of catalytically exchanged deuterium atoms per molecule. ^dControl experiment, verified twice. ^eMaximum theoretical % deuterium incorporation is 96.77%. ^f1,4-dioxane (40 μl) used as internal standard. ^gCatalyst used 0.01 mmol.

Sertraline **6** is an antidepressant, used for the treatment of anxiety disorders, post-traumatic stress disorder (PTSD), and premenstrual dysphoric disorder (PMDD). When reacted with deuterium oxide and catalyst **1** under the experimental conditions established for the amino acids, 94% deuteration (96.77% maximum theoretical % deuterium) at the N-methyl protons of sertraline occurred (Scheme 10.1). Deuteration

occurred selectively on N-methyl protons over the α -proton on the cyclohexyl ring, perhaps due to the steric hindrance. Similarly, pregabalin **7**, a medicine used for treating pain caused by nerve damage due to diabetes, shingles (herpes zoster) infection, and fibromyalgia, exhibited 71% deuteration at the α -CH₂ protons to the amine group. Conditions for deuteration catalyzed by **1** can be further optimized for individual drug molecules to achieve higher deuteration.

Scheme 10.1 Catalytic Deuteration of Pharmaceuticals



Stoichiometric reactions of complex **1** with benzylamine at rt led to immediate formation of a new cationic mononuclear Ru(IV) hydride complex **2**, resulting from an unprecedented N–H bond activation²⁰ of benzylamine, which showed the corresponding hydride signal at δ –5.5 ppm in ¹H NMR spectroscopy.²¹ The structure of complex **2** is unequivocally corroborated using single-crystal X-ray analysis,²² which displayed capped pseudo octahedral geometry around the ruthenium center (Figure 10.1). Upon using isolated **2** (0.5 mol %) as a catalyst, similar deuteration as for catalyst **1** was obtained for benzylamine, indicating the involvement of **2** in catalysis.

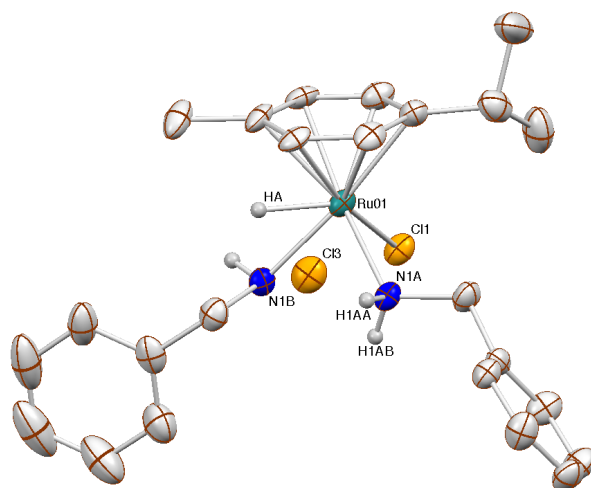
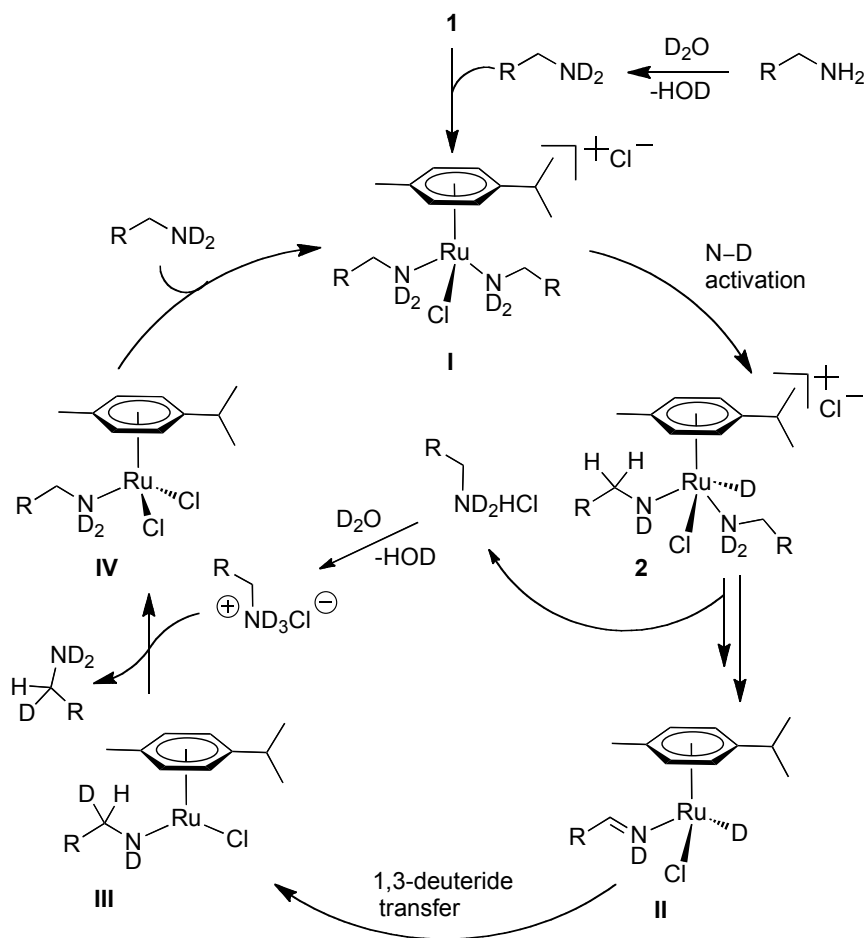


Figure 10.1 X-ray structure of [$\{\eta^6\text{-}p\text{-cymene}\}\text{RuHCl}\}\text{(NHCH}_2\text{Ph)(NH}_2\text{CH}_2\text{Ph)]Cl$ **2** (thermal ellipsoids are drawn with 50% probability)

Further, addition of mercury (50 mol %) to the catalytic deuteration (**1**, 0.5 mol %) of benzylamine and hexylamine resulted in an insignificant effect and 90% and 83% α -deuteration occurred, respectively, indicating (although not proving) the involvement of molecular organometallic intermediates. On the basis of these experimental observations, a catalytic cycle is proposed as described in Scheme 10.2. The reaction of **1** with amine provided an initial cationic ruthenium(II) coordination complex **I**. Subsequent N–H bond activation of a coordinated amine provided the observed mononuclear Ru(IV) cationic complex **2**. Further β -hydride elimination and concomitant dissociation of ammonium salt generates imine ligated Ru(II) complex **II**. A 1,3-deuteride transfer on **II** leads to the reduction of ligated imine to provide amide coordinated Ru(II) intermediate **III**. Further, reaction of **III** with quaternary amine and subsequent decooordination of amine from **III** provided partial (α -CHD) deuterated amine and a Ru(II) complex **IV**, which upon coordination of a benzylamine regenerates **I** and closes a catalytic cycle.

Scheme 10.2 Proposed Mechanism for α -Selective Deuteration of Amines and Amino Acids



10.4 CONCLUSIONS

In conclusion, a ruthenium-catalyzed selective α -deuteration of primary amines, secondary amines, amino acids and commercial drugs is demonstrated. Stoichiometric reactions revealed the involvement of Ru(IV) intermediate. The mechanism involving an unprecedented N–H activation by a cationic ruthenium complex and subsequent 1,3-deuteride transfer to in situ formed imine is proposed. High deuterium incorporation, exceptional selectivity for α -CH₂ protons to the amine functional group, and low loadings of catalyst **1** make this protocol attractive and advantageous for both laboratory and large-scale preparation of highly useful deuterated amines and amino acids.

10.5 EXPERIMENTAL SECTION

General experimental: All catalytic reactions were performed under nitrogen atmosphere. All stoichiometric reactions were performed in nitrogen atmosphere MBraun glove box. Chemicals were purchased from Acros, Sigma-Aldrich, Alfa-esar, Spectrochem and used without further purification. ^1H , ^{13}C , and DEPT spectra were recorded at Bruker AV-400 (^1H : 400 MHz, ^{13}C : 100.6 MHz, ^2H : 61 MHz). ^1H and $^{13}\text{C}\{^1\text{H}\}$ NMR chemical shifts were reported in ppm downfield from tetramethyl silane. Multiplicity is abbreviated as: s, Singlet; d, doublet; t, triplet; q, quartet; sept, septet; m, multiplet. Assignment of spectra was done based on one dimensional (dept-135) NMR technique.

Preparation of $[(\eta^6\text{-}p\text{-cymene})\text{RuCl}]_2(\mu\text{-H-}\mu\text{-Cl})$ **1:** Complex **1** is prepared by following our previous reports.¹⁷ The stock solution of **1** is prepared by dissolving 145 mg of $[(\eta^6\text{-}p\text{-cymene})\text{RuCl}]_2(\mu\text{-H-}\mu\text{-Cl})$ in 2 mL of 1,4-dioxane. The prepared stock solution then stored in glove-box freezer and further used as catalyst (solution standard concentration: $1.45 \text{ mg}/20 \mu\text{l} = 0.0025 \text{ mmol} = 0.5 \text{ mol\%}$ of **1**).

General Procedure for the Deuteration of Primary Amines: To a screw cap scintillation vial primary amine (0.5 mmol), catalyst **1** (0.0025 mmol, 20 μl stock solution), and D_2O (0.4 mL, 20 mmol) were added under nitrogen atmosphere. The reaction vial was sealed and immersed into a pre-heated oil bath of 135 $^\circ\text{C}$ and the reaction mixture was stirred for 24 h. If the reaction mixture is not homogeneous, the solvent was evaporated under reduced pressure and the resulted residue was extracted with dichloromethane. The combined organic phase is dried over sodium sulfate. Removal of solvent under reduced pressure provided pure products.

Precaution!!! Owing to the thin walled nature of the scintillation vial this is potentially a hazardous operation and must be conducted in a fume hood behind a blast shield.

Spectral Data of the Deuterated Primary Amines:

Benzylamine-d4 (3a):²³ Colorless oil. Yield 45 mg (81%). ¹H NMR (D₂O, 400 MHz) δ 7.17-7.03 (m, 5H, ArCH), 4.46 (0.1H, α -CH₂). ¹³C NMR (101 MHz, CDCl₃) δ 130.85 (quat-C), 128.49 (ArCH), 128.27 (ArCH), 127.06 (ArCH), 52.95 (m, α -CH₂).

***p*-Tolylmethanamine-d4 (3b):**²⁴ Colorless oil. Yield 49 mg (79%). ¹H NMR (CDCl₃, 400 MHz) δ 7.24-7.13 (m, 4H, ArCH), 3.76 (s, 0.53H, α -CH₂), 2.34 (s, 3H, CH₃). ¹³C NMR (101 MHz, CDCl₃) δ 136.42 (quat-C), 129.27 (ArCH), 129.16 (quat-C), 127.10 (ArCH), 46.00 (m, CH₂), 21.09 (CH₃).

Naphthalen-1-ylmethanamine-d4 (3c): Dark yellow liquid. Yield 71 mg (89%). ¹H NMR (D₂O, 400 MHz) δ 8.04 (d, 1H, J = 8 Hz, ArCH), 7.86 (t, 1H, J = 8 Hz, ArCH), 7.76 (d, 1H, J = 8 Hz, ArCH), 7.51 (m, 3H, ArCH), 7.43 (d, 1H, J = 8 Hz, ArCH), 3.81 (0.37H, α -CH₂). ¹³C NMR (101 MHz, CDCl₃) δ 138.63 (quat-C), 133.81 (quat-C), 131.10 (quat-C), 128.80 (ArCH), 127.51 (ArCH), 126.14 (ArCH), 125.65 (ArCH), 125.56 (ArCH), 124.40 (ArCH), 123.10 (ArCH), 43.61 (m, CH₂). HRMS (ESI): m/z calcd for C₁₁H₇ND₄ (M+H)⁺ 162.1221, found: 162.1216.

Pyridin-3-ylmethanamine-d4 (3d): Brown liquid. Yield 39 mg (69%). ¹H NMR (CDCl₃, 400 MHz) δ 8.47 (s, 1H, ArCH), 8.40 (d, 1H, J = 4 Hz, ArCH), 7.58 (d, 1H, J = 8 Hz, ArCH), 7.18 (d, 1H, J = 4 Hz, ArCH), 3.60 (t, 0.07H, α -CH₂). ¹³C NMR (101 MHz, CDCl₃) δ 147.64 (ArCH), 147.12 (ArCH), 137.48 (quat-C), 136.49 (ArCH), 124.17 (ArCH), 42.02 (m, CH₂). HRMS (ESI): m/z calcd for C₆H₅N₂D₄ (M+H)⁺ 113.1017, found: 113.1011.

Pyridin-2-ylmethanamine-d4 (3e): Brown liquid. Yield 35 mg (62%). ¹H NMR (D₂O, 400 MHz) δ 8.27 (d, 1H, J = 4 Hz, ArCH), 7.67 (t, 1H, J = 8 Hz, ArCH), 7.26 (d, 1H, J = 8 Hz, ArCH), 7.16 (t, 1H, J = 8 Hz, ArCH), 3.41 (t, 0.07H, α -CH₂). ¹³C NMR (101 MHz, CDCl₃) δ 160.31 (quat-C), 148.18 (ArCH), 138.17 (ArCH), 122.61

(ArCH), 121.84 (ArCH), 45.35 (m, CH₂). HRMS (ESI): m/z calcd for C₆H₅N₂D₄ (M+H)⁺ 113.1017, found: 113.1012.

2-Phenylethanamine-d₄ (3f):²³ Yellow liquid. Yield 45 mg (72%). ¹H NMR (CDCl₃, 400 MHz) δ 7.05 (m, 5H, ArCH), 2.71 (t, 0.39H, α-CH₂), 2.52 (s, 1.92H, CH₂). ¹³C NMR (101 MHz, CDCl₃) δ 139.72 (quat-C), 128.76 (ArCH), 128.40 (ArCH), 126.10 (ArCH), 42.81 (m, α-CH₂), 39.77 (t, CH₂).

Butan-1-amine-d₄ (3g):²⁵ Light yellow liquid. Yield 20 mg (51%). ¹H NMR (D₂O, 400 MHz) δ 2.57 (t, 0.87H, α-CH₂), 1.31 (m, 4H, CH₂), 0.83 (t, 3H, CH₃).

Pentan-1-amine-d₄ (3h): Light yellow liquid. Yield 29 mg (64%). ¹H NMR (CDCl₃, 400 MHz) δ 2.64 (t, 0.19H, α-CH₂), 1.31 (m, 4H, CH₂), 0.88 (t, 3H, CH₃). ¹³C NMR (101 MHz, CDCl₃) δ 29.78 (m, α-CH₂), 22.74 (CH₂), 22.66 (CH₂), 22.57 (CH₂), 14.16 (CH₃). HRMS (ESI): m/z calcd for C₇H₁₃ND₄Na (M+Na)⁺ 142.1510, found: 142.1504.

Hexan-1-amine-d₄ (3i):²⁶ Yellow liquid. Yield 36 mg (68%). ¹H NMR (CDCl₃, 400 MHz) δ 2.58 (0.17H, α-CH₂), 1.26 (m, 8H, CH₂), 0.83 (t, 3H, J = 8 Hz, CH₃). ¹³C NMR (101 MHz, CDCl₃) δ 41.44 (m, α-CH₂), 33.53 (CH₂), 31.76 (CH₂), 26.58 (CH₂), 22.69 (CH₂), 14.07 (CH₃).

Heptan-1-amine-d₄ (3j): Yellow liquid. Yield 40 mg (67%). ¹H NMR (CDCl₃, 400 MHz) δ 2.50 (0.15H, α-CH₂), 1.51-1.18 (m, 8H, CH₂), 0.82 (t, 3H, J = 8 Hz, CH₃). ¹³C NMR (101 MHz, CDCl₃) δ 49.63 (m, α-CH₂), 31.91 (CH₂), 29.33 (CH₂), 29.25 (CH₂), 27.22 (CH₂), 22.69 (CH₂), 14.13 (CH₃). HRMS (ESI): m/z calcd for C₇H₁₄ND₄ (M+H)⁺ 120.1960, found: 120.1965.

Octan-1-amine-d₄ (3k):²⁷ Yellow liquid. Yield 46 mg (70%). ¹H NMR (CDCl₃, 400 MHz) δ 2.64 (0.18H, α-CH₂), 1.49-1.22 (br s, 10H, CH₂), 0.87 (t, 3H, J = 8 Hz, CH₃).

^{13}C NMR (101 MHz, CDCl_3) δ 49.51 (m, $\alpha\text{-CH}_2$), 33.49 (CH_2), 31.81 (CH_2), 29.44 (CH_2), 29.27 (CH_2), 26.84 (CH_2), 22.63 (CH_2), 14.06 (CH_3).

Dodecan-1-amine-d4 (3l): White solid. Yield 74 mg (78%). ^1H NMR (CDCl_3 , 400 MHz) δ 2.54 (t, 0.39H, $\alpha\text{-CH}_2$), 1.26 (m, 20H, CH_2), 0.86 (t, 3H, CH_3). ^{13}C NMR (101 MHz, CDCl_3) δ 49.55 (m, $\alpha\text{-CH}_2$), 32.05 (CH_2), 29.80 (CH_2), 29.77 (4 CH_2), 29.76 (CH_2), 29.71 (CH_2), 29.48 (CH_2), 22.81 (CH_2), 14.23 (CH_3). HRMS (ESI): m/z calcd for $\text{C}_{12}\text{H}_{24}\text{ND}_4$ ($\text{M}+\text{H}$) $^+$ 190.2473, found: 190.2467.

Octadecan-1-amine-d4 (3m): White solid. Yield 112 mg (82%). ^1H NMR (CDCl_3 , 400 MHz) δ 2.64 (t, 0.18H, $\alpha\text{-CH}_2$), 1.25 (m, 32H, CH_2), 0.87 (t, 3H, CH_3). ^{13}C NMR (101 MHz, CDCl_3) δ 49.65 (m, $\alpha\text{-CH}_2$), 32.07 (CH_2), 29.84 (11 CH_2), 29.80 (CH_2), 29.68 (CH_2), 29.51 (CH_2), 22.83 (CH_2), 14.25 (CH_3). HRMS (ESI): m/z calcd for $\text{C}_{18}\text{H}_{36}\text{ND}_4$ ($\text{M}+\text{H}$) $^+$ 274.3412, found: 274.3406.

Cyclohexylmethanamine-d4 (3n): Yellow liquid. Yield 43 mg (73%). ^1H NMR (CDCl_3 , 400 MHz) δ 2.49 (d, 0.46H, $\alpha\text{-CH}_2$), 1.68 (m, 4H, CH_2), 1.21 (m, 5H, CH_2), 0.88 (m, 2H, CH_2). ^{13}C NMR (101 MHz, CDCl_3) δ 48.25 (m, CH_2), 41.01 (CH), 30.70 (CH_2), 26.61 (CH_2), 25.98 (CH_2). HRMS (ESI): m/z calcd for $\text{C}_7\text{H}_{12}\text{ND}_4$ ($\text{M}+\text{H}$) $^+$ 118.1528, found: 118.1525.

Cyclohexanamine-d4 (3o):²⁸ Yellow liquid. Yield 32 mg (62%). ^1H NMR (CDCl_3 , 400 MHz) δ 2.54 (m, 0.30H, $\alpha\text{-CH}_2$), 1.64 (m, 4H, CH_2), 1.07 (m, 6H, CH_2).

3-Morpholinopropan-1-amine-d4 (3p): Brown liquid. Yield 38 mg (52%). ^1H NMR (D_2O , 400 MHz) δ 3.64 (t, 4H, $J = 8$ Hz, OCH_2), 2.75 (t, 0.29 H, $\alpha\text{-CH}_2$), 2.47 (m, 6H, NCH_2), 1.59 (m, 2H, CH_2). ^{13}C NMR (101 MHz, D_2O) δ 66.15 (OCH_2), 55.73 (CH_2), 52.59 (CH_2), 38.68 (m, $\alpha\text{-CH}_2$), 27.86 (t, CH_2). HRMS (ESI): m/z calcd for $\text{C}_7\text{H}_{12}\text{ON}_2\text{D}_4\text{Na}$ ($\text{M}+\text{Na}$) $^+$ 171.1411, found: 171.1406.

Octane-1,8-diamine-d8 (3q): Yellow liquid. Yield 37 mg (49%). ^1H NMR (CDCl_3 , 400 MHz) δ 2.34 (0.73H, $\alpha\text{-CH}_2$), 1.12-1.01 (m, 12H, CH_2). ^{13}C NMR (101 MHz, CDCl_3) δ 40.76 (m, $\alpha\text{-CH}_2$), 32.84 (CH_2), 28.95 (CH_2), 26.30 (CH_2). HRMS (ESI): m/z calcd for $\text{C}_8\text{H}_{13}\text{N}_2\text{D}_8$ ($\text{M}+\text{H}$) $^+$ 153.2201, found: 153.2209.

General Procedure for the Deuteration of Secondary Amines:

To a screw cap scintillation vial secondary amine (0.5 mmol), catalyst **1** (0.005 mmol, 40 μl stock solution), and D_2O (0.4 mL, 20 mmol) were added under nitrogen atmosphere. The reaction vial was sealed and immersed into a pre-heated oil bath of 135 $^\circ\text{C}$ and the reaction mixture was allowed to stir for 24 h. The resultant reaction mixtures were characterized by NMR spectroscopy. If the reaction mixture is not homogeneous, the solvent was evaporated under reduced pressure and the residue was extracted with dichloromethane. Combined organic phase is dried over sodium sulfate. Removal of solvent under reduced pressure provided pure products.

Spectral Data of the Deuterated Secondary Amines:

***N*-Methyl-1-phenylmethanamine-d4 (4a):** Yellow liquid. Yield 46 mg (73%). ^1H NMR (D_2O , 400 MHz) δ 7.29-7.22 (m, 5H, ArCH), 3.58 (s, 2H, NCH_2), 2.36 (m, 0.14 H, $\alpha\text{-NCH}_3$). ^{13}C NMR (101 MHz, D_2O) δ 137.84 (quat-C), 128.70 (ArCH), 128.59 (ArCH), 127.61 (quat-C), 53.88 (CH_2), 33.22 (m, $\alpha\text{-CH}_3$). HRMS (ESI): m/z calcd for $\text{C}_8\text{H}_8\text{ND}_4$ ($\text{M}+\text{H}$) $^+$ 126.1220, found: 126.1215.

Dibutylamine-d5 (4b):²⁹ Yellow liquid. Yield 45 mg (67%). ^1H NMR (D_2O , 400 MHz) δ 2.87 (m, 1.15 H, $\alpha\text{-CH}_2$), 1.55 (t, 4H, $J = 8$ Hz, CH_2), 1.32 (m, 4H, CH_2), 0.88 (t, 6H, $J = 8$ Hz, CH_3). ^{13}C NMR (101 MHz, D_2O) δ 47.22 (m, $\alpha\text{-CH}_2$), 27.56 (CH_2), 19.19 (CH_2), 12.85 (CH_3).

Dihexylamine-d5 (4c):²⁸ Yellow liquid. Yield 71 mg (75%). ^1H NMR (CDCl_3 , 400 MHz) δ 2.52 (t, 0.43H, $\alpha\text{-CH}_2$), 1.22 (m, 16H, CH_2), 0.82 (t, 3H, CH_3). ^{13}C NMR (101

MHz, CDCl₃) δ 48.61 (m, α -CH₂), 31.62 (CH₂), 28.60 (CH₂), 26.80 (CH₂), 22.54 (CH₂), 13.96 (CH₃).

Pyrrolidine-d₅ (4d):³⁰ Yellow liquid. Yield 23 mg (61%). ¹H NMR (D₂O, 400 MHz) δ 2.77 (t, 1H, α -CH₂), 1.65 (s, 4H, CH₂). ¹³C NMR (101 MHz, CDCl₃) δ 45.21 (m, α -CH₂), 24.39 (CH₂).

Piperidine-d₅ (4e):^{27,30} Yellow liquid. Yield 29 mg (64%). ¹H NMR (D₂O, 400 MHz) δ 2.79 (0.84H, α -CH₂), 1.51 (br s, 6H, CH₂). ¹³C NMR (101 MHz, CDCl₃) δ 44.20 (m, α -CH₂), 23.81 (CH₂), 22.78 (CH₂).

1,3-Di(piperidin-4-yl)propane-d₁₀ (4f): Yellow liquid. Yield 78 mg (71%). ¹H NMR (CDCl₃, 400 MHz) δ 2.82 (0.31H, α -CH₂), 2.34 (0.34H, α -CH₂), 2.04 (0.70H, α -CH₂), 1.45-0.84 (m, 14H, CH₂). ¹³C NMR (101 MHz, D₂O) δ 46.19 (m, α -CH₂), 37.84 (CH₂), 35.65 (CH₂), 35.45 (CH₂), 31.38 (CH₂), 25.01 (CH₂). HRMS (ESI): m/z calcd for C₁₃H₁₇N₂D₁₀ (M+H)⁺ 221.2803, found: 221.2796.

Piperazine-d₁₀ (4g): Yellow liquid. Yield 26 mg (54%). ¹H NMR (D₂O, 400 MHz) δ 2.73 (br s, 1.35H, α -CH₂). ¹³C NMR (101 MHz, D₂O) δ 44.61 (m, α -CH₂). HRMS (ESI): m/z calcd for C₄N₂D₁₀ (M+Na)⁺ 119.1364, found: 119.1372.

General Procedure for the Deuteration of Amino Acids:

In a screw cap scintillation vial amino acid (0.5 mmol) and KOH (0.5 mmol, 28 mg) were dissolved in D₂O (0.6 mL, 30 mmol) and stirred at room temperature for 30 minutes. Then the catalyst **1** (0.005 mmol, 40 μ l stock solution) is added to the vial under nitrogen atmosphere sealed and immersed into a pre-heated oil-bath of 135 °C and the reaction mixture was allowed to stir for 36 h. The cooled reaction mixture is transferred to a NMR tube and analyzed by NMR spectroscopy.

Spectral Data of the Deuterated Amino Acids:

Phenylalanine-d3 (5a):³¹ ¹H NMR (D₂O, 400 MHz) δ 7.29 (m, 5H, ArCH), 3.44 (m, 0.16H, α-CH), 2.97 (d, 1H, J = 8 Hz, CH₂), 2.75 (d, 1H, J = 8 Hz, CH₂). ¹³C NMR (101 MHz, D₂O) δ 181.96 (COOK), 138.43 (quat-C), 129.51 (ArCH), 128.68 (ArCH), 126.70 (ArCH), 57.36 (m, α-CH), 40.90 (d, CH₂).

Tyrosine-d4 (5b):³² ¹H NMR (D₂O, 400 MHz) δ 7.07-6.57 (m, 4H, ArCH), 3.39 (m, 0.60H, α-CH), 2.82 (d, 1H, J = 8 Hz, CH₂), 2.64 (d, 1H, J = 8 Hz, CH₂).

Glycine-d4 (5c):³³ ¹H NMR (D₂O, 400 MHz) δ 3.08 (0.21 H, α-CH₂). ¹³C NMR (101 MHz, D₂O) δ 181.31 (COOH), 44.11 (m, α-CH₂).

Alanine-d3 (5d):^{29,34} ¹H NMR (D₂O, 400 MHz) δ 3.33 (m, 0.32 H, α-CH), 1.20 (s, 3H, CH₃). ¹³C NMR (101 MHz, D₂O) δ 182.55 (COOK), 50.84 (m, α-CH), 19.32 (CH₃).

Serine-d4 (5e):³¹ ¹H NMR (D₂O, 400 MHz) δ 3.68 (m, 2H, OCH₂), 3.33 (m, 0.14H, α-CH) . ¹³C NMR (101 MHz, D₂O) δ 180.34 (COOK), 64.51 (OCH₂), 57.12 (t, α-CH).

Methionine-d3 (5f):³³ ¹H NMR (D₂O, 400 MHz) δ 3.31 (m, 0.3H, α-CH), 2.54 (t, 2H, J = 8 Hz, CH₂), 2.09 (s, 3H, CH₃), 1.84 (m, 2H, CH₂). ¹³C NMR (101 MHz, D₂O) δ 182.55 (COOK), 54.88 (m, α-CH), 34.02 (CH₂), 29.74 (CH₂), 14.20 (CH₃).

Isoleucine-d3 (5g):³⁵ ¹H NMR (D₂O, 400 MHz) δ 3.09 (d, 0.5H, α-CH), 1.63 (m, 1H, CH), 1.36 (m, 1H, CH), 1.10 (m, 1H, CH), 0.85 (m, 6H, CH₃). ¹³C NMR (101 MHz, D₂O) δ 182.27 (COOK), 37.95 (m, α-CH), 24.13 (CH), 15.54 (CH), 11.12 (CH₃).

Aspartic acid-d3 (5h):^{32,35} ¹H NMR (D₂O, 400 MHz) δ 3.53 (m, 0.27H, α-CH), 2.59 (d, 1H, J = 16 Hz, CH), 2.30 (d, 1H, J = 16 Hz, CH). ¹³C NMR (101 MHz, D₂O) δ 181.38 (COOK), 179.92 (COOK), 53.38 (m, α-CH), 42.33 (CH₂).

Methyl 2-amino-3-hydroxypropanoate-d4 (5i): ^1H NMR (D_2O , 400 MHz) δ 3.70 (m, 2H, OCH_2), 3.34 (s, 3H, OCOCH_3). ^{13}C NMR (101 MHz, D_2O) δ 180.53 (COOMe), 64.77 (OCH_2), 57.25 (t, $\alpha\text{-CH}$), 49.08 (OCH_3). HRMS (ESI): m/z calcd for $\text{C}_4\text{H}_5\text{NO}_3\text{D}_4\text{Na}$ ($\text{M}+\text{Na}$) $^+$ 146.0731, found: 146.0726.

Valine-d3 (5j):^{29,35} ^1H NMR (D_2O , 400 MHz) δ 3.02 (d, 0.2H, $\alpha\text{-CH}$), 1.90 (sept, 1H, $^i\text{PrCH}$), 0.88 (dd, 6H, $J_1 = 28$ Hz, $J_2 = 8$ Hz, $^i\text{PrCH}_3$). ^{13}C NMR (101 MHz, D_2O) δ 182.73 (COOK), 61.48 (m, $\alpha\text{-CH}$), 31.72 ($^i\text{PrCH}$), 19.21 ($^i\text{PrCH}_3$), 16.86 ($^i\text{PrCH}_3$).

Proline-d4 (5k):³⁵ ^1H NMR (D_2O , 400 MHz) δ 3.43 (0.20H, $\alpha\text{-CH}$), 2.98 (m, 0.64 H, $\alpha\text{-CH}_2$), 2.70 (m, 0.37 H, $\alpha\text{-CH}_2$), 2.05 (t, $J = 8$ Hz, 1H, CH_2), 1.69-1.64 (m, 3H, CH_2). ^{13}C NMR (101 MHz, D_2O) δ 179.51 (COOK), 61.05 (m, $\alpha\text{-CH}$), 46.02 ($\alpha\text{-CH}_2$), 30.02 (CH_2), 24.67 (CH_2).

General Procedure for Selective Deuteration of Pharmaceuticals:

To a screw cap scintillation vial commercial drugs (0.5 mmol) and KOH (0.5 mmol, 28 mg) were dissolved in D_2O (0.6 mL, 30 mmol) and stirred at room temperature for 30 minutes. Excipients were removed by centrifuge. The clear supernatant liquid was transferred into another scintillation vial and catalyst (0.01 mmol, 80 μl stock solution) is added under nitrogen atmosphere, sealed and immersed into a pre-heated oil-bath of 150 $^\circ\text{C}$ and the reaction mixture stirred for 24 h. The cooled reaction mixture is transferred to a NMR tube and analyzed by NMR spectroscopy.

Sertraline-d4 (6):³⁶ ^1H NMR (D_2O , 400 MHz) δ 8.81 (d, 1H, $J = 8$ Hz, ArCH), 8.46 (s, 1H, ArCH), 8.39 (d, 2H, $J = 8$ Hz, ArCH), 8.23 (t, 3H, $J = 8$ Hz, ArCH), 7.92 (d, 1H, $J = 8$ Hz, ArCH), 5.42 (t, 1H, $J = 6$ Hz, CH), 5.05 (t, 1H, $J = 8$ Hz, CH), 3.35 (0.16H, $\alpha\text{-CH}_2$), 3.32-3.12 (m, 4H, CH_2).

Pregabalin-d4 (7): ^1H NMR (D_2O , 400 MHz) δ 3.54-3.49 (m, 0.55H, $\alpha\text{-CH}_2$ to COOK), 3.02-3.04 (m, 0.55H, $\alpha\text{-CH}_2$ to COOK), 2.56 (m, 0.64H, $\alpha\text{-CH}_2$ to NH_2), 1.57 (m, 1H, $^i\text{PrCH}$), 1.36-1.24 (m, 2H, CH_2), 0.90 (d, 6H, $J = 8$ Hz, $^i\text{PrCH}_3$). ^{13}C

NMR (101 MHz, D₂O) δ 180.86 (COOK), 48.24 (m, α -CH₂ to NH₂), 43.19 (CH₂), 32.26 (α -CH₂ to COOK), 25.77 (CH), 24.72 (ⁱPrCH), 22.27 (ⁱPrCH₃). HRMS (ESI): m/z calcd for C₈H₁₂D₄KNO₂ (M)⁺ 201.1069, found: 201.1061.

Synthesis of $\{(\eta^6\text{-}p\text{-cymene})\text{RuHCl}\}(\text{NHCH}_2\text{Ph})(\text{NH}_2\text{CH}_2\text{Ph})\text{Cl } \mathbf{2}$:

In a screw cap scintillation vial [$\{(\eta^6\text{-}p\text{-cymene})\text{RuCl}\}_2(\mu\text{-H-}\mu\text{-Cl})$] **1** (0.017 mmol, 10 mg), benzylamine (5 equiv, 0.086 mmol, 9 μ l) and 1,4-dioxane (0.5 mL) were added and the resulting mixture was allowed to stir at room temperature for 2 h. The volume of reddish-brown solution was reduced under vacuum and kept at -30 °C for 24 h, which provided reddish-brown precipitate. The solution decanted and the precipitate was characterized by NMR and IR spectroscopy. IR (C₆D₆) 3427 (N-H), 2934, 2756, 2100, 2011 (Ru-H), 1552, 1431, 1328, 1187, 971, 823, 677 cm⁻¹. ¹H NMR (C₆D₆, 400 MHz) δ 7.86 (d, 4H, J = 8 Hz, ArCH), 7.49-7.33 (m, 6H, ArCH), 5.78 (d, 2H, J = 8 Hz, ArCH), 5.53 (d, 2H, J = 8 Hz, ArCH), 4.61 (br m, 2H, NH₂), 3.22 (m, 1H, ⁱPrCH), 2.70 (s, 3H, CH₃), 1.45 (d, 6H, J = 8 Hz, ⁱPrCH₃), -5.56 (1H, Ru-H). ¹³C NMR (101 MHz, CDCl₃) δ 141.07 (quat-C), 129.50 (ArCH), 129.25 (ArCH), 128.83 (ArCH), 104.95 (quat-C), 94.75 (quat-C), 83.08 (ArCH), 81.32 (ArCH), 54.51 (CH₂), 31.59 (CH), 22.58 (ⁱPrCH₃), 19.05 (CH₃).

Determination of the Molecular Structure of **2 in the Solid State by X-ray Single Crystal Diffraction:** A suitable single crystals of complex **2** for X-ray analysis was obtained from a solution of toluene. A suitable crystal was mounted on a glass fiber. Geometry and intensity data were collected with a Bruker SMART D8 goniometer equipped with an APEX CCD detector and with an Incoatec microsource (Mo-K α radiation, λ = 0.71073 Å, multilayer optics). Temperature was controlled using an Oxford Cryostream 700 instrument. Intensities were integrated with SAINT³⁷ and

corrected for absorption with SADABS.³⁸ The structure was solved by direct methods and refined on F^2 with SHELXL-97.^{39,40}

Crystal Data of Ru-Complex 2: $C_{48}H_{64}Cl_4N_4Ru_2$, crystal dimensions: $0.19 \times 0.15 \times 0.12$, triclinic with space group P-1 $a = 11.418 (12)\text{\AA}$, $b = 13.809 (15)\text{\AA}$, $c = 15.565 (17)\text{\AA}$, $\alpha = 71.93 (14)^\circ$, $\beta = 89.77 (14)^\circ$, $\gamma = 86.05 (14)^\circ$, $V = 2327 (4)\text{\AA}^3$, $Z = 2$, $T = 100\text{ K}$, $2\theta_{\max} = 24.03$, $\rho_{\text{calcd}} = 1.485\text{ g/cm}^3$, $\mu (\text{MoK}\alpha) = 0.916\text{ mm}^{-1}$. Min/max transmission factors = 0.5402/0.7457, 11856 Reflections collected, 6483 unique ($R1 = 0.058$), $WR2 = 0.1374$ (all data). The structure has been deposited at the CCDC data center and can be retrieved by using the number CCDC 1481309.

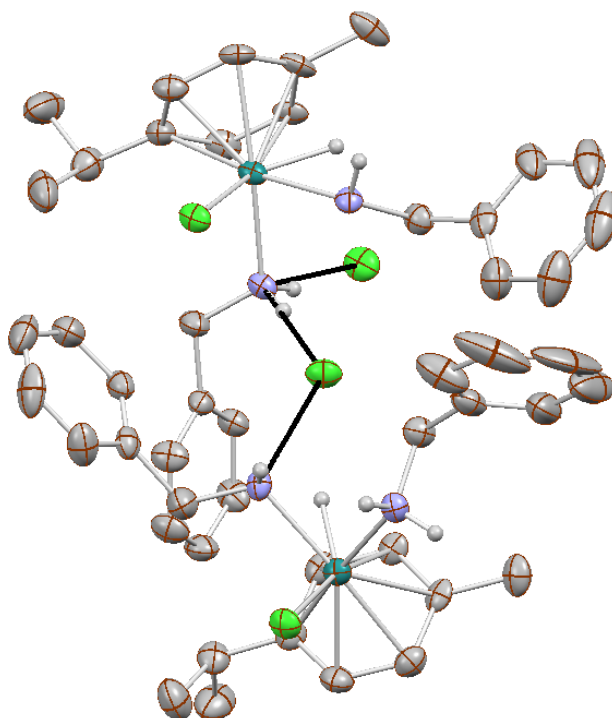


Figure 10.2 Structure of complex **2** with two molecules in unit cell showing hydrogen bond between $\text{PhCH}_2\text{NH}_2 \cdots \text{Cl} \cdots \text{NHCH}_2\text{Ph}$ (thermal ellipsoids are drawn with 50% probability)

10.6 NOTES AND REFERENCES

(1) For comprehensive reviews, see: (a) Lockley, W. J. S.; Heys, R. J. *Labelled*

Compd. Radiopharm. **2010**, *53*, 635-644. (b) Atzrodt, J.; Derdau, V.; Fey, T.; Zimmermann, J. *Angew. Chem., Int. Ed.* **2007**, *46*, 7744-7765. (c) *Synthesis and Application of Isotopically Labeled Compounds*; Pleiss, U., Voges, R., Eds.; Wiley: New York, 2001; Vol. 7. (d) Junk, T.; Catallo, W. J. *Chem. Soc. Rev.* **1997**, *26*, 401-406. (e) Lowry, T. H.; Richardson, K. S. *Mechanism and Theory in Organic Chemistry*; Harper & Row: New York, 1987.

(2) (a) Atzrodt, J.; Derdau, V. *J. Labelled Compd. Radiopharm.* **2010**, *53*, 674-685. (b) Stokvis, E.; Rosing, H.; Beijnen, J. H. *Rapid Commun. Mass Spectrom.* **2005**, *19*, 401-407. (c) Kao, C.-Y.; Giese, R. *Chem. Res. Toxicol.* **2005**, *18*, 70-75. (d) Wang, H.; Hussain, A. A.; Pyrek, J. S.; Goodman, J.; Wedlund, P. J. *J. Pharm. Biomed. Anal.* **2004**, *34*, 1063-1070. (e) Allen, G. D.; Brookes, S. T.; Barrow, A.; Dunn, J. A.; Grosse, C. M. *J. Chromatogr., Biomed. Appl.* **1999**, *732*, 383-393.

(3) (a) Tong, C. C.; Hwang, K. C. *J. Phys. Chem. C* **2007**, *111*, 3490-3494. (b) Kaino, T.; Jinguji, K.; Nara, S. *Appl. Phys. Lett.* **1983**, *42*, 567-569.

(4) Miyashita, M.; Sasaki, M.; Hattori, I.; Sakai, M.; Tanino, K. *Science* **2004**, *305*, 495-499.

(5) (a) Harbeson, S. L.; Tung, R. D. *Annu. Rep. Med. Chem.* **2011**, *46*, 403-417. (b) Meanwell, N. A. *J. Med. Chem.* **2011**, *54*, 2529-2591.

(c) Davidova, I. A.; Gieg, L. M.; Nanny, M.; Kropp, K. G.; Suflita, J. M. *Appl. Environ. Microbiol.* **2005**, *71*, 8174-8182. (d) Kushner, D. J.; Baker, A.; Dunstall, T. G. *Can. J. Physiol. Pharmacol.* **1999**, *77*, 79-88. (e) Foster, A. B. *Trends Pharmacol. Sci.* **1984**, *5*, 524-527.

(6) (a) Isin, E. M.; Elmore, C. S.; Nilsson, G. N.; Thompson, R. A.; Weidolf, L. *Chem. Res. Toxicol.* **2012**, *25*, 532-542. (b) Harbeson, S. L.; Tung, R. D. *Annu. Rep. Med. Chem.* **2011**, *46*, 403-417.

- (7) (a) Arockiam, P. B.; Bruneau, C.; Dixneuf, P. H. *Chem. Rev.* **2012**, *112*, 5879-5918. (b) Choi, J.; MacArthur, A. H. R.; Brookhart, M.; Goldman, A. S. *Chem. Rev.* **2011**, *111*, 1761-1779.
- (8) (a) Lockley, W. J. S.; Hesk, D. *J. Labelled Compd. Radiopharm.* **2010**, *53*, 668-673. (b) Bhatia, S.; Spahlinger, G.; Boukhumseen, N.; Boll, Q.; Li, Z.; Jackson, J. E. *Eur. J. Org. Chem.* **2016**, *2016*, 4230-4235.
- (9) (a) Takahashi, M.; Oshima, K.; Matsubara, S. *Chem. Lett.* **2005**, *34*, 192-193. (b) Alexakis, E.; Hickey, M. J.; Jones, J. R.; Kingston, L. P.; Lockley, W. J. S.; Mather, A. N.; Smith, T.; Wilkinson, D. J. *Tetrahedron Lett.* **2005**, *46*, 4291-4293.
- (10) Neubert, L.; Michalik, D.; Bähn, S. B.; Imm, S.; Neumann, H.; Atzrodt, J.; Derdau, V.; Holla, W.; Beller, M. *J. Am. Chem. Soc.* **2012**, *134*, 12239-12244.
- (11) Pieters, G.; Taglang, C.; Bonnefille, E.; Gutmann, T.; Puente, C.; Berthet, J.-C.; Dugave, C.; Chaudret, B.; Rousseau, B. *Angew. Chem., Int. Ed.* **2014**, *53*, 230-234.
- (12) Taglang, C.; Martínez-Prieto, L. M.; del Rosal, I.; Maron, L.; Poteau, R.; Philippot, K.; Chaudret, B.; Perato, S.; Lone, A. S.; Puente, C.; Dugave, C.; Rousseau, B.; Pieters, G. *Angew. Chem., Int. Ed.* **2015**, *54*, 10474-10477.
- (13) Maegawa, T.; Akashi, A.; Esaki, H.; Aoki, F.; Sajiki, H.; Hirota, K. *Synlett* **2005**, 845-847.
- (14) (a) Elemes, Y.; Ragnarsson, U. *J. Chem. Soc., Perkin Trans. 1* **1996**, *1*, 537-540. (b) Elemes, Y.; Ragnarsson, U. *Chem. Commun.* **1996**, 935-936. (c) Lankiewicz, L.; Nyasse, B.; Fransson, B.; Grehn, L.; Ragnarsson, U. *J. Chem. Soc., Perkin Trans. 1* **1994**, *1*, 2503-2510.
- (15) (a) Schollkopf, U.; Groth, U.; Deng, C. *Angew. Chem., Int. Ed. Engl.* **1981**, *20*, 798-799. (b) Schollkopf, U.; Hartwig, W.; Groth, U. *Angew. Chem., Int. Ed. Engl.* **1979**, *18*, 863-864.

- (16) (a) Chatterjee, B.; Gunanathan, C. *Org. Lett.* **2015**, *17*, 4794-4797. (b) Chatterjee, B.; Gunanathan, C. *Chem. Commun.* **2016**, *52*, 4509-4512.
- (17) (a) Chatterjee, B.; Gunanathan, C. *Chem. Commun.* **2014**, *50*, 888-890. (b) Kaithal, A.; Chatterjee, B.; Gunanathan, C. *Org. Lett.* **2015**, *17*, 4790-4793. (c) Kaithal, A.; Chatterjee, B.; Gunanathan, C. *Org. Lett.* **2016**, *18*, 3402-3405.
- (18) Tse, S. K. S.; Xue, P.; Lau, C. W. S.; Sung, H. H. Y.; Williams, I. D.; Jia, G. *Chem. - Eur. J.* **2011**, *17*, 13918-13925.
- (19) Ambrogelly, A.; Palioura, S.; Söll, D. *Nat. Chem. Biol.* **2007**, *3*, 29-35.
- (20) Khaskin, E.; Iron, M. A.; Shimon, L. J. W.; Zhang, J.; Milstein, D. *J. Am. Chem. Soc.* **2010**, *132*, 8542-8543.
- (21) Reaction of **1** with benzylamine in H₂O also led to immediate formation of **2** at rt. Upon heating, **2** remained with decreased intensity and two new signals appeared in hydride region of ¹H NMR (δ -19.02 and -19.20 ppm), and the corresponding complexes remain elusive to isolation and characterization.
- (22) Two molecules were present in unit cell. See Figure 10.2.
- (23) Tsukinoki, T.; Tsuzuki, H.; Ishimoto, K.; Nakayama, K.; Kakinami, T.; Mataka, S.; Tashiro, M. *J. labelled comp. radiopharm.*, **1994**, *34*, 839-844
- (24) Liu, D.; Yu, J.; Cheng, J. *Tetrahedron*, **2014**, 1149-1153.
- (25) Moritz, F.; Grottemeyer, *J. Mass. Spectrom.*, **1993**, *28*, 207-15.
- (26) Pieters, G.; Taglang, C.; Bonnefille, E.; Gutmann, T.; Puente, C.; Berthet, J. C.; Dugave, C.; Chaudret, B.; Rousseau, B. *Angew. Chem. Int. Ed.*, **2014**, 230-234.
- (27) Takahashi, M.; Oshima, K.; Matsubara, S. *Chem. Lett.* **2005**, *34*, 192-193.
- (28) Bhatia, S.; Spahlinger, G.; Boukhumseen, N.; Boll, Q.; Li, Z. Jackson, J. E. *Eur. J. Org. Chem.*, **2016**, 4230-4235.

- (29) Alexakis, E.; Hickey, M. J.; Jones, J. R.; Kingston, L. P.; Lockley, W. J. S.; Mather, A. N.; Smith, T.; Wilkinson, D. J. *Tetrahedron Lett*, **2005**, *46*, 4291-4293.
- (30) Frosig, L.; Tureeek, F. *J. Am. Soc. Mass. Spectrom.* **1998**, *9*, 242-254.
- (31) Pearce, C. M.; Williams, D. H. *J. Chem. Soc. Perkin Trans. 2*, **1995**, 153-157.
- (32) Panufnik, E.; Kanska, M. *J. labelled comp. radiopharm.*, **2007**, *50*, 85-89.
- (33) Moozeh, K.; So, S. M.; Chin, J. *Angew. Chem. Int. Ed.*, **2015**, *54*, 9381-9385.
- (34) Taglang, C.; Martinez-Prieto, L. M.; Rosal, I-D.; Maron, L.; Poteau, R.; Philippot, K.; Chaudret, B.; Perato, S.; Lone, A. S.; Puente, C.; Dugave, C.; Rousseau, B. Pieters, G. *Angew. Chem. Int. Ed.*, **2015**, *54*, 10474-10477.
- (35) Oppolzer, W.; Pedrosa, R.; Moretti, R. *Tetrahedron Lett*, **1986**, *27*, 831-834.
- (36) Czarnik, A. W. *Deuterium Enriched Sertraline*. US 2009/0062399 A1, Mar. 5, 2009
- (37) Bruker AXS, SAINT⁺, *Program for Reduction of Data collected on Bruker CCD Area Detector Diffractometer V. 6.02*. Bruker AXS Inc., Madison, Wisconsin, USA, 1999.
- (38) Bruker AXS, SADABS, *Program for Empirical Absorption Correction of Area Detector Data V 2004/1*, Bruker AXS Inc., Madison, Wisconsin, USA, 2004.
- (39) Sheldrick, G. M. *Acta Crystallogr.*, **2008**, *A64*, 112-122.
- (40) Dolomanov, O. V.; Bourhis, L. J.; Gildea, R. J.; Howard, J. A. K.; Puschmann, H. J. *Appl. Crystallogr.*, **2009**, *42*, 339-341.

^1H and ^{13}C NMR Spectra of Deuterated Amines

Figure 10.3 ^1H NMR spectrum of N-methyl-1-phenylmethanamine-d4 (**4a**) (400 MHz, D_2O):

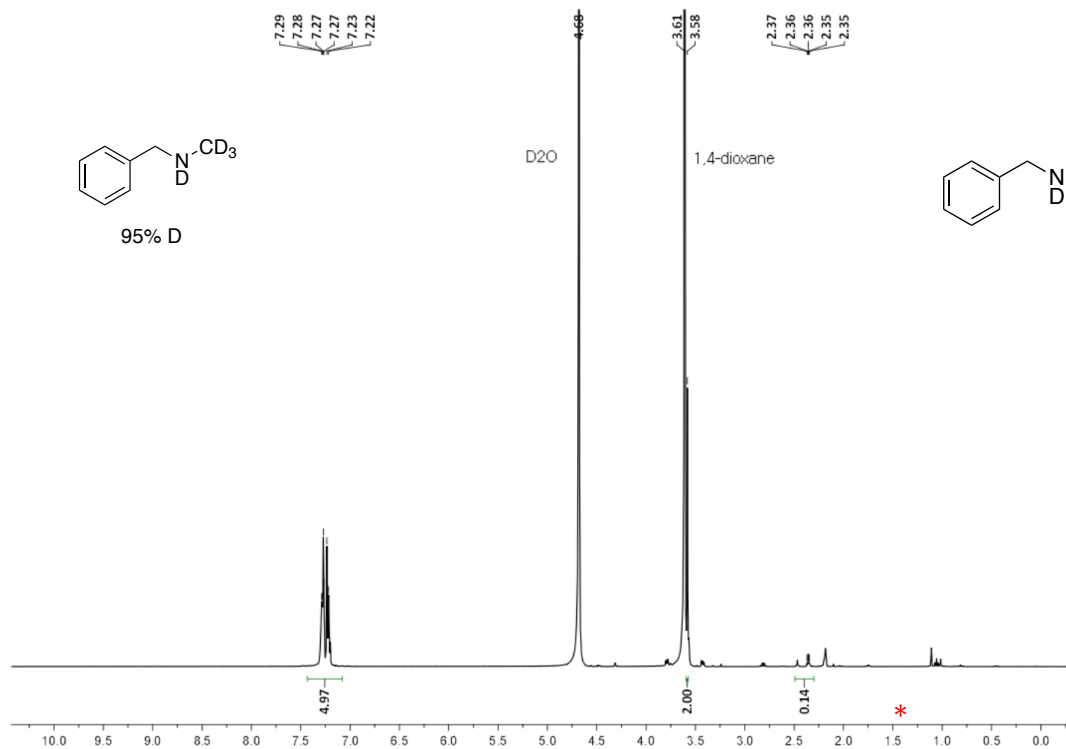


Figure 10.4 ^{13}C NMR spectrum of N-methyl-1-phenylmethanamine-d4 (**4a**) (101 MHz, D_2O):

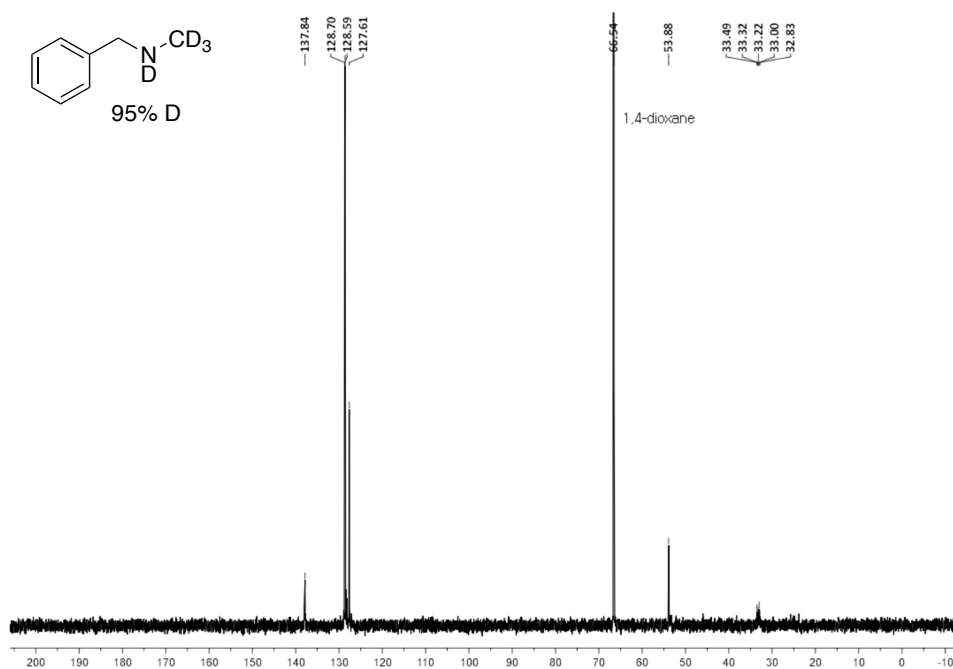


Figure 10.5 ^1H NMR spectrum of pyrrolidine-d₅ (**4d**) (400 MHz, D₂O):

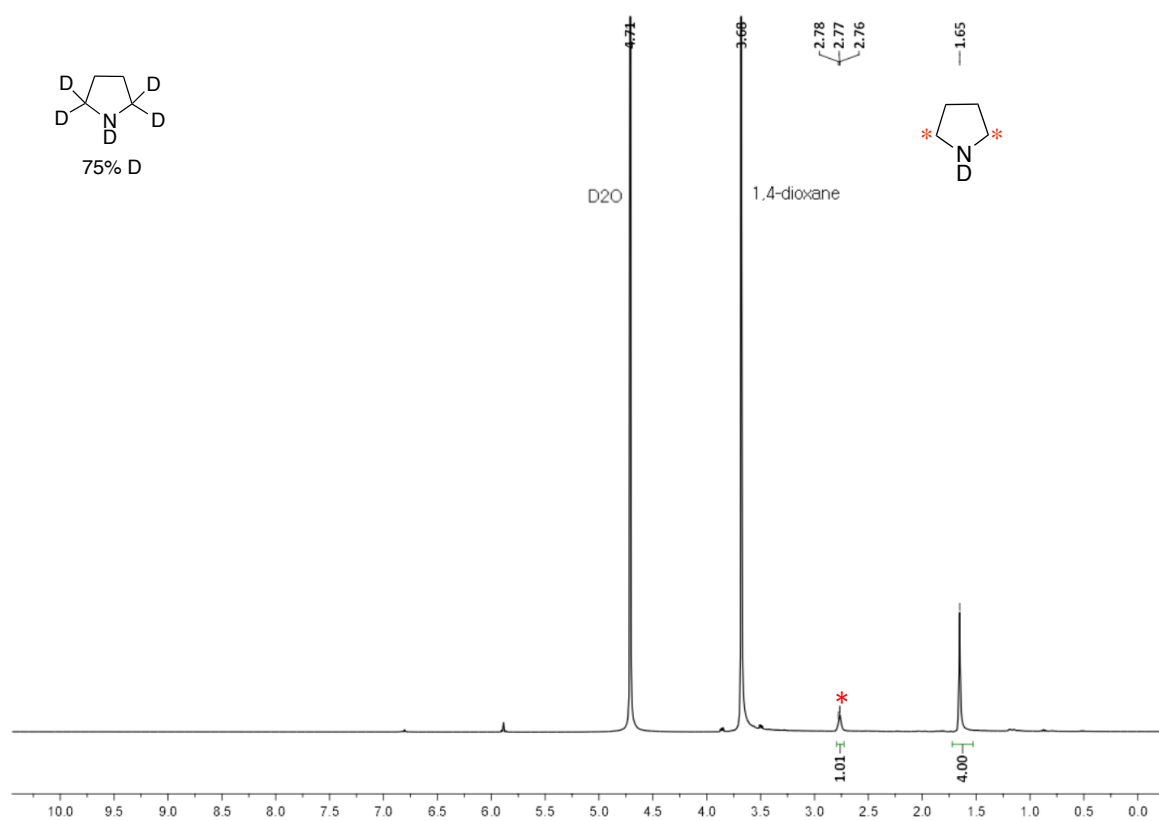


Figure 10.6 ^{13}C NMR spectrum of pyrrolidine-d₅ (**4d**) (101 MHz, D₂O):

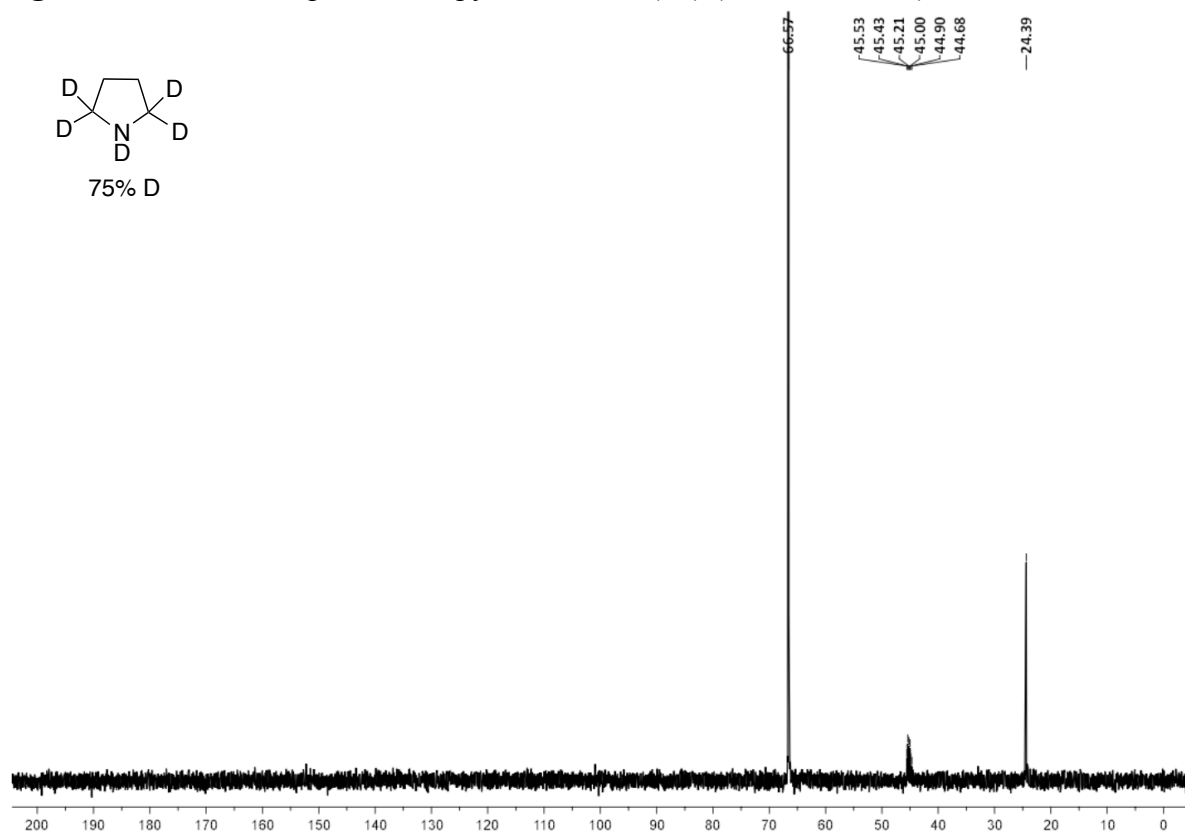


Figure 10.7 ^2H NMR spectrum of pyrrolidine-d5 (**4d**) (61 MHz, D_2O): D_2O peak is omitted for clarity

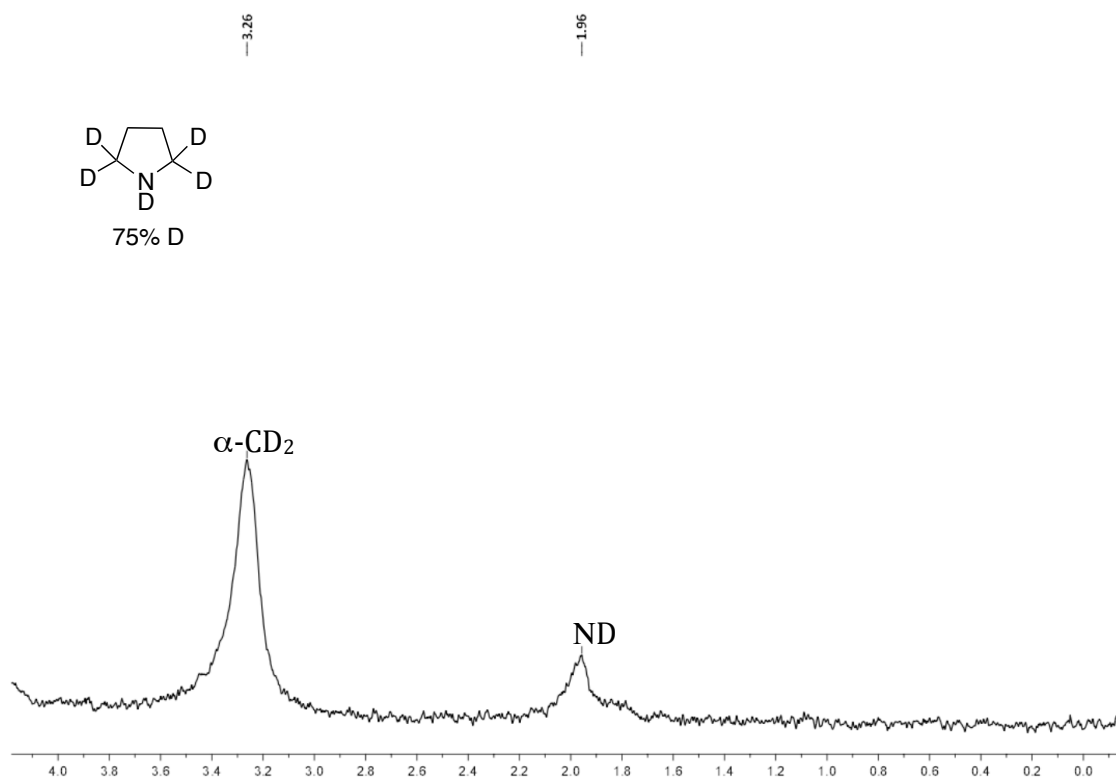


Figure 10.8 ^1H NMR spectrum for potassium salt of L-phenylalanine-d3 (**5a**) (400 MHz, D_2O):

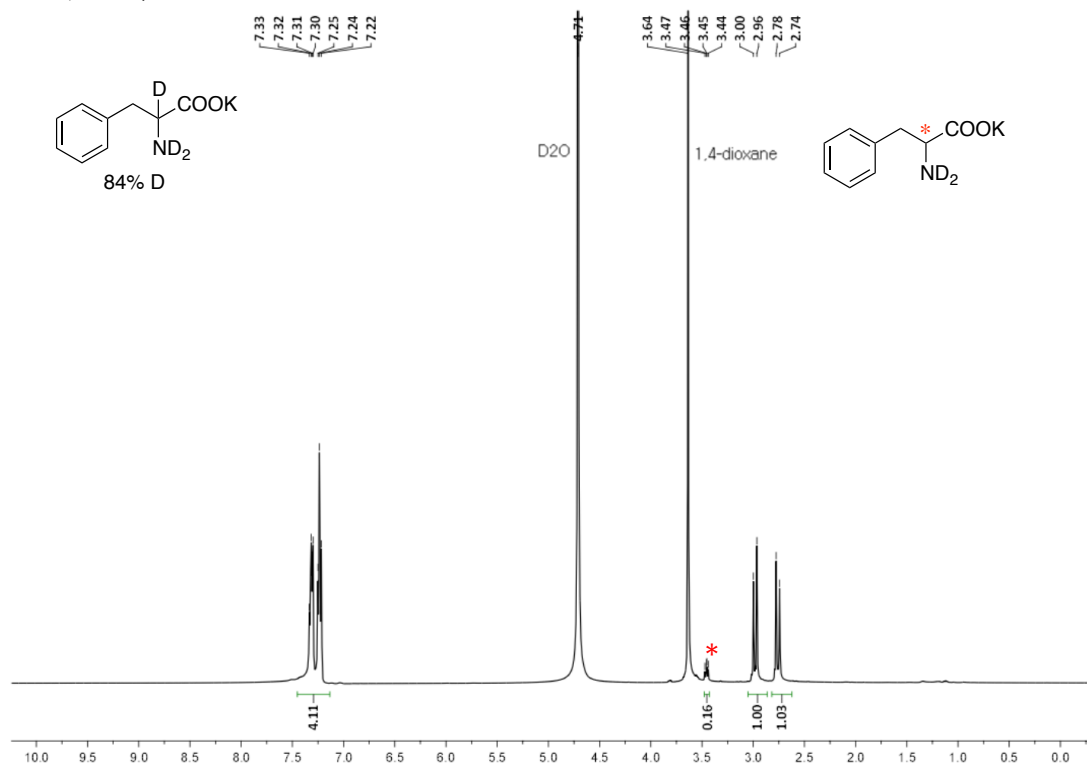
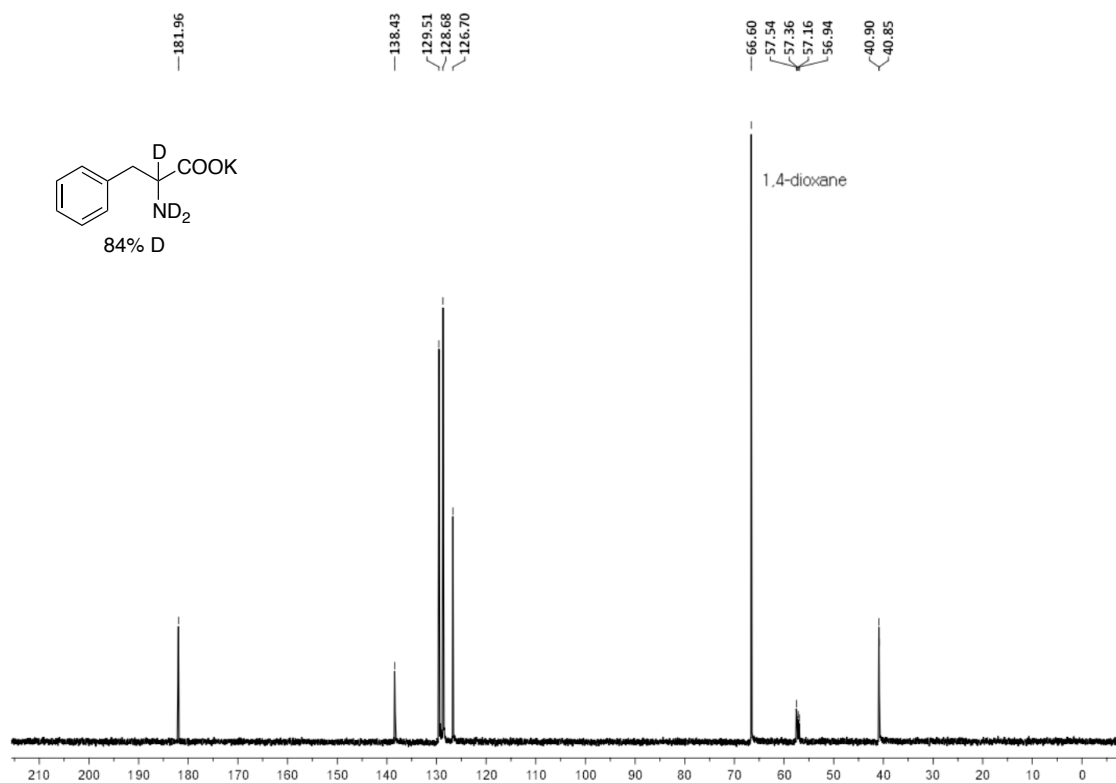


Figure 10.9 ^{13}C NMR spectrum for potassium salt of L-phenylalanine-d3 (**5a**) (101 MHz, D_2O):



SUMMARY

Isolation and characterization of intermediates in catalytic processes are uncommon and challenging owing to their inevitable low stability. However, overcoming this barrier and succeeding in isolation and characterization of the intermediates involved in the catalytic transformations can be highly beneficial in further fine tuning and optimization of catalysts, and for the fundamental understanding of reaction mechanisms. The work delineated in this thesis is an attempt to uncover such mechanistic information, which is corroborated by isolation and characterization of transient intermediates. The evidences gathered lead us to rationalize and establish the plausible reaction mechanisms for the catalytic processes presented.

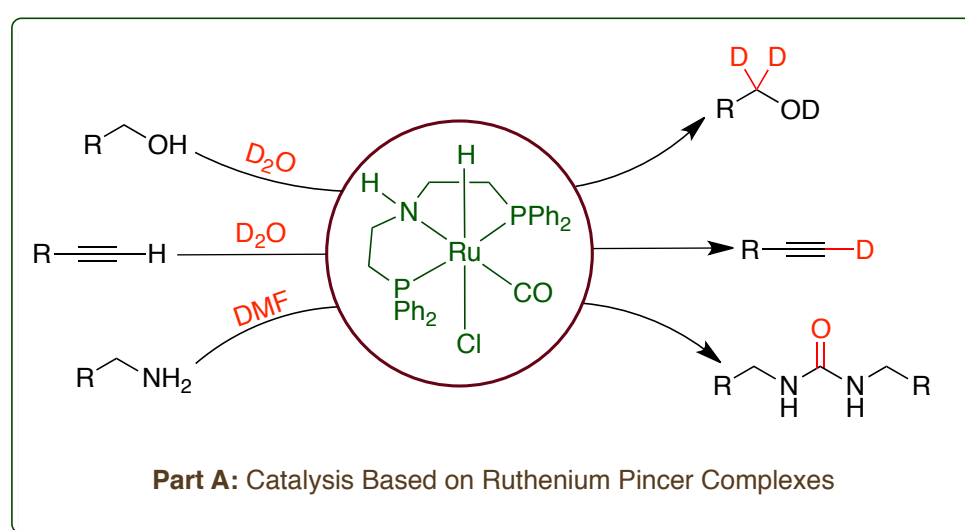
By employing pincer and half-sandwich ruthenium complexes, simple, atom-economical and important catalytic transformations were developed in which interesting and hitherto unknown intermediates were identified and disclosed. Identified catalytic intermediates were independently synthesized, characterized and further successfully used as efficient catalysts.

The **Part A** revealed the selective deuteration of alcohols and terminal alkynes (Chapter 2 and 3) using deuterium oxide as deuterium source. Mild reaction conditions, low loadings of catalyst and wide substrate scopes made these protocols highly efficient and practical. During these studies we realized the efficiency of Ru-macho complex in catalytic activation of O–H/or O–D and sp-C–H bonds to provide useful chemical transformations, which thus far was performed by employing stoichiometric bases and additives. Experiments performed in Chapter 2 disclosed the highly selective α -deuteration of primary alcohols and α,β -deuteration of secondary alcohols. Substrates embedded with different functional groups and activated C–H

protons, sensitive towards catalytic exchange are well tolerated under the optimized conditions, which demonstrates highly selective bond activations under this catalytic conditions. Further, selective sp-C–H bond activation and subsequent deuteration of terminal alkyne functionality revealed the high potential of Ru-macho complex in selective bond activations. The Ru-acetylide intermediate was isolated and structurally characterized, which allowed us to propose an oxidative reaction mechanism for this transformation. Notably, deuterium oxide is used as deuterium source in all these reactions.

After successfully demonstrating the application of O–H/or O–D and sp-C–H bond activation, the activation of N–H bond was planned. Thus, chapter 4 described a facile N–H bond activation of amines. This bond activation is further applied for developing an efficient protocol for the synthesis of valuable urea derivatives using DMF as a CO surrogate. The reactions are proposed to proceed via N–H activation of amines followed by CO insertion from DMF and with liberation of dihydrogen. The schematic summary for **Part A** is presented in Scheme A.

Scheme A Schematic Summary of Part A



The **Part B** disclosed the catalytic protocols based on half-sandwich ruthenium complexes. Highly efficient catalytic chemoselective hydroelementation reactions (hydroboration and hydrosilylation), and atom-economical synthesis of borasiloxanes were demonstrated (Chapter 6, 7, 8 and 9). Simple and commercially available ruthenium complex, $[\text{Ru}(p\text{-cymene})\text{Cl}_2]_2$ was used as catalyst precursor in all these transformations. Our studies uncovered the unknown reaction intermediate, “monohydrido-bridged dinuclear ruthenium complex” involved in the hydroelementation reactions. Using the simple catalyst precursor or isolated intermediate as catalyst, 990% TON was attained hydroelementation reactions.

Ruthenium catalyzed regioselective 1,4-hydroboration of pyridine derivatives using pinacolborane was also described (chapter 8). Mechanistic investigation of this transformation revealed the involvement of two intermediate half-sandwich ruthenium complexes, which are identified and independently synthesized and successfully used as efficient catalysts. Further in situ analyses of the catalytic experiments allowed us to identify the two other transient intermediates involved in the regioselective hydroboration of pyridine compounds. On the basis of the experimental evidence a new reaction mechanism consists of selective 1,5-hydride transfer from the metal center leading to the selective 1,4-addition on pyridine is proposed.

We established selective atom economical catalytic synthesis of borasiloxanes using a multi-component approach directly from the one-pot ruthenium catalyzed reaction of boranes, silanes and water. The pyridine ligated mononuclear ruthenium and monohydrido-bridged dinuclear ruthenium complexes were found to be suitable catalysts. This new catalytic protocol is highly efficient, water and molecular

hydrogen are the only byproducts and thus can be employed for the synthesis of boron and silicon containing useful inorganic materials.

Interestingly, monohydrido-bridged dinuclear ruthenium complex, which was identified as intermediate in the hydroelementation reactions turned out to be an efficient catalyst for the challenging selective deuteration of amines and amino acids using deuterium oxide. Upon reaction of this dinuclear monohydrido-bridged complex with amines, formation of rare cationic ruthenium complex was identified as a result of N–H bond activation (Chapter 10). The schematic summary of **Part B** is presented in Scheme B.

Scheme B Schematic Summary of Part B

